



Mechanism of action of metformin on glucose 6-phosphate in hepatocytes

Tabassum Naher Moonira

Thesis submitted for the degree of Doctor of Philosophy

Newcastle University

Faculty of Medical Sciences

Institute of Cellular Medicine

January 2019

Declaration

I declare that this thesis is my own work and that I have correctly acknowledged the work of others. This thesis has not been previously submitted for assessment at Newcastle University or elsewhere and is in accordance with University and School guidance on good academic conduct.

Abstract

The anti-hyperglycaemic drug metformin is the first-line oral therapy for Type 2 Diabetes, yet its mechanism of action remains contentious. We tested the hypothesis that metformin counteracts the effect of high glucose on gene regulation in hepatocytes by lowering cell glucose 6-phosphate (G6P) and we investigated the possible candidate mechanisms for the lowering of G6P by metformin.

Rat and mouse hepatocytes were treated with metformin (0.1-1.0mM) in incubation conditions to achieve cellular loads of metformin within the therapeutic range and higher (1-10 nmol / mg protein) as determined from cellular accumulation of [¹⁴C] metformin. Rates of flux of glucose metabolism were determined using ³H-labelled (2,3 and 5 positions) or ¹⁴C-labelled glucose (1,6 or uniformly labelled) in hepatocytes incubated with metformin, allosteric activators of AMPK (AMP-activated protein kinase), and allosteric modulators of enzymes that alter flux and G6P levels in hepatocytes.

Metformin, at cellular loads corresponding to the therapeutic range (1-2 nmol/mg), counteracted the elevation in G6P caused by 15-25mM glucose, dihydroxyacetone, xylitol and fructose in conditions where cell adenosine triphosphate (ATP) levels were maintained, but had little effect on cell G6P at basal glucose (5mM). In conditions of high glucose or gluconeogenic precursors the metformin efficacy in lowering G6P was greater at high cell G6P levels as occurs during compromised hydrolysis of G6P with a chlorogenic acid inhibitor of the G6P-transporter encoded by *Slc37a4*. Metformin also counteracted the effects of high glucose on both gene induction (*Pklr* and *G6pc*) and *Gck* gene repression and the latter was not mimicked by AMPK activators. The G6P lowering effect of metformin was not mimicked by pharmacological activators of AMPK (A769662, C13 and 991) but was mimicked by inhibitors of complex 1, mitochondrial uncouplers, an inhibitor of nicotinamide nucleotide transhydrogenase (NNT) which is coupled to the mitochondrial proton gradient, and phenazine methosulphate which oxidizes NADPH. Inhibition of glucokinase and glucose phosphorylation were excluded as a mechanism for the lowering of G6P by therapeutic concentrations of metformin. However, inhibition of glucose phosphorylation, estimated from metabolism of [2-³H] glucose, and glucokinase translocation occurred with diverse selective AMPK activators and also at higher metformin concentrations ≥ 1.0 mM. We excluded the possibility that

metformin lowers G6P by stimulating glycogen synthesis or inhibiting glycogen degradation from measurement of glycogen accumulation and correlation of glycogen synthesis with G6P using an allosteric inhibitor of phosphorylase. These studies showed inhibition of glycogen synthesis by metformin which paralleled the lowering of G6P suggesting that it is “secondary to” rather than “causative of” the G6P lowering. Metformin raised cell NADP indicating possible increased flux of G6P through the pentose phosphate pathway, and dehydroepiandrosterone (DHEA), an inhibitor of glucose 6-phosphate dehydrogenase (G6PD), abolished the increase in NADP with 0.5mM metformin and partially counteracted the decrease in G6P consistent with a possible increased pentose phosphate pathway flux by metformin. However, this could not be confirmed by knock down of G6PD. We excluded the possibility that inhibition of NNT by metformin is a major mechanism in lowered G6P because metformin lowered G6P in hepatocytes from mice with a deletion in the NNT gene. With high glucose as substrate, low metformin increased production of lactate and pyruvate, and metabolism of [3-³H] glucose but not [2-³H] glucose in conditions of negligible inhibition of [U-¹⁴C] glucose oxidation indicating increased glycolysis downstream of G6P. Targeting the first regulated site of glycolysis by allosteric inhibition of phosphofructokinase-1 (with either aurintricarboxylic acid a potent inhibitor, or by selective lowering of fructose 2,6-P₂ by expressing a kinase-deficient variant of *PFKFB1*) caused marked elevation in G6P for a small fractional inhibition of flux through glycolysis. This suggests the phosphofructokinase-1 / fructose biphosphatase-1 site is a strong candidate target for the stimulation of glycolysis and lowering of G6P by metformin. Elevated inorganic phosphate was identified as one candidate allosteric activator of phosphofructokinase-1 that is raised by metformin.

In summary, metformin lowers G6P in hepatocytes at least in part by stimulation of glycolysis and most likely by altered allosteric control at phosphofrucokinase-1 through raised inorganic phosphate or other effectors. The stimulation glycolysis by metformin is not mimicked by allosteric activators of AMPK. The lowering of hepatocyte G6P by metformin contributes to the counter-effects of metformin on gene regulation by high glucose.

Acknowledgements

Firstly, I am extremely grateful to Diabetes UK for my PhD Studentship, without which this project would not have been possible.

I would especially like to thank my supervisor Professor Lorraine Agius for her continued guidance and support throughout this project. I am indebted to Lorraine for her encouragement and dedication as a mentor, and I have truly loved being a part of the Liver Metabolism Group.

I would also like to express my gratitude to Dr Catherine Arden, Dr Ziad Al-Oanzi and Kirsty Cullen for their time in teaching me many of the techniques I have used in this study. I am also thankful to Ahmed Alshawi, Dr Francesco Zummo, Dr Brian Ford, Dr Shruti Chachra and to all the friends I have made in the lab for their help and for making my experience so enjoyable.

Finally, I could not have completed this project without the love and support of my family Alhamdulillah. I would like to dedicate this thesis to my parents who have taught me what hard work and perseverance is, and for always encouraging me to aim high and achieve my goals. Also, to my siblings Siddiquha, Adil, Aakib and Mahfuzah for their understanding and patience throughout this project and for their unwavering faith in me.

Table of Contents

Chapter 1: Introduction	1
1.1 Type 2 Diabetes	2
1.2 Metformin background	2
1.2.1 Metformin uptake and excretion	3
1.2.2 Metformin levels in animal models	5
1.2.3 Metformin inhibits gluconeogenesis in the liver	6
1.3 Metformin mechanism- Inhibition of complex 1	7
1.3.1 AMPK activation is implicated in the metformin mechanism	8
1.3.1.1 Gene regulation of gluconeogenic enzymes by AMPK mediated mechanisms	9
1.3.1.2 Metformin activates AMPK by inhibiting AMP deaminase independently of LKB1... 10	
1.3.1.3 Metformin activates AMPK through a lysosomal pathway through LKB1	11
1.3.2 Metformin effects that are AMPK independent and associated with gluconeogenesis... 11	
1.3.2.1 Inhibition of glucokinase translocation	12
1.3.2.2 Inhibition of glucagon signalling by AMP	13
1.3.2.2.1 Inhibition of glucagon signalling by AMPK activation	14
1.3.2.3 Inhibition of mitochondrial glycerophosphate dehydrogenase independently of AMPK or ATP depletion	14
1.4 AMPK maintains intracellular ATP homeostasis.....	16
1.4.1 Small molecule AMPK activators	17
1.4.1.1 AICAR	17
1.4.1.2 A769662.....	17
1.4.1.3 Compound 991	19
1.4.1.4 Compound-13	19
1.5 Glucose regulated gene expression is mediated by the transcription factor ChREBP-Mlx.....	20
1.6 Metformin lowers cell G6P in hepatocytes	23
1.6.1 Potential mechanisms for the lowering of G6P by metformin	23
1.7 Current status of hypotheses on the metformin mechanism	25
Chapter 2: Materials and Methods	38
2.1 Materials.....	39
2.1.1 Animals	39
2.1.2 Chemicals and Reagents	39
2.1.3 Enzymes.....	42
2.1.4 Antibodies.....	43
2.1.5 Adenoviral vectors.....	44

2.1.6 Primers for Real time RT-qPCR.....	44
2.2 Hepatocyte isolation and culture.....	45
2.2.1 Rat hepatocytes	45
2.2.2 Mouse hepatocytes.....	46
2.3 Methods.....	47
2.3.1 Preparation of radioactive substrates for metabolic studies	47
2.3.1.1 Determination of metformin accumulation	47
2.3.1.2 Determination of glycogen synthesis.....	47
2.3.1.3 Determination of glucose phosphorylation and glycolysis.....	48
2.3.1.4 Determination of glucose oxidation	49
2.3.2 Metabolite determination	50
2.3.2.1 Glucose 6-phosphate (G6P)	50
2.3.2.2 Glycerol 3-phosphate (G3P).....	51
2.3.2.3 Adenosine triphosphate (ATP).....	53
2.3.2.4 Lactate production.....	53
2.3.2.5 Pyruvate production	54
2.3.2.6 Glucose production.....	54
2.3.3 G6PD activity.....	55
2.3.4 Cell glycogen determination	56
2.3.5 NADP determination.....	56
2.3.6 Inorganic phosphate determination	57
2.3.7 Determination of mRNA expression (RT-qPCR)	57
2.3.7.1 Reverse transcription.....	58
2.3.8 Western blotting	58
2.3.9 Determination of cellular protein by Bradford method	59
2.3.10 Determination of cellular protein by Lowry method.....	59
2.3.11 Immunostaining	60
2.3.11.1 Fixation.....	60
2.3.11.2 Immunofluorescence	60
2.3.11.3 Mounting and imaging of coverslips.....	61
2.3.12 Statistical analysis	61
Chapter 3: Results 1	62
3.1 Metformin accumulation in hepatocytes	63
3.2 Metformin lowers cell G6P in hepatocytes incubated with high glucose or gluconeogenic precursors	64
3.2.1 Mitochondrial depolarisation mimics the G6P lowering effect of metformin	66

3.2.2 Potential link of G6P depletion with raised cell NADP	67
3.2.2.1 Elevation in NADP in conditions of lowered cell G6P: possible role of compromised NNT activity	67
3.2.2.2 Metformin lowers G6P in hepatocytes deficient in NNT activity	68
3.2.3 AMPK activators do not mimic the metformin effect on G6P	69
3.2.3.1 Testing the effects of AMPK activators on cellular G6P in hepatocytes	69
3.2.3.2 Testing the effects of AMPK activators on glucose production in hepatocytes.....	71
3.3 Metformin counteracts the effect of high glucose on hepatic gene expression	72
Chapter 4: Results 2.....	100
4.1 Effects of metformin and AMPK activators and glucose phosphorylation	101
4.1.1 AMPK activators but not low metformin concentrations inhibit glucokinase translocation or glucose phosphorylation	101
4.1.2 Metformin but not AMPK activators increase glucose metabolism at or downstream of G6P	101
4.1.3 The lowering of G6P by metformin is not explained by inhibition of glucose phosphorylation	102
4.2 Lowering of G6P by metformin is not secondary to altered glycogen metabolism.....	104
4.2.1 Metformin mimics CP-91149 on G6P lowering but has converse effects on glycogen synthesis	105
4.2.2 Metformin but not A769662 inhibits glycogen accumulation with both glucose and DHA as substrates	105
4.2.3 The inhibition of glycogen synthesis by metformin correlated with the lowering of G6P	105
4.3 Exclusion of hexosamine biosynthesis pathway	106
4.4 Exclusion of stimulation of H6PD metabolism	107
4.5 Metformin may lower G6P partially by stimulating flux through the pentose phosphate pathway	108
4.5.1 DHEA partially counteracts the effect of metformin on NADP and G6P.....	108
4.5.2 Lowering of G6P by DHEA could be due to its metabolism.....	109
4.5.3 CB72 as a G6PD inhibitor	110
4.5.4 Adenoviral knockdown of ShG6PD does not counteract the effect of metformin on cell G6P	110
4.5.5 Estimation of flux through the pentose phosphate pathway with [1- ¹⁴ C] glucose.....	111
4.6 Stimulation of glycolysis can explain the lowering of G6P by metformin.....	113
4.6.1 Depletion of F-2,6-P ₂ raises cell G6P, which is counteracted by metformin	114
4.6.2 The PFK1 inhibitor ATA raised cell G6P which is counteracted by metformin.....	114
4.6.3 Inhibition of FBP1 lowers cell G6P.....	115

4.6.4 The lowering of G6P by metformin is not mimicked in conditions of a more reduced cytoplasmic redox state	115
4.6.5 Metformin elevates cell phosphate: a potent allosteric activator of PFK1	116
Chapter 5: Discussion.....	149
5.1 Current status of hypotheses on the metformin mechanism	150
5.2 Metformin lowers G6P in hepatocytes	153
5.3 Lowering of G6P by metformin is mimicked by inhibition of mitochondrial complex 1	154
5.4 Metformin action involves mechanisms other than AMPK.....	155
5.5 Metformin does not inhibit glucose phosphorylation	155
5.6 Metformin inhibits glycogen synthesis: Possible roles of G6P depletion and Pi elevation ...	156
5.7 Low metformin stimulates lactate and pyruvate formation but high metformin inhibits substrate oxidation	157
5.8 Metformin counteracts the effects of high glucose on glucose regulated gene expression.	159
5.9 Summary	160

List of Tables and Figures

Table 2-1 Chemicals and Reagents	39
Table 2-2 Enzymes	43
Table 2-3 Antibodies.....	44
Table 2-4 Adenoviral Vectors	44
Table 2-5 Primers for real time RT-qPCR.....	44
Table 3-1 Control metabolite results for rat hepatocytes expressed in nmol/mg protein.....	74
Table 3 2 Control metabolite results for mouse hepatocytes expressed in nmol/mg protein	74
Figure 1.1 Chemical structure of metformin and the biguanide family of insulin-sensitising drugs (Bailey., 2017).....	28
Figure 1.2 Transporters involved in metformin uptake and excretion (Florez et al., 2017)	29
Figure 1.3 Chemical structure of metformin and its metabolic product, guanyurea (Trautwein et al., 2014).....	30
Figure 1.4 Proposed mechanisms by which metformin inhibits hepatic gluconeogenesis	31
Figure 1.5 Crystal structure of AMPK consisting of α , β and γ subunits	33
Figure 1.6 AICAR is transported across the plasma membrane and phosphorylated into ZMP in the cytoplasm (Corton et al., 1995).....	34
Figure 1.7 Structures of direct small molecule AMPK activators and inhibitors.....	35
Figure 1.8 G6P formation and metabolism	36
Figure 1.9 The chlorogenic acid derivative S4048 is an inhibitor of the glucose 6-phosphate transporter (G6PT).....	37
Figure 3.1 Cell metformin content and intracellular to extracellular metformin ratio in mouse hepatocytes	75
Figure 3.2 The chlorogenic acid derivative, S4048 increases cell G6P with high glucose or with gluconeogenic precursors	76
Figure 3.3 Metformin lowers G6P in hepatocytes with high glucose as substrate.....	77
Figure 3.4 Metformin lowers G6P but not ATP in hepatocytes with gluconeogenic precursors as substrate.....	78
Figure 3.5 Rotenone lowers G6P and increases lactate and pyruvate production in hepatocytes79	79
Figure 3.6 DNP lowers both G6P and lactate and pyruvate production with high glucose and gluconeogenic precursors as substrate.....	80
Figure 3.7 Glucose oxidation is stimulated by DNP and inhibited by both rotenone and a high metformin concentration	81
Figure 3.8 Berberine mimics the effect of metformin on G6P and lactate and pyruvate production	82
Figure 3.9 Possible consequences of mitochondrial depolarisation	83
Figure 3.10 Elevation in NADP by Rhein, metformin and ammonium ion	84
Figure 3.11 Metformin lowers G6P in hepatocytes from mice with a deletion in the NNT gene..	85
Figure 3.12 Stimulation of AMPK phosphorylation by high metformin is comparable with A769662 with high glucose	86

Figure 3.13 Stimulation of ACC phosphorylation by high metformin is comparable with A769662 with high glucose	87
Figure 3.14 Stimulation of AMPK phosphorylation by high metformin and A769662 is comparable with a gluconeogenic substrate	88
Figure 3.15 Stimulation of ACC phosphorylation by metformin is comparable with A769662 with a gluconeogenic substrate	89
Figure 3.16 A769662 does not mimic the effect of metformin on G6P or lactate and pyruvate production.....	90
Figure 3.17 The AMPK activators C13, 991 and A769662 stimulate ACC phosphorylation with high glucose	91
Figure 3.18 Stimulation of ACC phosphorylation by A769662 and C13 is comparable to high metformin concentrations.....	92
Figure 3.19 Opposite effects of AMPK activators and metformin on G6P and lactate and pyruvate production from DHA.....	93
Figure 3.20 Diverse effects of AMPK activators and metformin on G6P and glycolysis.....	94
Figure 3.21 Cell ATP for experiments in figures 3.19 (A-F) and 3.20 (G-L)	95
Figure 3.22 Opposite effects of metformin and AMPK activators on gluconeogenesis	96
Figure 3.23 High metformin causes comparable stimulation of AMPK phosphorylation as A769662	97
Figure 3.24 High metformin causes comparable stimulation of AMPK as A769662	98
Figure 3.25 Metformin counteracts the effect of high glucose on gene regulation	99
Figure 4.1 Sequestration of GK in the nucleus is abolished by high metformin, A769662 and GKA	118
Figure 4.2 AMPK activators but not metformin inhibit metabolism of [2- ³ H] glucose and [5- ³ H] glucose	119
Figure 4.3 Metformin and ammonium ion stimulate metabolism of [3- ³ H] glucose but not [2- ³ H] glucose	120
Figure 4.4 Lowering of G6P by GKR overexpression correlates with inhibition of glucose phosphorylation.....	121
Figure 4.5 Inhibition of glucose phosphorylation by glucosamine (GlcN) but not by metformin.....	122
Figure 4.6 Metformin lowers G6P in the presence of the GK inhibitor mannoheptulose.....	123
Figure 4.7 Metformin lowers G6P but inhibits glycogen synthesis	124
Figure 4.8 Metformin decreases glycogen accumulation with high glucose and DHA as substrates	125
Figure 4.9 Inhibition of glycogen synthesis with metformin with not A769662 correlates with G6P	126
Figure 4.10 Metformin lowers G6P independently of the hexosamine biosynthesis pathway ..	127
Figure 4.11 Metformin lowers G6P independently of hexose 6-phosphate dehydrogenase	128
Figure 4.12 PMS increases NADP and decreases G6P	129
Figure 4.13 DHEA increases NADP and decreases G6P	130
Figure 4.14 DHEA attenuates the decrease in G6P by metformin.....	131
Figure 4.15 Effects of DHEA on [¹⁴ C] metformin accumulation	132
Figure 4.16 G6P is lowered by DHEA and metyrapone.....	133
Figure 4.17 Menadione and miconazole lower G6P.....	134
Figure 4.18 CB72 lowers G6P	135
Figure 4.19 G6PD mRNA and protein in hepatocytes treated with short-hairpin RNA.....	136

Figure 4.20 shG6PD decreases G6PD enzyme activity at high concentrations only	137
Figure 4.21 Metformin lowers G6P in the presence of ShG6PD	138
Figure 4.22 Higher rate of $^{14}\text{CO}_2$ formation from $[6\text{-}^{14}\text{C}]$ glucose than from $[1\text{-}^{14}\text{C}]$ glucose in mouse hepatocytes	139
Figure 4.23 Inhibition of $[6\text{-}^{14}\text{C}]$ and $[\text{U-}^{14}\text{C}]$ glucose oxidation by high ethanol	140
Figure 4.24 DHEA increases oxidation of $[6\text{-}^{14}\text{C}]$ glucose and $[\text{U-}^{14}\text{C}]$ glucose	141
Figure 4.25 Inhibition of glycolysis and raised G6P by expression of a kinase deficient variant of PFK2/ FBP2	142
Figure 4.26 Inhibition of glycolysis and raised G6P with an inhibitor of PFK1	143
Figure 4.27 ATA inhibits the metabolism of $[3\text{-}^3\text{H}]$ and $[2\text{-}^3\text{H}]$ glucose	144
Figure 4.28 Lowering of G6P with an inhibitor of FBP1	145
Figure 4.29 Inhibition of the malate-aspartate shuttle increases the lactate/ pyruvate ratio and causes a small increase in G6P	146
Figure 4.30 AOA inhibits glucose oxidation when combined with a pyruvate transport inhibitor	147
Figure 4.31 Metformin and DNP raise inorganic phosphate (Pi)	148

Abbreviations

3PG	3-Phosphoglycerate
6-PG	6-Phosphogluconate
6PGD	6-Phosphogluconate Dehydrogenase
6PGL	6-Phosphogluconolactone
AAT	Aspartate Aminotransferase enzyme
ACC	Acetyl – CoA Carboxylase
ADaM	Allosteric Drug and Metabolite
ADP	Adenosine Diphosphate
AICAR	5-Aminoimidazole-4- Carboxamide-1- β -D-Ribofuranoside
AMP	Adenosine Monophosphate
AMPD	AMP Deaminase
AMPK	AMP-Activated Protein Kinase
AOA	Aminooxyacetic Acid
ATA	Aurintricarboxylic Acid
ATM	Ataxia Telangiectasia Mutated Gene
ATP	Adenosine Triphosphate
bHLHLZ	Basic Helix-Loop-Helix-Leucine Zipper
BPG	1,3-Bisphosphoglycerate
CaMKK2	Calcium/ Calmodulin- Dependent Protein Kinase Kinase 2
cAMP	Cyclic AMP
CBM	Carbohydrate-Binding Module
CBP	CREB Binding Protein
CBS	Cystathionine- β -Synthase
cGPD	Cytosolic Glycerophosphate Dehydrogenase
ChoRE	Carbohydrate Response Element
ChREBP	Carbohydrate Response Element Binding Protein
CPT1	Carnitine Palmitoyltransferase
CRE	cAMP Response Element
CREB	cAMP Response Element Binding Protein
CRTC2	CREB Regulated Transcription Coactivator 2
DHA	Dihydroxyacetone
DHAP	Dihydroxyacetone Phosphate
DHEA	Dehydroepiandrosterone
DNP	2,4-Dinitrophenol
DON	6-Diazo-5- oxo-L-norleucine
EHNA	Erythro-9-(2-hydroxy-3-nonyl)-adenine
ER	Endoplasmic Reticulum
F-1,6-P₂	Fructose 1,6-bisphosphate
F1P	Fructose 1-phosphate
F-2,6-P₂	Fructose 2,6-bisphosphate
F6P	Fructose 6-phosphate
FAS	Fatty Acid Synthase
FBP1	Fructose 1,6-bisphosphatase
FBP2	Fructose 2,6-bisphosphatase

FBPi	Fructose 1,6-bisphosphatase inhibitor (5-Chloro-2-[N-(2,5-dichlorobenzenesulfonamido)]-benzoxazole)
G1P	Glucose 1-phosphate
G3P	Glycol 3-phosphate
G6P	Glucose 6-phosphate
G6pc	Glucose 6-phosphatase
G6PD	Glucose 6-phosphate Dehydrogenase
G6PT	Glucose 6-phosphate Transporter
GA3P	Glyceraldehyde 3-phosphate
GAPDH	Glyceraldehyde 3-phosphate Dehydrogenase
GBD	Glycogen Binding Domain
GFAT	Glutamine:Fructose-6-phosphate Amidotransferase
GH	Growth Hormone
GK	Glucokinase
GKA	Glucokinase Activator
GKRP	Glucokinase Regulatory Protein
GKT	Glucokinase Translocation
GlcN	Glucosamine
GlcN 6-P	Glucosamine 6-phosphate
GIK	Glycerol Kinase
GLP-1	Glucagon-like Peptide 1
GP	Glycogen Phosphorylase
GPDH	Glycerol-3-phosphate Dehydrogenase
GS	Glycogen Synthase
GYS2	Liver Glycogen Synthase
H6PD	Hexose 6-phosphate Dehydrogenase
HBP	Hexosamine Biosynthesis Pathway
IMP	Inosine Monophosphate
IP3R	Inositol-1,4,5-trisphosphate Receptor
KO	Knockout
LDH	Lactate dehydrogenase
LKB1	Liver kinase B1
Ma-CoA	Malonyl Coenzyme A
MATE1	Multidrug and Toxin Extrusion 1
MATE2	Multidrug and Toxin Extrusion 2
mGPD	Mitochondrial Glycerophosphate Dehydrogenase
Mlx	Max-like Factor X
NAD	Nicotinamide Adenine Dinucleotide
NADH	Nicotinamide Adenine Dinucleotide (Reduced)
NADP	Nicotinamide Adenine Dinucleotide Phosphate
NADPH	Nicotinamide Adenine Dinucleotide Phosphate (reduced)
NH₄	Ammonium
NNT	Nicotinamide Nucleotide Transhydrogenase
OAA	Oxaloacetate
OCT 1	Organic Cation Transporter 1
OCT 3	Organic Cation Transporter 1

OGT	O-linked N-acetylglucosamine Transferase
PDE	Phosphodiesterase
PEP	Phosphoenolpyruvate
PEPCK	Phosphoenolpyruvate Carboxykinase
PFK1	Phosphofructokinase 1
PFK2	Phosphofructokinase 2
PFK2-KD	Kinase Deficient Phosphofructokinase 2
PGC-1α	Peroxisome Proliferator-Activated Receptor- γ Coactivator-1 α
PGI	Phosphoglucose Isomerase
Pi	Inorganic Phosphate
PKA	Protein Kinase A
Pkfr	Pyruvate Kinase
PMAT	Plasma Membrane Monoamine Transporter
PMS	Phenazine Methosulfate
PP2A	Protein Phosphatase 2A
PP-2Cα	Protein Phosphatase
SHP	Small Heterodimer Partner
T2D	Type 2 Diabetes
TCA	Tricarboxylic Acid Cycle
TXNIP	Thioredoxin Interacting Protein
UDP-GlcNAc	UDP-N-acetylglucosamine
Xu-5P	Xylulose 5-phosphate
ZMP	5-Aminoimidazole-4- Carboxamide-1- β -D-Ribonucleotide
α-AID	α -Autoinhibitory Domain
α-KD	α -Kinase Domain

Chapter 1: Introduction

1.1 Type 2 Diabetes

Diabetes is a chronic disease characterised by raised blood glucose levels that is prevalent in an estimated 425 million adults (age 20-79) worldwide. This is predicted to increase to 629 million by 2045 (International Diabetes Federation., 2017). Type 2 diabetes mellitus (T2D) (previously known as non-insulin-dependent or adult-onset diabetes) accounts for around 90% of all diabetes cases. The pathogenesis of this disorder is multifactorial resulting from a combination of lifestyle, genetic and epigenetic factors which lead to dysfunction of the β -cells in the pancreas and insulin resistance. Under normal conditions a feedback system between islet β -cells in the pancreas and insulin-sensitive tissues operates to maintain blood glucose homeostasis. When blood glucose is elevated, stimulation of β -cells results in insulin release which targets the liver to suppress hepatic glucose production and stimulates the uptake of glucose, amino acids and lipids in muscle and adipose tissue to maintain blood glucose within a narrow range. When these tissues develop insulin resistance the β - cells compensate by increasing insulin output, and an inability to do so results in impaired glucose tolerance and manifests as T2D (Kahn et al., 2014).

1.2 Metformin background

According to national and international guidelines metformin (1,1-dimethylbiguanide hydrochloride) is the first line oral therapy for the treatment of T2D and is taken by over 150 million people each year (UK Prospective Diabetes Study (UKPDS) group., 1998; An & He., 2016; Sanchez-Rangel & Inzucchi., 2017). Metformin is a member of the biguanide family of insulin-sensitising drugs which effectively lower insulin resistance and improve insulin sensitivity, reducing blood glucose in states of hyperglycaemia in T2D (Bailey., 2017; Rena et al., 2017). Biguanides were developed from the compound guanidine (figure 1.1) extracted from the plant *Galega* (French lilac) which has been used for centuries as a treatment for diabetes due to its blood glucose lowering properties (Witters., 2001; Bailey., 2017; Rena et al., 2017). Metformin was first proposed as a treatment for adult-onset diabetes in 1957, yet the more potent biguanides phenformin and buformin (figure 1.1) were more commonly used until their withdrawal in 1977 due to the high risk of lactic acidosis. Further research led to the clinical introduction of metformin which is preferential to its counterparts phenformin

and buformin as it effectively reduces hepatic gluconeogenesis with a lower risk of unwanted side effects such as hypoglycaemia, weight gain, or potentially fatal lactic acidosis (Bailey., 2017).

Metformin (200-250 mg/kg) demonstrates properties as an anti-tumour agent by inhibiting mTORC1 involved in the metabolism, growth and proliferation of cancer cells via AMPK activation (Manning et al., 2012). Metformin has also demonstrated properties as an anti-aging agent (Cabreiro et al., 2013; Martin-Montalvo et al., 2013; Wu et al., 2016; Sosnicki et al., 2016; Novelle et al., 2016; Heckman-Stoddard., 2017; Valencia et al., 2017; Wang et al., 2017; Howell et al., 2017) and has exhibited effects that could lower the risk of cardiovascular disease (Bannister et al., 2014; Vasamsetti et al., 2015; Cameron et al., 2016; Griffin et al., 2017; Wang et al., 2017; Varjabedian et al. 2018) and neurodegenerative diseases (such as Alzheimer, Parkinson, Huntington and dementia) (Wang et al., 2017). Additionally, it is a current treatment for polycystic ovary syndrome alleviating its metabolic symptoms likely through increased insulin sensitivity (Wang et al., 2017; Patel., 2018). However, the mechanism of metformin action in T2D has not yet been fully elucidated as it was discovered before the use of targeted drug discovery techniques (Rena et al., 2013; Rena et al., 2017).

1.2.1 Metformin uptake and excretion

Metformin is administered as an oral dose of 500-1000mg with a maximum dose of 2550-3000mg/day (2000mg/day in children) and is rapidly absorbed into the small intestine (Bailey et al., 2008; Graham et al., 2011; Gormsen et al., 2016; Bailey., 2017). It takes approximately 2.5 hours for metformin to reach its maximum plasma concentration (T_{max}) (of 8-23 μ M for a 0.5-1.5g dose in man) with an oral bioavailability of 50-60% and a half-life ($t_{1/2}$) of 5 hours (Graham et al., 2011; Bailey., 2017).

There are a number of metformin transporters present at varying levels in different tissues involved in the absorption, distribution and excretion of cationic drugs. In the small intestine the cation transporters plasma membrane monoamine transporter (PMAT encoded by SLC29A4) and OCT3 (encoded by SLC22A3, a member of the solute carrier family 22) are responsible for metformin uptake from the gut lumen into enterocytes, whereas OCT1 (encoded by SLC22A1) facilitates the transport of metformin into the interstitium (figure 1.2) (Wang et al., 2002; Zhou et al., 2009; McCreight et al.,

2016; Florez., 2017). These transporters account for 5-10% of metformin uptake, as the majority of metformin is transported via the paracellular route although metformin accumulation in the enterocyte is high (Proctor et al., 2008; Bailey et al., 2008). In the gut metformin increases glucose uptake and utilisation, and also increases levels of glucagon-like peptide 1 (GLP-1) (Bailey et al., 1994; Massollo et al., 2013; McCreight et al., 2016., Buse et al., 2016; DeFronzo et al., 2016; Preiss et al., 2017) and has been implicated as a major site for metformin action and its associated side effects (Cubeddu et al., 2000; Zhou et al., 2009; Cabreiro et al., 2013; Shin et al., 2014; Forslund et al., 2015; Duca et al., 2015; Zhou et al., 2016; Dujic et al., 2016 (a); Dujic et al., 2016 (b); Buse et al., 2016).

Further to its role in the small intestine, in humans OCT1 is principally expressed in the liver transporting metformin into hepatocytes (figure 1.2) (McCreight et al., 2016). Metformin uptake and accumulation is significantly reduced in OCT1 knock out mice, and the ability of metformin to lower fasting plasma glucose is lost (Shu et al. 2007). Furthermore, polymorphisms in the SLC22A1 gene encoding OCT1 affect the pharmacokinetics of metformin suggesting the liver is an important target of metformin (Shu et al., 2007; Sundelin et al., 2017). In liver OCT3 (figure 1.2) is expressed to a lesser extent than OCT1 (Nies et al., 2009) and the reduction of blood glucose by metformin is not apparent in OCT3 knockout mice (Chen et al., 2015).

Metformin is a small molecule which does not bind to plasma proteins allowing it to be readily filtered at the glomerulus. It is also a substrate for several kidney transporters including OCT1, MATE1 (multidrug and toxin extrusion 1) and MATE2 (multidrug and toxin extrusion 2) which promote the transport of metformin into urine (figure 1.2). OCT2 is mainly expressed in the kidney facilitating metformin uptake into renal epithelial cells for its excretion (figure 1.2). Reabsorption of metformin by passive diffusion is insignificant due to its low lipid solubility (McCreight et al., 2016).

It is acknowledged that metformin is excreted unchanged with peak concentrations of metformin in the urine of > 5mM after an oral dose of 50mg/kg and a urinary excretion $t_{1/2}$ of 20 hours (Wilcock & Bailey., 1994), however in some studies 14-20% of the drug was unaccounted for in urine (Graham et al., 2011). One possibility is that a small percentage of metformin is metabolised to guanylurea in hepatocytes (figure 1.3) (Gabr

et al., 2017). Although only a small percentage of metformin may be subject to metabolism, the drug is taken in large quantities meaning the metabolite could have a considerable role in its therapeutic mechanism (Gabr et al., 2017).

1.2.2 Metformin levels in animal models

The antihyperglycaemic effects of metformin are attributed to targeting of multiple tissues including stimulation of glucose absorption and stimulation of glucose utilisation in the small intestine, stimulation of glucose uptake and oxidation in skeletal muscle, and inhibition of gluconeogenesis in the liver (Wilcock & Bailey., 1994). Wilcock & Bailey., (1994) showed that when mice were given an oral load of 50mg/kg metformin, accumulation was greatest in the gastrointestinal tract particularly in the small intestine where metformin accumulated at concentrations greater than 1000 μ mol/kg wet weight of tissue over a 4-hour time period and fell to <2% of peak values after 24 hours. High metformin concentrations were also observed in the kidney and fell to <2% of the maximum values after 24 hours. The plasma concentrations after 0.5 hours in the hepatic portal vein were 52 μ M and 62 μ M in the normal mouse and the diabetic mouse respectively, and the hepatic content at 0.5 hours was significantly higher in the diabetic mouse at 282 μ mol/kg wet weight in comparison with 182 μ mol/kg wet weight in the normal mouse. Therefore, assuming a hepatocyte number per gram of liver of 100 million and a hepatocyte protein content of 1.7mg per million cells, the liver metformin content at 0.5h after an oral therapeutic load was 1-2nmol/mg cell protein. After 4 hours liver metformin concentration fell to 3% of the peak concentration. These values equate to the maximum concentrations observed in humans after a single dose of 0.5 or 1.5g of metformin, indicated by the maximum inferior vena cava plasma concentration of around 30 μ mol/l (Wilcock & Bailey., 1994). Furthermore, rats treated orally with 50mg/kg [¹⁴C] metformin accumulated a maximum metformin concentration of 15 μ mol/l in the hepatic portal vein after 1 hour and the metformin in the liver declined to a half-maximal concentration at 4 hours. The majority of [¹⁴C] metformin was localised to the cytosol, with 7-10% localised in the mitochondrial and lysosomal fraction (Wilcock & Bailey 1991).

1.2.3 Metformin inhibits gluconeogenesis in the liver

Chronic therapy with metformin in man for ~ 3 months shows a lowering of blood glucose by 25-30% which is attributed to inhibition of hepatic glucose production by inhibition of gluconeogenesis (Stumvoll et al., 1995; Hundal et al., 2000; Petersen et al., 2017) although inhibition of glycogenolysis had also been reported (Cusi et al., 1996). A lowering of plasma free fatty acids by metformin was also reported in some (Hundal et al., 2000) but not in other (Stumvoll et al., 1995) studies of gluconeogenesis, suggesting a potential role of the lowering of free fatty acids in contributing to the decrease in gluconeogenesis, because elevated fatty acid levels stimulate gluconeogenic flux through raised levels of mitochondrial acetyl-CoA levels with activate pyruvate carboxylase or other mechanisms (Rui., 2014). Whether the decrease in gluconeogenesis by metformin in man is due to changes in gene expression of gluconeogenic enzymes or a direct inhibitory effect of metformin on gluconeogenic flux is not known. However, a study testing the rapid effects of metformin in man by intravenous infusion of metformin to plasma concentrations of 13-50 μM in conjunction with a hyperglycaemic clamp found no effect of metformin on either uptake of glucose by the periphery or on inhibition of glucose production, and concluded that the therapeutic effect on inhibition of glucose production results from chronic therapy (Sum CF et al., 1992) and presumably therefore either indirect mechanisms or changes in liver gene expression.

Several studies reported inhibited of gluconeogenesis by metformin in perfused rat liver (Radzuik J et al., 1997) and in isolated rat hepatocytes by a direct effect that is most likely not secondary to changes in gene expression because it manifests within a few hours (Wollen & Bailey., 1988; Argaud et al 1993; Owen et al., 2000; Fulgencio et al., 2001; Zhou et al., 2001; Foretz et al., 2010; Madiraju et al., 2014). However, inhibition of gluconeogenesis by metformin in hepatocytes through changes in gene expression has been observed (Kim et al., 2008; He et al., 2009; Lee et al., 2010; Kim et al., 2012; Sajan et al., 2013; Cao et al., 2014). There is no evidence for inhibition of glycogenolysis by metformin in hepatocytes although inhibition of glycogen synthesis in hepatocytes has been reported (Otto et al., 2003; Hansen et al., 2002). The animal studies concur with the conclusion that inhibition of glucose production in man by metformin is through inhibition of gluconeogenesis.

1.3 Metformin mechanism- Inhibition of complex 1

Metformin is positively charged and accumulates in hepatocytes because of the electrochemical gradient (Owen et al., 2000; Bridges et al., 2014). Likewise, it accumulates slowly in the mitochondria in accordance with mitochondrial membrane potential where it is proposed to inhibit mitochondrial respiratory chain complex 1 (NADH: ubiquinone oxoreductase) (figure 1.4) (Schafer et al., 1976; Pryor et al., 1987; Owen et al., 2000; El-Mir et al., 2000; Ota et al., 2009; Bridges et al., 2014). Complex 1 is a multi-subunit protein that couples the transfer of electrons from NADH to ubiquinone reduction providing electrons to respiratory complex III and complex IV for the reduction of oxygen to water, which drives proton transport across the inner membrane to generate a protonmotive force for ATP synthesis, and produces reactive oxygen species dependent on the NADH/NAD⁺ pool in the mitochondrial matrix (Bridges et al., 2014). El-Mir et al., (2000) showed that high concentrations of metformin (1-10mM) inhibited complex 1 in hepatocytes, likely by an indirect mechanism, accompanied by a decrease in the ATP/ADP ratio. Owen et al., (2000) also showed inhibition of complex 1 by 10mM metformin and a decrease in the ATP/ADP ratio, although they proposed that this was a direct effect of metformin. Bridges et al., (2014) also proposed that metformin is a reversible non-competitive inhibitor of complex 1 that stabilises complex 1 in its inactive conformation, and inhibits the rate determining step that is mechanistically coupled to ubiquinone reduction, and that metformin inhibits ATP synthesis consequently to complex 1 inhibition. It was also reported that metformin binds to mitochondrial copper ions which may inhibit mitochondrial function, also this is less well understood (Logie et al., 2012; Repiscak et al., 2014; Quan et al., 2015).

These studies used high metformin concentrations that exceed the pharmacological dose. Bridges et al., (2014) proposed that metformin can accumulate in mitochondria at concentrations of up to 1000 times greater than the extracellular environment, justifying the use of high concentrations of metformin in mitochondrial experiments although they exceed the clinical extracellular levels. However, metformin does not accumulate to this degree in organs, and radioactive metformin accumulation has not been observed in *Xenopus laevis* oocyte mitochondria at concentrations that inhibit complex 1 suggesting

metformin accumulation in the mitochondria may not reach the required concentrations for complex 1 inhibition (Fontaine et al., 2014).

1.3.1 AMPK activation is implicated in the metformin mechanism

Zhou et al., (2001) reported that metformin exerts its effects by stimulating AMP-activated protein kinase (AMPK), a serine/ threonine kinase responsible for sensing and regulating intracellular and whole-body energy metabolism, and that this mechanism provides a unified explanation for its diverse metabolic effects on gluconeogenesis, lipogenesis and fatty acid oxidation. One possible mechanism is that metformin inhibition of complex 1 and the subsequent inhibition of mitochondrial ATP production increases the cytoplasmic ADP: ATP and AMP: ATP ratios leading to activation of AMPK which restores the energy balance by stimulating catabolic processes to generate ATP and by reducing energy consumption, for example by inhibiting gluconeogenesis (figure 1.4) (Rena et al., 2017). Zhou et al., (2001) showed that metformin (10-2000 μ M) activated AMPK and suppressed acetyl CoA-carboxylase (ACC) activity, a downstream target of AMPK that catalyses fatty acid synthesis and is negatively regulated by AMPK mediated phosphorylation. They also showed stimulation of fatty acid oxidation and inhibition of fatty acid and lipogenic gene expression by metformin (0.2-0.5mM) (Zhou et al., 2001).

In response to an increase in cellular AMP and its binding to the γ unit of AMPK, the upstream serine/ threonine kinase liver kinase B1 (LKB1) phosphorylates the conserved threonine residue in the activation loop of AMPK α (Thr172 α 1), activating AMPK (Zhang et al., 2013). Shaw et al. (2005) suggested that AMPK activation is required for the therapeutic effects of metformin as metformin (250mg/kg) was unable to reduce blood glucose in mice lacking hepatic LKB1 which exhibit a marked decrease in AMPK phosphorylation. Cao et al. (2014) also showed that metformin was unable to phosphorylate AMPK and inhibit glucose production in LKB1 knockdown hepatocytes. Therefore, the increase in AMP by metformin could account for stimulation of AMPK. Furthermore, chronic metformin treatment (50mg/kg) failed to inhibit hepatic glucose production in ACC double knock-in (ACCDKI) mice with alanine-knock in mutations at both ACC1 (at Ser79) and Acc2 (at Ser212) (Fullerton et al., 2013) consistent with the study by Zhou et al., (2001) that inhibitory phosphorylation of ACC by AMPK is involved

in the therapeutic actions of metformin. Meng et al., (2015) showed that metformin (0.1-1.0mM) inhibited hepatic gluconeogenesis and gluconeogenic gene expression, and stimulated AMPK phosphorylation and activity. When AMPK was overexpressed in hepatocytes, metformin stimulated AMPK phosphorylation and enhanced the suppression of glucose production (He et al., 2016) suggesting the action of metformin is mediated by AMPK.

1.3.1.1 Gene regulation of gluconeogenic enzymes by AMPK mediated mechanisms

Glucagon signalling activates cAMP-PKA and phosphorylation of the transcription factor cAMP response element binding protein (CREB) and dephosphorylation of CREB-regulated transcriptional co-activator 2 (CRTC2) forming the CREB-CBP-CRTC2 complex on a cAMP response element site. This complex increases transcription of gluconeogenic genes including peroxisome proliferator-activated receptor- γ coactivator-1 α (PGC-1 α) and its downstream targets phosphoenolpyruvate carboxykinase (PEPCK) and G6pc (figure 1.4) (He et al., 2009). He et al. (2009) showed that both metformin and the AMPK activator Amino-4-imidazolecarboxamide riboside (AICAR) stimulated CBP (CREB binding protein) phosphorylation dissociating this complex and subsequently inhibiting gluconeogenic gene expression. This was also mimicked by AMPK overexpression suggesting this effect of metformin involves activation of AMPK.

AMPK activation also phosphorylates CRTC2 inhibiting gluconeogenic gene expression (Koo et al., 2005; He et al., 2009). Lee et al. (2010) proposed that acute metformin treatment activates AMPK promoting CRTC2 phosphorylation, whereas chronic metformin treatment inhibits gluconeogenic gene expression by induction of SHP (small heterodimer partner) gene expression. SHP gene expression in hepatocytes inhibits CRTC2 binding to CREB and CRE (cAMP response element) promoter activity inhibiting PEPCK and G6pc gene expression. In this study, metformin (0.1-1.0mM) upregulated SHP gene expression in hepatocytes. Additionally, with constitutively active CRTC2 the ability of metformin (2mM) to inhibit glucose production was lost in SHP knockdown hepatocytes. SHP knockdown also blocked AMPK mediated inhibition of PEPCK and G6pc promoter activity (Lee et al., 2010). Together this suggests AMPK activation by metformin inhibits gluconeogenic gene expression by upregulating SHP.

Kim et al. (2012) provided evidence that metformin stimulates SHP gene expression through activation of ATM (ataxia telangiectasia mutated gene) which encodes a serine/threonine protein kinase, counteracting the effect of growth hormone (GH) on gluconeogenic gene expression. GH stimulates PEPCK and G6pc gene expression and glucose production, which is inhibited by 2mM metformin (Kim et al., 2012). It has been proposed that activation of ATM by metformin activates AMPK (Zhou et al., 2001; Kim et al., 2012), upregulating SHP, inhibiting GH mediated induction of gluconeogenic gene expression (Kim et al., 2012). However, these studies used the ATM inhibitor KU-55933 to draw this conclusion and Yee et al. (2012) observed that metformin-mediated AMPK phosphorylation with the ATM inhibitor KU-55933 was due to inhibition of metformin uptake via OCT1 independently of ATM rather than direct AMPK activation. Therefore, the results in which metformin-mediated inhibition of gluconeogenic gene expression and glucose production was counteracted by KU-55933 (Kim et al., 2012), may have been due to inhibition of metformin uptake by KU-5933, questioning whether metformin exerts its effects via activation of ATM.

1.3.1.2 Metformin activates AMPK by inhibiting AMP deaminase independently of LKB1

Ouyang et al., (2011) proposed that metformin activates AMPK by inhibiting AMP deaminase (AMPD) which converts AMP to IMP (inosine monophosphate). Metformin (10mM) inhibited purified rabbit muscle AMPD activity and stimulated AMPK phosphorylation, glucose uptake and fatty acid oxidation in L6 cells which was mimicked by the AMPD inhibitor erythro-9-(2-hydroxy-3-nonyl)-adenine (EHNA), the effects which were not additive (Ouyang et al., 2011) suggesting metformin and EHNA exert their effects by similar mechanisms. Additionally, metformin failed to stimulate glucose uptake in AMPD1 knockdown cells and LKB1 knockdown had no effect on metformin stimulated glucose uptake indicating glucose uptake is affected by the metformin effect on AMPD rather than via LKB1 (Ouyang et al., 2011). Vytla et al., (2013) showed that metformin stimulated fatty acid oxidation in L6 cells whereas the complex 1 inhibitor rotenone had the converse effect, and that both metformin (15mM) and EHNA raised cell AMP without affecting ATP. Therefore, metformin could inhibit AMPD by stimulating

electron transport in the mitochondria rather than via inhibition of complex 1 (Vytla et al., 2013).

1.3.1.3 Metformin activates AMPK through a lysosomal pathway through LKB1

AMPK activation by LKB1 is initiated on the late endosome/ lysosome. Under conditions of glucose starvation AXIN bound LKB1 translocates to the endosome where it interacts with the v-ATPase-Ragulator complex and AMP bound AMPK allowing AMPK phosphorylation by LKB1, switching on catabolic metabolism (Zhang et al., 2013; Zhang et al., 2014). Zhang et al., (2016) proposed that metformin promotes AXIN/LKB1 translocation onto the lysosome surface where it forms a complex with v-ATPase-Ragulator resulting in AMPK activation. They found that metformin (50mg/kg/day) mediated AMPK phosphorylation and activation was not observed in AXIN-liver-specific knockout mice (AXIN^{LKO}) and in AXIN^{LKO} hepatocytes treated with 70 μ M metformin. Metformin mediated AMPK phosphorylation and activation was also lost with knockout and knockdown models of the regulator complex components (LAMTOR1 and ATP6v0c), indicating metformin activates AMPK by promoting the formation of the v-ATPase-Ragulator-AXIN/LKB1-AMPK complex on the lysosomal surface. Subsequently the v-ATPase-Ragulator complex dissociates Raptor and mTOR, inactivating mTORC1- a regulator of anabolic pathways (Zhang et al., 2016).

1.3.2 Metformin effects that are AMPK independent and associated with gluconeogenesis

The studies discussed above prove evidence for inhibition of gluconeogenesis by metformin in an AMPK dependent manner. However, Foretz et al., (2010) reported that metformin was able to inhibit gluconeogenesis independently of AMPK as metformin (0.25-1mM) retained its ability to inhibit glucose production in AMPK α 1 α 2-null hepatocytes (knockout) in the absence of AMPK/ ACC phosphorylation. The AMP mimetic AICAR also inhibited glucose production in wild type and AMPK knockout hepatocytes whereas the direct AMPK activator A769662 did not have a significant effect on glucose production in either the wild type or the knockout. Metformin and AICAR also inhibited gluconeogenic gene expression (G6pc) in wild type and AMPK knockout hepatocytes whereas A769662 (\leq 100 μ M) had no effect on either wild type or

knockout (Foretz et al., 2010). Therefore, both metformin and AICAR were able to inhibit gluconeogenesis independently of AMPK.

As discussed above, Lee et al., (2010) proposed that metformin activates AMPK, promoting CRTC2 phosphorylation, inhibiting transcription of gluconeogenic genes. However, Foretz et al., (2010) showed that CRTC2 dephosphorylation was similar in both wild type and AMPK knockout hepatocytes, and that metformin stimulated CRTC2 phosphorylation in wild type but not AMPK knock out hepatocytes, suggesting metformin inhibits glucose production by a CRTC2 independent mechanism. Metformin also inhibited glucose production in LKB1 knock out hepatocytes in the absence of CRTC2 phosphorylation suggesting the LKB1 pathway does not mediate the inhibition of glucose production by metformin. These effects were also observed with AICAR and both metformin and AICAR lowered cell ATP, with metformin (0.2-2mM) also increasing the AMP/ ATP ratio. This was not mimicked by A769662 suggesting metformin inhibits hepatic gluconeogenesis independently of LKB1 and AMPK due to the decrease in the hepatic energy state (Foretz et al., 2010). Hawley et al., (2010) also showed that both AICAR and metformin activated AMPK in wild type cells but not HEK293 cells carrying the R531G mutated form of AMPK (RG) which is insensitive to AMP. However, the direct AMPK activator A769662 activated AMPK signalling in both wild type and RG cells suggesting metformin activates AMPK by raising cell AMP rather than direct AMPK activation (Hawley et al., 2010).

1.3.2.1 Inhibition of glucokinase translocation

The enzyme glucokinase (GK) catalyses the phosphorylation of glucose in the first step of glucose metabolism. In the post-absorptive state when blood glucose is 5mM, GK is bound to its regulatory inhibitory protein (GKRP) and sequestered in the nucleus in an inactive form. When the glucose concentration is elevated in the portal vein after a meal GK dissociates from GKRP and translocates to the cytoplasm where it resides in its active form. GK activity is also affected by allosteric regulators of GKRP such as the negative regulator fructose 1-phosphate (F1P) (the first intermediate of fructose metabolism) and the positive regulator fructose 6-phosphate (F6P) (an intermediate of glycolysis) (Choi et al., 2013; Agius., 2016). Guigas et al., (2006) showed that both metformin (3-10mM) and AICAR inhibited liver glucose phosphorylation, correlating with AMPK activation and an

increase in ACC phosphorylation however, this relationship was not linear suggesting AMPK activation could not fully explain inhibition of glucose phosphorylation. Both metformin and AICAR also inhibited glucokinase translocation (GKT) in both wild type mice and in mice lacking AMPK α_1 and α_2 catalytic subunits (AMPK α_1 $\alpha_{2LS}^{-/-}$) indicating that inhibition of glucose phosphorylation was due to impaired GKT independently of AMPK. The ATP synthase inhibitor oligomycin had similar effects as metformin and AICAR on glucose phosphorylation, and all three compounds were associated with a drop in ATP- a substrate for GK. Therefore Guigas et al. (2006) proposed that metformin depletes intracellular ATP, inhibiting GK translocation to the cytosol resulting in inhibition of glucose phosphorylation.

However, Mukhtar et al. (2008) found that AICAR (50-200 μ M) inhibited glucose-induced GKT and glucose phosphorylation in conditions where ATP was not depleted. This involved phosphorylation of 6-phosphofructo-2-kinase/ fructose-2,6-bisphosphatase (PFK2) and phosphorylation of GKRP. In this study metformin (0.5mM and 5mM) stimulated AMPK and inhibited GKT at concentrations that lowered ATP meaning the role of ATP depletion could not be measured independently of AMPK activation (Mukhtar et al., 2008).

1.3.2.2 Inhibition of glucagon signalling by AMP

Binding of glucagon to its receptor on hepatocytes activates adenylyl cyclase and stimulates production of the second messenger cyclic AMP (cAMP) causing activation of protein kinase A (PKA) which increases glucose output by phosphorylating target proteins. Miller et al., (2013) reported that metformin (125 μ M-1Mm) raised cell AMP, an allosteric inhibitor of adenylyl cyclase, and inhibited glucagon stimulated cAMP accumulation and glucose output in primary hepatocytes (figure 1.4). Metformin (500mg/kg) also counteracted the increase in cAMP and PKA activity as well as the phosphorylation of the PKA target proteins PFK1/FBP1 (6-Phosphofructo-2-Kinase/Fructose-2,6-biphosphatase 1) and IP3R (inositol-1,4,5-trisphosphate receptor) in both fasted and diabetic mice indicating metformin inhibits glucagon signalling. Although metformin activated AMPK, phenformin and AICAR antagonised the accumulation of cAMP by glucagon in AMPK α deleted hepatocytes suggesting

biguanides inhibit glucagon signalling by increasing AMP and independently of AMPK activation (figure 1.4) (Miller et al., 2013).

1.3.2.2.1 Inhibition of glucagon signalling by AMPK activation

Johanns et al., (2016) also found that metformin inhibited glucagon signalling although they suggested this was an AMPK dependent effect. They found that direct AMPK activation with an allosteric activator compound 991 (1-10 μ M) inhibited glucagon signalling and phosphorylation of its targets (glycogen phosphorylase and CREB) without altering intracellular adenine nucleotide concentrations. This action of compound 991 was dependent on phosphodiesterase (PDE) activation and was lost in AMPK deleted hepatocytes (AMPK $\alpha 1^{-/-}/\alpha 2^{LS^{-/-}}$) although, glucagon still activated PDE in knockout mice as AMPK and PKA phosphorylate and activate PDE at distinct sites. Therefore Johannis et al., (2016) suggested that hepatic AMPK activation activates PDE4B which counteracts glucagon signalling (figure 1.4). Metformin (100-300 μ M) increased the activity of PDE suggesting that metformin inhibits glucagon signalling by stimulation of AMPK either directly or indirectly via an increase in AMP (Johanns et al., 2016).

1.3.2.3 Inhibition of mitochondrial glycerophosphate dehydrogenase independently of AMPK or ATP depletion

Madiraju et al., (2014) proposed that metformin inhibits hepatic gluconeogenesis by non-competitive inhibition of the mitochondrial enzyme glycerophosphate dehydrogenase (mGPD) (figure 1.4), a flavin linked respiratory chain dehydrogenase that operates at the intersection between glycolysis, oxidative phosphorylation and fatty acid metabolism, catalysing the oxidation of glycerol-3-phosphate (G3P) to dihydroxyacetone phosphate (DHAP). They reported that metformin treatment (50mg/kg) in rats increased the hepatic lactate/ pyruvate ratio and decreased the β -hydroxybutyrate/ acetoacetate ratio suggestive of an increase in cytoplasmic NADH/ NAD⁺ ratio and a decreased mitochondrial NADH/ NAD⁺ ratio respectively (Madiraju et al., 2014). However, whether the latter can be explained by a decrease in plasma fatty acids as was shown previously in a metformin study in man (Hundal et al., 2000) was not discussed. It was assumed that a more reduced cytosolic redox state and more oxidised mitochondrial redox state could be explained by metformin inhibition of mGPD, and that the latter could also explain inhibition of gluconeogenesis from lactate (Madiraju et al., 2014). Consistent

with this, both metformin and knockdown of mGPD inhibited glucose production when the lactate: pyruvate ratio was high but not when the redox state was lowered in primary hepatocytes. Additionally, metformin inhibited glucose production from lactate and glycerol which are reduced substrates and were proposed to require mGPD for the conversion to DHAP in gluconeogenesis. However, metformin did not inhibit glucose production from DHAP, alanine and pyruvate which do not require changes in the cytosolic redox state for gluconeogenesis. This substrate selectivity was also observed in mGPD knockdown hepatocytes. Therefore, Madiraju et al., (2014) proposed that metformin inhibits mGPD, increasing cytosolic NADH and inhibiting the conversion of lactate and glycerol to glucose.

However, Baur & Birnbaum (2014) proposed a number of issues arising from this conclusion and the experimental methods used. Firstly, previous studies have shown an increase in both the cytoplasmic and mitochondrial NADH/NAD⁺ ratios in hepatocytes with biguanides (Owen et al., 2000) consistent with inhibition of complex 1 by metformin. Baur & Birnbaum., (2014) suggested the increase in cytosolic NADH may represent NADH production by cGPD (cytosolic glycerophosphate dehydrogenase) operating in reverse rather than inhibition of mGPD. Additionally, the NADH generated from lactate dehydrogenase in the conversion of lactate to pyruvate is used by GAPDH meaning the importance of mGPD in gluconeogenesis is uncertain. Furthermore, the glycerophosphate shuttle accounts for only ~0.5% of ATP production indicating it would have little effect on gluconeogenesis from lactate, because the malate-aspartate shuttle is more prominent in humans than the glycerophosphate shuttle. Likewise, the malate aspartate shuttle is also more important in mice and its disruption lowers fasting glycaemia whereas disruption of the glycerophosphate shuttle has no effect on glycaemia in mice (Saheki et al., 2007; Baur & Birnbaum 2014).

Madiraju et al., (2014) also found that acute and chronic treatment of 50mg/kg metformin inhibited endogenous glucose production in rats, in parallel with AMPK/ ACC activation and reduced CREB phosphorylation after chronic treatment but not after acute exposure. On this basis they argued that acute inhibition of gluconeogenesis was independent of AMPK however, they could not rule out an increase in AMP and

consequent inhibition of adenylyl cyclase rather than direct AMPK activation or mGPD inhibition (Madiraju et al., 2014; Baur & Birnbaum., 2014).

1.4 AMPK maintains intracellular ATP homeostasis

AMPK is a serine/ threonine kinase responsible for sensing and regulating intracellular and whole-body energy metabolism (Cool et al., 2006). Its activation leads to the generation of ATP by activation of catabolic pathways such as fatty acid oxidation (Velasco et al., 1997), and inhibition of anabolic enzymes involved in fatty acid synthesis (such as acetyl-CoA carboxylase) and ATP consuming processes such as gluconeogenesis (Zhou et al., 2001) in order to maintain homeostasis of intracellular ATP, ADP and AMP. AMPK exists as a heterotrimer comprised of a catalytic α subunit with protein kinase activity, a scaffolding β subunit and a regulatory γ subunit which exist in multiple isoforms (figure 1.5). The α and β subunit are encoded by 2 genes each, while the γ subunits is encoded by 3 genes generating the isoforms $\alpha 1/ \alpha 2$, $\beta 1/ \beta 2$ and $\gamma 1/ \gamma 2/ \gamma 3$ resulting in 12 potential heterotrimeric combinations which vary in their tissue distribution, regulatory properties and subcellular localisations. AMPK is activated by phosphorylation of Thr172 within the activation loop of the kinase domain of the α subunit (α -KD) which is catalysed by the upstream kinases liver kinase B1 (LKB1) and calcium/ calmodulin- dependent protein kinase kinase 2 (CaMKK2) (Hardie et al., 2012; Ross et al., 2016 a; Ross et al., 2016 b; Hardie et al., 2018). At low levels of AMP, AMPK is maintained in its inactive conformation by the autoinhibitory domain (α -AID) which is connected to the C-terminal domain (α -CTD) by the regulatory α -linker segment. In conditions of energy depletion cell AMP exceeds that of ATP as a product of the reaction catalysed by adenylate kinase. AMP binds directly to the cystathionine- β -synthase (CBS) domain of the AMPK γ subunit promoting phosphorylation of Thr172 within the α -KD by LKB1 and decreasing the rate of Thr172 dephosphorylation by protein phosphatases, activating AMPK 100-fold. In the presence of AMP, the catalytic subunit is more closely associated with the nucleotide binding module physically protecting Thr172 from dephosphorylation, while binding of the α -linker to the γ subunit also separates the α -KD from the α -AID contributing to the allosteric activation of AMPK by AMP which can increase P-AMPK activity by more than 10-fold (Cordero et al., 2016; Hardie et al., 2018; Olivier et al., 2018). AMPK can also be activated by CaMKK2 which is activated in

response to increased intracellular Ca^{2+} concentrations mediated by hormones.

Downstream of its activation, AMPK phosphorylates and inactivates both isoforms of the enzyme acetyl-CoA carboxylase (ACC1/ ACC2) which requires ATP to produce malonyl-CoA for the synthesis of fatty acids. This relieves malonyl-CoA inhibition of carnitine palmitoyltransferase (CPT1) and stimulates fatty acid oxidation (Hardie et al., 2018).

Furthermore, AMP is an allosteric inhibitor of the gluconeogenic enzyme fructose-1,6-bisphosphatase (FBP1), potentially inhibiting glucose production (McGrane et al., 1983) and like fructose 2,6-bisphosphate, AMP is an allosteric activator of the glycolytic enzyme PFK1. The inhibition of gluconeogenesis by AICAR (see below) -which when phosphorylated functions as an AMP analogue- is explained by inhibition of FBP1 (Vincent et al., 1991). In addition to AICAR, a number of small molecule activators of AMPK are available which are discussed below.

1.4.1 Small molecule AMPK activators

1.4.1.1 AICAR

AICAR (5-aminoimidazole-4- carboxamide-1- β -D-ribofuranoside) was identified as an inhibitor of gluconeogenesis and potential anti-hyperglycaemic compound (Vincent et al., 1991; Vincent et al., 1992) and was later shown to cause activation of AMPK (Sullivan et al., 1994). AICAR itself is not a direct AMPK activator, but it is taken up in cells and phosphorylated by adenosine kinase into ZMP (5-aminoimidazole-4- carboxamide-1- β -D-ribonucleotide) (figure 1.6) which is a structural analogue of AMP (Corton et al., 1995; Cordero et al., 2016). Therefore, it mimics the effects of AMP, activating AMPK allosterically and promoting its phosphorylation without altering intracellular levels of ATP/ADP/AMP (Corton et al., 1995). Like AMP, AICAR also allosterically inhibits FBP1 in rat hepatocytes and this was the proposed mechanism for the inhibition of gluconeogenesis (Vincent et al., 1991). AICAR has also been shown to inhibit glycolysis in hepatocytes and other cell types although it was concluded that AICAR is a stronger inhibitor of glycolysis than gluconeogenesis (Vincent et al., 1992).

1.4.1.2 A769662

The selective AMPK activator A769662 discovered by Cool et al., (2006) is a thienopyridone that is specific for heterotrimers containing the β 1 subunit (figure 1.7). It

reversibly binds to the “ADaM” (allosteric drug and metabolite) site on AMPK located at the interface between α -KD and carbohydrate-binding module (CBM) of the β subunit, stabilising the α -KD in the active conformation. Like AMP, A769662 is an allosteric activator of AMPK which requires autophosphorylation on Ser108 within the CBM (Sanders et al., 2007; Scott et al., 2008; Xiao et al., 2013; Landgraf et al., 2013; Scott et al., 2014; Calabrese et al., 2014). Goransson et al. (2007) showed that A769662 (100 μ M) and ionomycin (which activates AMPK via increasing intracellular Ca^{2+} and activating CaMKK β) phosphorylated and activated AMPK in HeLa cells which lack LKB1 expression. This was counteracted by the CaMKK β inhibitor STO-609, although phosphorylation of ACC by A769662 remained indicating A769662 activates non-phosphorylated AMPK. Furthermore, Sanders et al. (2007) showed that STO-609 inhibited A769662 (200 μ M) mediated AMPK activation in LKB1 knockout CCL13 cells but not in HEK293 cells expressing LKB1, and A769662 did not directly affect AMPK phosphorylation by LKB1 and CaMKK β in cell-free assays suggesting A769662 acts independently of upstream kinases. A769662 also inhibited Thr172 dephosphorylation on the α subunit by inhibiting protein phosphatase (PP-2C α) (Sanders et al., 2007) and A769662 (1 μ M) protected purified rat liver AMPK incubated with recombinant PP-2C α against P-Thr172 dephosphorylation to a greater extent than with 200 μ M AMP (Goransson et al., 2007).

Cool et al. (2006) showed that A769662 directly stimulated partially purified rat liver AMPK ($EC_{50}=0.8\mu$ M in comparison with AMP $EC_{50}=38\mu$ M) and did not significantly alter the AMP: ATP ratio in primary rat hepatocytes. Additionally, both A769662 (30mg/kg) and metformin (500mg/kg) reduced the respiratory exchange ratio (VCO_2/VO_2) and reduced malonyl-CoA in the liver, indicating increased fatty acid utilisation and reduced fatty acid synthesis. Like metformin (450mg/kg) and AICAR (375mg/kg), A769662 lowered fed plasma glucose and liver triglycerides in chronically treated diabetic ob/ob mice in parallel with reduced ACC activity and a decrease in G6pc, PEPCK and FAS gene expression (Cool et al., 2006). Additionally, in hepatocytes from β 1 knock-out mice the ability of 100 μ M A769662 to stimulate fatty acid oxidation and AMPK/ACC phosphorylation was lost highlighting its preference for β 1 containing isomers (Hawley et al., 2012). Ducommun et al. (2014) showed that AMPK phosphorylation and activation by 1-30 μ M A769662 was synergistic with AICAR, and AICAR-induced phosphorylation of

the AMPK downstream targets ACC and CRTC2 as well as the inhibition of lipogenesis was enhanced in the presence of A769662 in hepatocytes (Foretz et al., 2010). A769662 and AICAR also behaved synergistically in protecting hepatocytes against PP2C α mediated AMPK dephosphorylation (Ducommun et al., 2014), and both AMP and the direct AMPK activator C2 activated AMPK synergistically with A769662 in λ -phosphatase treated AMPK- α 1 complexes (Langendorf et al., 2016) highlighting distinct target sites of AMP/ ZMP and A769662.

1.4.1.3 Compound 991

Like A769662, the cyclic benzimidazole derivative compound 991 (also known as ex229) binds AMPK at the ADaM site (figure 1.7) although with 5-10 times greater potency than A769662, and lower concentrations are needed to activate AMPK and to protect against Thr172 dephosphorylation. Compound 991 also preferentially binds to the AMPK β 1 subunit with 10 times greater affinity than the β 2 isoform (Xiao et al., 2013). In rat skeletal muscle compound 991 increased AMPK activity in α 1, α 2, β 1 and β 2 containing complexes and stimulated glucose uptake without altering intracellular adenine nucleotide levels. Compound 991 also stimulated fatty acid oxidation in L6 myotubes, and the increase in glucose uptake and ACC phosphorylation by compound 991 was abolished in AMPK α 1/ α 2 catalytic subunit double knock out myotubes (Lai et al., 2014). In mouse primary hepatocytes 991 (0.1-30 μ M) stimulated hepatic fatty acid oxidation and inhibited lipogenesis which was not observed in AMPK α 1 α 2 knock out mice (Boudaba et al., 2018). Additionally, co-treatment of compound 991 with either AICAR or the AMPK activator C13 enhanced stimulation of AMPK activity and inhibition of lipogenesis in mouse hepatocytes, and enhanced activation of AMPK γ 1/3 containing complexes and glucose transport in skeletal muscle cells (Bultot et al., 2016).

1.4.1.4 Compound-13

The prodrug compound-13 (C13) (figure 1.7) is converted by intracellular esterases to its active form C2 which behaves as an AMP analogue directly activating AMPK (Hardie et al., 2014) in the absence of altered adenine nucleotide levels (Hunter et al., 2014). C2 is selective for α 1 containing isoforms and activates human AMPK (EC_{50} =6.3nM in comparison with AMP EC_{50} =5.9 μ M) similarly to rat AMPK (EC_{50} =21nM) (Gomez-Galeno et al., 2010) as well as recombinant human AMPK complexes (EC_{50} =10-30nM) in

comparison with AMP ($EC_{50}=2-4\mu\text{M}$)), and sensitivity of AMPK to C2 is lost in the γ 2-R531G AMP insensitive mutant (Hunter et al., 2014). Two C2 molecules bind at the interface of the CBS binding sites 1,3 and 4 with the phosphate groups overlapping the phosphate binding sites of AMP at sites 1 and 4 (γ -pSite-1 and γ -pSite-4) (Langendorf et al., 2016). Like AMP, C2 protects against Thr172 dephosphorylation although it has no effect on AMP-regulated enzymes such as glycogen phosphorylase, PFK1 or FBP1 at up to $100\mu\text{M}$ suggesting it is a selective AMPK activator (Hunter et al., 2014). Gomez-Galeno et al., (2010) showed that administration of 30mg/kg of the prodrug compound-13 in rat reached plasma concentrations of $200-300\mu\text{M}$ and inhibited de novo lipogenesis, Boudaba et al., (2018) demonstrated that $1-30\mu\text{M}$ of compound-13 stimulated hepatic fatty acid oxidation and inhibited lipogenesis in mouse primary hepatocytes.

1.5 Glucose regulated gene expression is mediated by the transcription factor ChREBP-Mlx

T2D is associated with increased expression of enzymes involved in gluconeogenesis and lipogenesis in the liver (Brown & Goldstein., 2008). Because insulin inhibits gluconeogenesis but stimulates lipogenesis, one hypothesis that has been proposed by Brown & Goldstein (2008) to explain the simultaneous elevation of both pathways in T2D is of selective insulin resistance of the gluconeogenic pathway but not the lipogenic pathway. This hypothesis assumes that the changes in gene expression in liver in T2D are explained exclusively by defects in insulin signalling. An alternative explanation is that T2D represents a condition of either relative glucose excess or relative elevation of intracellular glucose 6-phosphate (G6P) and downstream intermediates of metabolism (Agius., 2014).

The transcription factor carbohydrate response element binding protein (ChREBP) mediates the changes in gene expression in response to raised intracellular concentrations of phosphate ester metabolites of glucose and is found at high levels in liver and adipose tissue. ChREBP belongs to the Mondo family of transcription factors. It comprises of a basic helix-loop-helix-leucine zipper (bHLHLZ) which upon activation heterodimerizes with Max-like protein X (Mlx) (a member of the Myc/Max family of bHLHLZ transcription factors) (Stoekman et al., 2004; Havula & Hietakangas., 2012;

Filhoulaud et al., 2013). Under fasting blood glucose levels ChREBP is sequestered in the cytosol by cAMP dependent protein kinase (PKA) phosphorylation of serine 196 on the N-terminus. An elevation in blood glucose results in increased cellular levels of phosphorylated intermediates of glycolysis, for example G6P (formed in the first step of glycolysis), xylulose 5-phosphate (Xu-5P) and fructose-2,6-bisphosphate (F-2,6-P₂) which promotes ChREBP activation and nuclear entry allowing heterodimerization with Mlx (Kabashima et al., 2003; Li et al., 2010; Dentin et al., 2012; Arden et al., 2012). The ChREBP-Mlx complex can then bind to specific regulatory sites in the promotor regions of glucose regulated genes named carbohydrate response elements (ChoRE), inducing genes encoding enzymes of glycolysis, lipogenesis and gluconeogenesis (Shih et al., 1994; Koo et al., 2000; Yamashita et al., 2001). The ChoRE sequence consists of a tandem E-box element separated by five nucleotides (5'-CACGTGnnnnnCACGTC) (Shih et al., 1994). The loop region of the Mlx bHLHLZ domain mediates the interaction of two heterodimers which each binds an E box, stabilising the ChREBP-Mlx-ChoRE interaction (Billin et al., 1999; Meroni et al., 2000).

ChREBP-Mlx is a key transcription factor that mediates the effects of high glucose on hepatic gene expression (Ma et al., 2006). Targets of ChREBP-Mlx include enzymes of glycolysis and the pentose phosphate pathway (e.g. pyruvate kinase (Pklr) and glucose 6-phosphate dehydrogenase (G6PD)), fatty acid synthesis (e.g. acetyl-coA carboxylase (ACC)), triglyceride formation (e.g. glycerol 3-phosphate dehydrogenase (GPDH)), lipid metabolism (e.g. fatty acid synthase (FAS)) and gluconeogenesis (e.g. glucose 6-phosphatase (G6pc)) (Wang et al., 2002; Ishii et al., 2004; Ma et al., 2005; Ma et al., 2006; Wang et al., 2006; Iizuka et al., 2009; Havula & Hietakangas., 2012).

Initially, Kabashima et al., (2003) proposed that the pentose phosphate pathway intermediate Xu-5P activated protein phosphatase 2A (PP2A) promoting dephosphorylation of ChREBP and its subsequent activation. However, Tsatsos et al. (2006) and Davies et al. (2008) showed that high glucose could activate ChREBP independently of PP2A activation suggesting other mechanisms are involved in its regulation. The phosphorylated intermediate G6P is formed by glucokinase (GK) mediated phosphorylation of glucose as well as by gluconeogenesis and glycogenolysis. G6P has been implicated as a regulator of ChREBP as the glucose analogue 2-

deoxyglucose (which like glucose is phosphorylated by GK to 2-deoxyglucose 6-phosphate but is not metabolised further) stimulated ChREBP activation in proliferating cell lines (Li et al., 2010), and stimulates Gal4-ChREBP activity in HepG2 cells (Dentin et al., 2012). A key consideration is that the effect of 2-deoxyglucose on induction of ChREBP target genes is not observed in hepatocytes (Towle et al., 1997; Arden et al., 2012; Al-Oanzi et al., 2017) but only in proliferating cell lines. Although this does not rule out a role for G6P, it clearly suggests that metabolites other than G6P that are elevated by glucose but not by 2-deoxyglucose are essential. One such metabolite is F-2,6-P₂ an allosteric activator of PFK1 and inhibitor of FBP1 (Van Schanftingen., 1993). Arden et al. (2012) showed that depletion of F-2,6-P₂ in hepatocytes by expressing a kinase deficient variant of the bifunctional protein PFK2/FBP2 (PFK2-KD) increased cell G6P and prevented glucose induced ChREBP translocation and binding to the G6pc promoter and its transcription. Additionally, overexpression of the wild type PFK2/FBP2 variant enhanced ChREBP mediated G6pc transcription. This implicates F-2,6-P₂ as an essential regulator of glucose regulated ChREBP mediated gene expression, although the mechanism remains unknown. This does not exclude the involvement of additional metabolites such as G6P.

ChREBP also regulates transcription of thioredoxin interacting protein (TXNIP) which is induced by high glucose concentrations and is implicated in the regulation of glucose transport in several cell types that express GLUT1 and GLUT4 transporters. Shaked et al. (2011) and Li et al. (2015) showed that metformin repressed TXNIP transcription in pancreatic β -cells and also in endothelial cells, and that metformin inhibited the nuclear accumulation of ChREBP and its negative regulator forkhead box O1 (FOXO1) as well as its binding to the TXNIP promoter with high glucose that cannot be explained fully by AMPK activation (Li et al., 2015). Sato et al. (2016) proposed that AMP allosterically inhibits the nuclear localisation of ChREBP by stimulating its interaction with 14-3-3 proteins that regulate nuclear/cytosol trafficking of ChREBP in rat liver. Therefore, the increase in AMP/ATP ratio with metformin may explain the inhibition of ChREBP nuclear localisation. Like F-2,6-P₂, AMP is also an allosteric inhibitor of FBP1 and an increase in AMP by metformin inhibits gluconeogenesis both directly and also indirectly by changes in gene expression (Rena et al., 2013).

1.6 Metformin lowers cell G6P in hepatocytes

Several studies have reported that metformin lowers G6P in hepatocytes (Owen et al., 2000; Fulgencio et al., 2001). Owen et al., (2000) showed that metformin (2mM) inhibited gluconeogenesis in rat hepatocytes and also lowered cell G6P and F6P by approximately 50%. Additionally, rats administered with 150-200mg/kg or 450-600mg/kg metformin lowered hepatic G6P content by 60% and 61% respectively. This was accompanied by a drop in the ATP/ADP ratio (by >70%) (Owen et al., 2000). Fulgencio et al., (2001) showed that metformin (5mM) lowered G6P by ~50% in hepatocytes and lowered cell ATP by 70%. Guigas et al. (2006) also observed that metformin (5mM) lowered G6P by 20% and lowered ATP by approximately 40%. These studies on isolated hepatocytes or freeze clamped liver determined several metabolites of glycolysis. They showed lowering of F6P and elevation of triose phosphates. In the study on freeze-clamped liver, cell fructose 1,6-bisphosphate (F1,6P₂) was not decreased by metformin (Owen et al., 2000). Therefore, a tentative hypothesis is that metformin lowers G6P and F6P (which are assumed to be in near equilibrium because of the high activity of phosphoglucose isomerase (PGI) (Zalitis & Oliver., 1967)), but not more distal metabolites of glycolysis.

1.6.1 Potential mechanisms for the lowering of G6P by metformin

The metabolite G6P lies in the intersection of a number of metabolic pathways meaning there are a number of possible target sites that may be implicated in the lowering of G6P by metformin in hepatocytes (figure 1.8). In the GK reaction, G6P is formed by the ATP dependent phosphorylation of glucose at carbon 6. Under basal glucose conditions GK is bound and sequestered by its inhibitory protein glucokinase regulatory protein (GKRP) in the nucleus of hepatocytes. In response to elevated glucose concentrations GKRP dissociated from GK allowing GK translocation (GKT) from the nucleus to the cytoplasm and subsequent glucose phosphorylation. One possible explanation for the lowering of G6P by metformin is inhibition of glucose induced GKT and glucose phosphorylation which has been observed at high metformin concentrations in conditions of ATP depletion (Guigas et al., 2006) and maintained ATP (Mukhtar et al., 2008).

In the final step of glucose production from gluconeogenesis and glycogenolysis, G6P is hydrolysed by the membrane bound enzyme glucose 6-phosphatase (G6pc) in the endoplasmic reticulum (ER) after transport of G6P into the ER by the SLC37 family of ER associated sugar-phosphate/ phosphate (Pi) exchangers consisting of 4 members (SLC37A1-4). SLC37A4 (also known as the glucose 6-phosphate transporter or G6PT) is a Pi-linked G6P antiporter that is associated with G6pc (figure 1.9). (Chen et al., 2008; Pan et al., 2011). Both SLC37A1/ A2 also exhibit Pi-linked G6P antiporter activity however unlike SLC37A4 they are not coupled with G6pc and are expressed at low levels in the liver suggesting they are not involved in the control of blood glucose homeostasis (Pan et al., 2011). Therefore, metformin could lower cell G6P by activating G6PT (Van de Werve et al., 2000) or G6pc as occurs during overexpression of G6pc in hepatocytes (Seoane et al., 1997; Aiston et al., 1999). Functionally it is possible to distinguish between SLC37A4 and the other transporters (SLC37A1-3) by using chlorogenic acid derivatives which selectively inhibit SLC37A4 (Arion et al., 1997; Herling et al., 1998; Harndahl et al., 2006) but not SLC37A1-3 (Pan et al., 2011).

G6P is also metabolised by glycolysis to pyruvate and lactate. Stimulation of glycolysis by metformin at a number of potential target sites could in principle deplete cell G6P. One possibility is stimulation of phosphofruktokinase-1 (PFK1) at the first regulated site of glycolysis. Alternatively, inhibition of gluconeogenesis by metformin by inhibition of fructose 1,6-bisphosphatase-1 (FBP1) would explain the decrease in G6P (figure 1.8).

Another potential site for lowering G6P is the pentose phosphate pathway. In the cytoplasm glucose 6-phosphate dehydrogenase (G6PD) catalyses the metabolism of G6P to 6-phosphogluconolactone generating NADPH from NADP in the rate limiting step of the pentose phosphate pathway (Stincone et al., 2015). In the ER, hexose 6-phosphate dehydrogenase (H6PD) catalyses the first two reactions of the pentose phosphate pathway, essentially the NADP dependent conversion of G6P to phosphogluconate, thereby providing NADPH for luminal reductases (Senesi et al., 2010). In addition, the ER mechanism may involve transport of F6P into the ER by a mechanism that is insensitive to chlorogenic acid derivatives (Senesi et al., 2010). Metformin may target either G6PD in the cytoplasm or H6PD in the ER, lowering G6P (figure 1.8).

G6P is an allosteric activator of glycogen synthase and it promotes its dephosphorylation by stabilising a conformation that is a better substrate for synthase phosphatase (Villar-Palasi & Guinovart., 1997; Pederson et al., 2000). Likewise, glycogen phosphorylase also has a binding site (Johnson et al., 1993) and raised G6P in hepatocytes promotes net dephosphorylation of phosphorylase (Agius., 2015). This in turn leads to activation of glycogen synthase because the phosphorylated form of phosphorylase is a potent allosteric inhibitor of glycogen synthase phosphatase through the glycogen targeting protein encoded by PPP1R3B (Hampson & Agius 2005; Aiston et al., 2003). Therefore, one possibility is that metformin lowers G6P by either stimulating glycogen synthesis or inhibiting glycogen degradation. G6P is also a substrate for glutamine: fructose-6-phosphate amidotransferase (GFAT) in the hexosamine biosynthesis pathway, a possible target for metformin stimulation and G6P depletion (Robinson et al., 1995) (figure1.8).

1.7 Current status of hypotheses on the metformin mechanism

There remains a long-standing debate on which of the proposed mechanisms of metformin described above can account for the metformin mechanism including: (i) inhibition of Complex 1; (ii) activation of AMPK either by mechanisms downstream of Complex 1 or by other mechanisms which manifest at lower drug concentration; (iii) AMPK independent mechanisms linked to ATP depletion; (iv) inhibition of glucagon signalling by raised AMP; (v) inhibition of cAMP signalling or (vi) mGPD inhibition.

Three factors can be considered for this lack of consensus on the mechanism:

1. Experimental versus therapeutic doses of metformin: One view is that many of the cellular studies on the metformin mechanism have used concentrations that are far higher than the therapeutic range. It is thought that at therapeutic doses of the drug, metformin may have several effects that are individually small but collectively effective at lowering blood glucose. The latter assumes that inhibition of complex 1, ATP depletion and possibly also activation of AMPK may not be major components of the metformin mechanism at therapeutic doses of the drug (Wilcock and Bailey., 1994; He & Wondisford., 2015).
2. Chronic versus acute effects: Another consideration is that metformin may be more effective during chronic therapy and may be relatively ineffective after a

single exposure at therapeutic doses in T2D in man (Sum et al., 1992). Indeed, most of the clinical evidence for inhibition of glucose production by metformin is based on chronic rather than acute studies (Stumvol et al., 1995; Hundal et al., 2000; Petersen et al., 2017). Although there are relatively few acute studies, there is evidence that there are no significant short-term effects observed in man on either glucose production or peripheral glucose disposal during an intravenous metformin infusion (Sum et al 1991).

3. Compromised versus non-compromised metabolic homeostasis: Another important consideration is that the effect of metformin on blood glucose is dependent on the physio-pathological state. Accordingly, in animal models, metformin (300 mg/kg) is much more effective at lowering blood glucose in a model of obesity and T2D than in the non-diabetic state (Lloyd et al., 2013). This contrasts with the effect of other classes of drugs such as sulphonylureas or direct activators of glucokinase, which are similarly effective.

Previous work has focused on the role of AMPK in the metformin effect on gluconeogenic gene expression observed in isolated hepatocytes (as discussed above). One of the key target genes repressed by metformin in the db/db mouse is G6pc (Heishi et al., 2006) which is regulated by AMPK mediated signalling (Lee et al., 2010; Cao et al., 2014) and also by ChREBP in response to raised levels of glucose metabolites in hepatocytes (e.g. F-2,6-P₂ and G6P) (Arden et al., 2011; Arden et al., 2012). G6pc is one of a number of genes induced by high glucose (Al-Oanzi et al., 2017). Previous work has shown that high glucose (25mM) elevates cell G6P and downstream phosphorylated intermediates in hepatocytes, stimulating the expression of ChREBP target genes including G6pc and Pklr (Al-Oanzi et al., 2017). Work leading up to this project showed that:

- Metformin (1mM) counteracted the effect of high glucose on the recruitment of ChREBP-Mlx to the G6pc and Pklr promoters and on the induction of these genes but did not affect gene expression at basal glucose (Al-Oanzi et al., 2017).
- Additionally, metformin lowered F-2,6-P₂ (Al-Oanzi et al., 2017) which regulates ChREBP translocation (Arden et al., 2012; Arden et al., 2011).

- Furthermore, a higher metformin concentration (5mM) lowered cell ATP and inhibited GK translocation (Guigas et al., 2006). Whether this effect of metformin occurs at concentrations where ATP is maintained has not been explored.

G6P, the first intermediate of glucose metabolism, is also generated from glycogen breakdown and gluconeogenesis, and is metabolised by several pathways (figure 1.8). Changes in G6P could therefore arise as a result of altered activity of several enzymes, and the effects of metformin on lowering G6P could be a consequence of metformin targeting multiple possible sites. Accordingly, G6P can be used as a marker to investigate the effects of metformin on these candidate pathways.

HYPOTHESIS:

The aims of this study were to test the hypothesis that the counter-regulatory effect of metformin on gene regulation at high glucose is due to inhibition of GK translocation and glucose phosphorylation, and thereby due to lowering of cell G6P and downstream metabolites. To investigate this, a number of research questions need to be considered:

- First, does metformin counteract the effect of high glucose on elevated G6P at cellular metformin levels that are within the therapeutic range for this drug?
- Does this effect of metformin occur in conditions of maintained or compromised ATP?
- Is the metformin effect mediated by activation of AMPK?
- Is the effect of metformin on cell metabolites in conditions of elevated glucose fully accounted for by inhibition of GK translocation or does it involve effects of metformin on other metabolic pathways?
- Does the lowering of G6P by metformin account for its counter-regulatory effect on gene regulation?

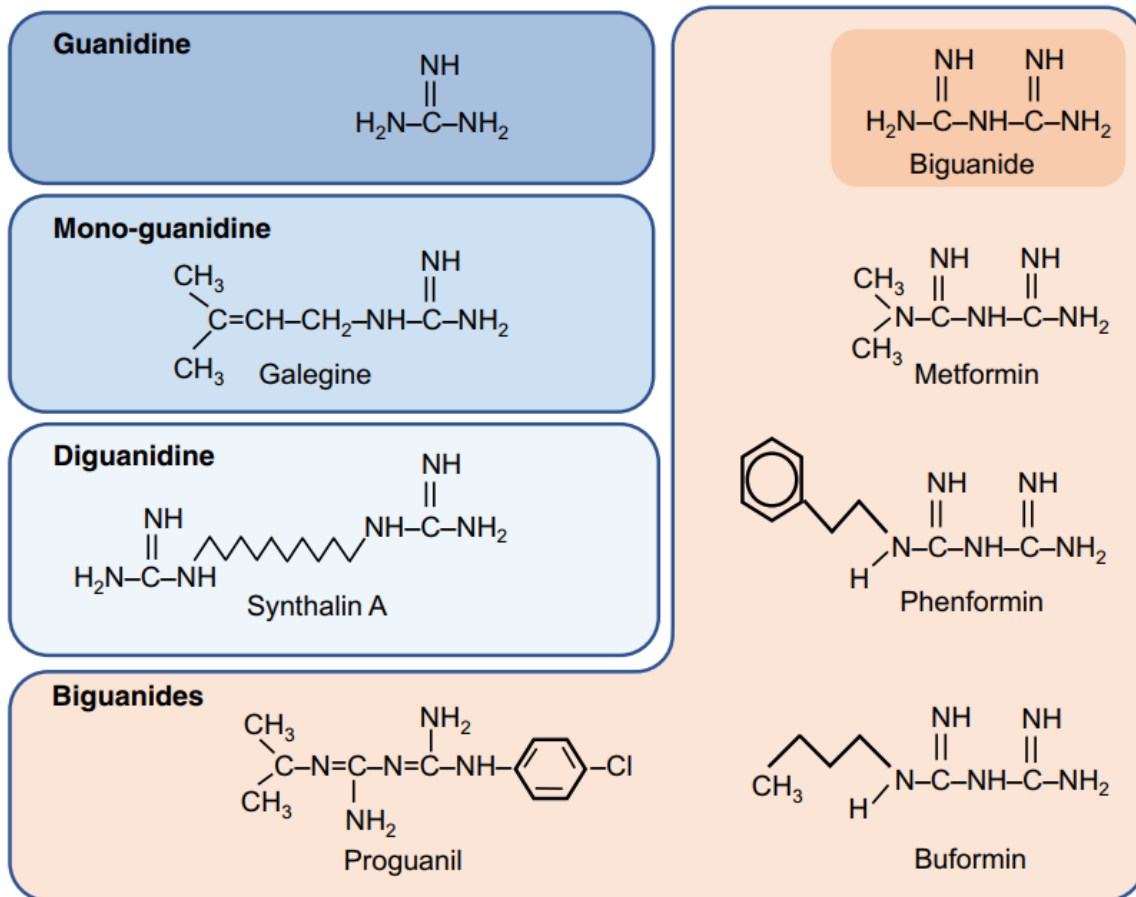


Figure 1.1 Chemical structure of metformin and the biguanide family of insulin-sensitising drugs (Bailey., 2017)

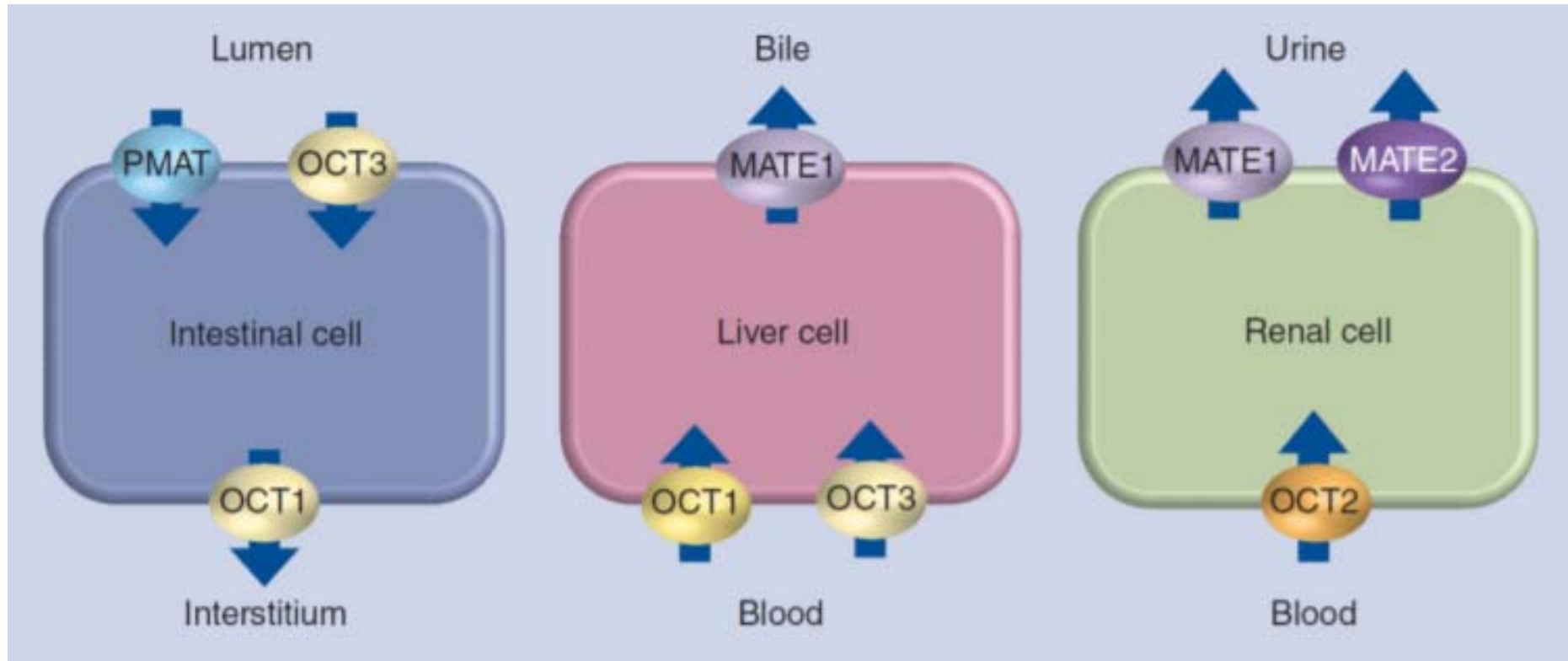


Figure 1.2 Transporters involved in metformin uptake and excretion (Florez et al., 2017)

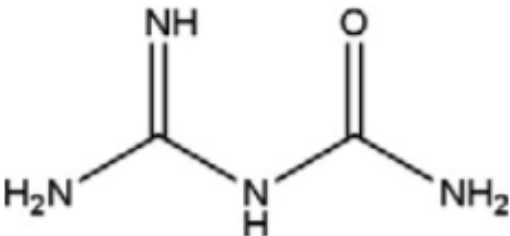
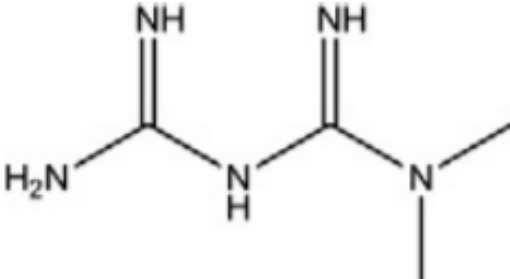
Compound	Molecular structure
Guanyurea	 <p>The chemical structure of Guanyurea is shown. It consists of a central nitrogen atom bonded to two hydrogen atoms and two carbonyl groups. Each carbonyl group is further bonded to an amino group (NH₂).</p>
Metformin	 <p>The chemical structure of Metformin is shown. It consists of a central nitrogen atom bonded to two hydrogen atoms and two carbonyl groups. Each carbonyl group is further bonded to an amino group (NH₂) and a methyl group (CH₃).</p>

Figure 1.3 Chemical structure of metformin and its metabolic product, guanyurea (Trautwein et al., 2014)

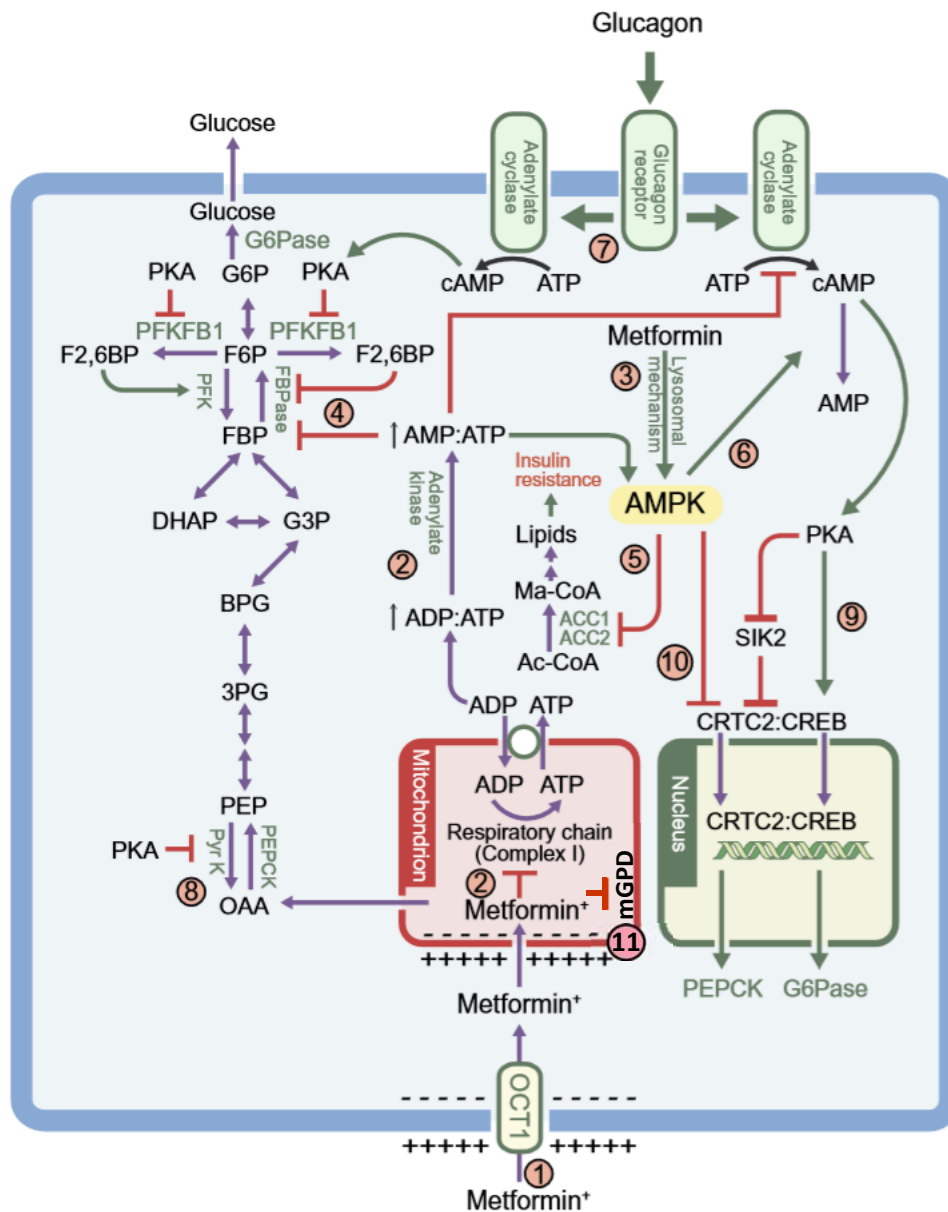


Figure 1.4 Proposed mechanisms by which metformin inhibits hepatic gluconeogenesis

(1) Metformin is taken up into hepatocytes by OCT1 (2) and accumulates in the mitochondria where it inhibits complex 1. This results in an increased AMP:ATP ratio which activates AMPK. (3) Alternatively, metformin may activate AMPK by a lysosomal pathway. (4) An increase in AMP also inhibits fructose-1,6-bisphosphatase (FBPase) inhibiting gluconeogenesis, and inhibits glucagon signalling by inhibition of cAMP production. (5) Activated AMPK phosphorylates ACC, promoting fatty acid oxidation. (6) AMPK activation also phosphorylates and activates phosphodiesterase 4B (PDE4B), lowering cAMP production. (7) Glucagon signalling stimulates cAMP production and activates protein kinase A (PKA), phosphorylating and inactivating PFKFB1, lowering fructose-2,6-bisphosphate which is an allosteric activator of phosphofruktokinase (PFK1)

and inhibitor of FBPase, stimulating gluconeogenesis. (8) PKA also phosphorylates and inactivates pyruvate kinase (Pyr K) in glycolysis and (9) stimulates gluconeogenic gene expression. (10) AMPK activation counteracts the effect of PKA on phosphoenolpyruvate carboxykinase (PEPCK) and glucose 6-phosphatase (G6Pase) expression, inhibiting gluconeogenic gene expression. (11) Metformin is also proposed to inhibit mitochondrial glycerophosphate dehydrogenase (mGPD) (adapted from Rena et al., 2017).

Ac-CoA, acetyl coenzyme A; BPG, 1,3-bisphosphoglycerate; DHAP, dihydroxyacetone phosphate; FBP, fructose 1,6-bisphosphate; F6P, fructose 6-phosphate; G3P, glyceraldehyde 3-phosphate; G6P, glucose 6-phosphate; Ma-CoA, malonyl coenzyme A; OAA, oxaloacetate; PEP, phosphoenolpyruvate; 3PG, 3-phosphoglycerate.

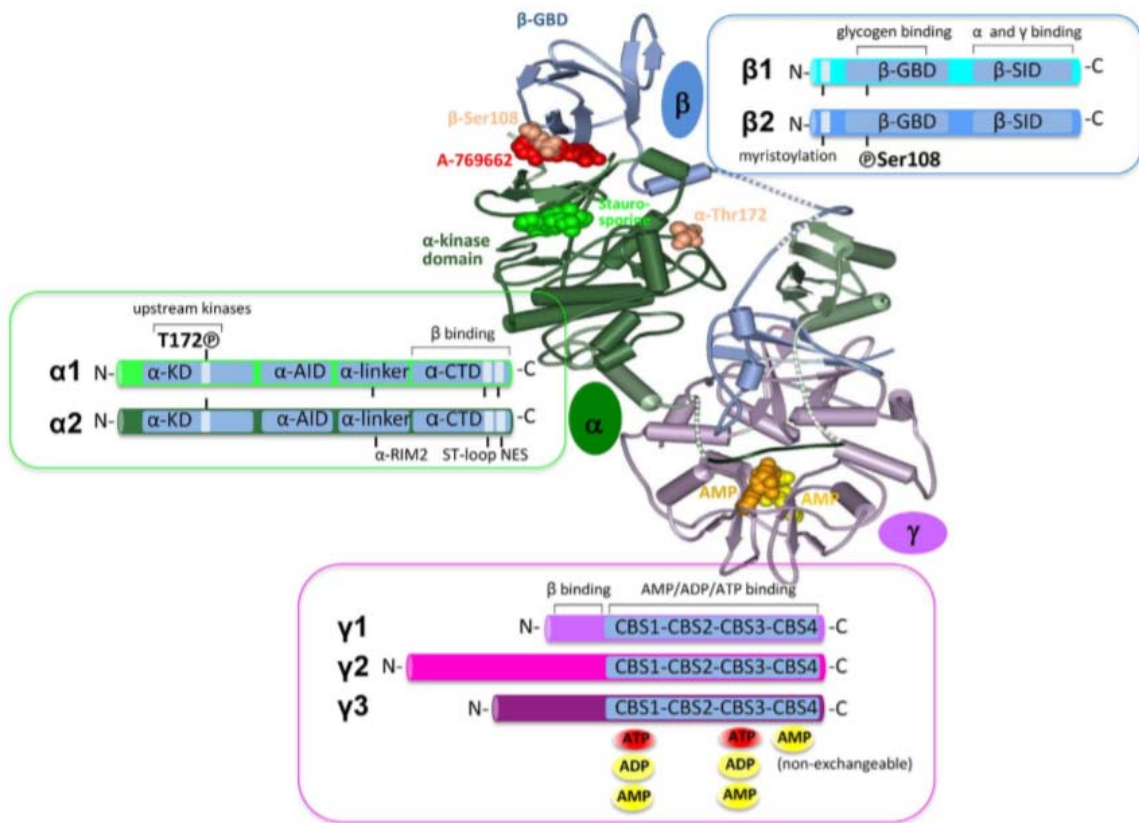


Figure 1.5 Crystal structure of AMPK consisting of α , β and γ subunits

AMPK is phosphorylated at α -Thr172 and β -Ser108. AMP binds at the CBS (cystathionine- β -synthase) sites in the γ subunit. A769662 binds at the interface between the α -kinase domain and β -glycogen binding domain (GBD) (Olivier et al., 2018).

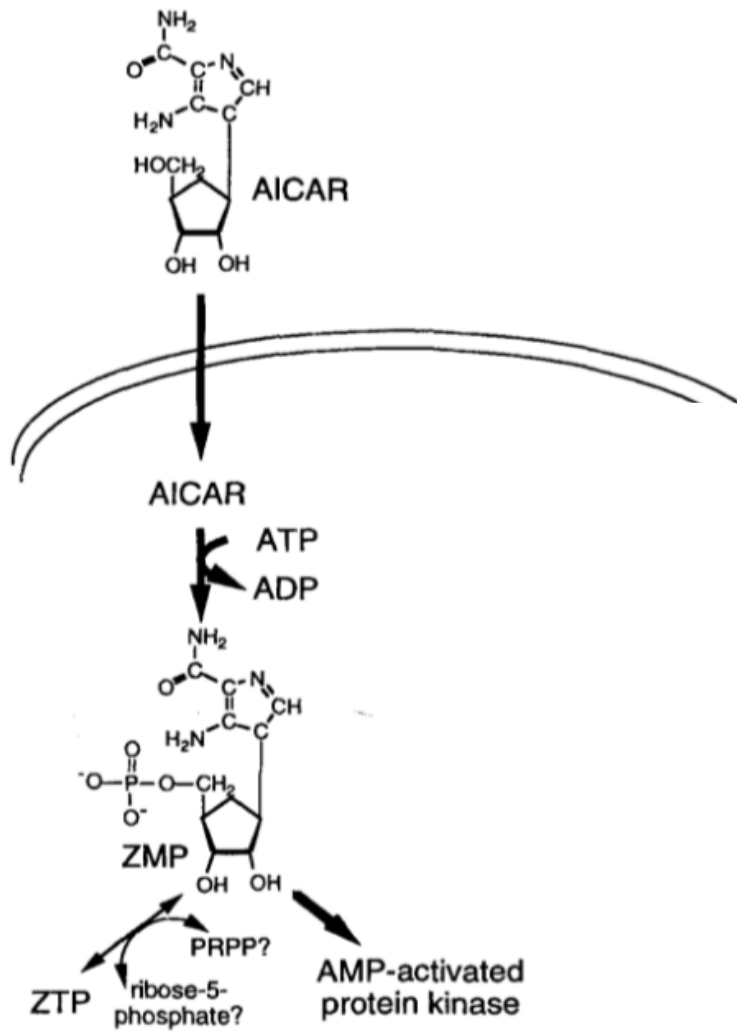


Figure 1.6 AICAR is transported across the plasma membrane and phosphorylated into ZMP in the cytoplasm (Corton et al., 1995)

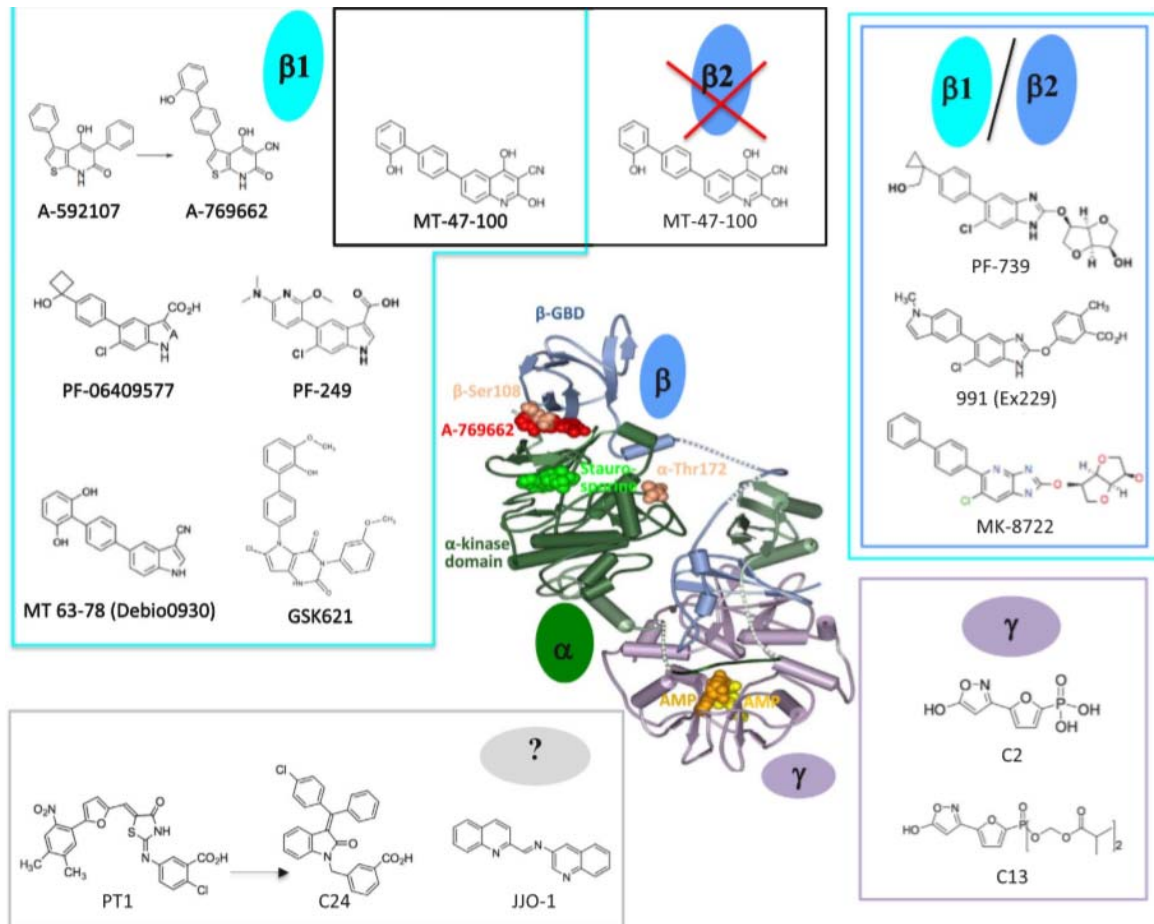


Figure 1.7 Structures of direct small molecule AMPK activators and inhibitors

Small molecule AMPK activators and inhibitors bind to the ADaM site selective for the β 1- isoform (turquoise frame), or both β 1 and β 2 containing isoforms (turquoise/ blue frame), bind to the γ isoform (purple frame) or with unknown interaction (grey frame) (Olivier et al., 2018).

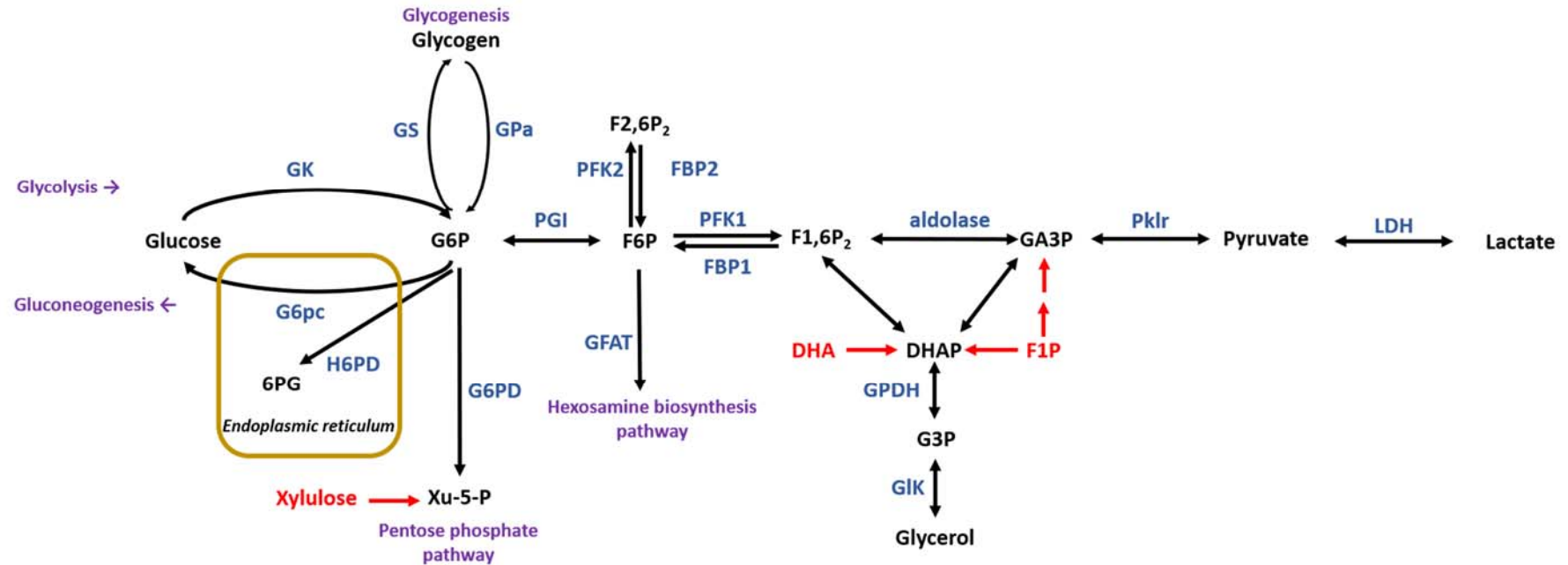


Figure 1.8 G6P formation and metabolism

G6P is generated by glucokinase (GK), glycogen degradation by glycogen phosphorylase (GPa) and in gluconeogenesis. G6P is metabolised by glycolysis, glycogen synthesis by glycogen synthase (GS), glucose 6-phosphate dehydrogenase (G6PD) in the pentose phosphate pathway, and by glucose 6-phosphatase (G6pc) and hexose 6-phosphate dehydrogenase (H6PD) in the endoplasmic reticulum (yellow).

6-PG, 6-phosphogluconate; DHA, dihydroxyacetone; DHAP, dihydroxyacetone phosphate; F16P₂, fructose 1,6-bisphosphate; F1P, fructose 1-phosphate; F26P₂, fructose 2,6-bisphosphate; F6P, fructose 6-phosphate; FBP1, fructose 1,6-bisphosphatase; FBP2, fructose 2,6-bisphosphatase; G3P, glycerol-3-phosphate; G6P, glucose 6-phosphate; G6pc, glucose 6-phosphatase; G6PD, glucose 6-phosphate dehydrogenase; GA3P, glyceraldehyde 3-phosphate; GFAT, glutamine: fructose 6-P amidotransferase; GK, glucokinase; GIK, glycerol kinase; GPa, glycogen phosphorylase; GPDH, glycerol-3-phosphate dehydrogenase; GS, glycogen synthase; H6PD, hexose 6-phosphate dehydrogenase; LDH, lactate dehydrogenase; PFK1, phosphofructokinase 1; PFK2, phosphofructokinase 2; PGI, phosphoglucose isomerase; Pklr, pyruvate kinase; Xu-5P, xylulose-5-phosphate.

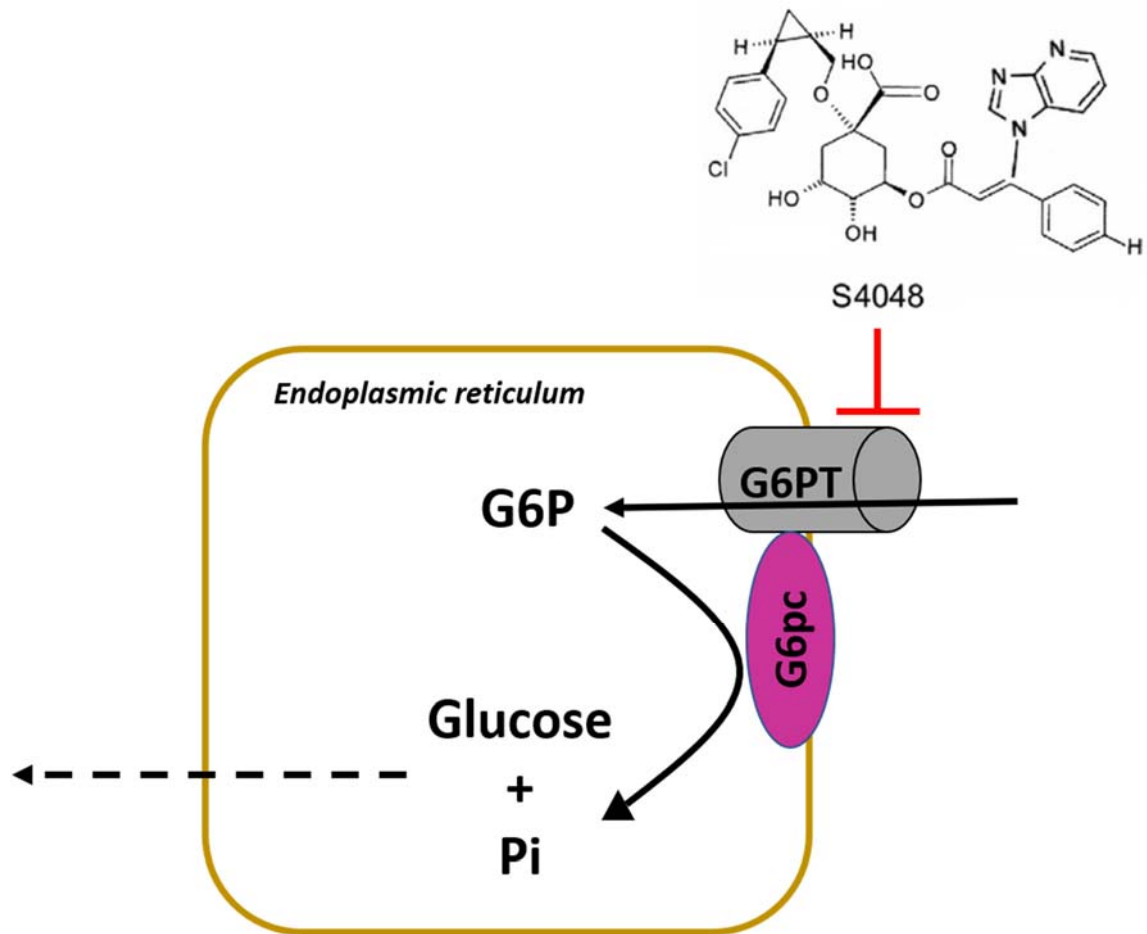


Figure 1.9 The chlorogenic acid derivative **S4048** is an inhibitor of the glucose 6-phosphate transporter (**G6PT**)

In the ER, G6P transport is coupled to G6P metabolism by glucose 6-phosphatase (**G6pc**).

Chapter 2: Materials and Methods

2.1 Materials

2.1.1 Animals

Male Wistar rats (body weight 200-300g) were obtained from Envigo (Bicester, UK).

Male C57BL/6J mice aged 8-10 weeks were obtained from Charles River (UK).

Male C57BL/6J-OlaHsd mice aged 8-10 weeks were obtained from Envigo (Bicester, UK).

Hexose 6-phosphate dehydrogenase knockout mice were obtained from Professor G. Lavery, University of Birmingham, UK (Lavery et al., 2006).

2.1.2 Chemicals and Reagents

General chemicals and solvents were obtained from BDH, VWR, Sigma or Santa Cruz.

Other reagents are indicated in Table 2-1.

Chemical	Supplier	Catalogue Number
Ammonium Chloride	BDH	10017
Ammonium Molybdate	Fisher Scientific	A7302
Aminooxyacetic Acid	Sigma	A4508
Aurintricarboxylic Acid (ATA)	Sigma	A1895
Adenosine triphosphate (ATP)	Sigma	A3377
A769662	Tocris	3336
Benzamidine	Sigma	B6506
Berberine	Sigma	B3412
Protein Assay Dye Reagent Concentrate	Bio-Rad	5000006
Bovine Serum Albumin	Sigma	A2153
Calyculin A	Sigma	C5552
CB72	ChemBridge	6049458
5-Chloro-N-[(1S,2R)-3-(dimethylamino)-2-hydroxy-3-oxo-1-(phenylmethyl)propyl]-1H-indole-2-carboxamide	Gift from Pfizer Global Research and Development (Groton/New London	

CP-91149	Laboratories, Groton, CT)	
Dihydroxyacetone (DHA)	Sigma	PHR1430
Dehydroepiandrosterone (DHEA)	US Biological	78590177
2-Deoxy-D-glucose	Sigma	D6134
6-Diazo-5-oxo-L-norleucine (DON)	Sigma	D2141
Dithiothreitol (DTT)	Sigma	D5545
Emodin	Sigma	E7881
Folin-Ciocalteu's Phenol Reagent	Sigma	F9252
Fructose	Sigma	F0127
Glucokinase Activator (GKA)	Axon MedChem	RO281675
Glucosamine	Sigma	G4875
Glucose	BDH	28450
Glucose 6-phosphate	Sigma	G7879
Glycerol 3-phosphate	Sigma	G7886
L-Lactic Acid Sodium Salt	Sigma	L7022
Malachite Green	Sigma	229105
Mannoheptulose	Brunschwig Chemicals	M4375
Menadione	Sigma	M5625
Metformin	Sigma	D5035
Metyrapone	Sigma	856525
Miconazole	Sigma	M1880000
NAD ⁺	Calbiochem	481911
NADH	Calbiochem	481913
NADP	Sigma	N0505
Perchloric Acid	Sigma	244252
Phosphate Standard	Sigma	20-103
Protease Inhibitor Cocktail	Sigma	P8340

Phenazine Methosulfate	Sigma	P9625
Phenylmethanesufonyl Fluoride (PMSF)	Sigma	P7626
Sodium Pyruvate	Sigma	P2256
Random Primers	Roche	11034731001
Resazurin Sodium Salt	Sigma	R7017
Rhein	Sigma	275611
Rotenone	Sigma	R8875
S4048 (1-[2-(4-chloro-phenyl)-cyclopropylmethoxy]-3, 4-dihydroxy-5-(3-imidazo[4,5-b]pyridin-1-yl-3-phenylacryloyloxy)-cyclohexanecarboxylic acid)	Gift from Dr. D. Schmoll, Aventis, Pharma GnbH, Frankfurt, Germany	
Sodium Borohydride	Sigma	S9125
5-Sulfosalicylic Acid	Sigma	S2130
LightCycler Faststart DNA Master SYBR	Roche	3003230
TRIS	VWR	0826
TRIzol	ThermoFisher Scientific	15596018
UK5099	Tocris	4186
Xylitol	Sigma	X3375
S4048	Gift from Dr. D. Schmoll, Aventis, Pharma GnbH, Frankfurt, Germany	
[1- ¹⁴ C] glucose	ARC	ARC0120A
[1- ¹⁴ C] glucose	Hartmann Analytic	MC228
[2- ³ H] glucose	Perkin Elmer	NET238C005MC
[3- ³ H] glucose	Perkin Elmer	NET331A250UC
[5- ³ H] glucose	Perkin Elmer	NET531005MC
[6- ¹⁴ C] glucose	ARC	ARC0121B

[U- ¹⁴ C] Glucose	Perkin Elmer	NEC042B005MC
[¹⁴ C] Metformin	Hartmann Analytic	MC2043
2,4-Dinitrophenol (DNP)	Sigma	81F5051
5-Chloro-2-[N-(2,5-dichlorobenzenesulfonamido)]-benzoxazole	Calbiochem	344267

Table 2-1 Chemicals and Reagents**2.1.3 Enzymes**

Commercial enzymes are indicated in Table 2-2.

Enzyme	Supplier	Catalogue Number
Amyloglucosidase (from <i>Aspergillus niger</i>)	Sigma	A7420
Diaphorase (from <i>Clostridium kluyveri</i>)	Sigma	D2197
DNase I (RNase free)	Roche	04716728001
Glucose 6-phosphate dehydrogenase (from Yeast)	Roche	10127655001
Glycerol 3-phosphate dehydrogenase (from Rabbit muscle)	Roche	10127752001
Hexokinase (from Yeast)	Roche	11426362001
L-lactate dehydrogenase (from Rabbit muscle)	Roche	10127884001
Luciferin-luciferase	Sigma	FLAA
M-MLV reverse transcriptase	Promega	M1701
Phosphoglucose isomerase (from Yeast)	Roche	10128139001

6-phosphogluconic dehydrogenase (from Yeast)	Sigma	P4553
--	-------	-------

Table 2-2 Enzymes

2.1.4 Antibodies

Commercial antibodies are indicated in Table 2-3.

Antibodies	Host	Supplier	Catalogue Number
Acetyl-CoA Carboxylase	Rabbit	Cell Signaling Technology	3662
Alexa fluor 488 Goat anti-Rabbit IgG	Goat	ThermoFisher Scientific	A11008
AMPK α	Rabbit	Cell Signaling Technology	2603
G6PD2	Rabbit	Proteintech	172191AP
GAPDH	Mouse	HyTest	5G4
GK H-88	Rabbit	Santa Cruz Biotechnology, Inc.	Sc7908
Glucokinase (GK)	Rabbit	AstraZeneca	
Glucokinase Regulatory protein (GKRP)	Rabbit	AstraZeneca	
Mouse Immunoglobulins (HRP-conjugated)	Rabbit	Dako	P0260
Phospho-Acetyl-CoA Carboxylase (Ser79-P)	Rabbit	Cell Signaling Technology	3661
Phospho-AMPK α (Thr172-P)	Rabbit	Cell Signaling Technology	2535

Rabbit Immunoglobulins (HRP-conjugated)	Goat	Dako	P0448
---	------	------	-------

Table 2-3 Antibodies**2.1.5 Adenoviral vectors**

Adenoviral vectors are indicated in Table 2.4.

Adenoviral Vector	Source	Catalogue Number/ Reference
Ad-CMV-GKL	Gift from Dr. C. Newgard (Duke University, Durham, NC)	Becker et al., 1996
Ad-CMV-GKRP	Rat liver GKRP cDNA	De la Iglesia et al., 2000
Ad-GFP-U6-m-G6PDX- shRNA	VectorBioLabs, Malvern PA, USA	shADV-279685
PFK-KD	Gifts from A. Lange	Arden et al., 2012

Table 2-4 Adenoviral Vectors**2.1.6 Primers for Real time RT-qPCR**

Primers for PCR are indicated in Table 2.5.

Gene	Primers
Glucokinase (<i>GK</i>)	FWD: GATACCTGGGGAACAGCAA REV: TAGGTGGAGACCCTGCTGAT
Glucose 6-phosphatase (<i>G6pc</i>)	FWD: CTACCTTGCGGCTCACTTC REV: ATCCAAGTGCGAAACCAAAC
Glucose 6-phosphate dehydrogenase (<i>G6PD</i>)	FWD: TTAAATGGGCCAGCGAAG REV: TGCTCTGCCATGATGTTTTTC
L-type Pyruvate Kinase (<i>Pk1r</i>)	FWD: CTGGAACACCTCTGCCTTCTG REV: CACAATTTCCACCTCCGACTC
Nicotinamide Nucleotide Transhydrogenase (<i>NNT</i>) EXON7	FWD: GGAAGGGTCAGTTGTTGTGG REV: CCGGCTTAGTCGTTTCAAAG

Table 2-5 Primers for real time RT-qPCR

2.2 Hepatocyte isolation and culture

2.2.1 Rat hepatocytes

Hepatocytes were prepared by a two-step collagenase perfusion of the liver of male Wistar rats (200-300g body weight) obtained from Harlan, Bicester, UK. They were allowed free access to standard rodent chow and water *ad libitum* on a 12h light / 12h dark cycle at 20 ± 2 °C and a controlled relative humidity of $50 \pm 10\%$. Procedures conformed to Home Office Regulations and were approved by the University Ethics Committee. The rat was anaesthetized in a chamber containing 15ml isoflurane (IsoFlo 100%, Zoetis UK Ltd). The rat was then removed from the chamber, attached to the dissection tray, wiped in 70% ethanol and a laparotomy was performed. The portal vein and superior vena cava were cannulated and the liver was perfused with Ca^{2+} -free EGTA-containing buffer (148 mM NaCl, 6.7 mM KCl, 10 mM HEPES, 0.2 mM EGTA, 10 $\mu\text{g}/\text{ml}$ phenol red, pH 7.4) at 20-30 ml/min for 15 min, followed by Ca^{2+} containing collagenase buffer (100 ml) (20mg/100 ml collagenase, 124 mM NaCl, 6.7 mM KCl, 2 mM CaCl_2 , 1 mM MgSO_4 , 20 mM HEPES, 10 $\mu\text{g}/\text{ml}$ phenol red, pH 7.4) until digestion (15-20 min). On termination of the perfusion the liver was transferred to a petri dish and gently dissociated in ~ 40 ml Minimum Essential Medium. The medium used for washing and cell culture was MEM with Earle's salts (Gibco #21430-020), supplemented with Non-Essential Amino acids (Gibco #11140-035); 2mM glutamine; penicillin (75mg/l) and streptomycin sulphate (50mg/l) (designated MEM). The cell suspension was filtered through 80 μm nylon mesh and centrifuged at 50 g for 2 min. The cell pellet was washed 3 times and hepatocytes were suspended in Minimum essential medium (MEM) containing 5 % (v/v) neonatal calf serum. Cell viability was checked with Trypan Blue (Lonza 19-942E) by mixing equal volumes of cell suspension and Trypan Blue and checking for dye exclusion. The cells were seeded at cell density of 4×10^4 cells / cm^3 on gelatin-coated (1mg/ml) multi-well plates. Cells were incubated for 3 hours at 37°C equilibrated with 5% CO_2 / air. After cell attachment (3h) the medium was replaced by serum-free MEM containing 5mM glucose and 10nM dexamethasone and 1nM insulin and the hepatocytes were cultured for 18 h.

2.2.2 Mouse hepatocytes

Male adult mice of the C57BL/6J OlaHsd strain or C57BL/6J strains were housed in the Comparative Biology Centre at Newcastle University Medical School. They were allowed free access to standard rodent chow and water *ad libitum* on a 12h light / 12h dark cycle at 20 ± 2 °C and a controlled relative humidity of $50 \pm 10\%$. Procedures for hepatocyte isolation conformed to Home Office Regulations and were approved by the University Ethics Committee. The mouse was anaesthetized in a 2-litre chamber containing 8 ml of isoflurane (IsoFlo 100%, Zoetis UK Ltd). After 2 min the mouse was weighed, injected intraperitoneally with 300 μ l heparin (Sigma H9399; 3mg (9000U) / ml sterile 150 mM NaCl) and then returned to the isoflurane chamber. After 4 min from first exposure to isoflurane the mouse was removed from the chamber, attached to the dissection tray, wiped in 70% ethanol and dissected to expose the heart and liver. A suture was placed below the heart under the vena cava. The heart was then gripped with fine forceps from the right atrium and stretched upwards and a 20 Gauge x 32 mm i.v. catheter (Versatus, SR+DU2032PX) was inserted into the inferior vena cava. The needle insert was then removed and when the cannula filled with blood, the suture was tied securely and the portal vein was cut approximately 1 cm distal to the liver. The cannula was then connected to a first peristaltic pump linked to calcium-free perfusate (containing per litre: 8000mg NaCl, 400mg KCl, 130mg KH_2PO_4 , 76mg EGTA, 20mg phenol red, 10 mmol HEPES, pH 7.4). The liver was perfused at 5 ml / min for 6 min. The cannula was then connected to a calcium plus collagenase Hanks medium buffered with 5mM NaHCO_3 , 20mM HEPES and containing 10 mg / 100 ml collagenase (Sigma Collagenase Type IV, *Clostridium histolyticum* C5138) and it was perfused for between 15 and 20 min. On termination of the perfusion the liver was transferred to a petri dish and gently dissociated in \sim 40 ml Minimum Essential Medium. The medium used for washing and cell culture was MEM with Earle's salts (Gibco #21430-020), supplemented with Non-Essential Amino acids (Gibco #11140-035); 2mM glutamine; penicillin (75mg/l) and streptomycin sulphate (50mg/l) (designated MEM). The cell suspension was filtered through a 200 μ m mesh, sedimented at 50g (2 min) and the pellet was washed at 50g for 2 min. The pellet was suspended in Minimum Essential Medium (as above) but supplemented with 5% vol/vol newborn calf serum (Gibco, Heat inactivated #26010-074), 10 nM dexamethasone and 10 nM insulin. Cell viability was checked with Trypan

Blue (Lonza 19-942E) by mixing equal volumes of cell suspension and Trypan Blue and checking for dye exclusion. The final cell suspension was ~ 0.5 million cells / ml and the cells were plated at a density of approximately 10^5 cells / cm^2 and placed in an incubator at 37 °C equilibrated with 5% CO_2 / air.

2.3 Methods

2.3.1 Preparation of radioactive substrates for metabolic studies

For radiochemical assays, required amounts of [^{14}C] metformin (0.4 $\mu\text{Ci/ml}$), [$\text{U-}^{14}\text{C}$] glucose (0.2-2 $\mu\text{Ci/ml}$), [$2\text{-}^3\text{H}$] glucose (1.5 $\mu\text{Ci/ml}$), [$3\text{-}^3\text{H}$] glucose (1.5 $\mu\text{Ci/ml}$), [$5\text{-}^3\text{H}$] glucose (1.5 $\mu\text{Ci/ml}$), [$1\text{-}^{14}\text{C}$] glucose (0.4 $\mu\text{Ci/ml}$) and [$6\text{-}^{14}\text{C}$] glucose (0.4 $\mu\text{Ci/ml}$) were dried at room temperature to evaporate the ethanol solvent.

2.3.1.1 Determination of metformin accumulation

Total cell accumulation of metformin was determined by pre-incubating hepatocytes with MEM, [^{14}C] metformin, and indicated metformin concentrations for 2 hours. Glucose (25mM) was then added to the medium for a further 1 hour. Cells were washed twice with 300mM sucrose, then extracted in 400 μl 0.1M NaOH. 1ml scintillation cocktail was added to 300 μl of cell extract and radioactivity was measured. Results expressed as nmol of metformin per mg protein.

Calculation

$$\text{Specific activity} = \frac{\text{dpm}/\mu\text{l}}{\text{nmol metformin}/\mu\text{l}}$$

$$= \text{dpm}/\text{nmol}$$

$$\frac{\text{dpm}}{\text{SA}} \times \frac{\text{Total vol. of cell ext.}}{\text{Vol of cell ext. measured}} \times \frac{1}{\text{Protein}}$$

(dpm/nmol)

(mg/ well)

= nmol of metform accumulated in cells per mg of protein

2.3.1.2 Determination of glycogen synthesis

Glycogen synthesis was determined from the incorporation of [$\text{U-}^{14}\text{C}$] glucose into cellular glycogen. Hepatocytes were pre-incubated with indicated conditions for 2 hours,

then incubated with MEM containing [U-¹⁴C] glucose and indicated additions for 3 hours. 50µl of medium was collected for calculation of specific activity. The remaining medium was then removed and cells were washed with 150mM NaCl, then extracted with 0.1M NaOH (0.5ml/ well) and frozen. For protein precipitation, 300µl of cell extract was added to 300µl of 20% trichloroacetic acid (TCA) containing 0.75mg/ ml glycogen. The mixture was vortexed, then centrifuged at 13,000g, 4°C for 10 minutes. Supernatant (500µl) was added to 1ml of 95% ethanol and centrifuged at 13,000g, 4°C for 10 minutes. The supernatant was aspirated and the glycogen pellet was washed twice with 1ml of 66% ethanol, and centrifuged at 13,000g, 4°C for 15 minutes. After the second wash, the pellet was left to dry at room temperature. 150µl of deionised water was added to the pellet and the pellet was left to dissolve overnight. The following day, 1ml of scintillation cocktail was added to the samples and vortexed until clear. Radioactivity was measured and results were expressed as nmol of glucose incorporated into glycogen per 3 hours per mg of protein.

Calculation

$$\begin{aligned} \text{Specific activity} &= \frac{\text{dpm}/\mu\text{l}}{\text{nmol glucose}/\mu\text{l}} \\ &= \text{dpm}/\text{nmol} \end{aligned}$$

$$\begin{aligned} \frac{\text{dpm}}{\text{SA}} \times \frac{\text{Total vol of cell ext. in well}}{\text{Vol added to glycogen/ TCA}} \times \frac{\text{Total vol. of cell ext. + glycogen/ TCA}}{\text{Vol. added to ethanol}} \\ \times \frac{1}{\text{protein}} \end{aligned}$$

(dpm/nmol)

(mg/ well)

= nmol of glucose incorporated into glycogen per mg of protein.

2.3.1.3 Determination of glucose phosphorylation and glycolysis

Glucose phosphorylation was measured from detritiation of [2-³H] glucose, and glycolysis was measured from detritiation of [3-³H] glucose and [5-³H] glucose.

Hepatocytes were pre-incubated with indicated conditions for 2 hours, then incubated with MEM containing [2-³H] glucose, 25mM glucose and indicated additions for 1 hour. The medium was collected and acidified with 10% 1M HCl. 50µl unincubated medium was acidified for calculation of specific activity. Acidified sample (100µl) or unincubated medium for blank correction was transferred to a 500µl microcentrifuge tube which was placed inside a 5ml scintillation vial containing 750µl deionised H₂O and stoppered. The tubes were incubated at 37°C for a minimum of 2 days to allow the ³H₂O to equilibrate between the two solutions. To determine the level of tritiated water, the microcentrifuge tube was removed and scintillation cocktail was added to the scintillation vial and counted. Results expressed as nmol of glucose detritiated per 3 hours per mg of protein.

Calculation

$$\text{Specific activity} = \frac{\text{dpm}/\mu\text{l}}{\text{nmol glucose}/\mu\text{l}}$$

$$= \text{dpm}/\text{nmol}$$

$$\frac{\text{dpm samples} - \text{dpm blank}}{\text{SA (dpm/nmol)}} \times \frac{\text{Vol of medium in well}}{\text{Vol taken for assay}} \times \frac{\text{Total vol in well} + 1\text{M HCl}}{\text{Total vol in well}}$$

$$\times \frac{1}{\text{Recovery}} \times \frac{1}{\text{protein (mg/well)}}$$

= nmol of glucose detritiated per 3h per mg cell protein

$$\text{Recovery factor} = \frac{{}^3\text{H}_2\text{O in ependorf}}{{}^3\text{H}_2\text{O} + 750\mu\text{l H}_2\text{O (total recovery)}}$$

2.3.1.4 Determination of glucose oxidation

Hepatocytes were plated into gelatine coated 25ml flasks. The following day hepatocytes were pre-incubated with indicated conditions for 2 hours. Medium containing [1-¹⁴C] glucose, [6-¹⁴C] glucose or [U-¹⁴C] glucose, 15mM glucose and indicated additions was added to the flasks. A 2ml microcentrifuge tube containing a paper wick was inserted carefully into each flask, and the flasks were stoppered and incubated at 37°C for 2-3 hours. The reaction was stopped by injection of 300µl hyamine

hydroxide to the microcentrifuge followed by 300µl 2M HCl into the main flask and left for 2 hours to allow for absorption of the $^{14}\text{CO}_2$ by the hyamine. The outer surface of the microcentrifuge tubes was rinsed in decontamination solution and transferred into a 20ml vial with 15ml scintillation cocktail and counted. The flasks were rinsed with 150mM NaCl and cells were extracted in 900µl of 1M NaOH. 20µl unincubated medium was used to calculate specific activity.

Calculation

$$\begin{aligned} \text{Specific activity} &= \frac{\text{dpm}/\mu\text{l}}{\text{nmol glucose}/\mu\text{l}} \\ &= \text{dpm}/\text{nmol} \end{aligned}$$

$$\frac{\text{dpm samples} - \text{dpm blank}}{\text{SA (dpm/nmol)}} \times \frac{1}{\text{Protein}}$$

= nmol of glucose decarboxylated per 2/3 hours per mg of protein

2.3.2 Metabolite determination

2.3.2.1 Glucose 6-phosphate (G6P)

Cell G6P was determined fluorometrically based on G6P oxidation by glucose 6-phosphate dehydrogenase (G6PD) to yield NADPH which is coupled to the reduction of resazurin in the presence of diaphorase to produce resorufin. The fluorescence of resorufin is detected by excitation at 530nm and emission at 590nm on a fluorimeter.

Principle of the reaction:



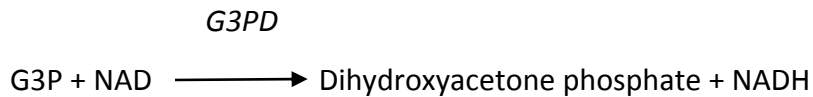
After incubation, hepatocytes were snap frozen in liquid nitrogen and the plates were stored at -80°C until extraction. Cells were extracted in $300\mu\text{l}$ 0.6M perchloric acid (PCA) or $300\mu\text{l}$ (2.5% weight/ vol) sulfosalicylic acid (SSA).

SSA extracts were transferred to a microfuge tube and centrifuged at $13,000g$, 4°C for 10 minutes. The supernatant ($200\mu\text{l}$) was neutralised with $3\text{M KOH}/ 1\text{M K}_2\text{HPO}_4$ (1:2, vol:vol). G6P standards (blank, 2, 5, 10, 20, $40\mu\text{M}$) were prepared in 2.5% SSA from a freshly prepared 10mM stock solution and neutralised similarly to the samples. The main reagent consisted of 50mM Tris base neutralised with acetic acid to pH 7.8, 2mM MgCl_2 , 0.2mM NADP, $0.02\mu\text{M}$ resazurin, 0.1 units/ ml G6PD, 0.03 units/ ml diaphorase. The sample volume was $40\mu\text{l}$ and the main reagent volume was $160\mu\text{l}$. G6P was assayed from resorufin fluorescence at Ex 530 nm , Em 590 nm (Spectramax M5e Microplate reader) and the G6P concentration in the samples was determined from the standard curve using Softmax Pro Software.

Perchlorate extracts were transferred to a microfuge tube and centrifuged at $13,000g$, 4°C for 10 minutes for precipitating the protein. The supernatant ($200\mu\text{l}$) was neutralised with KOH. Samples were cooled to precipitate the potassium perchlorate and centrifuged at $13,000g$, 4°C for 10 minutes. G6P standards (blank, 2, 5, 10, 20, $40\mu\text{M}$) were prepared from a freshly prepared 10mM stock solution in 0.6M PCA and neutralised similarly to the samples. The main reagent consisted of 50mM Tris base neutralised with acetic acid to pH 7.8, 2mM MgCl_2 0.2mM NADP, 0.1 units/ ml G6PD. The sample volume was $40\mu\text{l}$ and the main reagent volume was $160\mu\text{l}$. G6P was assayed from the rate of formation of NADPH. For PCA extracts NADH fluorescence was detected at Ex 340nm , Em 450nm (Spectramax M5e Microplate reader) and the G6P concentration in the samples was determined from the standard curve using Softmax Pro Software.

2.3.2.2 Glycerol 3-phosphate (G3P)

Cell G3P was determine fluorometrically based on G3P oxidation by glycerol 3-phosphate dehydrogenase (G3PD) to yield NADH which is coupled to the reduction of resazurin in the presence of diaphorase to produce resorufin. The fluorescence of resorufin can be detected by excitation at 530nm and emission at 590nm on a fluorimeter.

Principle of the reaction:

After incubation, hepatocytes were snap frozen in liquid nitrogen and the plates were stored at -80°C until extraction. Cells were extracted in 300µl 0.6M perchloric acid (PCA) or 300µl (2.5% weight/ vol) sulfosalicylic acid (SSA).

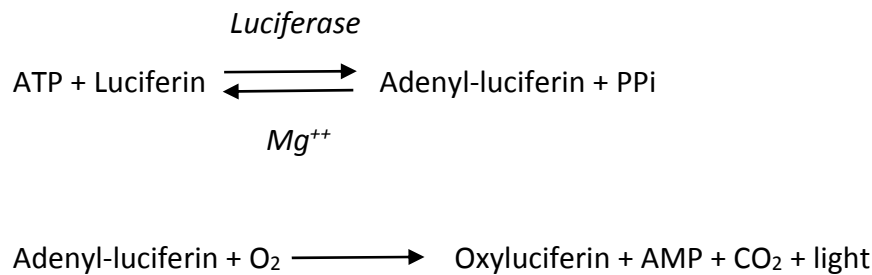
SSA extracts were transferred to a microfuge tube and centrifuged at 13,000g, 4°C for 10 minutes. The supernatant (200µl) was neutralised with 3M KOH/ 1M K₂HPO₄ (1:2, vol:vol). G3P standards (blank, 2, 5, 10, 20, 40µM) were prepared in 2.5% SSA from a freshly prepared 10mM stock solution and neutralised similarly to the samples. The main reagent consisted of 0.1M Tris/ hydrazine (pH 9.1), 0.4mM NAD, 0.02µM resazurin, 1.5 units/ ml G3PD, 0.04 units/ ml diaphorase (9µl). The sample volume was 40µl and the main reagent volume was 160µl. G3P was assayed from resorufin fluorescence at Ex 530 nm, Em 590 nm (Spectramax M5e Microplate reader) and the G3P concentration in the samples was determined from the standard curve using Softmax Pro Software

Perchlorate extracts were transferred to a microfuge tube and centrifuged at 13,000g, 4°C for 10 minutes for precipitating the protein. The supernatant (200µl) was neutralised with KOH. Samples were cooled and centrifuged at 13,000g, 4°C for 10 minutes to precipitate the potassium perchlorate. G3P standards (blank, 2, 5, 10, 20, 40µM) were prepared in in 0.6M PCA from a freshly prepared 10mM stock solution and neutralised similarly to the samples. The main reagent consisted of 0.1M Tris/ hydrazine (pH 9.1), 0.4mM NAD, 1.5 units/ ml G3PD (18ul). The sample volume was 40µl and the main reagent volume was 160µl. For PCA extracts NADH fluorescence was detected at Ex 340nm, Em 450nm (Spectramax M5e Microplate reader) and the G3P concentration in the samples was determined from the standard curve using Softmax Pro Software.

2.3.2.3 Adenosine triphosphate (ATP)

Cell ATP was determined by a luciferase assay comprising of a 2-step reaction. Luciferase catalyses the oxidation of luciferin, consuming ATP. Light is emitted in the second step which is detected by a luminometer.

Principle of the reaction:



After incubation, hepatocytes were snap frozen in liquid nitrogen and the plates were stored at -80°C until extraction. Cells were extracted in $300\mu\text{l}$ PCA or 2.5% SSA and processed and neutralised as described above or extracted in $300\mu\text{l}$ 0.1M NaOH. ATP standards were prepared from a freshly prepared 10mM stock solution and assayed in parallel (blank, 2, 5, 10, 20, $40\mu\text{M}$). The main reagent consisted of buffer (0.1M Tris/acetate pH 7.75, 10mM Mg-acetate, 1.8mM EDTA, 0.3g/l BSA) and 1:200 (v/v) ATP bioluminescent assay kit (Sigma). The sample volume was $20\mu\text{l}$ and the main reagent volume was $200\mu\text{l}$. Light emitted was measured on a luminescence protocol (Spectramax M5e Microplate reader) and the ATP concentration in the samples was determined from the standard curve using Softmax Pro Software.

2.3.2.4 Lactate production

Determination of lactate in the medium was based on lactate oxidation by NAD in the presence of lactate dehydrogenase (LDH) to yield NADH. The increase in NADH absorbance at 340nm was measured.

Principle of the reaction:

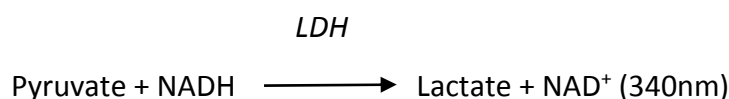


After incubation with hepatocytes, 200µl of media was transferred to a 96 well plate and stored at -20°C until required for assaying. The main reagent consisted of 0.1M Tris/ Hydrazine pH 9.1, 0.2mM NAD and 5.5 units/ml LDH. Lactate standards were prepared in MEM in from a 10mM stock solution (blank, 50, 100, 200, 500, 1000µM) and assayed in parallel. Main reagent (160µl) was added to 20µl of thawed media and NADH absorbance at 340nm was measured (Spectramax M5e Microplate reader). The lactate concentration in the samples was determined from the standard curve using Softmax Pro Software.

2.3.2.5 Pyruvate production

Determination of pyruvate in the medium was based on pyruvate reduction by NADH in the presence of lactate dehydrogenase (LDH) to yield NAD. The decrease in NADH absorbance at 340nm was measured.

Principle of the reaction:



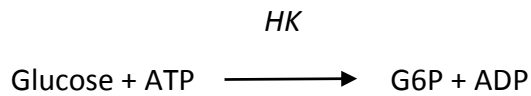
After incubation with hepatocytes, 200µl of media was transferred to a 96 well plate and stored at -20°C until required for assaying. Thawed media was acidified with 1:5 (v/v) 10% PCA: media. The main reagent consisted of 0.4M potassium phosphate buffer (K₂HPO₄/ KH₂PO₄), 0.14mM NADH and 1.1 units/ml LDH. Pyruvate standards were prepared in MEM from a 10mM stock solution and were acidified and assayed in parallel (blank, 25, 50, 100, 200, 500µM). Main reagent (180µl) was added to acidified media (20µl) and the decrease in NADH absorbance at 340nm was measured (Spectramax M5e Microplate reader). The pyruvate concentration in the samples was determined from the standard curve using Softmax Pro Software.

2.3.2.6 Glucose production

Glucose in the medium was measured by 2-step metabolism of glucose. Glucose is phosphorylated to G6P by hexokinase (HK) in the presence of ATP, then oxidised to 6-

phosphogluconate by G6PD leading to the formation of NADPH which is measured by the increase in absorbance and 340nm.

Principle of the reaction:



The main reagent consisted of 0.2M Tris pH 8.0, 20mM MgCl₂, 0.4mM NADP, 0.4mM ATP, 0.75 units/ml hexokinase and 0.1 units/ml G6PD. Glucose standards in MEM were prepared from a fresh 10mM stock solution (blank, 25, 50, 100, 200, 400µM) and were assayed in parallel. NADH absorbance at 340nm was measured (Spectramax M5e Microplate reader) and the glucose concentration in the samples was determined from the standard curve using Softmax Pro Software.

2.3.3 G6PD activity

Determination of G6PD activity was based on Rudack et al., (1971) on the basis that 1 unit of G6PD activity forms 1µmol NADPH per minute.

Principle of the reaction:

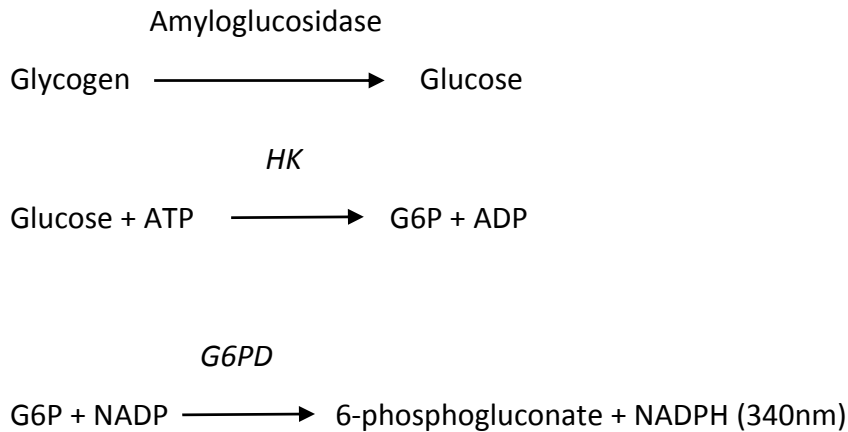


After incubation hepatocytes were snap frozen in liquid nitrogen and the plates were stored at -80°C until extraction. Cells were extracted in 100mM KCl, 10mM HEPES and 0.5mM DTT. Samples were sonicated and assayed for protein by a Bradford method (described below). Samples were centrifuged at 11,000 rpm, 4°C for 10 minutes. The supernatant was combined with main reagent (100mM Tris, 1.3mM G6P, 0.4mM NADP and 8mM MgCl₂ in water) and the absorbance of NADPH at 340nm was measured.

2.3.4 Cell glycogen determination

The glycogen content in cell extracts is determined in a 2-step process by glycogen digestion to glucose by amyloglucosidase, then spectrometric determination of glucose.

Principle of the reaction:



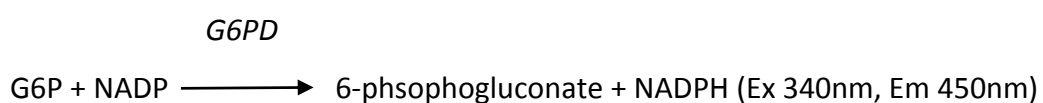
After incubation hepatocytes were snap frozen in liquid nitrogen and the plates were stored at -80°C until extraction. Cells were extracted in 0.2M NaOH (200µl) and incubated for 90 minutes with Amyloglucosidase/ acetate buffer (pH 4.8) at 55°C. Parallel incubations were carried out with either buffer alone or with amyloglucosidase to subtract from samples. A solution of glycogen (0.2mg/ml) was also incubated similarly to confirm amyloglucosidase digestion.

Glucose was measured by the hexokinase/glucose-6-phosphate dehydrogenase method described above.

2.3.5 NADP determination

Cell NADP was determined fluorometrically based on G6P oxidation by NADP to yield NADPH. The fluorescence of NADPH can be detected by excitation at 340nm and emission at 450nm on a fluorimeter.

Principle of the reaction:



After incubation, hepatocytes were snap frozen in liquid nitrogen and the plates were stored at -80°C until extraction. Cells were extracted in $300\mu\text{l}$ 0.6M perchloric acid (PCA) and transferred to a microfuge tube and centrifuged at $14,000\text{g}$, 4°C for 10 minutes for precipitating the protein. The supernatant ($200\mu\text{l}$) was neutralised with KOH. Samples were cooled and centrifuged at $14,000\text{g}$, 4°C for 10 minutes for precipitating the potassium perchlorate. NADP standards (blank, 1, 2, 5, 10, $20\mu\text{M}$) were prepared from a 1mM stock solution in PCA and neutralised similarly to the samples. The main reagent consisted of 50mM Tris base neutralised with acetic acid to pH 7.8, 2mM MgCl_2 , 5mM G6P, 0.1 unit/ml G6PD. The samples were treated with or without G6PD in the main reagent and NADPH fluorescence was measured in order to subtract the enzyme blanks to correct for the colour interference in the assay. NADH fluorescence was detected at Ex 340nm , Em 450nm (Spectramax M5e Microplate reader) and the NADP concentration in the samples was determined from the standard curve using Softmax Pro Software.

2.3.6 Inorganic phosphate determination

Determination of inorganic phosphate (Pi) was based on Itaya & Ui., (1966) on the basis that at lower pH malachite green complexes with phosphomolybdate, forming a green solution, shifting the maximum absorption.

After incubation, the medium was collected and the cells were washed twice with 300mM sucrose, then extracted in $400\mu\text{l}$ PCA. Samples were centrifuged at 9000g for 10 minutes. The main reagent consisted of 1% ammonium molybdate in 5M HCl, 0.12% malachite green in water. Absorbance at 660nm was measured. Pi standards (5 , 10 , 25 , 50 , $100\mu\text{M}$) were assayed in parallel.

2.3.7 Determination of mRNA expression (RT-qPCR)

mRNA expression was determined by semi-quantitative real-time (RT)-PCR. RNA was extracted from rat or mouse hepatocyte monolayers using $250\mu\text{l}$ Trizol reagent (24-well plates) and transferred to microfuge tubes, then frozen at -80°C until processing. Samples were thawed and incubated at room temperature for 10 minutes. $200\mu\text{l}$ of chloroform was added and samples were shaken vigorously followed by a 2-minute incubation at room temperature. Samples were centrifuged at $12,000\text{g}$, 4°C for 15 minutes and the aqueous upper phase was transferred to a fresh microcentrifuge tube. An equal volume of isopropanol was added and shaken vigorously followed by a 10-

minute incubation at room temperature. Samples were centrifuged at 12,000g, 4°C for 15 minutes and the supernatant was removed. Pellets were washed with 250µl 75% ethanol and centrifuged at 7,500g, 4°C for 5 minutes. Ethanol was aspirated and samples air dried at room temperature for 50 minutes. The pellets were resuspended in 10µl H₂O and incubated at 55°C for 10 minutes.

2.3.7.1 Reverse transcription

Genomic DNA was removed by treatment with Rnase free Dnase I for 15 minutes at 37°C, followed by denaturation of the enzyme at 70°C for 10 minutes. The RNA was quantified on Spectromax (260:280nm). Random primers (1µg/ml) were added to 1 µg RNA and samples incubated for 10 minutes at 70°C. Reverse transcriptase mix (M-MLV reverse transcriptase buffer (Promega), M-MLV reverse transcriptase (Promega), dNTP mix and molecular biology H₂O) was added to each sample and samples were incubated at 37°C for 50 minutes followed by a 15-minute incubation at 70°C. Samples were diluted 1:1 for a final cDNA concentration of 25ng/µl.

RT-PCR was performed with 50ng of reverse transcribed RNA with SYBR mix (Promega) and 5ng forward and reverse primers using a Roche capillary light cycler. Samples were denatured at 95°C for 10 minutes, followed by 40 cycles consisting of 95°C for 15 seconds, 58°C for 7 seconds and 72°C for 15 seconds.

2.3.8 Western blotting

For extraction of phosphorylated proteins, hepatocytes were extracted in a buffer containing 100mM KCl, 10mM EDTA, 20mM Kpi, 0.5mM PMSF, 0.5mM benzamidine, 1mM DTT, 1/1000 calyculin A and 1/1000 protease inhibitor cocktail. For extraction of unphosphorylated protein, hepatocytes were extracted in a buffer containing 100mM Tris-HCl (pH 7.4), 100mM NaCl, 2mM EDTA, 25mM NaF, 0.1% triton, 1mM benzamidine, 0.1mM Na₃VO₄, 1/1000 protease inhibitor cocktail.

Samples were sonicated and protein concentration was measured by a Bradford assay (see below). The samples (20µg) were diluted 1:5 with 4x SDS loading buffer containing 120mM Tris pH 6.8, 1:4 (v/v) 10 % SDS, 3mM glycerol, 4% (v/v) mercaptoethanol and 4% (v/v) 0.1% bromophenol blue in ethanol, and denatured at 100 °C for 5 min. The samples were loaded into SDS polyacrylamide gel for electrophoresis (90V for 15 minutes, then

180v for 45 minutes). After electrophoresis, the gels were electrophoretically transferred (semi-dry) onto PVDF membrane using a Trans-Blott SD semi-dry transfer cell from Biorad Laboratories Ltd. (Hertfordshire, UK) at 15V for 45 minutes with transfer buffer consisting of 25mM Tris, 0.2M glycine and 30% methanol in distilled water. After transfer the membranes were blocked in TBST, pH 7.4 (25mM Tris, 144mM NaCl, 0.2% concentrated HCl, 0.5% Tween in distilled water) containing 5% BSA (phosphorylated proteins) or 5% milk (unphosphorylated proteins). Membranes were incubated with the primary antibody overnight.

The following day, membranes were washed in TBST and incubated with peroxidase conjugated anti-rabbit/mouse IgG secondary antibody for 1 hour. After incubation, the membranes were washed in TBST and developed using ECL chemiluminescence reagent according to the manufacturer's instructions followed by brief exposure to ECL X-ray film.

For re-incubation of blots with different primary antibodies, blots were first incubated with stripping buffer pH 6.7 (0.06mM Tris base, 2% SDS, 0.8% mercaptoethanol in distilled water), then washed in PBS and TBST before being blocked with 5% milk and re-probed with primary antibody.

2.3.9 Determination of cellular protein by Bradford method

For western blotting, cellular protein was determined spectrometrically by a Bradford method. The assay is based on the binding of Coomassie blue to peptidyl residues that form a coloured complex measured at 595nm.

Samples were diluted 1:10 with 0.05% Triton and standards in 0.05% Triton-X100 (0.025, 0.05, 0.1, 0.2, 0.3, 0.5mg/ml) were used for the assay. Bradford reagent (Bio-Rad) diluted 1:5 was added to the standard/ samples.

2.3.10 Determination of cellular protein by Lowry method

Cellular protein was determined spectrometrically by a Lowry method. The assay is based on the reaction between Folin-phenol reagent (phosphomolybdic-tungstic acid) which is reduced by protein to form a coloured complex which can be measured at 750 nm.

After incubation hepatocytes were washed twice with 150mM NaCl, then snap frozen in liquid nitrogen and the plates were stored at -80°C until extraction. Cells were extracted in 1ml 0.1M NaOH and transferred to a microcentrifuge tube. The main reagent (10% (w/v) Na₂CO₃ in 0.5 M NaOH, H₂O, CuSO₄.5H₂O and Na⁺/K⁺ tartate in a 10:40:1:1 ratio) is activated with Folin and Ciocalteu's phenol diluted with distilled water in a 1:20 (v/v) ratio. BSA standards (blank, 0.2, 0.3, 0.4, 0.5, 0.75 and 1 mg/ml in 0.1M NaOH) were used for the standard curve.

2.3.11 Immunostaining

Immunostaining was performed to determine the changes in subcellular localisation of glucokinase in response to different compounds in hepatocytes. Hepatocytes were cultured in 24-well plates on glass coverslips that had been sterilised with ethanol and dried.

2.3.11.1 Fixation

After incubation, MEM was aspirated and coverslips were washed twice with PBS. Cells were fixed with 4% paraformaldehyde and incubated for 30 minutes at room temperature. Paraformaldehyde was then aspirated and coverslips were washed twice with PBS.

4% paraformaldehyde in 1X PBS: 2g paraformaldehyde was dissolved in 50ml nanopure H₂O (heated to 70-80°C) with 200µl 2M NaOH and 5ml 10x PBS. Paraformaldehyde was then cooled on ice before being used for fixation.

2.3.11.2 Immunofluorescence

Sodium borohydride (500µl 1mg/ml) (made up in PBS) was added to each coverslip and incubated for 10 min at room temperature to quench autofluorescence of hepatocytes. Coverslips were then washed twice with 1x PBS and 500µl 0.2% Triton-X100 (in PBS) was added and incubated for 10 min at room temperature to permeabilise the cells and improve antibody penetration. Coverslips were then washed twice with PBS and transferred onto parafilm. 25µl 1% BSA / 0.2% Triton-X100 was added to each coverslip and incubated for 10 min at room temperature to act as a blocking solution to reduce background and unspecific staining. Cells were then washed twice with PBS and 25µl/

slip of primary GK antibody (GK H-88, Santa Cruz) diluted 1:10 in 1% BSA/ 0.1% Triton/PBS and incubated at room temperature for 3 hours.

The primary antibody was removed and cells washed with PBS. Cells were incubated with 25 μ l/ slip of secondary antibody (Alexa fluor 488 Goat anti-Rabbit) diluted 1:50 in 10% BSA/ 10% triton/ PBS for 1 hour at room temperature. The secondary antibody was removed and cells were washed with PBS. 0.2 μ g/ml DAPI was then added to cells and incubated for 5 min at room temperature to stain nuclei before cells were washed twice with PBS, then placed on a paper towel and allowed to air dry for 30 minutes

2.3.11.3 Mounting and imaging of coverslips

Coverslips were mounted face down onto glass slides using Mowiol R-4088 containing 2.5% DABCO to help prevent fading of the immunofluorescent dyes. Coverslips were left to dry and then examined using a Nikon E400 fluorescent microscope. Images were taken at 40x magnification and captured using a Nikon DXM1200 digital camera. 10 fields were imaged for each incubation condition and the nuclear/ cytoplasmic ratio of GK was measured.

2.3.12 Statistical analysis

Results are expressed as mean \pm SEM of the number of experiments indicated. Statistical analysis was performed with the Student's paired t-test experiments. A P value of < 0.05 was considered to be statistically significant.

Chapter 3: Results 1

3.1 Metformin accumulation in hepatocytes

Metformin is positively charged at physiological pH and accumulates in the cells slowly in accordance with the transmembrane potential (Owen et al., 2000). In vivo the concentration of metformin in the liver measured at various time points (0.5 to 8 h) after an oral load of metformin exceeded that in the hepatic portal vein by approximately 2-6 fold (Wilcock & Bailey 1994). It has been reported that in a time course of metformin uptake in rat hepatocytes, metformin accumulation begins to plateau at around 2 hours incubation (Al-Oanzi et al., 2017). Therefore, throughout this study we used a pre-incubation time of 2 hours with metformin, before challenging the hepatocytes with the substrates indicated.

(Figure 3.1 A) shows the level of [^{14}C] metformin that accumulates in mouse hepatocytes during a 2-hour incubation with varying concentrations of extracellular metformin. Metformin accumulated in a dose dependent manner relative to the extracellular metformin concentration. Furthermore, based on a cellular water content of hepatocytes of 2 microlitres per mg cell protein (al-Habori et al., 1992) it can be calculated that the average cellular accumulation of metformin in incubations with 0.1-0.5mM metformin is 5-7 fold greater than the extracellular concentration, and with 1.0mM metformin is 10 fold greater than the extracellular concentration (figure 3.1 B) similar to previous reports (Wilcock & Bailey., 1994). Additionally, after incubations with 0.1-0.2mM metformin, cell metformin accumulation was 1.4-2.0 nmol/mg which is similar to the peak level in hepatocytes after an oral dose of 50mg/kg metformin in mice based on the cellular protein content of the liver of 200mg protein per 1g wet weight (Wilcock & Bailey., 1994; Berry et al., 1991, Laboratory Techniques, vol21. Isolated hepatocytes).

Therefore, we determined that incubating hepatocytes for 2 hours with 0.1-0.2mM metformin gave a comparable cell load as occurs in vivo after an oral therapeutic dose of metformin. Subsequent experiments were conducted following a protocol of pre-incubating hepatocytes for 2 hours with 0.1-1.0mM metformin and 5mM glucose followed by a 1-hour incubation with either 5mM glucose or substrate challenge to

determine the effect of metformin on glucose 6-phosphate (G6P) and adenine nucleotides at pharmacological concentrations of metformin and at concentrations that exceed the pharmacological dose.

3.2 Metformin lowers cell G6P in hepatocytes incubated with high glucose or gluconeogenic precursors

The hepatic portal vein provides the liver with the dietary sugars glucose and fructose (Niewoehner et al., 1984 a; Niewoehner et al., 1984 b). G6P is the first intermediate of glucose metabolism, generated by glucokinase (GK) mediated glucose phosphorylation. Owen et al., (2000) observed that cell G6P was decreased by approximately 50% with 2mM metformin in rat hepatocytes after a 3-hour incubation. Similar effects were observed in rats treated orally with 50-150mg/kg metformin in conjunction with a drop in the ATP/ ADP ratio (Owen et al., 2000). Additionally, in rat hepatocytes incubated with 10mM glucose, metformin at 3-10mM lowered cell G6P accompanied by a drop in cell ATP (Guigas et al., 2006). Therefore, the aim of the study was to test the effects of varying metformin concentrations inclusive of the therapeutic range on cell G6P, and to investigate whether metformin lowers cell G6P in the absence of lowering cell ATP.

Cellular levels of G6P in hepatocytes are dependent on the extracellular concentration of substrates (glucose or gluconeogenic precursors), and also on the intrinsic activities of GK and glucose 6-phosphatase (G6pc), which are major positive and negative modulators of cellular G6P respectively (Agius et al., 2002). In gluconeogenesis, G6P enters the endoplasmic reticulum (ER) via the glucose 6-phosphate transporter (G6PT) and is hydrolysed by the membrane bound enzyme glucose 6-phosphatase (G6pc) (van Shaftingen et al., 2002). The SLC37A4 exchanger is the only sugar-phosphate/ Pi exchanger in the liver that is coupled with G6pc (Chou & Mansfield., 2014) and that is inhibited by the chlorogenic acid derivative S4048 (1-[2-(4-chloro-phenyl)-cyclopropylmethoxy]-3,4-dihydroxy-5-(3-imidazo[4,5-*b*]pyridin-1-yl-3-phenyl-acryloyloxy)-cyclohexanecarboxylic acid), a potent competitive inhibitor of G6PT (Herling et al., 1999; Harndahl et al., 2006). S4048 is both an inhibitor of G6P hydrolysis and it also enhances the elevation in cell G6P during substrate challenge. To investigate the mechanism by which metformin affects G6P in hepatocytes we tested a variety of substrates in the absence or presence of S4048.

First, we compared the effects of basal glucose (5mM) with high glucose (25mM) simulating the raised blood glucose in the portal vein (15-25mM) on cell G6P. High glucose (25mM) was used as it has previously been shown to elevate G6P (Aiston et al., 2004) and downstream phosphorylated intermediates in hepatocytes (Arden et al., 2012), stimulating the expression of ChREBP target genes including G6pc and Pklr (Al-Oanzi et al., 2017).

High glucose increased cell G6P by 4-fold and S4048 had no effect on G6P with 5mM glucose (figure 3.2 A) but it increased G6P with 25mM glucose by a further 10-fold (figure 3.2 A) in agreement with previous findings (Harndahl et al., 2006). S4048 also increased cell G6P by 10-fold with the gluconeogenic precursor DHA as a substrate (figure 3.2 C). The fold elevation in G6P caused by S4048 was greater in rat hepatocytes (figure 3.3 C) than in mouse hepatocytes (figure 3.3 E).

Cell ATP was measured as a marker of cell viability. In some experiments ATP was lowered marginally by up to 16% with high metformin concentrations (0.5-1.0mM) but ATP was not lowered by moderate metformin concentrations (0.2-0.5mM) (figure 3.3 D, F) which result in cell loads of 2-5 nmol metformin/ mg that are within the therapeutic range and that cause lowering G6P (figure 3.3 C, E). Additionally, the lowering of ATP by S4048 in combination with high glucose in conditions of markedly elevated G6P (figure 3.2 B) can be explained by sequestration of inorganic phosphate (Pi) in the elevated G6P pool similar to the depletion of Pi that occurs in isolated hepatocytes or perfused livers challenged with millimolar concentrations of fructose (Morris et al., 1978).

Metformin concentrations of 0.1-0.2mM had little effect on cell G6P at 5mM glucose (both with and without S4048) (figure 3.3 A) however with high glucose, metformin caused a concentration dependent lowering of G6P (figure 3.3 C, E). This was also observed with the gluconeogenic substrates DHA, xylitol and fructose (figure 3.4 A, C, E) which are metabolised by pathways independent of glucokinase (Azzout & Peret., 1984; McCormick & Touster., 1957). Significant lowering of G6P by metformin occurred at an extracellular concentration of 0.1mM metformin (figure 3.3 C, E) and fractional lowering of G6P was greater in the presence of S4048 (figure 3.3 G, H) although the trends were similar. Due to this advantage later studies were conducted in the presence of S4048 only.

3.2.1 Mitochondrial depolarisation mimics the G6P lowering effect of metformin

We determined that metformin at 0.1-1.0mM lowered cell G6P. We next investigated possible mechanisms that mimic the G6P lowering effect of metformin. Firstly, evidence suggests that metformin inhibits complex 1 in isolated mitochondria and hepatocytes at elevated concentrations (10mM metformin) (Owen et al., 2000; El-Mir et al., 2000). Therefore, we tested whether the complex 1 inhibitor rotenone (Palmer et al., 1968; Heinz et al., 2017) mimicked metformin and lowered G6P with high glucose, and whether this was observed in conditions of depleted or maintained ATP.

In both mouse and rat hepatocytes 0.25 μ M rotenone lowered cell G6P by more than 30% (figure 3.5 A, D, G) and stimulated lactate and pyruvate production (figure 3.5 C, F, I) in the absence of ATP depletion (figure 3.5 B, E, H). However, higher concentrations of rotenone lowered ATP (figure 3.5 B, E). To test whether the decrease in G6P by metformin and rotenone is due to inhibition of complex 1 we tested the effect of a mitochondrial uncoupler as metformin depolarises the mitochondria (Owen et al., 2000). The mitochondrial uncoupler 2,4-dinitrophenol (DNP) (Starkov., 2006) (40 μ M) lowered cell G6P at 25mM glucose (figure 3.6 A, D, G) and with 5mM DHA (figure 3.6 J) with variable effects on cell ATP (figure 3.6 B, E, H, K). Additionally, in contrast with metformin and rotenone, DNP lowered total lactate and pyruvate at high concentrations (figure 3.6 C, F, I).

Furthermore, rotenone and DNP had opposite effects on the metabolism of [U-¹⁴C] glucose to ¹⁴CO₂. Rotenone inhibited substrate oxidation as expected for a complex 1 inhibitor, whereas DNP stimulated substrate oxidation by 2-fold as expected for a compound that dissipates the proton gradient (figure 3.7 A). Metformin had no effect on substrate oxidation up to 0.2mM but inhibited substrate oxidation at 0.5mM similarly to rotenone (figure 3.7 B). This indicates that metformin inhibits complex 1 at 0.5mM but may have other effects on mitochondrial function at lower concentrations which result in a cellular load < 5 nmol /mg protein corresponding to accumulation in the liver at the pharmacological dose (Wilcock & Bailey., 1994).

Emodin and berberine which occur naturally in several plant species and have been reported to mimic several effects of metformin on mitochondria (Turner et al., 2008; Zhang & Ye., 2012; Song et al., 2013; Xu et al., 2014) also lowered cell G6P with high

glucose and DHA (figure 3.8 A, D, F, I) and lowered total lactate + pyruvate at high concentrations (figure 3.8 C, H). This was observed in the absence of ATP depletion with berberine (figure 3.8 B, E) although emodin lowered ATP by up to 45% (figure 3.8 G, J). Cumulatively this shows that lowering of G6P is not unique to either metformin or inhibition of Complex 1.

3.2.2 Potential link of G6P depletion with raised cell NADP

3.2.2.1 Elevation in NADP in conditions of lowered cell G6P: possible role of compromised NNT activity

The above studies showed that pharmacological inhibition of complex 1 and depolarisation of the mitochondria mimicked the effect of metformin in lowering G6P in the absence of lowering of ATP. We next tested the hypothesis that the metformin effect on G6P lowering may be caused by mitochondrial depolarisation and/or a decrease in the mitochondrial proton gradient. Various mechanisms are linked to the transmembrane proton gradient including ATP-synthase (Bridges et al., 2014), nicotinamide nucleotide transhydrogenase (NNT) (Hoek & Rydström., 1988; Moyle & Mitchell., 1973) and various pH dependent transporters like the inorganic phosphate transporter. Our initial hypothesis to explain the G6P lowering by metformin, rotenone and DNP may involve inhibition of NNT as a result of a diminished proton gradient (figure 3.9). NNT on the inner mitochondrial membrane generates NADPH from NADH and NADP⁺, driven by the transmembrane proton gradient. In mitochondria, the reduction of NADP⁺ by NADH is coupled to the translocation of protons from the cytoplasmic side of the mitochondrial inner membrane to the matrix (Hoek & Rydström., 1988). Approximately one third of total NADPH + NADP⁺ is located in the cytosol and the rest in the mitochondria (Sies et al., 1977), and NNT is responsible for half of the NADPH generated in the liver (Hoek & Rydström., 1988).

To test the possible role of compromised NNT activity in the G6P lowering effect of metformin we first tested whether an NNT inhibitor mimics the G6P lowering effect of metformin. Rhein (4,5-dihydroxyanthraquinone-2-carboxylic acid), an anthraquinone present in rhubarb was identified as a competitive inhibitor of NNT (Kean et al., 1971). Rhein causes elevation in NADP in hepatocytes at 0.1mM (Sies et al., 1975) but also depletion of ATP and GSH at lower concentrations (Bironaite & Ollinger., 1997). Our

initial aim was to determine whether rhein causes depletion of G6P in association with elevation of NADP. Hepatocytes maintain the NADPH/NADP ratio at a very reduced state (Veech et al., 1969) however, an increase in NADP occurs with rhein or in conditions of NADPH consumption as occurs with ammonium ion (Sies et al., 1975). In preliminary experiments we confirmed ATP depletion by 0.1mM rhein, we therefore tested lower concentrations (10-40 μ M) during incubation with high glucose and S4048.

With high glucose, rhein (40 μ M) mimicked the effect of metformin, lowering cell G6P by 34 \pm 10% (figure 3.10 A) without lowering cell ATP (figure 3.10 B) and it increased NADP by 4-fold (figure 3.10 C) as expected from previous work (Sies et al., 1975). Although rhein was identified as a competitive inhibitor of NNT, it has also been reported to cause depolarisation of the mitochondrial membrane (Bironaite & Ollinger., 1997).

Accordingly, elevated NADP could be explained by either direct inhibition of NNT or indirect inhibition by mitochondrial depolarisation (figure 3.9). We next tested whether metformin raises NADP. These experiments were performed at either 5mM glucose or 25mM glucose with S4048. We also used ammonium ion as a positive control in these experiments as studies by Sies et al., (1975) showed that urea synthesis from ammonia elevates NADP. This was explained by preferential usage of NADPH in the reductive amination of 2-oxoglutarate to glutamate, when ammonia is the substrate for urea synthesis. In these experiments 2mM ammonium increased NADP 2-fold at both low and high glucose (figure 3.10 F) in agreement with the findings of Sies et al., (1975), and also lowered cell G6P to the same extent as 0.5mM metformin with high glucose (figure 3.10 D) without causing ATP depletion (figure 3.10 E). Cell NADP was higher at 5mM than at 25mM glucose (figure 3.10 F) suggesting a potential role of elevated glucose (and G6P) in maintaining a more reduced NADPH/ NADP state. Metformin had no effect on NADP at 0.2mM however, 0.5mM metformin raised NADP at high glucose but not at low glucose (figure 3.10 F). This finding is consistent with the hypothesis that the lowering of G6P by metformin at high glucose may be linked to the elevation in NADP.

3.2.2.2 Metformin lowers G6P in hepatocytes deficient in NNT activity

The hypothesis that the lowering of G6P by metformin could be explained by inhibition of NNT is supported by the following evidence: (i) Rhein, an NNT inhibitor raised NADP and lowered G6P; (ii) rotenone and DNP which are expected to cause attenuation of the

proton gradient also lowered G6P; (iii) metformin modestly raised NADP and lowered G6P. To further test this hypothesis, we determined the effects of metformin on G6P in hepatocytes from the C57BL/6J mouse which contains an in-frame deletion of exons 7-11 in the coding region of the NNT gene resulting in the formation of a truncated non-functional protein (Kraev., 2014; Meadows et al., 2011). These studies were conducted in parallel with studies on the C57BL/6J^{OlaHsd} strain which contains the intact NNT gene (Fontaine & Davis., 2016).

Firstly, we confirmed that mRNA levels of the NNT gene measured with primers spanning exon 7 were not detectable in hepatocytes from C57BL6/J mice (figure 3.11 A). In incubations with both 25mM glucose and 5mM DHA, hepatic G6P was similar in both mouse strains and metformin (0.2-0.5mM) lowered G6P similarly in both wild type and NNT deficient hepatocytes (figure 3.11 B, D, F, H) with little (13%) or no effect on ATP (figure 3.11 C, E, G, I). This suggests that mechanisms other than the NNT gene are involved in the G6P lowering effect of metformin.

3.2.3 AMPK activators do not mimic the metformin effect on G6P

3.2.3.1 Testing the effects of AMPK activators on cellular G6P in hepatocytes

Activation of AMPK is one of the most widely studied mechanisms of metformin that is implicated in mediating its blood glucose lowering effects in vivo and enhancement of insulin sensitivity by the inhibition of de novo lipogenesis, through phosphorylation of acetyl-CoA carboxylase (Cool et al., 2006; Rena et al., 2017). A role for AMPK in mediating the inhibition of gluconeogenesis by metformin in cellular studies was reported by Zhou et al., (2001) and Cao et al., (2014). Cool et al., (2006) also reported blood glucose lowering effects in vivo with the AMPK activator A769662. However, a study by Foretz et al., (2010) showed inhibition of gluconeogenesis in AMPK knock out hepatocytes in association with substantial lowering of cell ATP, indicating an AMPK-independent mechanism. However, the latter does not exclude the possibility that gluconeogenesis could be inhibited by both AMPK-dependent (Zhou et al., 2001; Cao et al., 2014) and AMPK-independent mechanisms (Foretz et al., 2010).

Various mechanisms have been proposed to mediate the activation of AMPK by metformin, including elevation in cell AMP as a result of attenuation of mitochondrial

function (Owen et al., 2000; Foretz et al., 2010), inhibition of AMP-deaminase (Ouyang et al., 2011; Vytla et al., 2013) and a lysosomal stress activated pathway (Zhang et al., 2014; Zhang et al., 2016). Since activation of AMPK could occur in response to a variety of stress conditions, a key question is whether activation of AMPK by small molecules mimics the effects of metformin in causing attenuation of cell G6P. The aim of this study was to test the direct effects of AMPK activation with small molecules on cell G6P and gluconeogenic flux and to compare this with metformin concentrations that do not lower cell ATP.

The initial aim was to compare metformin and the AMPK activators on AMPK-Thr172 phosphorylation and phosphorylation of ACC-Ser79, the downstream target of AMPK. We first used the allosteric activator A769662, a thienopyridone that targets the β 1-regulatory subunit in hepatocytes (Scott et al., 2008; Sanders et al., 2007; Goransson et al., 2007; Timmermans et al., 2014) and determined the concentration and pre-incubation time with A769662 that resulted in similar or greater phosphorylation of AMPK-Thr172 and ACC-S79 as metformin (0.5mM) with 25mM glucose as substrate (figure 3.12 A, 3.13 A, D), and as metformin (0.2mM) with 5mM DHA as substrate (figure 3.14 A, figure 3.15 A).

Unlike metformin, A769662 did not lower G6P in either rat or mouse hepatocytes with high glucose (figure 3.16 A, C). Because non-specific effects of A769662 that are independent of AMPK have been reported at high concentrations (100 μ M) (Foretz et al., 2010; Benziane et al., 2009) we compared A769662 with two other allosteric activators: Compound 991 also known as Ex229 (991) which like A769662 binds the AMPK ADaM site but with higher potency (Lai et al., 2014; Xiao et al., 2013), and Compound 13 (C13), a prodrug that is metabolised to an AMP analogue that binds to the α 1-catalytic unit and activates AMPK similarly to AMP (Hunter et al., 2014).

With concentrations of AMPK activator that stimulated ACC phosphorylation similarly (figure 3.17 A), all three AMPK activators differed from metformin in causing raised G6P with the gluconeogenic precursor DHA as substrate (figure 3.19 G, H, I). However, with high glucose as substrate, C13 (the AMP-mimetic) which stimulate ACC phosphorylation comparably to 0.5mM metformin (figure 3.18 A) caused a small lowering of G6P in both

the absence and presence of S4048 (figure 3.20 C, H), whereas A769662 had small but variable effects on G6P (figure 3.20 A, F) and 991 had non-significant trends (figure 3.20 B, G) without lowering cell ATP (figure 3.21 G-L). This contrasts with the lowering of G6P by metformin with both high glucose (figure 3.20 D, I) and DHA (figure 3.19 D, J). We also measured lactate and pyruvate accumulation which was increased by ≥ 0.2 mM metformin (figure 3.19 E, K; figure 3.20 E, J). In contrast, all three AMPK activators inhibited lactate and pyruvate production (figure 3.19 F, L; figure 3.20 K).

3.2.3.2 Testing the effects of AMPK activators on glucose production in hepatocytes

We also compared the effects of metformin and pharmacological AMPK activators on glucose production with DHA as substrate in a glucose-free medium. Metformin ≥ 0.2 mM inhibited glucose production by 24%-38% (figure 3.22 B). This was not mimicked by any of the AMPK activators tested, and A769662 and C13 stimulated glucose production by 42% and 17% respectively (figure 3.22 C). It is noteworthy that high concentrations of S4048, an inhibitor of SLC37A4, partially inhibited glucose production by 75% with DHA (figure 3.22 A). It is known that S4048 is selective for SLC37A4 and that other hexose 6-phosphate transporters that are encoded by SLC37A1 and SLC37A2 are insensitive to chlorogenic acid derivatives (Pan et al., 2011). Glucose production involving hexose 6-phosphate transporters other than SLC37A4 is a possible explanation for the residual glucose production in the presence of S4048. Metformin (0.1 to 1 mM) inhibited glucose production in the presence of S4048 (figure 3.22B) however, A769662 (but not 991 or C13) stimulated glucose production by 2-fold in the presence of S4048 (figure 3.22 C). A769662 also caused a larger elevation in G6P than C13 and compound 991 (figure 3.19 G, H, I). Cumulatively these results indicate opposite effects of AMPK activation and metformin on both gluconeogenic flux and cell G6P with gluconeogenic precursors as substrate.

The following conclusions can be drawn: first, that metformin has converse metabolic effects from AMPK activators on gluconeogenic flux, glycolytic flux and cellular levels of G6P. It can be concluded therefore that in conditions of maintained ATP levels, metformin inhibits gluconeogenesis and lowers cell G6P, most likely by an AMPK-independent mechanism. Second, since high concentrations of metformin (0.5 mM) induce activation of AMPK as shown by phosphorylation of ACC (figure 3.13 D), it can be

inferred that the AMPK-independent effect(s) of metformin predominate over the effect elicited by AMPK activation.

3.3 Metformin counteracts the effect of high glucose on hepatic gene expression

High glucose causes repression of GK expression and induction of glucose 6-phosphatase (G6pc) (which catalyses the final step of gluconeogenesis) and pyruvate kinase (Pklr) (which catalyses the transphosphorylation of phosphoenolpyruvate into pyruvate and ATP in the rate limiting step of glycolysis) in hepatocytes (Arden et al., 2011). These pathological changes associated with elevated glucose are often described as glucotoxicity as stimulation of gluconeogenesis in response to hyperglycaemia is counterintuitive (Gautier-Stein et al., 2012; Fujimoto et al., 2006). However, this mechanism benefits hepatocytes, maintaining intracellular homeostasis of phosphorylated intermediates such as G6P (Agius., 2015). Both G6pc and Pklr expression are regulated by the transcription factor ChREBP-Mlx in response to elevated concentrations of intracellular G6P (Towle et al., 1997; Argaud et al., 1997; Dentin et al., 2012), and expression of these genes correlates negatively with intracellular G6P, whereas GK mRNA expression correlates positively with cell G6P (Al-Oanzi et al., 2017). We therefore tested whether the changes in cell G6P with metformin correlated with changes in glucose regulated gene expression and whether these changes were mimicked by an AMPK activator.

The gene expression studies were conducted in conditions of high glucose. We therefore tested whether the concentrations of metformin used stimulated phosphorylation of AMPK to determine whether its effects could be AMPK dependent. Metformin at ≥ 0.5 mM stimulated phosphorylation of AMPK with 45 mM glucose, and AMPK phosphorylation by 20 μ M A769662 was comparable to that of 1.0 mM metformin (figure 3.23; figure 3.24).

First, we observed that high glucose repressed GK expression by two thirds (figure 3.25 A), induced G6pc expression 6-fold (figure 3.25 B), and induced Pklr expression by 4-fold (figure 3.25 C). Metformin counteracted the effect of high glucose on GK, G6pc and Pklr mRNA expression (figure 3.25 A, B, C) over the same concentration range (0.2-1.0 mM) that lowered cell G6P (figure 3.25 D) in the absence of ATP depletion (figure 3.25 E). The

effects of metformin on GK and G6pc were observed at concentrations that did not stimulate AMPK phosphorylation (0.2mM metformin) and also at concentrations that stimulated AMPK phosphorylation (≥ 0.5 mM metformin) (figure 3.23; figure 3.24). The AMPK activator A769662 had no effect on GK expression with high glucose (figure 3.25 A) but did partially counteract the effect of high glucose on G6pc and Pklr expression, although to a lesser extent than metformin (figure 3.25 B, C). This predicts an effect of therapeutic loads of metformin in attenuating the effects of high glucose on hepatic gene regulation. Although metformin at 1.0mM stimulated AMPK phosphorylation comparably to A769662 (figure 4.24 A), its effects on gene expression were greater suggesting that the mechanism for this cannot be fully explained by AMPK activation.

	G6P (nmol/mg protein)	ATP (nmol/mg protein)
5mM Glucose	1.6 ± 0.3	25.0 ± 2.0
5mM Glucose + S4048	1.7 ± 0.2	25.8 ± 3.0
25mM Glucose	6.8 ± 0.5	26.2 ± 2.2
25mM Glucose + S4048	69.2 ± 7.4	22.3 ± 2.3
5mM DHA	6.3 ± 0.7	20.2 ± 1.0
5mM DHA + S4048	51 ± 4.6	16.5 ± 0.8

Table 3-1 Control metabolite results for rat hepatocytes expressed in nmol/mg protein

Where metabolite results for control values are expressed as 100% in rat hepatocytes, they correspond to the cell metabolite concentration in nmol/mg protein in Table 3-1. Hepatocytes were pre-incubated in the absence of glucose or with 5mM glucose for 2 hours, then the indicated substrate for 1 hour. Mean ± SEM, n=8-17.

	25mM Glucose	25mM Glucose + S4048
G6P (nmol/mg protein)	2.3 ± 0.6	8.5 ± 0.8
ATP (nmol/mg protein)	9.1 ± 0.3	10.4 ± 0.3
Lactate + Pyruvate (nmol/mg protein)	542 ± 25	697 ± 24

Table 3-2 Control metabolite results for mouse hepatocytes expressed in nmol/mg protein

Where metabolite results for control values are expressed as 100% in mouse hepatocytes, they correspond to the cell metabolite concentration in nmol/mg protein in Table 3-1. Hepatocytes were pre-incubated in the absence of glucose or with 5mM glucose for 2 hours, then the indicated substrate for 1 hour. Mean ± SEM, n=6-135.

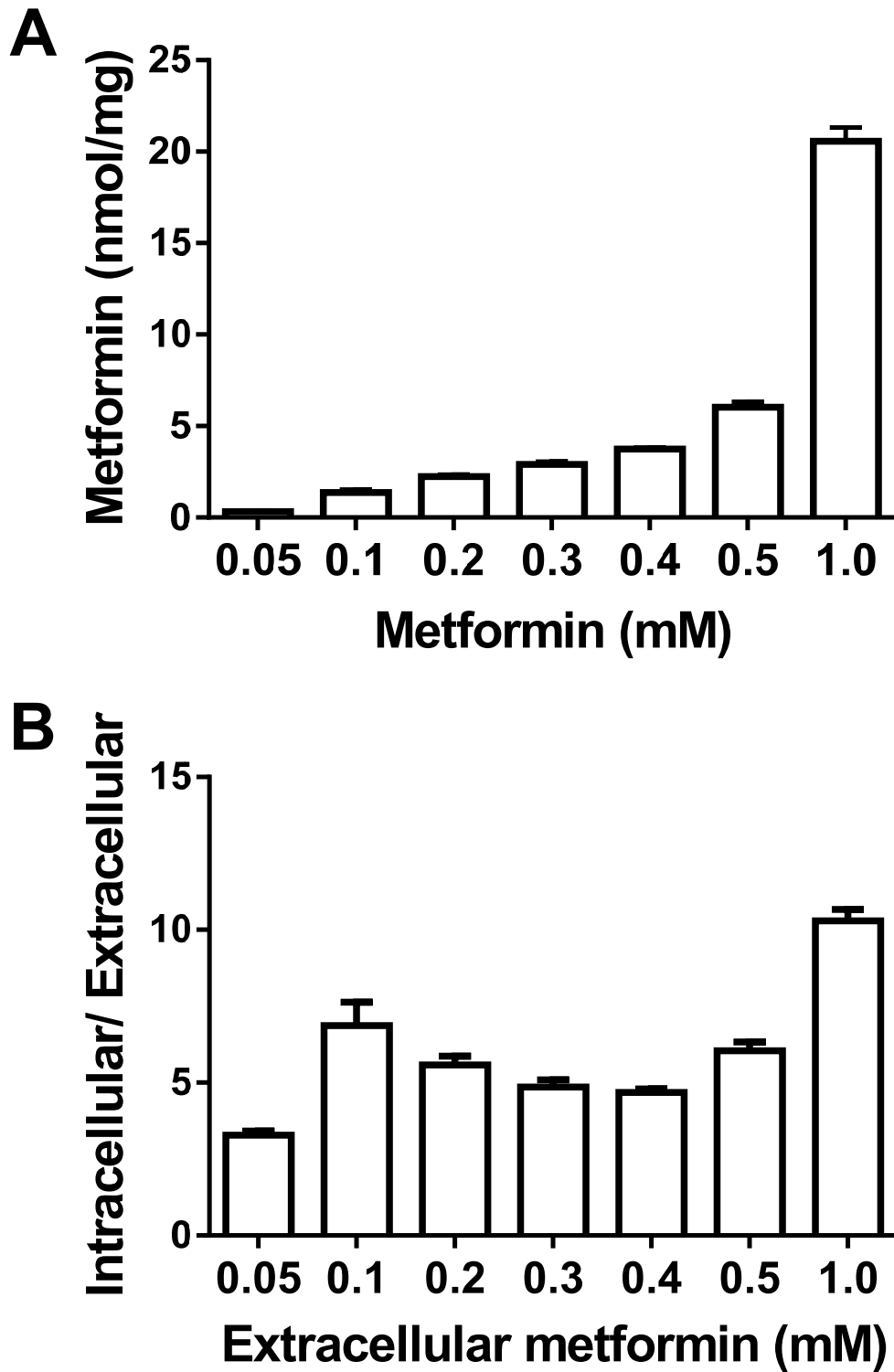


Figure 3.1 Cell metformin content and intracellular to extracellular metformin ratio in mouse hepatocytes

Mouse hepatocytes were incubated with [14 C] metformin and varying metformin concentrations for 2 hours, then 25mM glucose for a further 1 hour. Mean \pm SEM, n=2-10.

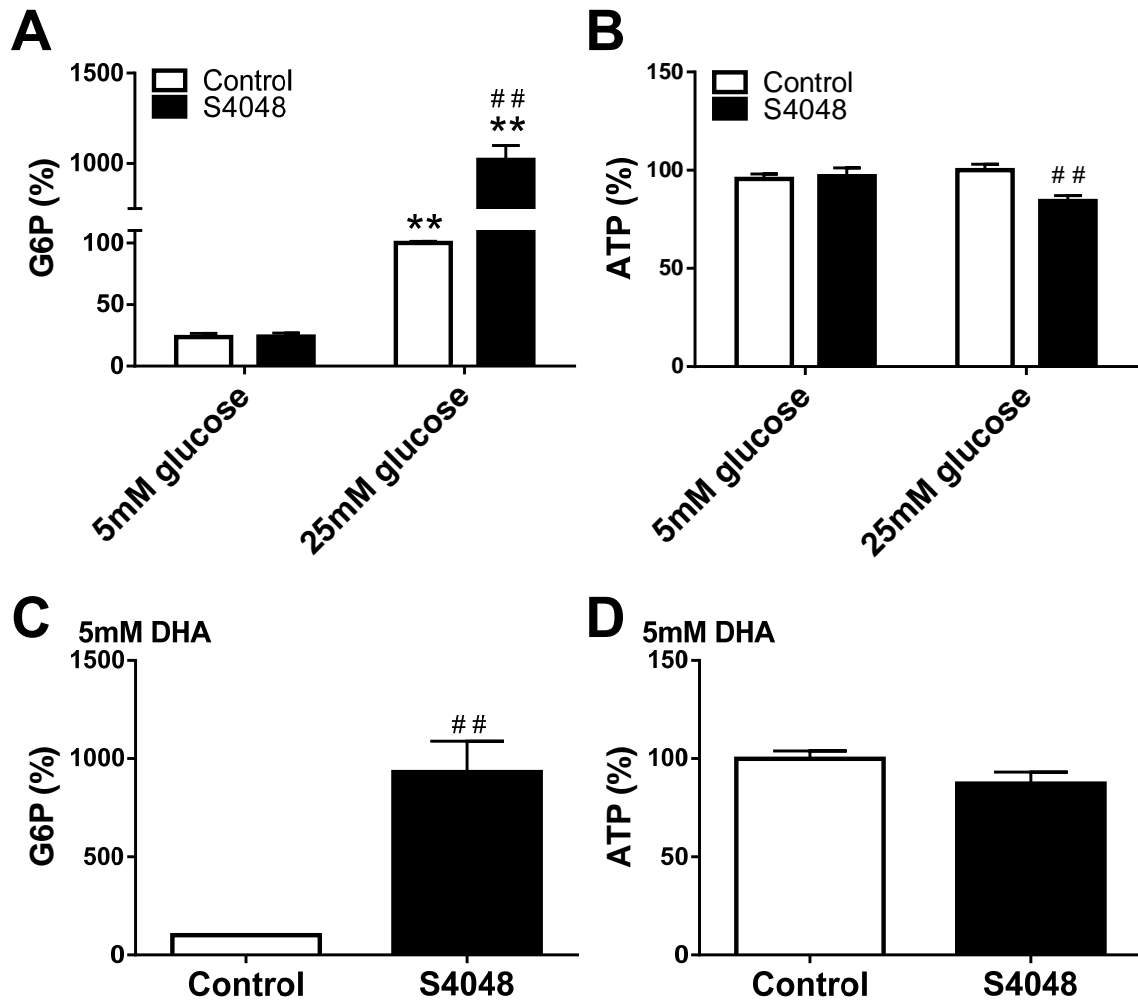


Figure 3.2 The chlorogenic acid derivative, S4048 increases cell G6P with high glucose or with gluconeogenic precursors

Rat hepatocytes were pre-incubated in the absence (white) or presence (black) of 0.2-2 μ M S4048 for 2 hours, then incubated for a further 1 hour with either 5mM glucose, 25mM glucose or 5mM DHA. Mean \pm SEM, n=4. **P<0.01 glucose effect. ## P<0.01 S4048 effect. Basal values were as in Table 3-1.

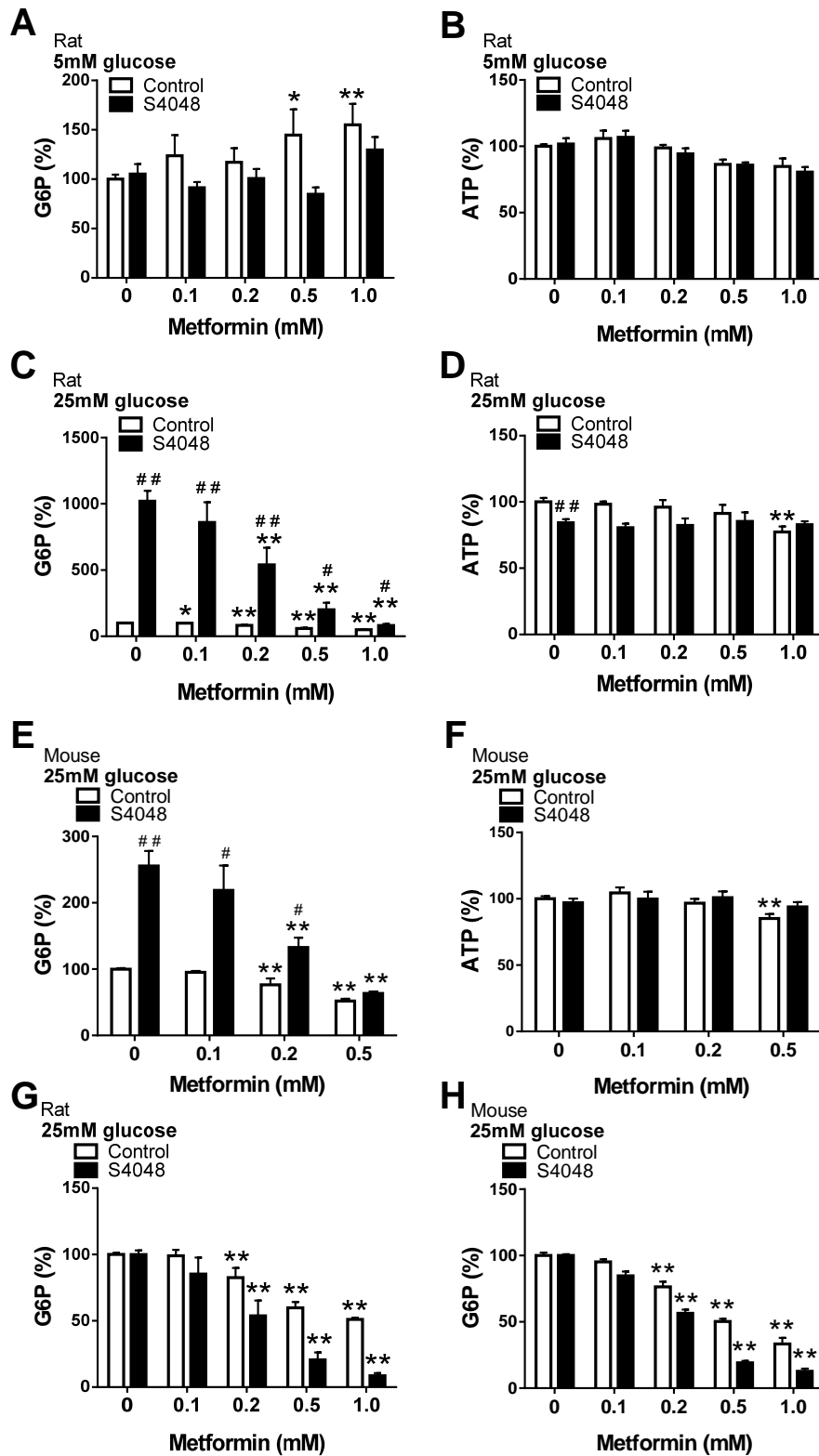


Figure 3.3 Metformin lowers G6P in hepatocytes with high glucose as substrate

Rat (A-D, G) and mouse (E, F, H) hepatocytes were pre-incubated in the absence (white) or presence (black) of 0.2–2 μ M S4048 and with metformin for 2 hours, then incubated for a further 1 hour with either 5mM glucose (A, B) or 25mM glucose (C-H). Mean \pm SEM, n=3-7. *P<0.05, **P<0.01 metformin effect. # P<0.05, ## P<0.01 S4048 effect. Basal values were as in Table 3-1 and Table 3-2.

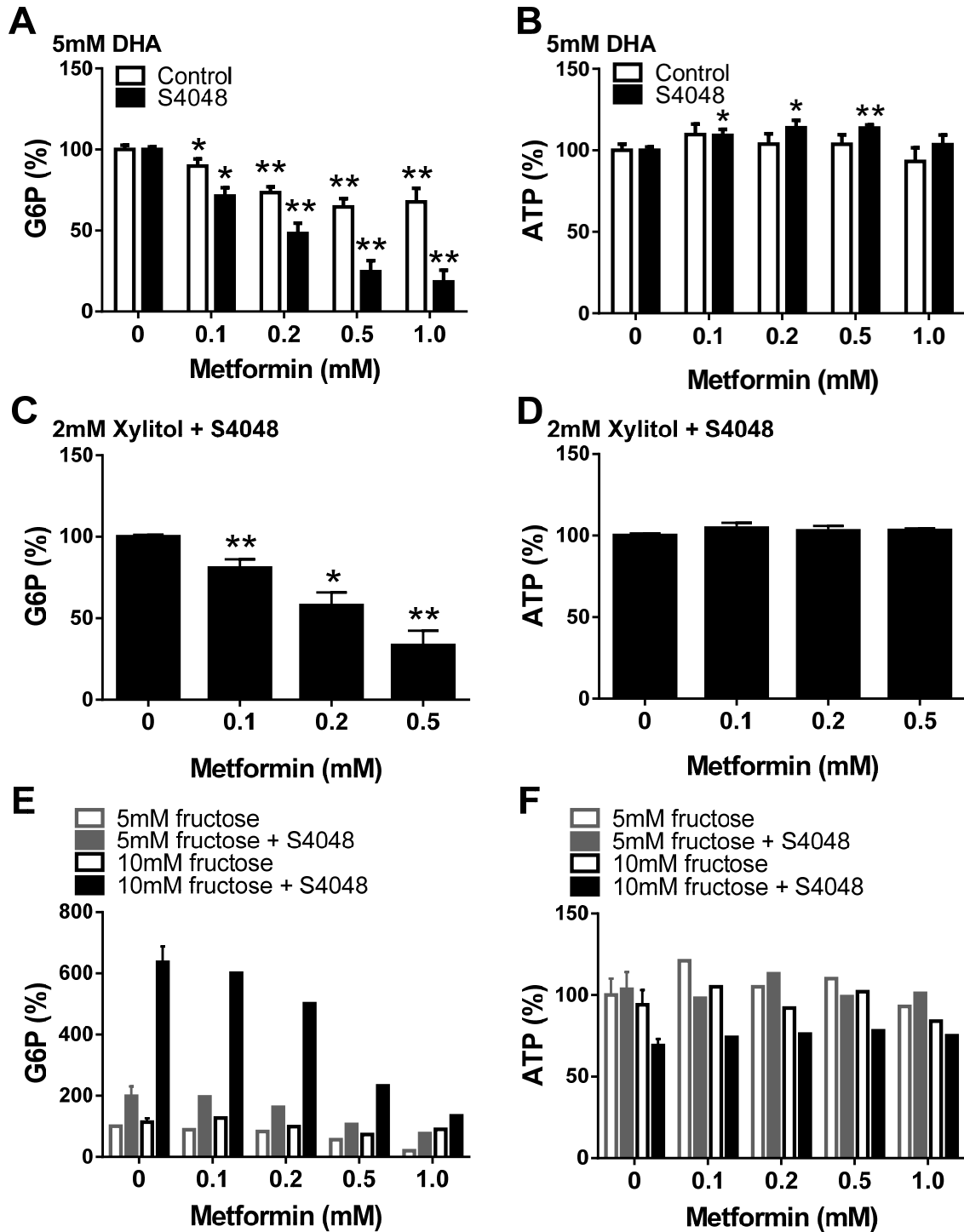


Figure 3.4 Metformin lowers G6P but not ATP in hepatocytes with gluconeogenic precursors as substrate

Rat hepatocytes were pre-incubated in the absence or presence of $2\mu\text{M}$ S4048 and metformin for 2 hours, then incubated for a further 1 hour with either 5mM DHA (A, B), 2mM xylitol (C, D) or 5-10mM fructose (E, F). Mean \pm SEM, (A-D) $n=3-7$, (E, F) $n=1$. * $P<0.05$, ** $P<0.01$ metformin effect.

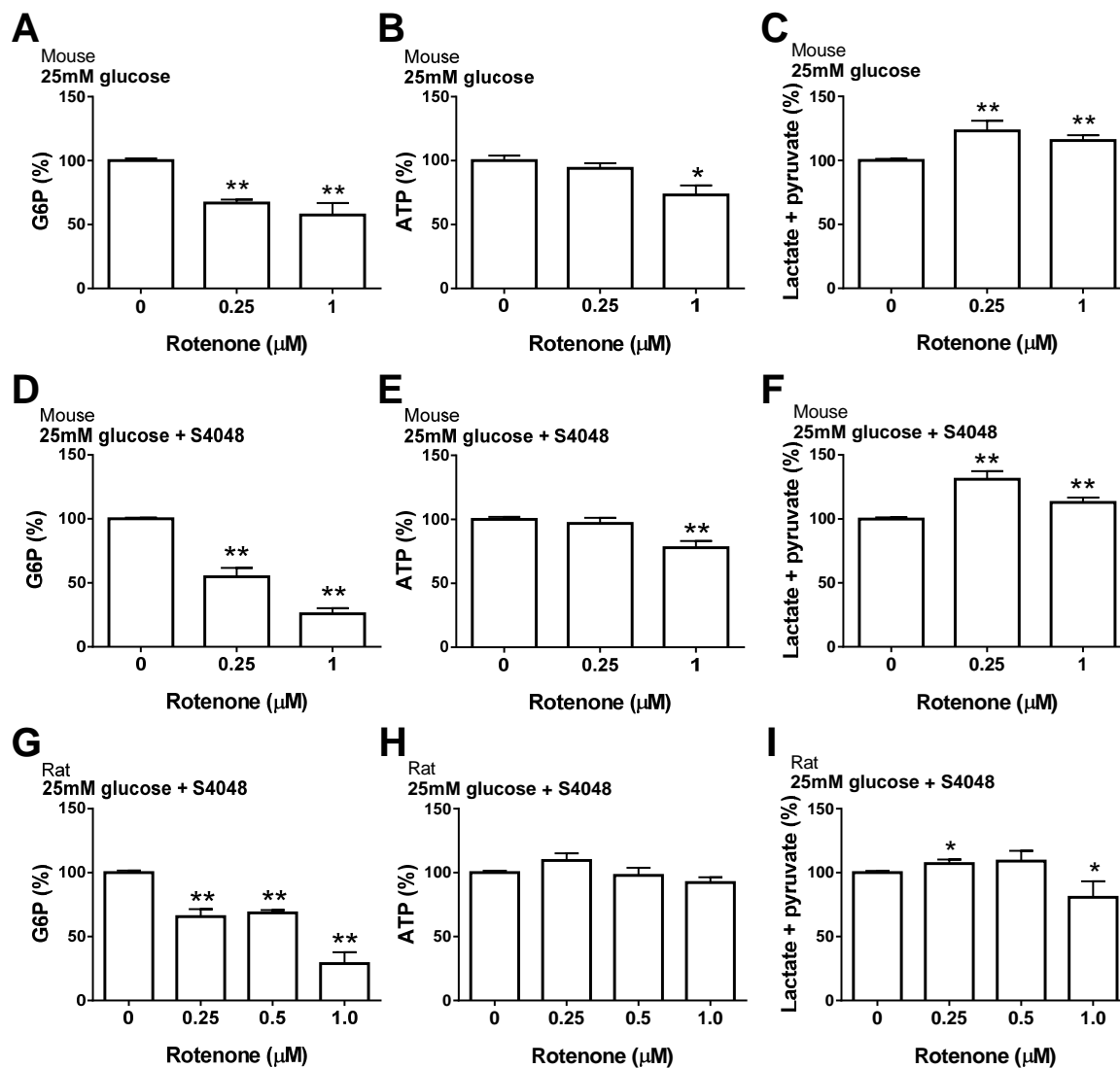


Figure 3.5 Rotenone lowers G6P and increases lactate and pyruvate production in hepatocytes

Mouse (A-F) and rat (G-I) hepatocytes were pre-incubated in the absence (A-C) or presence (D-I) of 0.2-2 μM S4048 and with rotenone for 2 hours, then incubated for a further 1 hour with 25mM glucose. Mean \pm SEM, n=2-10. *P<0.05, **P<0.01. Basal values were as in Table 3-1 and Table 3-2.

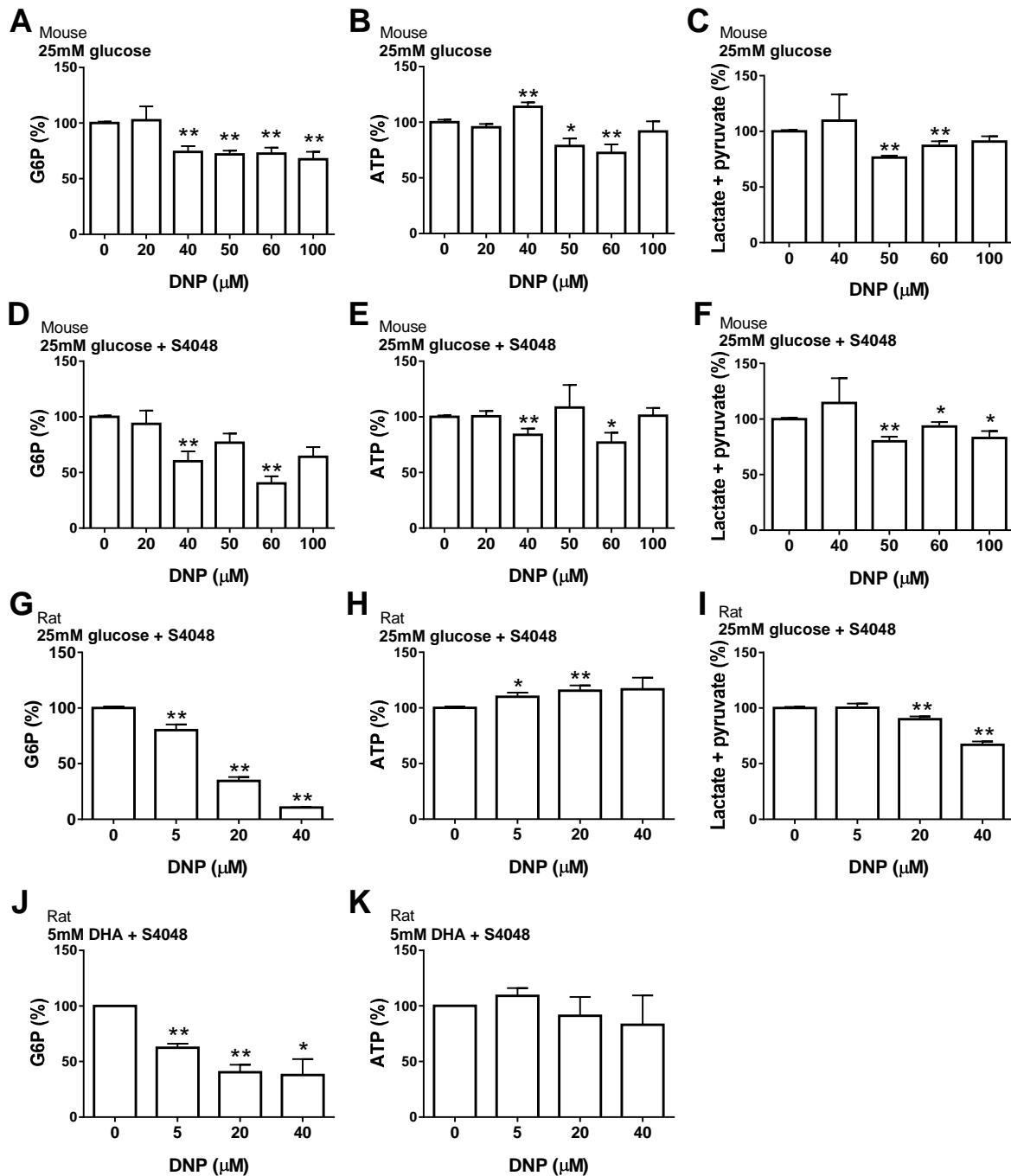


Figure 3.6 DNP lowers both G6P and lactate and pyruvate production with high glucose and gluconeogenic precursors as substrate

Mouse (A-F) and rat (G-K) hepatocytes were pre-incubated in the absence (A-C) or presence (D-K) of 0.2-2 μM S4048 and with DNP for 2 hours, then incubated for a further 1 hour with 25mM glucose (A-I) or 5mM DHA (J, K). Mean \pm SEM, n=2-10. *P<0.05, **P<0.01. Basal values were as in Table 3-1 and Table 3-2.

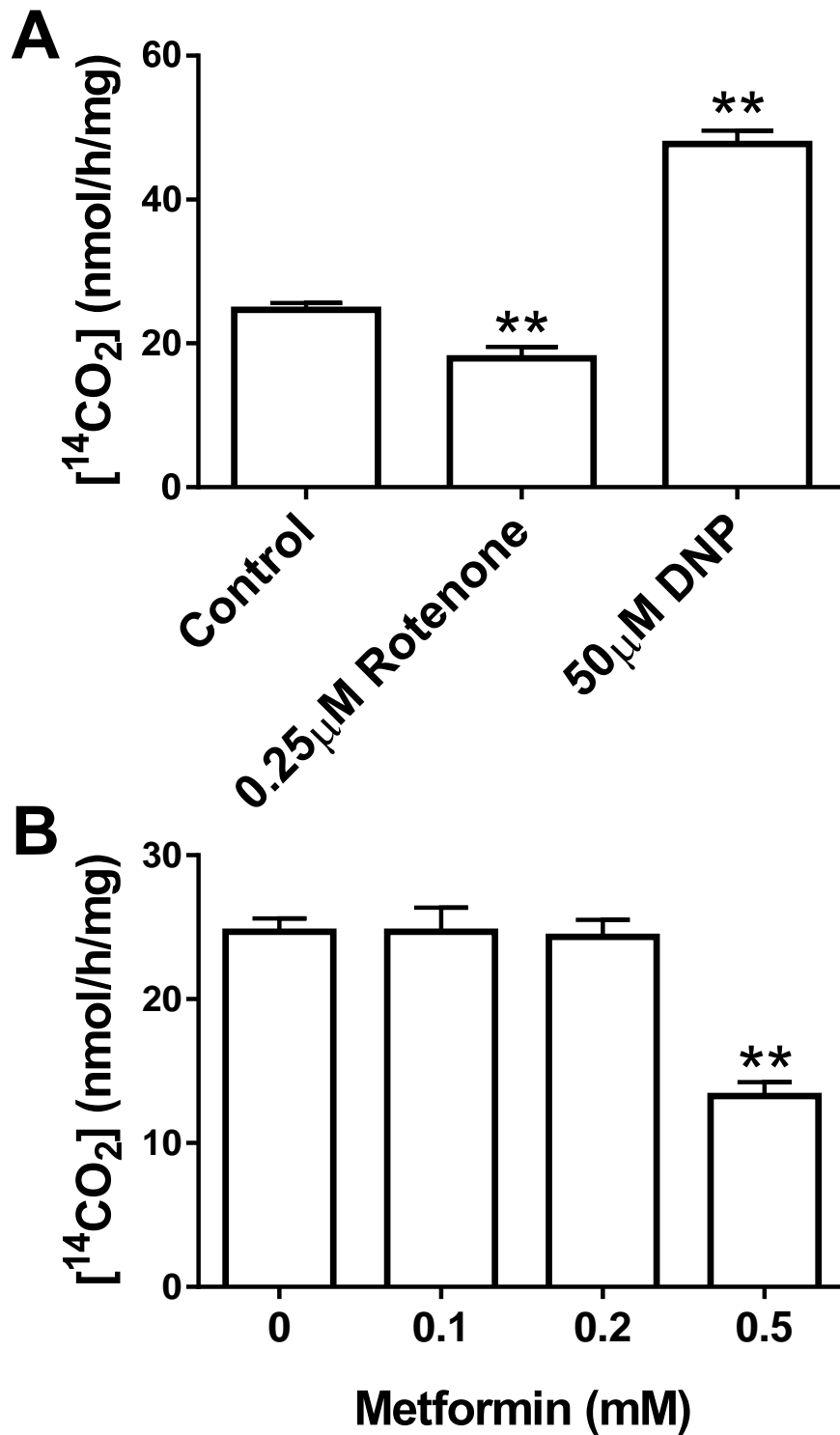


Figure 3.7 Glucose oxidation is stimulated by DNP and inhibited by both rotenone and a high metformin concentration

Mouse hepatocytes were pre-incubated with 0.2 μM S4048 and metformin for 2 hours, then a further 1 hour with 15mM glucose and [$\text{U-}^{14}\text{C}$] glucose and either rotenone or DNP. Mean \pm SEM, n=3. *p<0.05, **p<0.01.

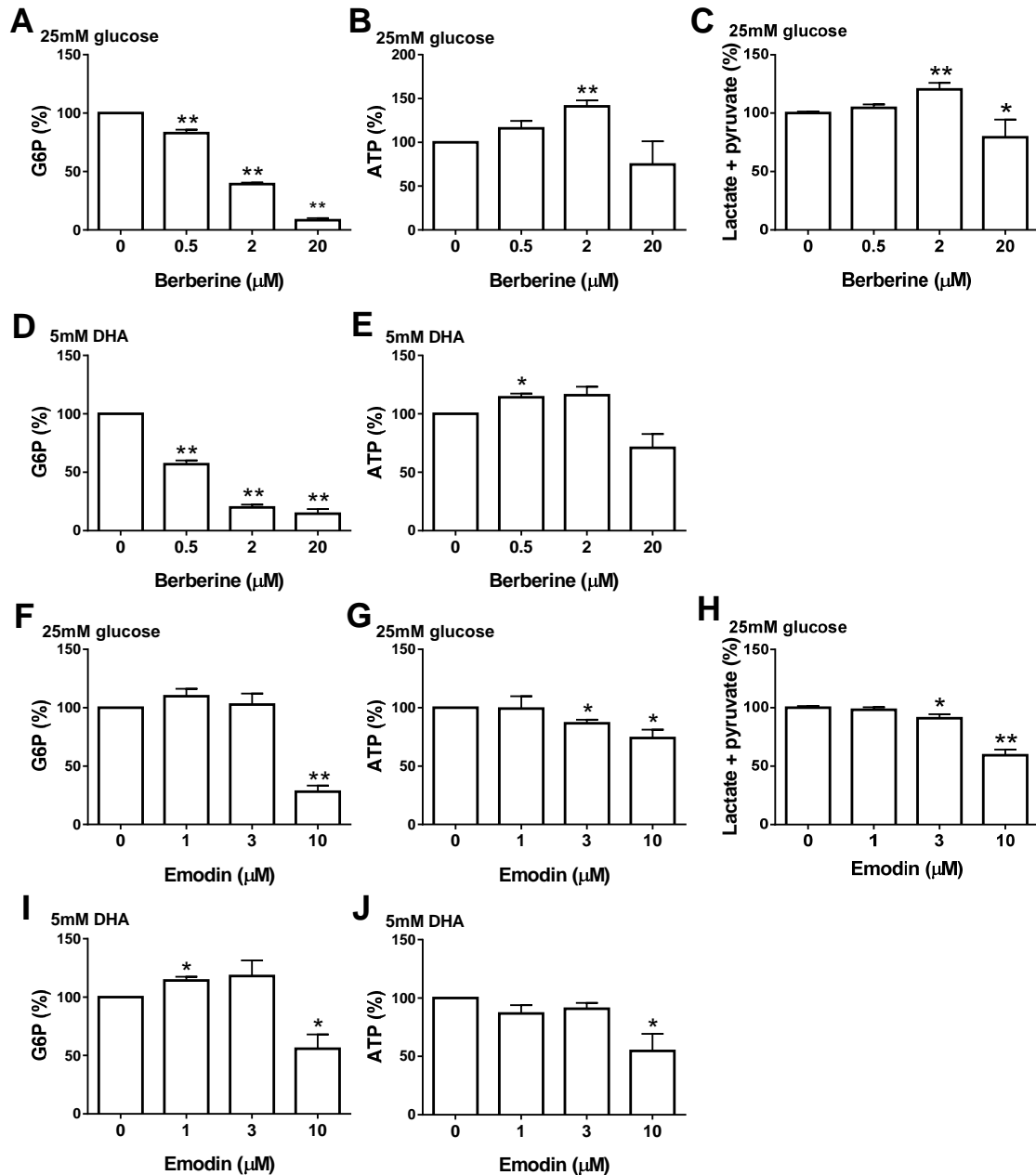


Figure 3.8 Berberine mimics the effect of metformin on G6P and lactate and pyruvate production

Rat hepatocytes were pre-incubated 0.2-2 μM S4048 and berberine (A-E) or emodin (F-J) for 2 hours, then incubated for a further 1 hour with 25mM glucose (A-C, F-H) or 5mM DHA (D, E, I, J). Mean ± SEM, n=2-3. *P<0.05, **P<0.01. Basal values were as in Table 3-1 and Table 3-2.

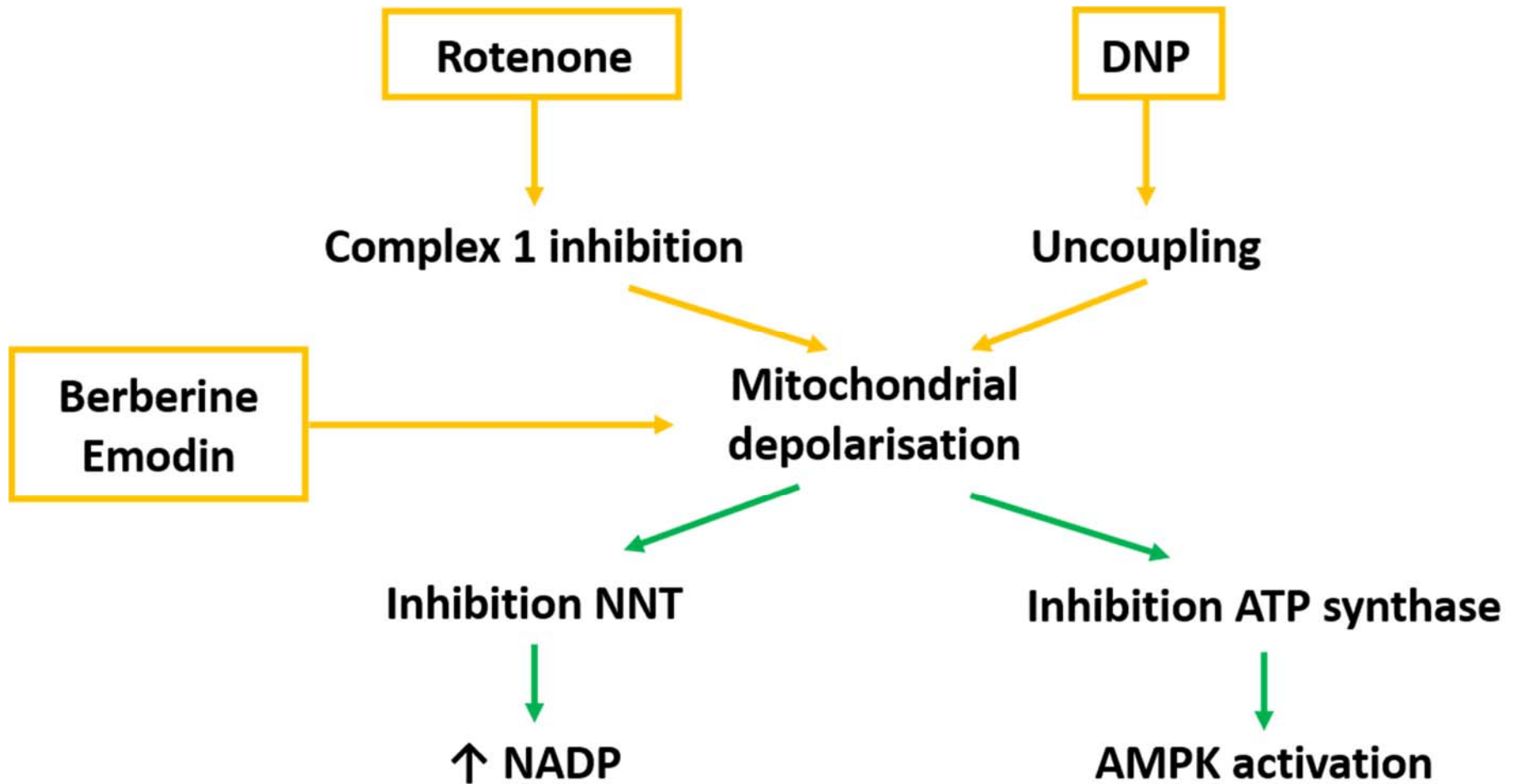


Figure 3.9 Possible consequences of mitochondrial depolarisation

Mitochondrial depolarisation by rotenone, DNP, berberine and emodin via inhibition of complex 1 or mitochondrial uncoupling diminishes the proton gradient which could result in inhibition of NNT and subsequently raised NADP, or inhibition of ATP synthase and subsequent AMPK activation.

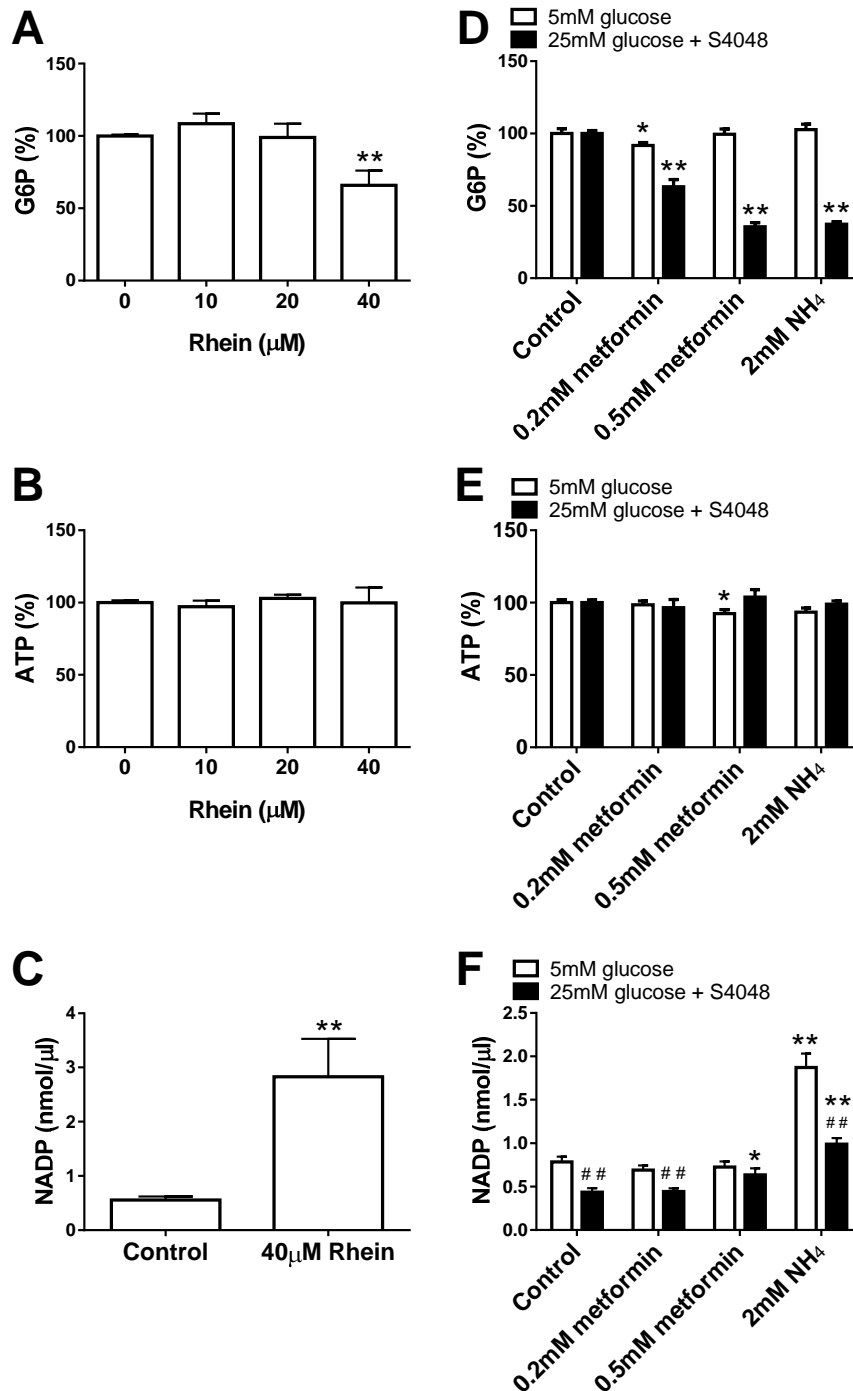


Figure 3.10 Elevation in NADP by Rhein, metformin and ammonium ion

Rat hepatocytes were pre-incubated with 2 μM S4048 and rhein for 2 hours, and a further 1 hour with 25mM glucose (A-C). Hepatocytes were pre-incubated in the absence or presence of 0.2-2 μM S4048 and metformin for 2 hours, and a further 1 hour with 2mM ammonium (NH₄) and either 5mM glucose or 25mM glucose (D-F). Mean \pm SEM, n=2-7. *p<0.05, **p<0.01 rhein/ metformin/ ammonium effect. # P<0.05, ## P<0.01 glucose effect.

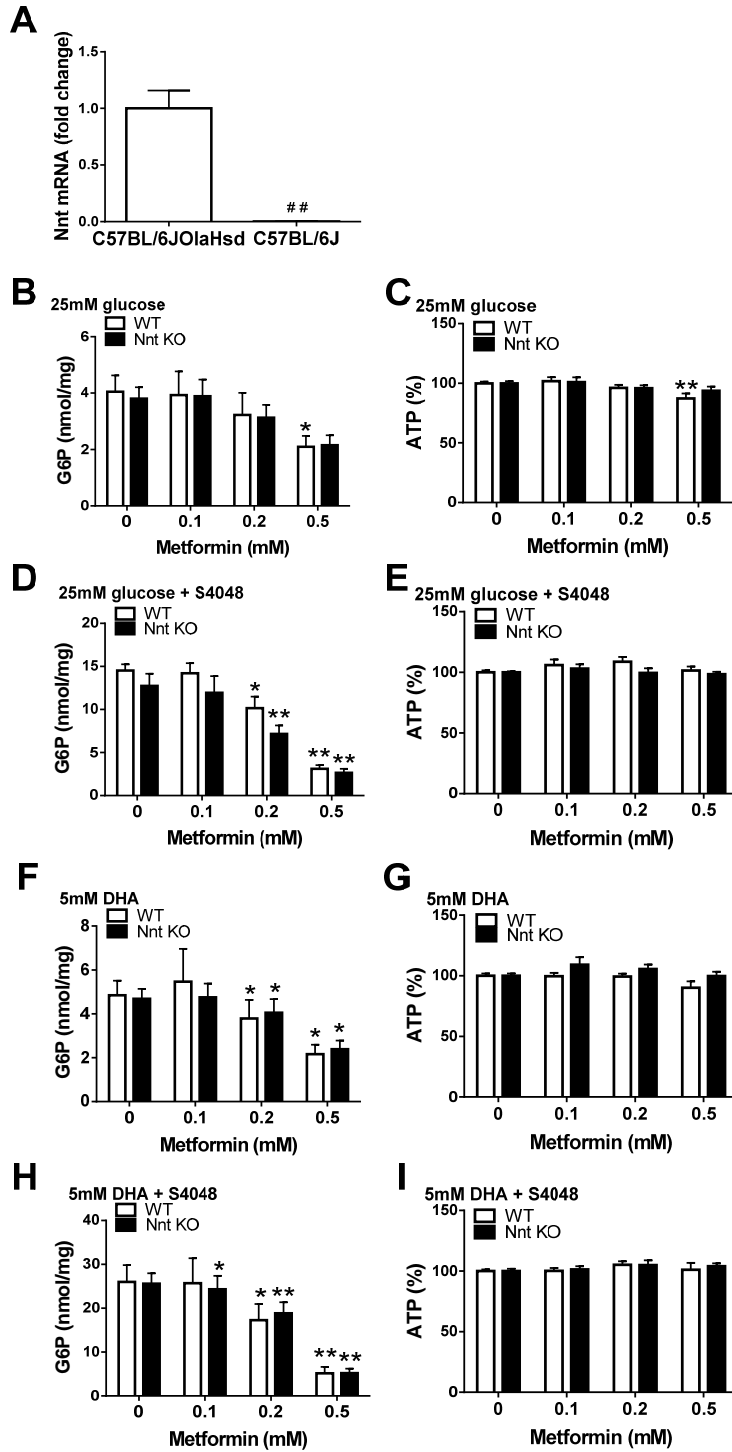


Figure 3.11 Metformin lowers G6P in hepatocytes from mice with a deletion in the NNT gene

(A) Nnt mRNA in mouse hepatocytes. Mean \pm SEM, $n=6$. **(B-I)** Mouse hepatocytes were pre-incubated with metformin for 2 hours in the absence (B, C, F, G) or presence (D, E, H, I) of $2\mu\text{M}$ S4048 and for a further 1 hour with either 25mM glucose (B-E) or 5mM DHA (F-I). Mean \pm SEM, $n=4-8$. * $p<0.05$, ** $p<0.01$ metformin effect. ## $p<0.01$ NNT knockout effect.

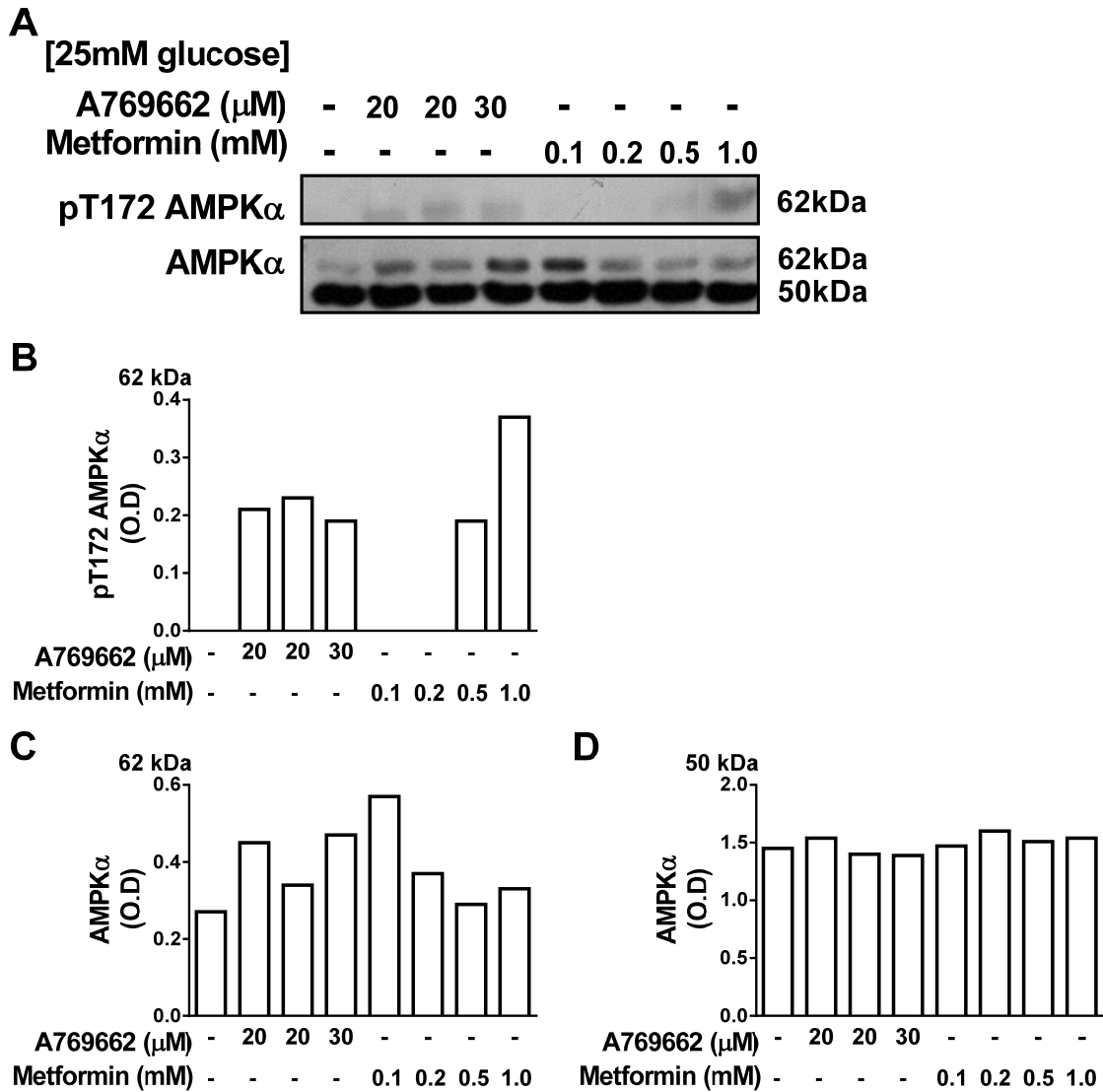


Figure 3.12 Stimulation of AMPK phosphorylation by high metformin is comparable with A769662 with high glucose

Rat hepatocytes were pre-incubated with metformin or A769662 for 2 hours, then for a further 1 hour with 25mM glucose. Cell extracts were immunoblotted for pT172 AMPK α and total AMPK α (A), and optical density (O.D) was calculated (B, C, D). AMPK α is variable (C), although a 50kDa non-specific band was also detected (A, D) suggesting equal loading concentrations of samples, which indicates stripping buffer for re-probing may be responsible for variable AMPK α .

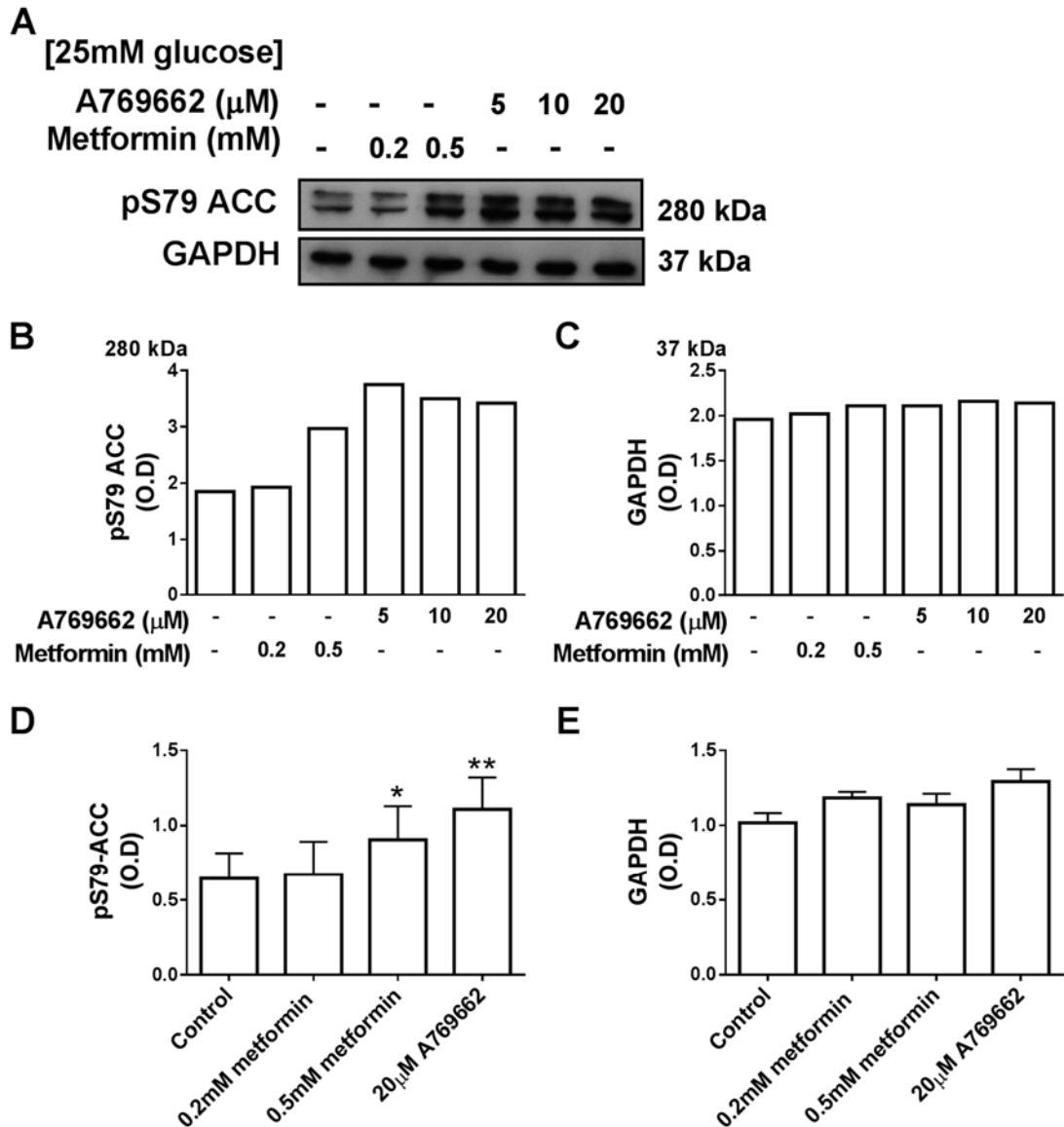


Figure 3.13 Stimulation of ACC phosphorylation by high metformin is comparable with A769662 with high glucose

Rat hepatocytes were pre-incubated with metformin or A769662 for 2 hours, then for a further 1 hour with 25mM glucose. Cell extracts were immunoblotted for pS79 ACC and GAPDH (A) and optical density (*O.D*) was calculated (B, C). (D, E) Mean *O.D* \pm SEM of $n=6$ experiments.

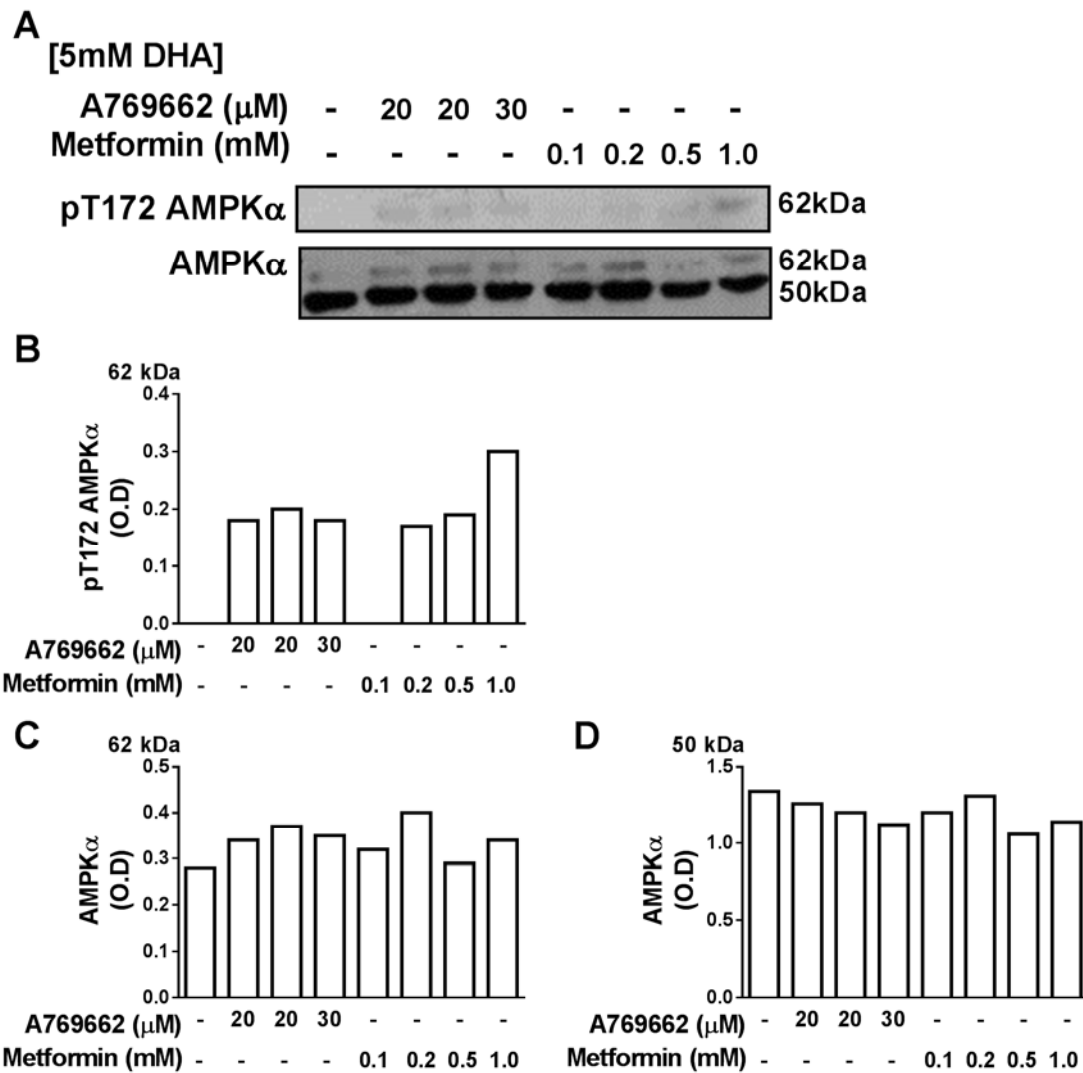


Figure 3.14 Stimulation of AMPK phosphorylation by high metformin and A769662 is comparable with a gluconeogenic substrate

Rat hepatocytes were pre-incubated with metformin or A769662 for 2 hours and for a further 1 hour with 5mM DHA. Cell extracts were immunoblotted for pT172 AMPK α and total AMPK α (A), and optical density (*O.D.*) was calculated (B, C, D). AMPK α is variable (C), although a 50kDa non-specific band was also detected (A, D) suggesting equal loading concentrations of samples, which indicates stripping buffer for re-probing may be responsible for variable AMPK α .

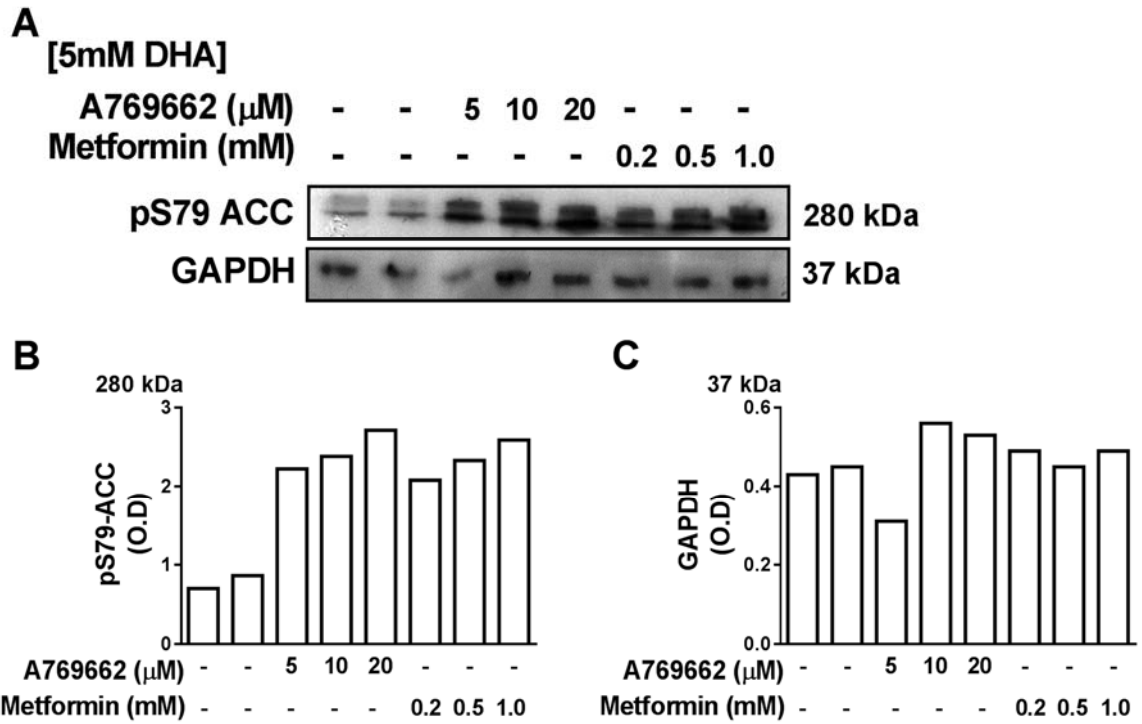


Figure 3.15 Stimulation of ACC phosphorylation by metformin is comparable with A769662 with a gluconeogenic substrate

Rat hepatocytes were pre-incubated with metformin or A769662 for 2 hours and for a further 1 hour with 5mM DHA. Cell extracts were immunoblotted for pS79 ACC and GAPDH (A) and optical density (*O.D*) was calculated (B, C).

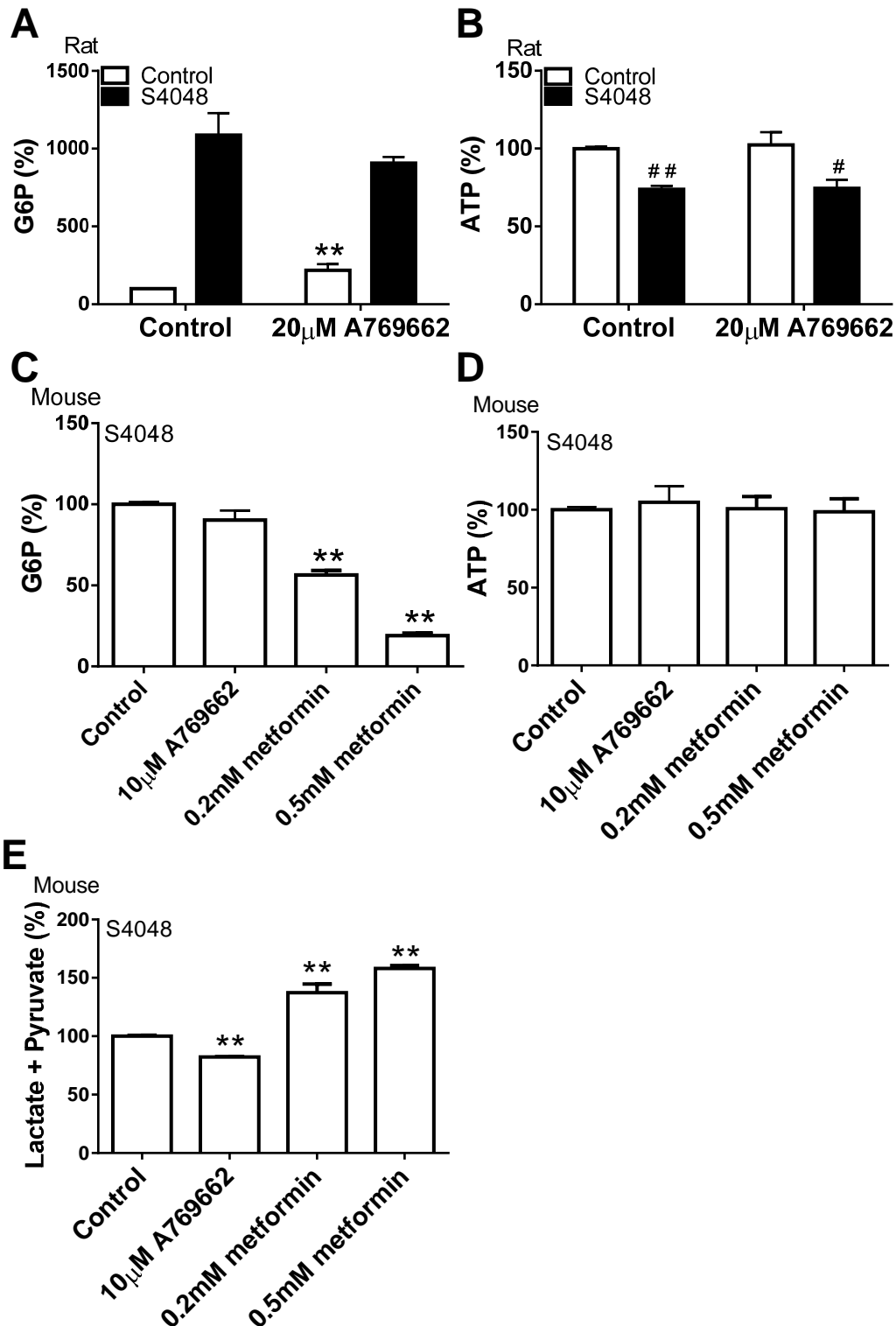


Figure 3.16 A769662 does not mimic the effect of metformin on G6P or lactate and pyruvate production

Rat (A, B) and mouse (C-E) hepatocytes were pre-incubated with 0.2-2 μ M S4048, metformin or A769662 for 2 hours, and a further 1 hour with 25mM glucose. Mean \pm SEM, n=3-11. *p<0.05, **p<0.01 A769662/ metformin/ effect. #P<0.05, ## P<0.01 S4048 effect. Basal values were as in Table 3-1 and Table 3-2.

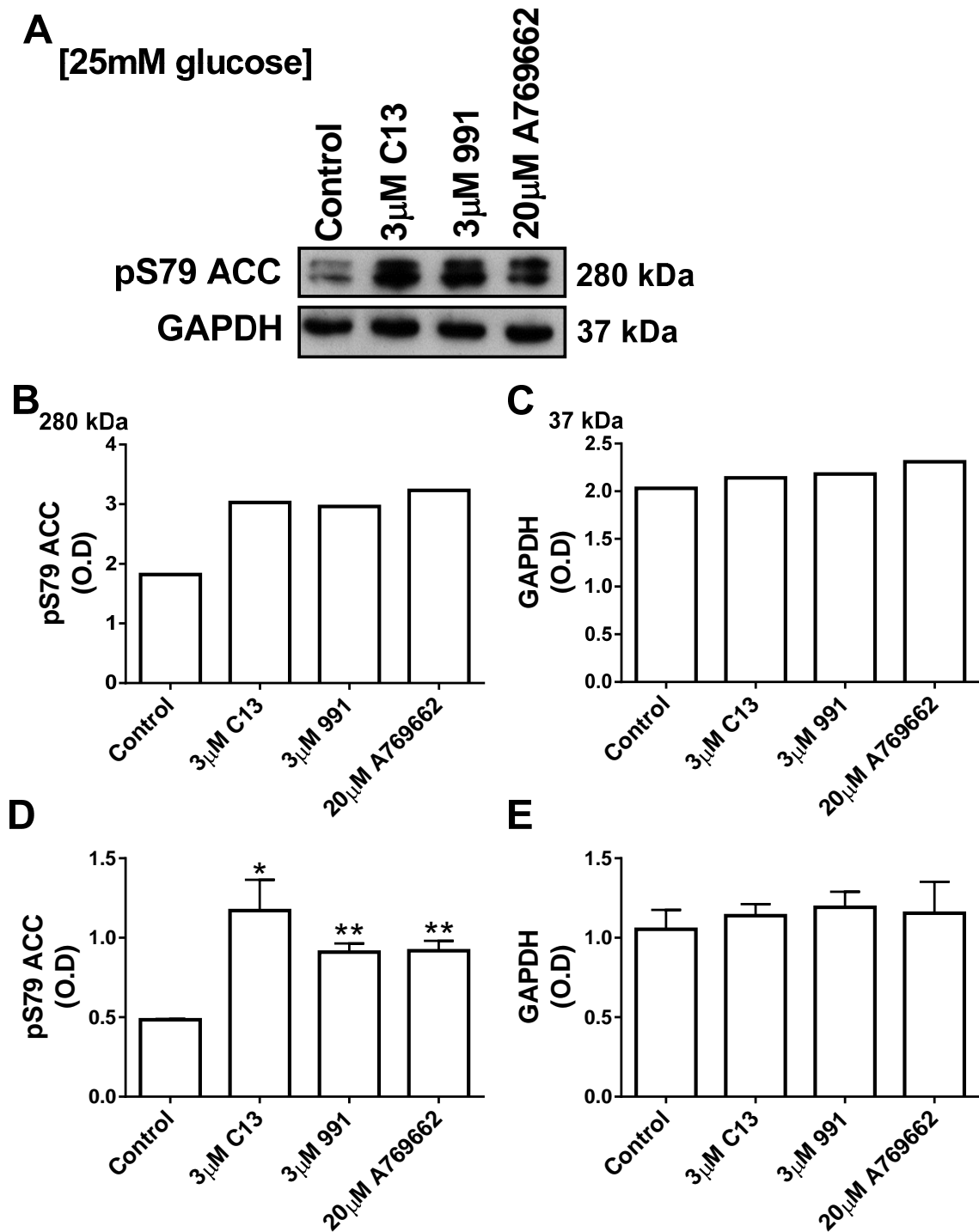


Figure 3.17 The AMPK activators C13, 991 and A769662 stimulate ACC phosphorylation with high glucose

Rat hepatocytes were pre-incubated with C13, 991 or A769662 for 2 hours and for a further 1 hour with 25mM glucose. Cell extracts were immunoblotted for pS79 ACC and GAPDH (A) and optical density (O.D) was calculated (B, C). (D, E) Mean O.D \pm SEM of n=4 experiments.

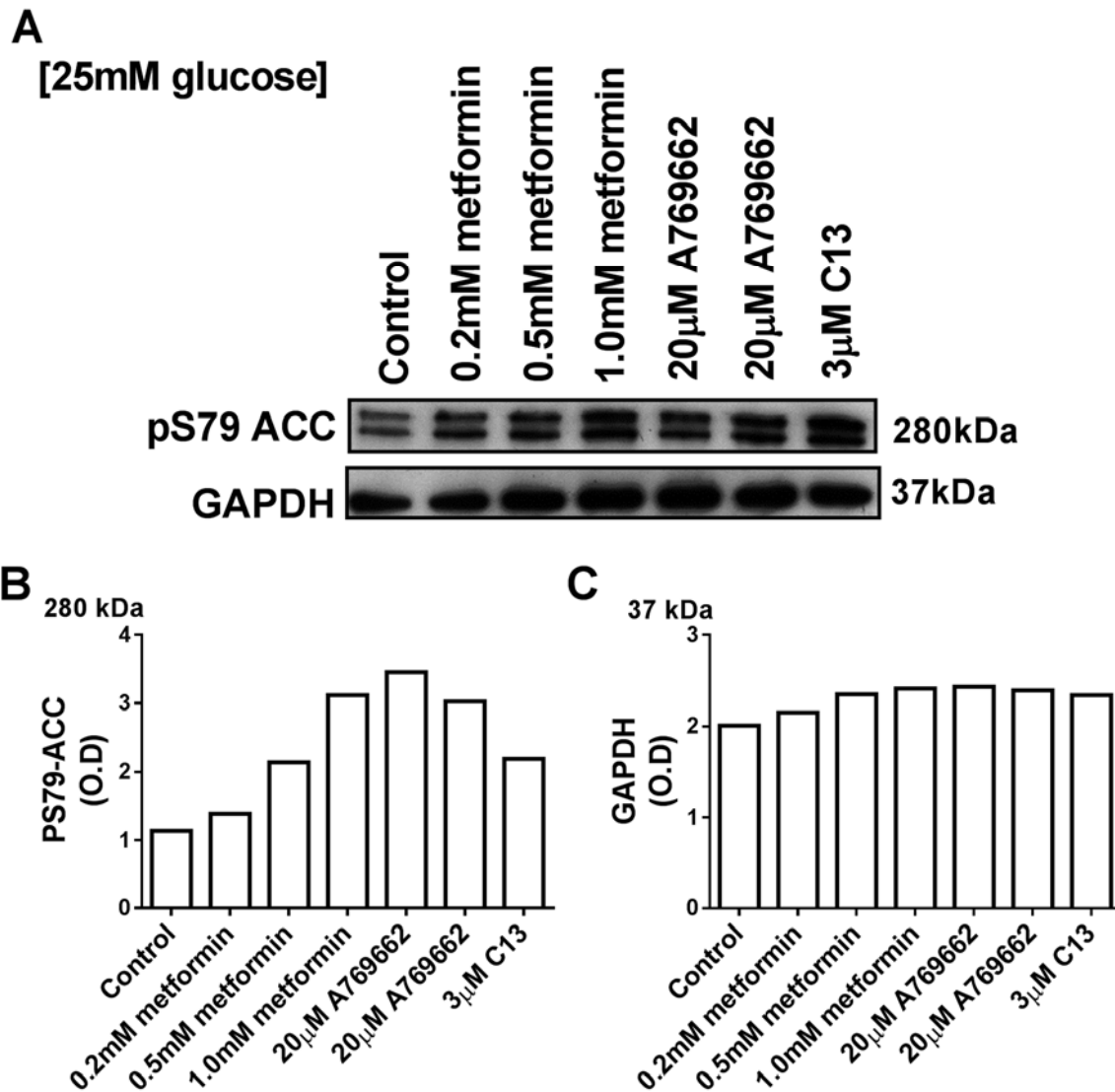


Figure 3.18 Stimulation of ACC phosphorylation by A769662 and C13 is comparable to high metformin concentrations

Rat hepatocytes were pre-incubated with metformin or A769662 for 2 hours and for a further 1 hour with 25mM glucose. Cell extracts were immunoblotted for pS79 ACC and GAPDH (A) and optical density (*O.D*) was calculated (B, C).

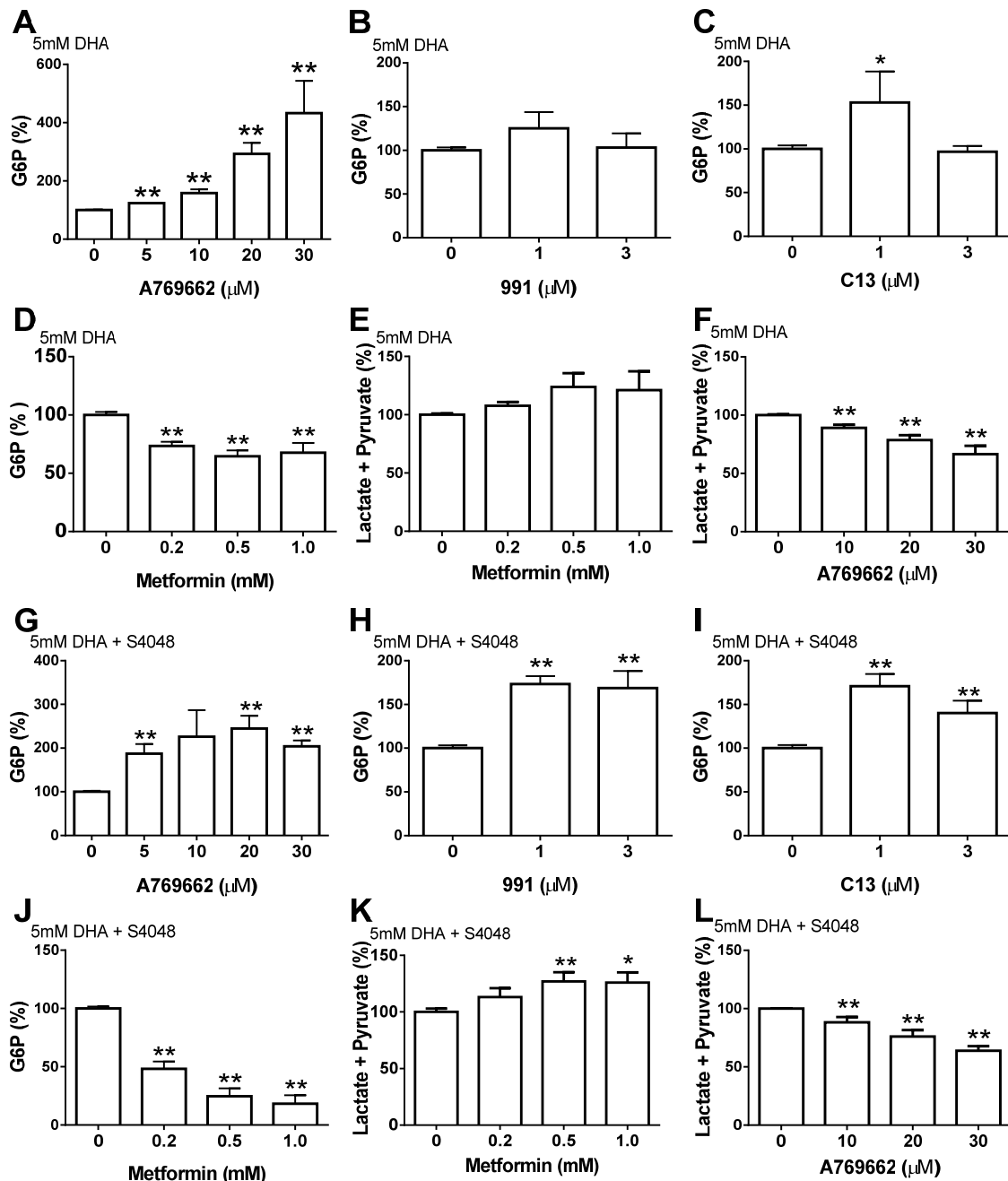


Figure 3.19 Opposite effects of AMPK activators and metformin on G6P and lactate and pyruvate production from DHA

Rat hepatocytes were pre-incubated with A769662, 991, C13 or metformin in the absence (A-F) or presence (G-L) of 0.2-2 μM S4048 for 2 hours, then for a further 1 hour with 5mM DHA. Mean \pm SEM, n=2-12. *P<0.05, **P<0.01. Basal values were as in Table 3-1 and Table 3-2.

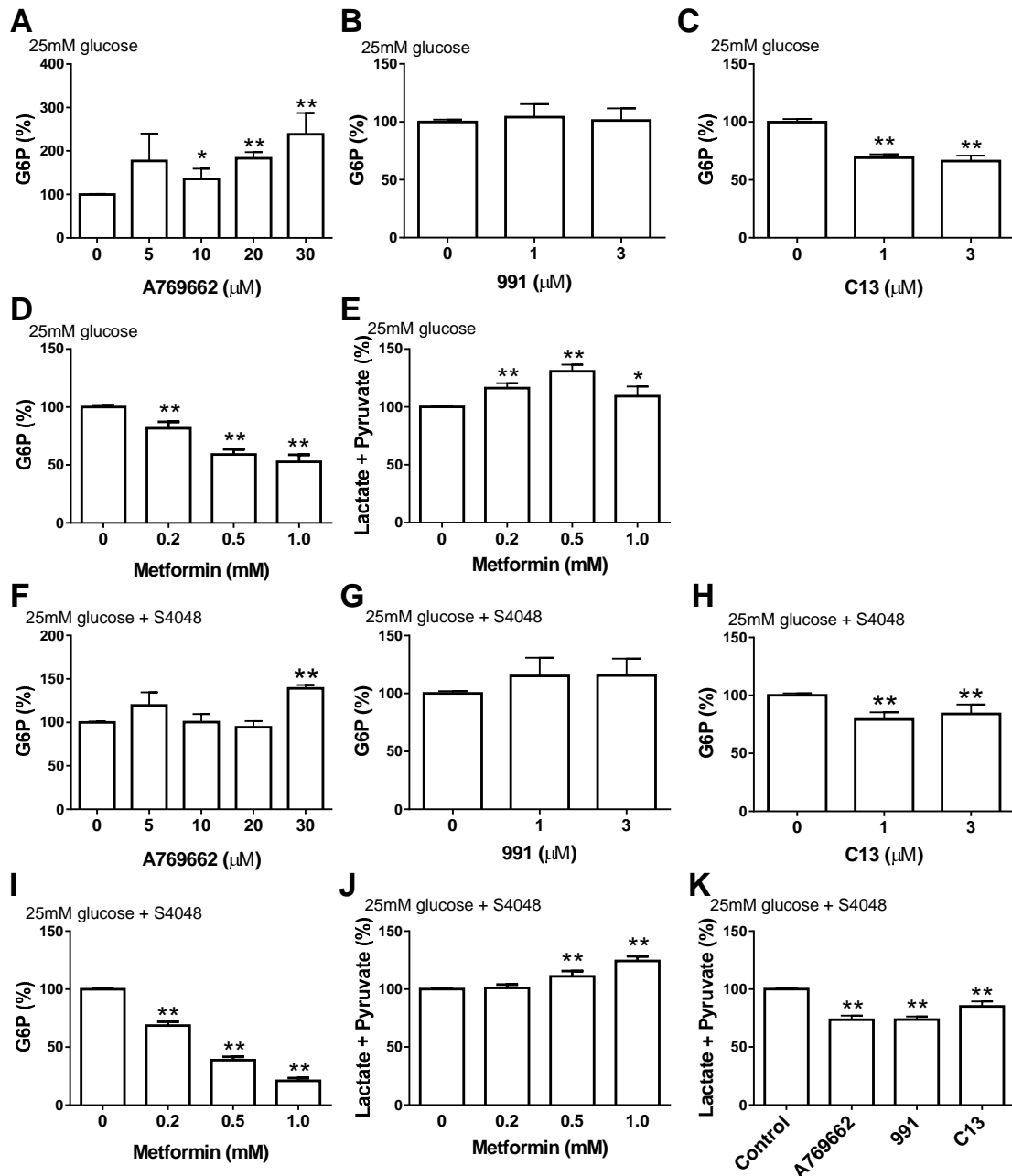


Figure 3.20 Diverse effects of AMPK activators and metformin on G6P and glycolysis

Rat hepatocytes were pre-incubated with A769662, 991 or C13 in the absence (A-E) or presence (F-K) of 0.2-2 μM S4048 for 2 hours, then for a further 1 hour with 25mM glucose. Mean \pm SEM, n=2-15. *P<0.05, **P<0.01. Basal values were as in Table 3-1 and Table 3-2.

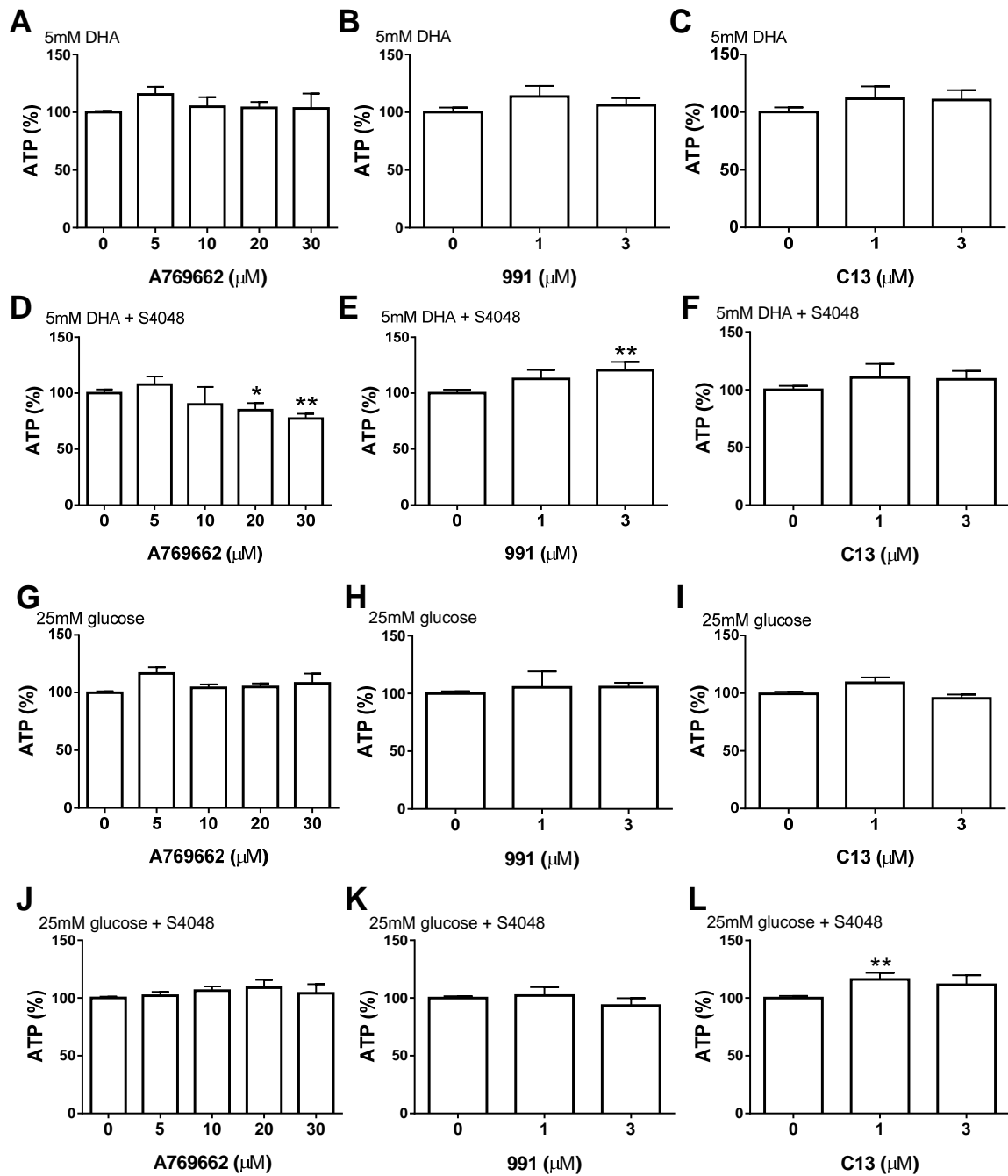


Figure 3.21 Cell ATP for experiments in figures 3.19 (A-F) and 3.20 (G-L)

Rat hepatocytes were pre-incubated with A769662, 991 or C13 in the absence or presence of 0.2-2 μM S4048 for 2 hours, then for a further 1 hour with 25mM glucose or 5mM DHA. Mean \pm SEM, n=2-15. *P<0.05, **P<0.01. Basal values were as in Table 3-1 and Table 3-2.

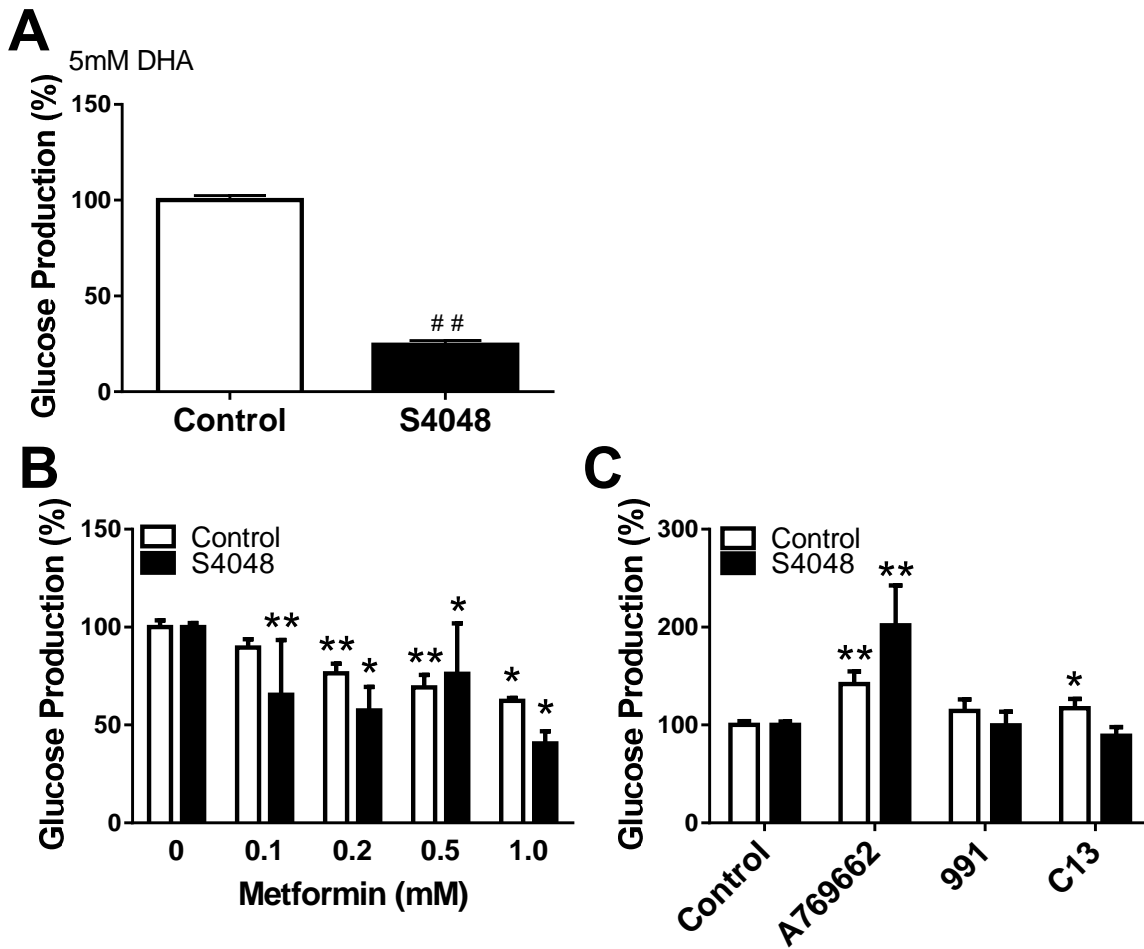


Figure 3.22 Opposite effects of metformin and AMPK activators on gluconeogenesis

Effects of S4048 (A), metformin (B) and AMPK activators (C) on glucose production. Rat hepatocytes were pre-incubated in glucose free medium with metformin, A769662, 991 or C13 in the absence (white) or presence (black) of 2 μ M S4048 for 2 hours, then for a further 2 hours with 5mM DHA. Mean \pm SEM, n=3-11. *P<0.05, **P<0.01 metformin, A769662, C13 or 991 effect. ##P<0.01 S4048 effect.

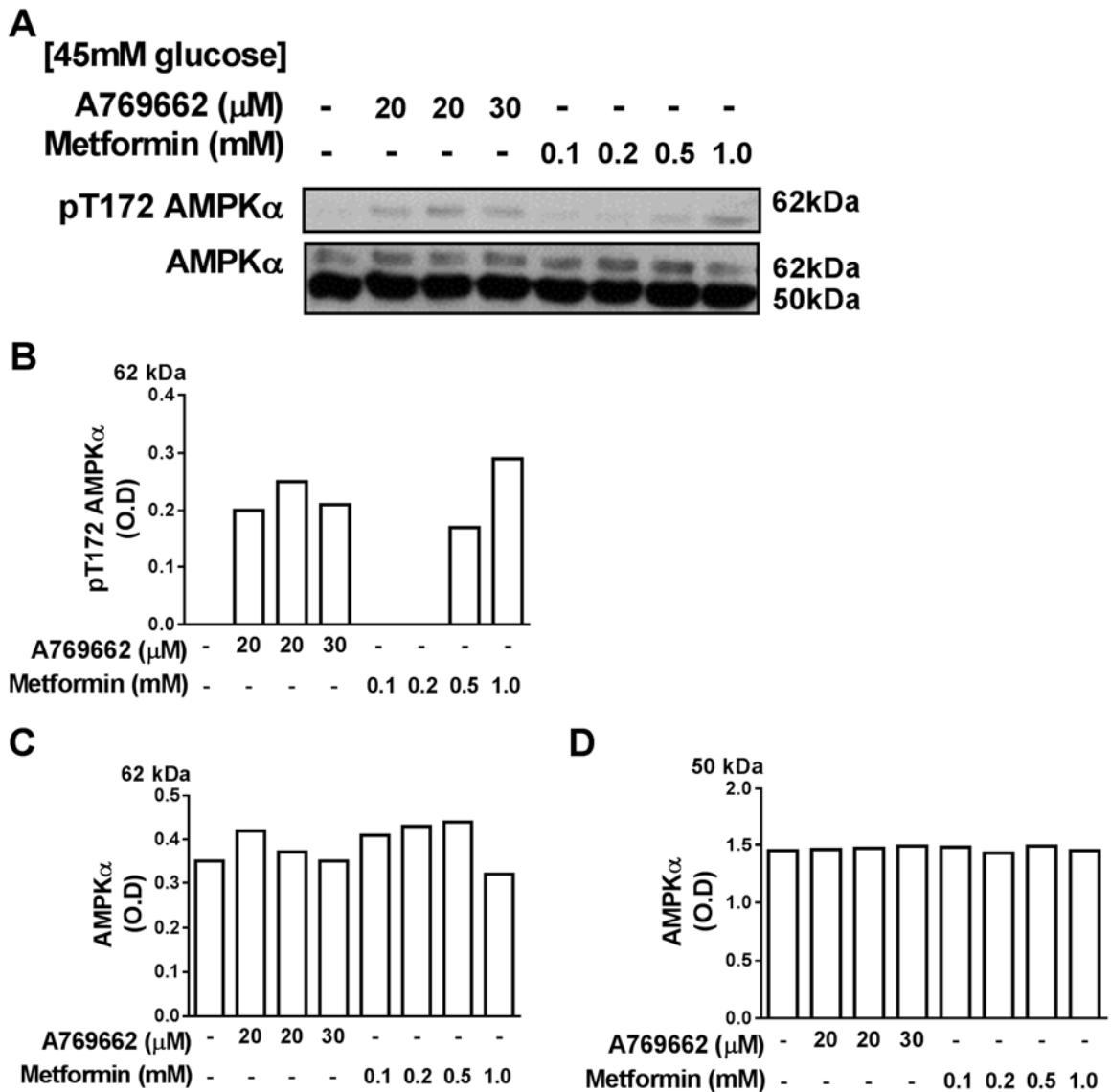


Figure 3.23 High metformin causes comparable stimulation of AMPK phosphorylation as A769662

Rat hepatocytes were pre-incubated with metformin or A769662 for 2 hours, then for a further 1 hour with 45mM glucose. Cell extracts were immunoblotted for pT172 AMPK α and total AMPK α (A), and optical density (*O.D*) was calculated (B, C, D). AMPK α is variable (C), although a 50kDa non-specific band was also detected (A, D) suggesting equal loading concentrations of samples which indicates stripping buffer for re-probing may be responsible for variable AMPK α .

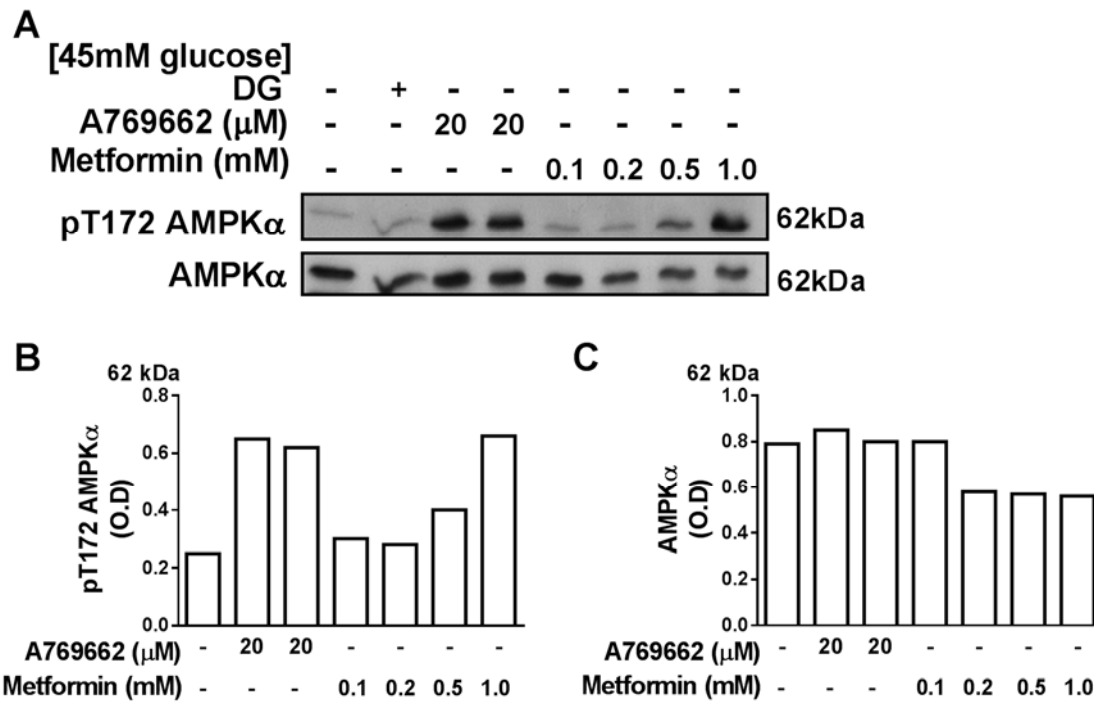


Figure 3.24 High metformin causes comparable stimulation of AMPK as A769662

Rat hepatocytes were pre-incubated with metformin or A769662 for 2 hours and for a further 1 hour with 10mM 2-deoxy-D-glucose (DG) and 45mM glucose. Cell extracts were immunoblotted for pT172 AMPK α and total AMPK α (A), and optical density (*O.D*) was calculated (B, C).

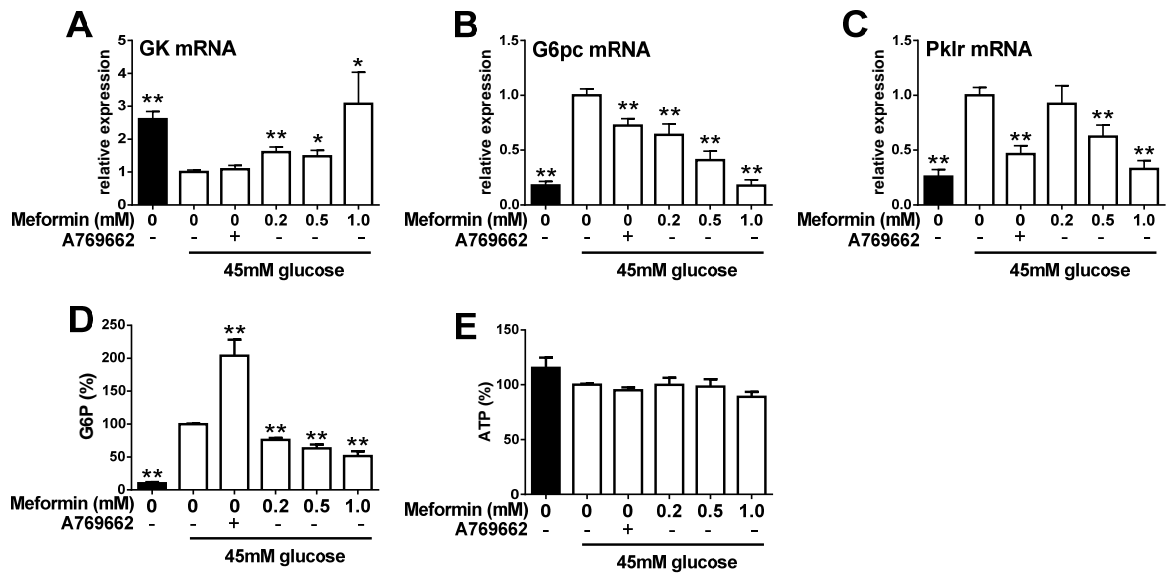


Figure 3.25 Metformin counteracts the effect of high glucose on gene regulation

(A-C) mRNA: rat hepatocytes were incubated in medium with 5mM (black) and 45mM (white) glucose for 4 hours with the metformin concentration indicated or 20 μ M A769662. (D-E) Rat hepatocytes were pre-incubated with metformin or A769662 for 2 hours, then a further 1 hour with 45mM glucose. Mean \pm SEM, n=4-8. *p<0.05, **p<0.01 effect compared with 45mM glucose.

Chapter 4: Results 2

4.1 Effects of metformin and AMPK activators and glucose phosphorylation

The above studies rule out involvement of either AMPK activation or NNT inhibition in the G6P lowering effect of metformin. Theoretically, metformin could lower G6P by inhibiting its production via glucose phosphorylation, gluconeogenesis or glycogenolysis, or by accelerating G6P metabolism by a variety of candidate pathways including glycogen synthesis, glycolysis, pentose phosphate pathway or other pathways within the endoplasmic reticulum or cytoplasm (figure 1.8). The action of metformin on G6P lowering may involve two or more pathways.

4.1.1 AMPK activators but not low metformin concentrations inhibit glucokinase translocation or glucose phosphorylation

We first tested the hypothesis that metformin may inhibit glucose phosphorylation by promoting enhanced binding of GK to its regulatory protein (GKRP) as reported previously at high metformin concentrations ($\geq 0.5\text{mM}$) (Guigas et al., 2006; Mukhtar et al., 2008). High glucose promoted glucokinase translocation (GKT) as shown by a significant decrease in the nuclear/ cytoplasmic ratio of GK (figure 4.1 A, B). This was observed in the presence of 0.5mM metformin but high metformin concentrations $\geq 1\text{mM}$ inhibited GKT at high glucose (figure 4.1 A, B). The AMPK activator A769662 (10 μM) also inhibited GKT (figure 4.1 A, B). As a control for comparison we tested a pharmacological GK activator (GKA) (Brocklehurst et al., 2004) which promoted GKT with both low and high glucose (figure 4.1 A, B). We also tested the metabolism of [2-³H] glucose as a measure of glucose phosphorylation of which there was no inhibition by metformin concentrations up to 1mM in rat or mouse hepatocytes (figure 4.2 A; figure 4.3A). However, both A769662 and C13 caused significant inhibition by 22% and 8% respectively in rat hepatocytes (figure 4.2 A). The latter could explain the small lowering of G6P by C13 at high glucose.

4.1.2 Metformin but not AMPK activators increase glucose metabolism at or downstream of G6P

Similarly to inhibition of glucose phosphorylation, A769662, C13 and 991 inhibited [5-³H] glucose metabolism whereas metformin (0.2-1.0mM) had no effect on [5-³H] glucose metabolism (figure 4.2 B). Loss of label as ³H₂O from tritium in the 5-position and in the 3-position of glucose indicates metabolism downstream of triose phosphate isomerase,

although loss of label is incomplete (Rognstad et al., 1975). Previous work showed that loss of label from the 5-position is greater than from the 3-position and the difference represents label exchange at the aldolase reaction. Loss of label from 3-position also includes flux from the pentose phosphate pathway, and flux through gluconeogenesis decreases loss of label from the 5 and 3-positions of glucose (Katz et al., 1975).

Therefore, the inhibition of [5-³H] glucose metabolism by the AMPK activators may be due to inhibition of glucose phosphorylation, or increased flux through gluconeogenesis.

In contrast, metabolism of [3-³H] glucose was increased by ≥ 0.2 mM metformin but not by A769662 (figure 4.3 B; figure 4.5 B). The increase in metabolism of [3-³H] glucose indicates increased flux through glycolysis and/ or the pentose phosphate pathway. Ammonium ion which causes elevation in NADP and therefore is predicted to cause increased flux through the pentose phosphate pathway (Sies et al., 1977) also increased metabolism of [3-³H] glucose (figure 4.3 B), consistent with increased flux through PPP or glycolysis.

4.1.3 The lowering of G6P by metformin is not explained by inhibition of glucose phosphorylation

The lack of inhibition of detritiation of [2-³H] glucose argues against inhibition of glucose phosphorylation as an explanation for the lowering of G6P by metformin. It is noteworthy however that loss of tritium from [2-³H] glucose is an underestimate of the rate of glucose phosphorylation because loss of 2-tritium at the phosphoglucoisomerase reaction is incomplete (Katz et al., 1975). Because the fractional retention of 2-tritium is dependent on the metabolic conditions we cannot firmly rule out inhibition by metformin of glucose phosphorylation that is not detectable from the metabolism of [2-³H] glucose. However various lines of evidence argue against this.

First, we determined the effects of titrated overexpression of GKR on cell G6P and metabolism of [2-³H] glucose. With GKR overexpression (figure 4.4 A) there was progressive lowering of G6P (figure 4.4 B) and also inhibition of metabolism of [2-³H] glucose (figure 4.4 D) in conditions of maintained ATP (figure 4.4 C). From this we infer that the lowering of G6P by metformin (0.1-0.5 mM) is unlikely to be due to increase binding of GK to GKR that is not detectable from the metabolism of [2-³H] glucose.

Secondly, the non-specific hexokinase inhibitor glucosamine inhibited [2-³H] glucose metabolism as expected by 35% (figure 4.5 A) and inhibited [3-³H] glucose metabolism to a similar extent (figure 4.5 B). Glucosamine significantly lowered G6P, and metformin (0.2mM) lowered G6P further (figure 4.5 C, D) but did not further inhibit [2-³H] glucose metabolism (figure 4.5 A). This occurred with minimal (<9%) or no ATP depletion (figure 4.5 G, H). Metformin increased lactate and pyruvate production by 13-16% in parallel with the lowering of G6P, although this was not significant (figure 4.5 E, F). This is consistent with the initial data suggesting the effects of metformin on G6P are unlikely to be due to inhibition of glucose phosphorylation.

We also tested the effects of metformin on cell G6P in incubations with mannoheptulose which inhibits GK activity but also blocks its interaction with GKRP (Niculescu et al., 1997; Agius & Stubbs., 2000). Mannoheptulose as expected lowered cell G6P (figure 4.6 A, B) and metformin lowered G6P further in the presence of mannoheptulose with S4048 (figure 4.6 B). This was observed in the absence of ATP depletion (figure 4.6 E, F). The lowering of G6P by metformin with mannoheptulose correlated with the stimulation of lactate and pyruvate production by metformin (figure 4.6 A-D). This agrees with the above data in which metformin lowered G6P further in the incubations with glucosamine which is a potent hexokinase inhibitor but is less effective than mannoheptulose in blocking the interaction of glucokinase with GKRP (Niculescu et al., 1997). Although we cannot exclude an effect of metformin on the interaction between glucokinase and GKRP we found no evidence for an inhibition of glucose phosphorylation to explain the lowering of G6P by metformin concentrations of 0.2mM.

Additionally, we tested the effects of GK overexpression which stimulated [2-³H] glucose metabolism by almost 2-fold (figure 4.4 D) and raised cell G6P by 4-fold (figure 4.4 B). Likewise, in accordance with the GKT data, a glucokinase activator (GKA) stimulated the metabolism of [2-³H] glucose (figure 4.5 A) and increased cell G6P by 2-6 fold (figure 4.5 C, D). However, metformin still lowered G6P in the presence of GKA (figure 4.5 C) without affecting the metabolism of [2-³H] glucose (figure 4.5 A), and the stimulation of [3-³H] glucose metabolism by metformin and GKA was additive (figure 4.5B) suggesting the lowering of G6P by 0.2mM metformin is unlikely to be due to inhibition of glucose phosphorylation.

Cumulatively, these results suggest that the lowering of G6P by metformin is most likely explained by increased metabolism of G6P by glycolysis and/ or pentose phosphate pathway rather than by inhibition of glucose phosphorylation. This effect of metformin is not mimicked by AMPK activators which have opposite effects from metformin on the metabolism of [2-³H] glucose and [3-³H] glucose.

4.2 Lowering of G6P by metformin is not secondary to altered glycogen metabolism

The lowering of G6P by metformin could be due to activation of various pathways downstream of G6P including glycogen synthesis. In hepatocytes, glycogen is synthesised by liver glycogen synthase (GYS2) from UDP-glucose derived from G6P, and glycogen is degraded by phosphorylase (GP) to glucose 1-phosphate (G1P) which is converted to G6P by phosphoglucomutase (Agius, 2015). Glycogen synthase and glycogen phosphorylase are regulated by covalent modification and by a range of allosteric effectors that include G6P and AMP (Fletterick & Madsen., 1980; Johnson et al., 1993). G6P is an allosteric activator of glycogen synthase and inhibitor of glycogen phosphorylase and promotes dephosphorylation of phosphorylase (inactivation) and synthase (activation) (Villar-Palasi & Guinovart 1997; Aiston et al., 2003, von Wilamowitz-Moellendorff et al., 2013). Conversely, AMP promotes activation (phosphorylation) of phosphorylase (Johnson & Barford., 1993). The phosphorylated form of phosphorylase is a very potent inhibitor of glycogen synthase phosphatase, to the extent that allosteric inhibitors of phosphorylase (e.g. G6P) can indirectly regulate glycogen synthase as well as having additional direct effects (Johnson & Barford., 1993). Previous work has identified small molecule allosteric inhibitors of phosphorylase such as the indole carboxamide inhibitor of phosphorylase (CP-91149), which promotes glycogen storage by inactivation of phosphorylase and activation of glycogen synthase (Aiston et al., 2001). Likewise, metabolic conditions that raise G6P, for example overexpression of GK (Seoane et al., 1996) or inhibition of G6PT with S4048 (van Dijk et al., 2001; Harndahl 2006) cause a strong activation of glycogen synthase and stimulation of glycogen synthesis which directly correlates with the raised G6P (Ciudad et al., 1986; Fernandez-Novell et al., 1994; Seoane et al., 1996). Glycogen storage is stimulated synergistically by raised G6P caused by GK overexpression and by allosteric inhibitors of phosphorylase (Hampson & Agius., 2005).

4.2.1 Metformin mimics CP-91149 on G6P lowering but has converse effects on glycogen synthesis

In this study we compared the effects of metformin with the phosphorylase inhibitor on glycogen synthesis in the absence and presence of S4048 to raise G6P. Firstly, S4048 stimulated glycogen synthesis 6-fold in mouse hepatocytes (figure 4.7 A) as expected from the increase in G6P. CP-91149 (2.5-10 μ M) stimulated glycogen synthesis by more than 3-fold in the absence of S4048 and by a further 29-37% in the presence of S4048 (figure 4.7 A). This was associated with a 37-42% decrease in G6P (figure 4.7 B). This concurs with previous work, combining CP-9149 with GK overexpression (Hampson & Agius, 2005). In contrast with CP-91149, metformin (0.2mM) inhibited glycogen synthesis by 44% and 67% in the absence and presence of S4048 respectively (figure 4.7 A) in parallel with a 27-33% decrease in G6P (figure 4.7 B). This indicates that the lowering of G6P by metformin cannot be explained by stimulation of glycogen synthesis.

4.2.2 Metformin but not A769662 inhibits glycogen accumulation with both glucose and DHA as substrates

Previous work showed that A769662 inactivated glycogen synthase through AMPK mediated phosphorylation of Ser-7 on GYS2 (Bultot et al, 2012). We therefore compared the effects of metformin (0.1-0.5mM) and A769662 (5-20 μ M) on glycogen accumulation in rat hepatocytes. Glycogen accumulation was stimulated by 2-fold with high glucose (figure 4.8 A) and the gluconeogenic precursor DHA (figure 4.8 B), and by up to 40% further with S4048 (figure 4.8 A, B). With high glucose and DHA in the absence of S4048, metformin (0.1-0.5mM) inhibited glycogen accumulation by 13-26% (figure 4.8 C, D). A769662 also caused a 12% inhibition with high glucose (figure 4.8 C) but had no effect on glycogen accumulation with DHA (figure 4.8 D).

4.2.3 The inhibition of glycogen synthesis by metformin correlated with the lowering of G6P

We next compared the effects of metformin (0.1-0.5mM) and A769662 (5-20 μ M) on glycogen synthesis in mouse hepatocytes with 25mM glucose as substrate. In the absence of S4048 metformin (0.2-0.5mM) caused similar inhibition (44-79%) of glycogen synthesis as the AMPK activator (figure 4.9 B). However, metformin but not A769662 lowered G6P (figure 4.9 D). In the presence of S4048 which increased glycogen synthesis

by more than 4-fold (figure 4.9 A), metformin (0.5mM) completely counteracted the stimulation by S4048, whereas A769662 had negligible effect (figure 4.9 B). In incubations with metformin without or with S4048, the rates of glycogen synthesis correlated with G6P ($r=0.96$, $r=0.99$ respectively) (figure 4.9 E, F). However, in incubations without or with A769662 the inhibition of glycogen synthesis is not paralleled by changes in G6P (figure 4.9 F). Accordingly, the counteraction of this effect by metformin is best explained by the lowering of G6P by metformin. The lack of effect of the AMPK activator in the presence of S4048 could be due to an over-riding effect of elevated G6P or because A769662 does not cause AMPK phosphorylation in conditions of raised G6P.

4.3 Exclusion of hexosamine biosynthesis pathway

We considered the hypothesis that metformin lowers G6P by stimulating flux through the hexosamine biosynthesis pathway (HBP) which accounts for 2-5% of glucose metabolism (Bouché et al., 2004; Filhoulaud et al., 2009). F6P generated from G6P by phosphoglucosomerase undergoes amidation with glutamine to glucosamine 6-phosphate (GlcN 6-P) catalysed by GFAT (glutamine:fructose-6-phosphate amidotransferase) which is metabolised to UDP-GlcNAc (UDP-N-acetylglucosamine), the substrate for O-glycosylation of serine/ threonine residues by O-linked N-acetylglucosamine transferase (OGT) (figure 4.10 A) (Bouché et al., 2004; Arden et al., 2012). Protein targets for glycosylation include transcription factors such as ChREBP which stimulates lipogenic gene expression (Guinez et al. 2011) and co-activators such as CRTC2 which stimulates gluconeogenic (G6pc) gene expression (Dentin et al. 2008).

We tested whether metformin could lower G6P by stimulating GFAT in the rate limiting step of HBP. Firstly, we tested the effect of glutamine which is required for F6P flux through GFAT (Bouché et al., 2004). Glutamine did not lower cell G6P (figure 4.10 B) supporting the literature that HBP accounts for a small percentage of glucose metabolism (Bouché et al., 2004; Filhoulaud et al., 2009). Furthermore, metformin lowered cell G6P similarly in the absence and presence of glutamine (by 63% and 61% respectively) (figure 4.10 B) indicating glutamine is not required for the metformin effect. We next tested whether inhibiting the rate limiting enzyme GFAT with the glutamine antagonist 6-diazo-5-oxo-L-norleucine (DON) abolished the decrease in G6P

observed with metformin. DON did not raise cell G6P significantly, and metformin lowered cell G6P similarly in the absence and presence of DON by 61% and 58% respectively (figure 4.10 B) without affecting cell ATP (figure 4.10 C).

Metformin lowered cell G6P and counteracted the stimulation of G6pc expression by high glucose (figure 3.25 B, D). However, if metformin stimulated flux through HBP we predict stimulation of G6pc expression and hepatic glucose production which is counter-intuitive. Nevertheless, the above results suggest the lowering of G6P by metformin is unlikely to be due to the stimulation of HBP and supports the literature that HBP accounts for a small percentage of glucose metabolism in hepatocytes (Bouché et al., 2004; Filhoulaud et al., 2009).

4.4 Exclusion of stimulation of H6PD metabolism

G6P enters the ER on G6PT encoded by SLC37A4 (which is inhibited by S4048 and other chlorogenic acid derivatives) (Herling et al., 1999; Harndahl et al., 2006), but most likely also on other hexose 6-phosphate transporters that are insensitive to chlorogenic acid derivatives. Senesi et al., (2010) reported that F6P can be transported into the ER independently of chlorogenic acid and can be converted to G6P as a substrate for hexose 6-phosphate dehydrogenase (H6PD). The ER associated Pi-linked antiporters SLC37A1 and SLC37A2 are not coupled with G6pc and are not inhibited by chlorogenic acid and so are possible transporters for F6P (Pan et al., 2011). G6P metabolism by H6PD is coupled to the conversion of cortisone to cortisol in man, and of 11-dehydrocorticosterone (11-DHC) to corticosterone in rodents via 11 β -hydroxysteroid dehydrogenase (11 β -HSD) (Zhou et al., 2012; Hult et al., 2004).

Metformin still exerted its effects in lowering G6P and inhibiting glucose production in the presence of S4048 (figure 3.3 G, H; figure 3.22 B). Therefore, we tested the hypothesis that decrease in G6P by metformin in the presence of S4048 may be due to stimulation of H6PD by comparing the effects of metformin in both wild type and H6PD knockout mice (H6PD KO). Firstly, cell G6P was 3-fold higher in H6PD KO hepatocytes compared to control (figure 4.11 A, B). Metformin at 0.2-0.5mM did not affect cell G6P in wild type or H6PD KO mice in the absence of S4048 (figure 4.12 A). However, with S4048 metformin lowered G6P similarly in WT and H6PD KO hepatocytes by 38% and

36% respectively with 0.2mM metformin, and by 48% and 61% with 0.5mM metformin in WT and H6PD KO hepatocytes respectively (figure 4.11 B) without lowering ATP (figure 4.11 D) suggesting an effect of metformin independent of H6PD.

4.5 Metformin may lower G6P partially by stimulating flux through the pentose phosphate pathway

Based on the results in earlier experiments indicating that rhein, ammonium and 0.5mM metformin all raised cell NADP but lowered cell G6P (figure 3.10 A-F), we investigated the hypothesis that metformin may lower G6P by stimulating flux through the pentose phosphate pathway, the first step in which G6P is metabolised to 6-phosphogluconolactone (6PGL) by glucose 6-phosphate dehydrogenase (G6PD) generating NADPH from NADP⁺ (Stincone et al., 2015). First, we tested whether stimulation of flux through the pentose phosphate pathway lowered cell G6P. The activity of G6PD in the rate limiting step of the pentose phosphate pathway is limited by the rate of NADPH oxidation. The electron acceptor phenazine methosulfate (PMS) is an NADPH oxidant that increases cell NADP stimulating flux through PPP, avoiding this limitation (Slater., 1967; Muirhead & Hothersall., 1995). In hepatocytes 10µM PMS increased cell NADP by more than 3-fold with high glucose (figure 4.12 A) and lowered cell G6P by 55% (figure 4.12 B) without lowering cell ATP (figure 4.12 C). This is consistent with increased flux through the pentose phosphate pathway in conjunction with a decrease in cell G6P.

4.5.1 DHEA partially counteracts the effect of metformin on NADP and G6P

The above studies suggest that stimulation of the pentose phosphate pathway lowers cell G6P. The next aim was to test whether the uncompetitive G6PD inhibitor dehydroepiandrosterone (DHEA) (Marks & Banks., 1960; Shantz et al., 1989; Schwartz & Pashko., 2004; Tabidi & Saggerson., 2012) had the opposite effect to PMS and raised cell G6P, which would indicate inhibition of the pentose phosphate pathway. We would also expect an inhibitor of G6PD to raise NADP. With DHEA (20-50µM) there was a small but significant increase in cell NADP (figure 4.13 A) in conditions where G6P was lowered by 11-31% (figure 4.13 B) and ATP was unchanged (figure 4.13 C). Although the increase in NADP is consistent with pentose phosphate pathway inhibition, there are two possible additional explanations for the accompanied effect on G6P; firstly, DHEA itself may be

metabolised by the P450 system (Fitzpatrick et al., 2001) involving NADPH conversion NADP. Secondly, DHEA may be exerting non-specific effects and may cause mitochondrial depolarisation similarly to rotenone, DNP and metformin, resulting in raised levels of NADP by inhibition of NNT.

The increase in NADP with DHEA (though not its effects on cell G6P) is consistent with DHEA inhibition of G6PD. Therefore, we next tested whether DHEA counteracts lowering of cell G6P by metformin. Under conditions where DHEA alone did not lower cell G6P, DHEA attenuated the decrease in G6P by 0.5mM metformin with both high glucose and DHA as substrates (figure 4.14 B, D, E) without lowering ATP (figure 4.14 C, G, H). This attenuation by DHEA was also observed with 0.2mM metformin with the substrate xylitol (figure 4.14 F). Additionally, DHEA did not counteract the decrease in G6P with ammonium with all substrates tested (figure 4.14 B, D, E, F) and the effects of ammonium and DHEA on NADP were additive (figure 4.14 A) suggestive of the different mechanisms by which DHEA and ammonium raise NADP.

To further investigate the mechanism by which DHEA attenuated the decrease in G6P with metformin, we next determined the effect of DHEA on cell metformin accumulation. Under the same pre-incubation conditions as the G6P experiments (figure 4.14 B), metformin accumulation was significantly lower (34%) in the presence of DHEA when the metformin concentration was 0.2mM but not at 0.5mM (figure 4.15 A). When the pre-incubation with DHEA was shortened from 2-hours to 30 minutes metformin accumulation at both 0.2mM metformin, and 0.5mM metformin was slightly but significantly lower by 36% and 15% respectively relative to no DHEA (figure 4.15 B). Therefore, the attenuation by DHEA of the G6P lowering by metformin may be at least in part due to a lower cellular metformin content.

4.5.2 Lowering of G6P by DHEA could be due to its metabolism

To investigate whether DHEA metabolism (Fitzpatrick et al., 2001) could account for its lowering of G6P, we tested whether compounds that are known to be metabolised in hepatocytes lower cell G6P. Firstly, the 11 β -HSD1 competitive inhibitor metyrapone (Sampath-Kumar., 1997) is reduced to metyrapol in human and mouse liver (Nagamine et al., 1997). Like DHEA, high concentrations of metyrapone (1.0mM) lowered cell G6P by 39% (figure 4.16 A) and ATP was lowered by 13% in parallel (figure 4.16 B), although

cell NADP was unaffected (figure 4.16 C). Metyrapone also lowered cell G6P with DHA as a substrate in the absence of ATP depletion (figure 4.16 D, E). Similar effects were observed with menadione (figure 4.17 A) -an oxidant that induces cytochrome P450 reductase and is reduced to 1,4-dihydroxy-2-methyldihydronaphthalene in the liver (Gray et al., 2016), and with the general P450 inhibitor miconazole (figure 4.17 C) (Miller et al., 2013) suggesting that compounds that are metabolised by hepatocytes lower cell G6P. Therefore, we cannot rule out DHEA metabolism as a possible mechanism for its G6P lowering effects.

4.5.3 CB72 as a G6PD inhibitor

Although DHEA increased cell NADP as expected of an inhibitor of G6PD, it did not raise cell G6P and had unexpected effects on metformin accumulation. We therefore tested whether the competitive G6PD inhibitor CB72 (Preuss et al., 2013) could be used as a tool to investigate flux through the pentose phosphate pathway. CB72 (10 μ M), unlike DHEA did not affect metformin accumulation in hepatocytes (figure 4.18 A). However, it lowered G6P by 46% (4.18 B) and it also lowered ATP by 27% (figure 4.18 C) but did not abolish the G6P lowering effect of 0.5mM metformin or ammonium (figure 4.19 D). In view of the lowering of G6P by CB72 alone no firm conclusions can be drawn on G6PD inhibition.

4.5.4 Adenoviral knockdown of ShG6PD does not counteract the effect of metformin on cell G6P

Based on the observation that DHEA partially attenuated the decrease in G6P with 0.5mM metformin in conditions where metformin accumulation is not lowered, we tested whether adenoviral knockdown of the G6PD gene in hepatocytes would also attenuate the decrease in G6P with metformin. First, we validated the knockdown of G6PD in mice with the adenoviral vector Ad-m-G6pdx-shRNA (ShG6PD) by establishing partial knockdown of G6PD mRNA expression (figure 4.19 A) after a 24-hour incubation with 10-20 μ l/ml of the vector (at 1-5 X10⁷ PFU/ μ l). However, we could not detect any changes in the levels of G6PD protein by immunoblotting (figure 4.19 B, C) which could be due to either (i) a long half-life of the G6PD protein, or (ii) small changes in G6PD protein may not have been detectable by immunoblotting.

We next tested whether we could measure a decrease in G6PD activity with ShG6PD. In rat hepatocytes and C57BL/6J mouse hepatocytes G6PD activity was unchanged by 2-10 $\mu\text{l/ml}$ of shG6PD (figure 4.20 A, B). However, in wild type mouse hepatocytes (figure 4.20 C) there was a small but significant 12% decrease in enzyme activity with 20 $\mu\text{l/ml}$ ShG6PD. Cell G6P was increased by 54% and 64% in mouse hepatocytes treated with 10 $\mu\text{l/ml}$ and 20 $\mu\text{l/ml}$ shG6pd respectively however, metformin still lowered G6P in these conditions (figure 4.21 A) with little (15%) or no ATP depletion (figure 4.21 B). Treatment with shG6PD also raised cell glycerol 3-phosphate (G3P) (figure 4.21 C) and metformin (0.2mM) stimulated lactate + pyruvate production in the absence but not in the presence of shG6PD (figure 4.21 D). In summary, unlike DHEA or CB72, treatment with shG6PD raised cell G6P but it did not attenuate the G6P lowering effects of metformin.

4.5.5 Estimation of flux through the pentose phosphate pathway with [1-¹⁴C] glucose

We aimed to measure flux through the oxidative branch of the pentose phosphate pathway by measuring the formation of ¹⁴CO₂ from [¹⁴C] glucose labelled in either the 1-position or the 6-position, taking into account the specific activity of glucose. ¹⁴CO₂ is released from [1-¹⁴C] glucose metabolism in the oxidative arm of the pentose phosphate pathway and in the TCA cycle, and from [6-¹⁴C] glucose metabolism in the TCA cycle. Accordingly, the difference in ¹⁴CO₂ between [1-¹⁴C] and [6-¹⁴C] represents flux through the pentose phosphate pathway. This method is based on the assumption that triose phosphate isomerization is sufficiently rapid such that GA3P and DHAP are in complete isotopic equilibrium (Katz & Rognstad., 1966). In these conditions generation of ¹⁴CO₂ via the TCA cycle from [1-¹⁴C] glucose and [6-¹⁴C] glucose would be identical (Katz & Rognstad., 1966), and has been widely used to estimate flux through the pentose phosphate pathway in several cell types including hepatocytes (Baranyai & Blum., 1989).

Our initial studies showed higher rates of ¹⁴CO₂ formation from [6-¹⁴C] glucose relative to [1-¹⁴C] glucose (figure 4.22 A). Accordingly, flux through the pentose phosphate pathways could not be determined from the difference between [1-¹⁴C] and [6-¹⁴C] decarboxylation. We assumed this to be due to lower purity of the [1-¹⁴C] glucose compared with [6-¹⁴C] glucose. Accordingly, we purchased a different preparation of [1-¹⁴C] glucose and determined the purity of the two batches of [1-¹⁴C] glucose (MC228 from Hartmann Analytic and ARC120B from PerkinElmer) by treatment of sample with

phosphoglucoisomerase, glucose 6-phosphate dehydrogenase and 6-phosphogluconate dehydrogenase, and determination of enzymic decarboxylation. We found both preparations to be greater than 90% pure (figure 4.22 B).

We next considered that the higher rate of $^{14}\text{CO}_2$ from $[6\text{-}^{14}\text{C}]$ glucose relative to $[1\text{-}^{14}\text{C}]$ glucose indicates a smaller contribution of $[1\text{-}^{14}\text{C}]$ than $[6\text{-}^{14}\text{C}]$ glucose to the TCA cycle because of lack of equilibration at the triose phosphate isomerase step (Rose & O'Connell., 1961; Katz & Rognstad., 1966). Because treatment with ethanol was reported to inhibit pyruvate entry into the TCA cycle by inhibition at the level of pyruvate dehydrogenase but not flux through the pentose phosphate pathway (Baranyai & Blum., 1989) we tested the effects of ethanol on the oxidation of $[\text{U}\text{-}^{14}\text{C}]$ glucose, $[6\text{-}^{14}\text{C}]$ glucose and $[1\text{-}^{14}\text{C}]$ glucose. Ethanol (20 mM) had negligible effect on the oxidation of both $[\text{U}\text{-}^{14}\text{C}]$ glucose and $[1\text{-}^{14}\text{C}]$ glucose (figure 4.23 A). However, 30 mM ethanol caused 70% inhibition of $[6\text{-}^{14}\text{C}]$ glucose but negligible inhibition of $[1\text{-}^{14}\text{C}]$ glucose (figure 4.23 B) and 50 mM ethanol caused 64% inhibition of $[\text{U}\text{-}^{14}\text{C}]$ glucose, 55% inhibition of $[6\text{-}^{14}\text{C}]$ glucose and negligible inhibition of $[1\text{-}^{14}\text{C}]$ glucose (figure 4.23 C). Since $[1\text{-}^{14}\text{C}]$ glucose like $[6\text{-}^{14}\text{C}]$ glucose is expected to be metabolised in the TCA cycle, we infer that the negligible inhibition by ethanol of $^{14}\text{CO}_2$ from $[1\text{-}^{14}\text{C}]$ glucose compared with $[6\text{-}^{14}\text{C}]$ glucose, is evidence for lack of loss of label from $[1\text{-}^{14}\text{C}]$ glucose in the TCA cycle and thereby for lack of equilibration at the level of triose phosphate isomerase as was proposed previously for liver (Rose & O'Connell., 1961; Katz & Rognstad., 1966). The ethanol experiments suggest that there is negligible decarboxylation of $[1\text{-}^{14}\text{C}]$ glucose by the TCA cycle. We therefore assume that decarboxylation of $[1\text{-}^{14}\text{C}]$ glucose provides an approximate estimate of the flux through the pentose phosphate pathway because it does not take into account recycling of hexose 6-phosphate derived from the non-oxidative branch into the pentose phosphate pathway

We next determined the effects of DHEA either alone (figure 2.24 A) or in combination with ethanol (figure 2.24 B) to eliminate the contribution of TCA cycle flux to the metabolism of $[1\text{-}^{14}\text{C}]$ glucose on decarboxylation of glucose. In the absence of ethanol, DHEA (both 20 and 100 μM) caused significant stimulation of $^{14}\text{CO}_2$ from $[6\text{-}^{14}\text{C}]$ glucose and a small but not significant stimulatory trend on the decarboxylation $[1\text{-}^{14}\text{C}]$ glucose (figure 2.24 A). In the presence of ethanol which caused a large suppression of

decarboxylation of [U-¹⁴C], DHEA stimulated [U-¹⁴C] glucose oxidation but had no effect on [1-¹⁴C] glucose oxidation (figure 2.24 B).

The following conclusions are drawn from this work. (1) Flux through the pentose phosphate pathway could not be determined from the difference in ¹⁴CO₂ between [1-¹⁴C] and [6-¹⁴C] glucose. (2) Based on the large inhibition by ethanol of metabolism of [6-¹⁴C] glucose but not [1-¹⁴C] glucose, we infer that the TCA cycle has a negligible contribution to decarboxylation of [1-¹⁴C] glucose (most likely because of lack of equilibration at the triose phosphate isomerase reaction; (3) we further conclude that decarboxylation of [1-¹⁴C] glucose approximates flux through the pentose phosphate pathway. This represents <1% of total lactate and pyruvate production. (4) The lack of inhibition by DHEA in the decarboxylation of [1-¹⁴C] glucose suggests that at the concentration of DHEA used in the present study there is negligible inhibition of the pentose phosphate pathway. (5) A tentative conclusion for the stimulation by DHEA of decarboxylation of [6-¹⁴C] glucose is that it may cause depolarisation of mitochondria and thereby stimulate pyruvate oxidation as occurs with the uncoupler. This would concur with the lower cellular accumulation of [¹⁴C] metformin in the presence of DHEA.

4.6 Stimulation of glycolysis can explain the lowering of G6P by metformin

We observed that metformin ≥ 0.2 mM stimulated metabolism of [3-³H] glucose (figure 4.3 B; figure 4.5 B), and that 0.2mM metformin increased lactate and pyruvate production in mouse hepatocytes (figure 4.25 A) without inhibiting [U-¹⁴C] glucose oxidation (figure 3.7 B). Previous studies reported stimulation of pyruvate kinase by metformin (Argaud et al., 1993) and that biguanides altered flux at the level of GAPDH / phosphoglycerate kinase by the decrease in free ATP/ADP (Owen & Halestrap, 1993; Owen et al., 2000). An alternative regulatory site for metformin is the phosphofructokinase-1/ fructose-1,6-bisphosphatase 1 (PFK1/FBP1) site. PFK1 and FBP1 are regulated in a converse manner by a large number of allosteric effectors including ATP, ADP, AMP, inorganic phosphate (Pi), citrate and fructose 2,6-bisphosphate (F-2,6-P₂) (Sugden & Newsholme., 1975; McGrane et al., 1983; Hers & Hue., 1983; Bosca et al., 1985). Of these the latter is the most potent allosteric activator of PFK1 and inhibitor of FBP1 (Hers & Hue., 1983). F-2,6-P₂ is synthesized from F6P and degraded to F6P by the

bifunctional enzyme 6-phosphofructo-2-kinase/fructose-2,6-bisphosphatase (PFK2/FBP2) (Hers & Hue., 1983).

4.6.1 Depletion of F-2,6-P₂ raises cell G6P, which is counteracted by metformin

Our initial aim was to test whether inhibition of glycolysis with selective targeting of the PFK1/FBP1 site by depleting F-2,6-P₂ with a kinase deficient phosphatase active variant of the bi-functional protein PFK2/FBP2 (PFK2-KD) would alter cell G6P levels. Expression of PFK2-KD inhibited total lactate and pyruvate production by 25% (figure 4.25 B) and increased cell G6P 3-fold (figure 4.25 C) without any change in cell ATP (figure 4.25 D). These results show that a small fractional change in flux through glycolysis (< 30%) by targeting PFK1/FBP1 causes a large elevation 200% above basal in G6P. Although 0.2mM metformin alone stimulated lactate and pyruvate production, this was not observed in the presence of PFK2-KD (figure 4.25 B). However, metformin ($\geq 0.2\text{mM}$) still attenuated the increase in G6P with PFK2-KD (figure 4.25 C). It is noteworthy however, that although PFK2-KD caused a large increase in G6P, inhibition of lactate and pyruvate production was smaller in comparison (25%). Therefore, as metformin (0.2mM) lowered G6P by 24% the corresponding stimulation of lactate and pyruvate production may be at levels that are not detectable (<5%).

The PFK1 activator ammonium (Sugden & Newsholme., 1975) which stimulated [$3\text{-}^3\text{H}$] glucose metabolism (figure 4.3 B) stimulated lactate and pyruvate production in the absence of PFK2-KD but not in its presence (figure 4.25 B). Ammonium still lowered G6P in control and PFK2-KD expressing cells (figure 4.25 C). This shows that the PFK1/FBP1 site is a major determinant of cell G6P content, and that metformin is still effective at lowering G6P when F-2,6-P₂ is depleted.

4.6.2 The PFK1 inhibitor ATA raised cell G6P which is counteracted by metformin

We next used a cell-permeable potent inhibitor of PFK1, the citrate analogue aurointricarboxylic acid (ATA) (McCune et al., 1989) to test its effects on glycolysis and G6P. Although ATA also inhibits other enzymes of glycolysis it was shown to be a much more potent inhibitor of PFK1 (McCune et al., 1989). Like PFK2-KD, cell G6P was increased by more than 2-fold with ATA (figure 4.26 A), although this was associated with partial lowering of cell ATP (figure 4.26 C). ATA (0.1-0.2mM) also inhibited lactate and pyruvate production by 36-51% as predicted of an inhibitor of PFK1 (figure 4.26 E).

However, 0.05mM ATA raised G6P without inhibiting lactate and pyruvate production (figure 4.26 A, E). This concurs with the above conclusion from the overexpression of PFK2-KD that a small fractional inhibition in flux through glycolysis results in a large increase in G6P. Metformin at 0.2mM partially attenuated the increase in G6P with 0.1-0.2mM ATA (figure 4.26 B). Unlike with PFK2-KD metformin still stimulated lactate and pyruvate production with low (0.1mM) concentrations of ATA but had no significant effect with higher concentrations of ATA (0.2mM) (figure 4.27 F). In this study ATA inhibited metabolism of both [$3\text{-}^3\text{H}$] glucose (figure 4.27 A) and [$2\text{-}^3\text{H}$] glucose (figure 4.27 B) but was a stronger inhibitor of [$3\text{-}^3\text{H}$] glucose in comparison

4.6.3 Inhibition of FBP1 lowers cell G6P

The above studies with PFK2-KD demonstrate the effects of metformin when inhibition of FBP1 by F-2,6-P₂ is removed. We next investigated the hypothesis that metformin lowers cell G6P by inhibiting FBP1 in gluconeogenesis, as was shown for AICAR (Vincent et al., 1991). We tested whether selective inhibition of FBP1 with the AMP site analogue FBPi (5-Chloro-2-[N-(2,5-dichlorobenzenesulfonamido)]-benzoxazole) mimicked the effects of metformin on cell G6P. FBPi lowered cell G6P in a concentration dependent manner (figure 4.28 A), consistent with inhibition of gluconeogenesis but this was also accompanied by a lowering of cell ATP (figure 4.28 C). Although both 5 μM FBPi and 0.2mM metformin lowered G6P similarly, when the two compounds were combined cell G6P was lowered by a further 15% although this was not significant (figure 4.28 B). However, FBPi had small inhibitory effects on lactate and pyruvate production which is not consistent with FBP1 inhibition (figure 4.28 E). Therefore, although FBPi mimicked the effect of metformin on lowering G6P, non-specific cytotoxic effects as shown by the lowering of ATP cannot be excluded.

4.6.4 The lowering of G6P by metformin is not mimicked in conditions of a more reduced cytoplasmic redox state

An alternative explanation for the raised lactate and pyruvate production with metformin is altered directionality of flux at the GAPDH and phosphoglycerate kinase equilibria which was also proposed by Halestrap and colleagues (Owen & Halestrap 1993; Owen et al., 2000). To investigate this, we used aminooxyacetate (AOA), an inhibitor of the aspartate aminotransferase enzyme (AAT), and thereby of the malate

aspartate shuttle which transfers reducing equivalents (NADH) from the cytoplasm to the mitochondria. The consequent increase in NADH/NAD would be expected to restrict flux through GAPDH (Kauppinen et al., 1987; Rognstad & Katz., 1970; Berry et al., 1992; Berry et al., 1994). A recent study suggested that metformin inhibits the glycerophosphate shuttle in the liver based on the increase in lactate/ pyruvate ratio as a measure of the cytoplasmic NADH/NAD redox state (Madiraju et al., 2014) but whether the latter shuttle has a major role in either rodents or man is contentious (Baur & Birnbaum., 2014).

AOA increased the lactate/ pyruvate ratio by more than 7-fold (figure 4.29 D), consistent with a major role for the malate aspartate shuttle in transfer of NADH equivalents (Baur & Birnbaum., 2014) and it increased cell G3P by more than 2-fold (figure 4.29 B) consistent with an increase in NADH/ NAD ratio which would be expected to reduce flux through GAPDH. AOA caused a relatively modest elevation in G6P (< 20%) with high glucose (figure 4.29 A, F) (compared with the 2-3 fold increase caused by either PFK2-KD or ATA), and metformin still lowered cell G6P with AOA (figure 4.29 F). AOA had no significant effect on total lactate + pyruvate accumulation in the medium (figure 4.29 C). This could be due to negligible inhibition of flux through GAPDH. It is noteworthy that total lactate and pyruvate accumulation is only an approximate measure of glycolysis because pyruvate can be transported into mitochondria or converted to alanine which can either be released into the medium or transported into mitochondria.

We tested for effects of AOA on $^{14}\text{CO}_2$ formation from [U- ^{14}C] glucose. There was no effect of AOA alone however when AOA was combined with the pyruvate transport inhibitor UK5099, AOA decreased $^{14}\text{CO}_2$ formation further to the inhibition by UK5099 alone as expected (figure 4.30). It can be concluded that pyruvate is transported into mitochondria in part directly and in part after conversion to alanine, and that only the combined inhibition with AOA and the pyruvate transport inhibitor blocks pyruvate oxidation. We conclude that a more reduced cytoplasmic NADH/NAD redox state as occurs in association with metformin cannot explain the lowering of G6P.

4.6.5 Metformin elevates cell phosphate: a potent allosteric activator of PFK1

The above studies cumulatively suggest that a change in the concentration of one or more allosteric effectors of PFK1/FBP1 by metformin is a potential explanation for the

small stimulation in flux through glycolysis (increased metabolism of [3-³H] glucose and formation of lactate and pyruvate) and the decrease in cell G6P. There are several allosteric effectors of these two enzymes which include ATP, ADP, AMP, Pi, ammonia, citrate, F-2,6-P₂ (Sugden & Newsholme., 1975; McGrane et al., 1983; Hers & Hue., 1983; Bosca et al., 1985). The latter can be excluded because it is decreased rather than increased by metformin (Al-Oanzi et al., 2017). Possible candidates for the metformin mechanism would include lowered citrate or raised ammonia or Pi. We tested for the latter possibility by measurement of cell Pi. Pi was significantly increased by 32-130% with 0.5-1.0mM metformin (figure 4.31 A, B). Pi was also raised by 100µM DNP but not by 1µM rotenone (figure 4.31 C, D). This indicates an increase in Pi as a possible allosteric effector (activator of PFK1 and inhibitor of FBP1) to explain the stimulation of glycolysis and the lowering of G6P by ≥0.5mM metformin.

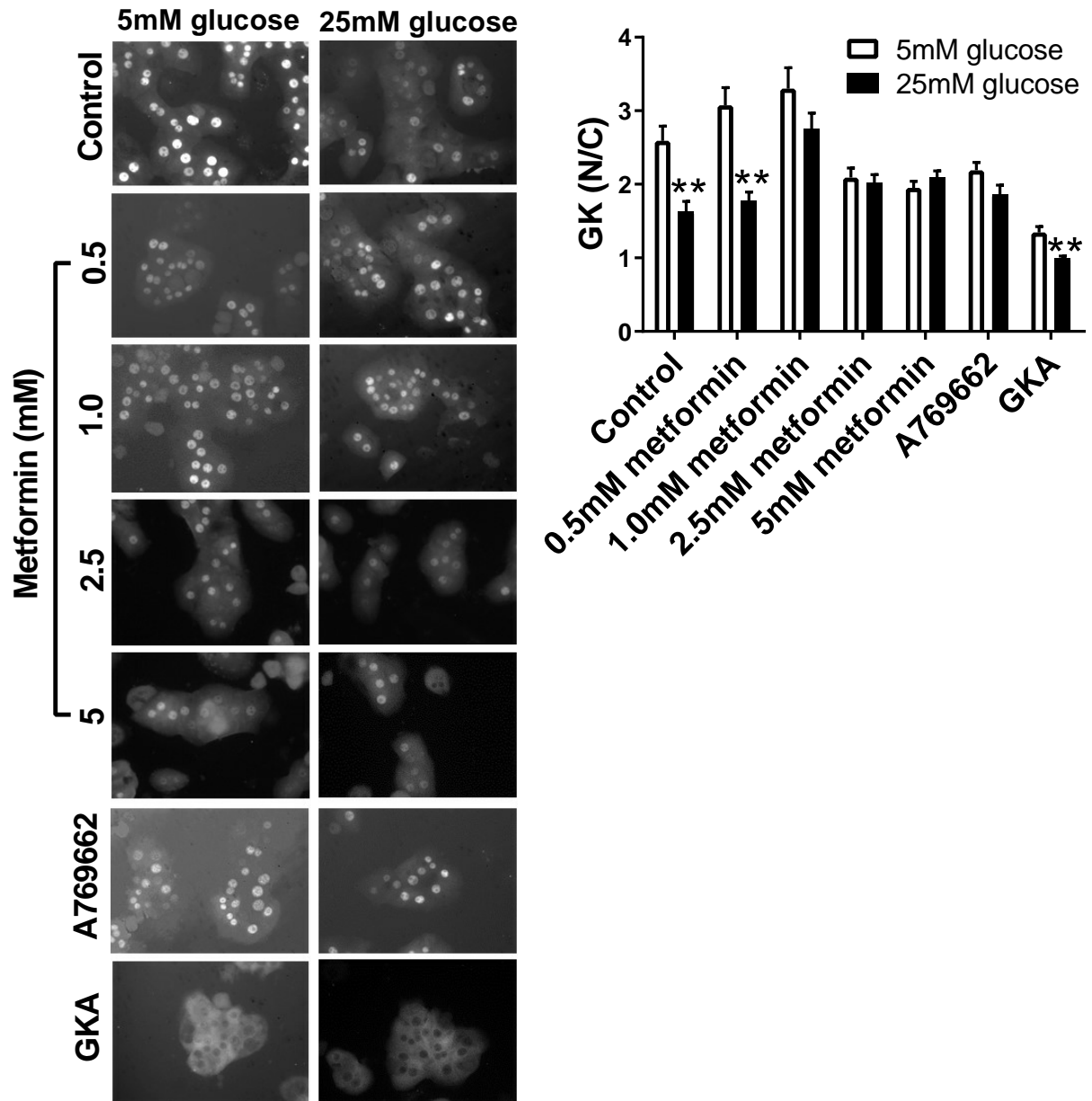


Figure 4.1 Sequestration of GK in the nucleus is abolished by high metformin, A769662 and GKA

Rat hepatocytes were pre-incubated with 5mM glucose and metformin or 20 μ M A769662 for 2 hours, then incubated for a further 1 hour with 10 μ M GKA and 5mM or 25mM glucose. Mean \pm SEM, n=1-3 (10 fields were imaged for each incubation condition). ** p <0.01 glucose effect.

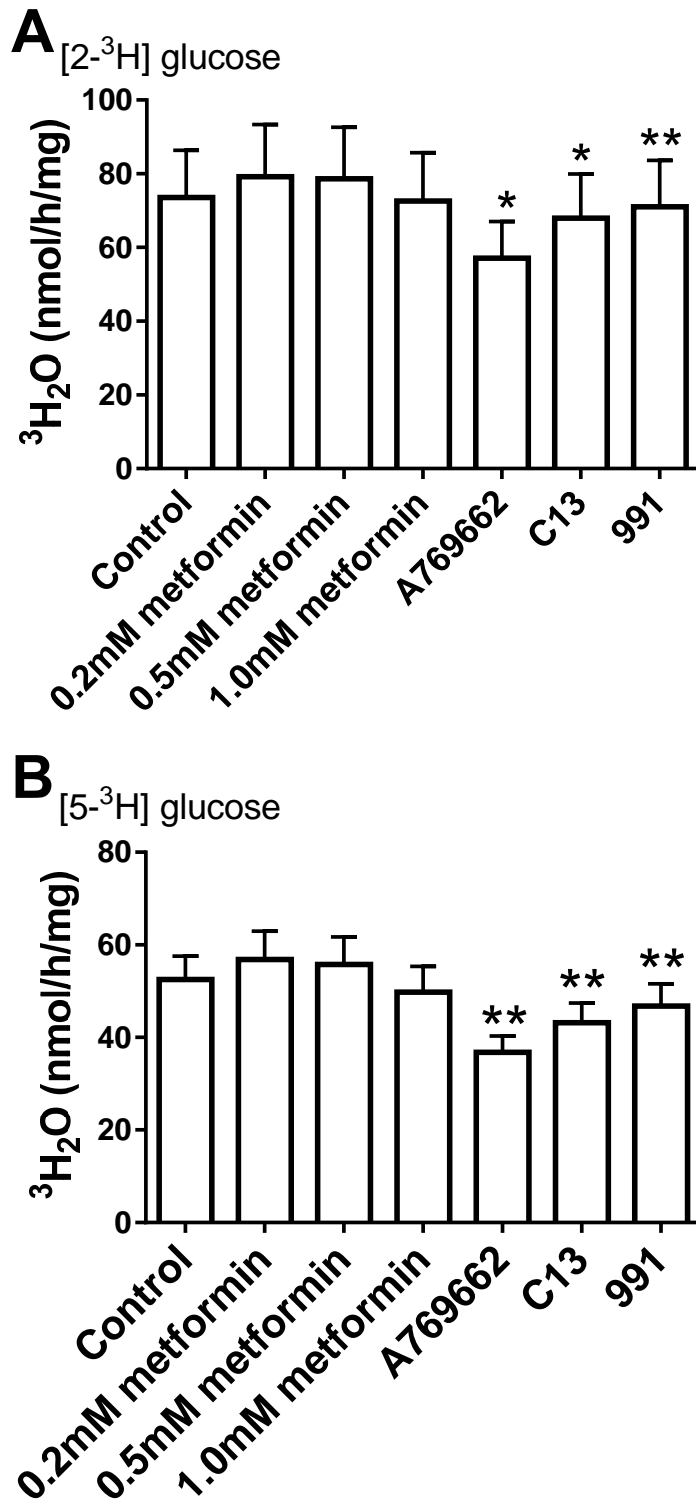


Figure 4.2 AMPK activators but not metformin inhibit metabolism of [2-³H] glucose and [5-³H] glucose

Rat hepatocytes were pre-incubated with 5mM glucose and metformin, 20 μ M A769662, 3 μ M C13 or 3 μ M 991 for 2 hours, then incubated for a further 1 hour with [2-³H] glucose or [5-³H] glucose, 25mM glucose and 2 μ M S4048. Mean \pm SEM, n= 7 (triplicate).

*p<0.05, **p<0.01.

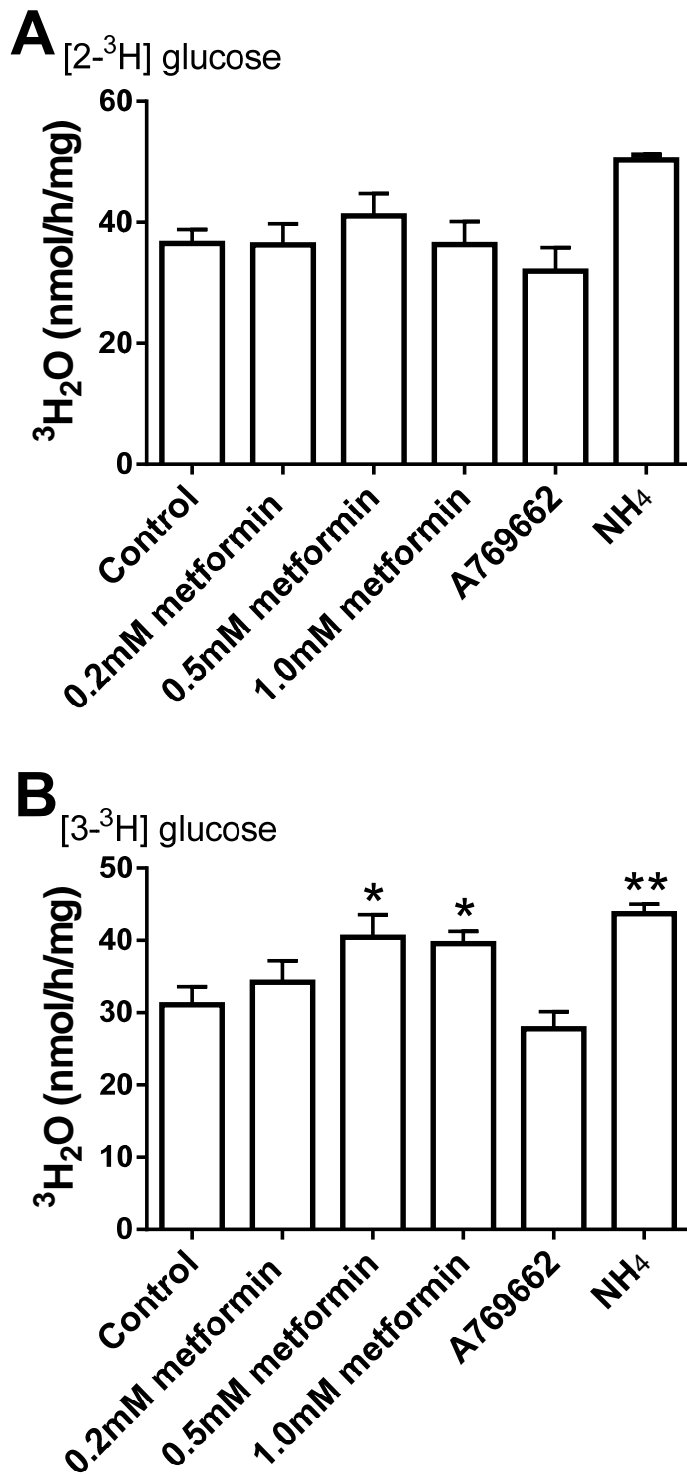


Figure 4.3 Metformin and ammonium ion stimulate metabolism of [3-³H] glucose but not [2-³H] glucose

Mouse hepatocytes were pre-incubated with metformin and 10 μ M A769662 for 2 hours, then 2mM ammonium (NH₄) and [2-³H]-glucose or [3-³H]-glucose, 25mM glucose and 0.2 μ M S4048 for 1 hour. Mean \pm SEM (triplicate), n=2-5. *p<0.05, **p<0.01.

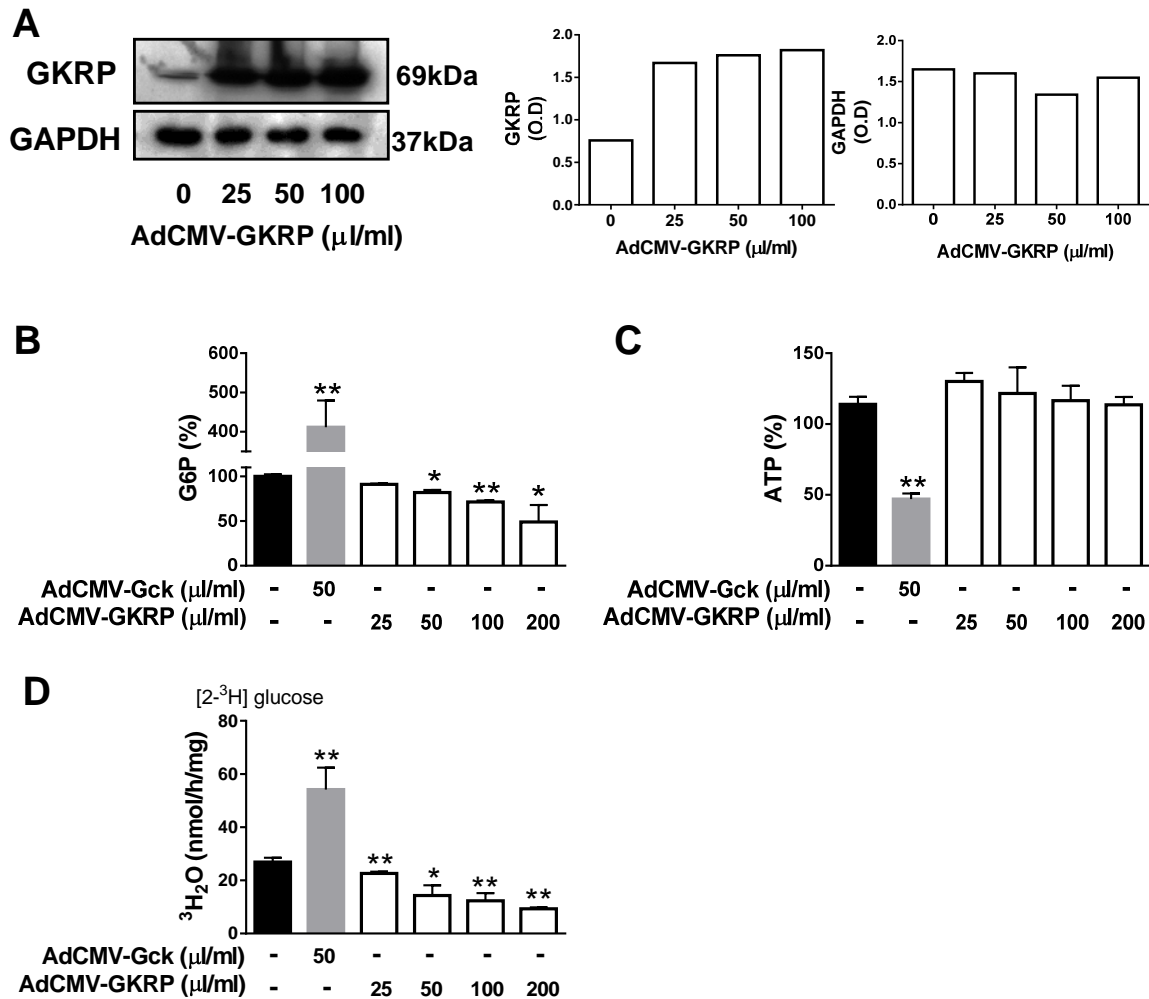


Figure 4.4 Lowering of G6P by GKR overexpression correlates with inhibition of glucose phosphorylation

Mouse hepatocyte monolayers treated with AdCMV-GK (50µl/ml) or AdCMV-GKRP (25-200µl/ml) were cultured overnight with 10nM dexamethasone and 1nM insulin. Cells were then incubated with [2-³H] glucose, 25mM glucose and 0.2µM S4048 for 1 hour. Results= mean ± SEM, n=1-2. *p<0.05, **p<0.01.

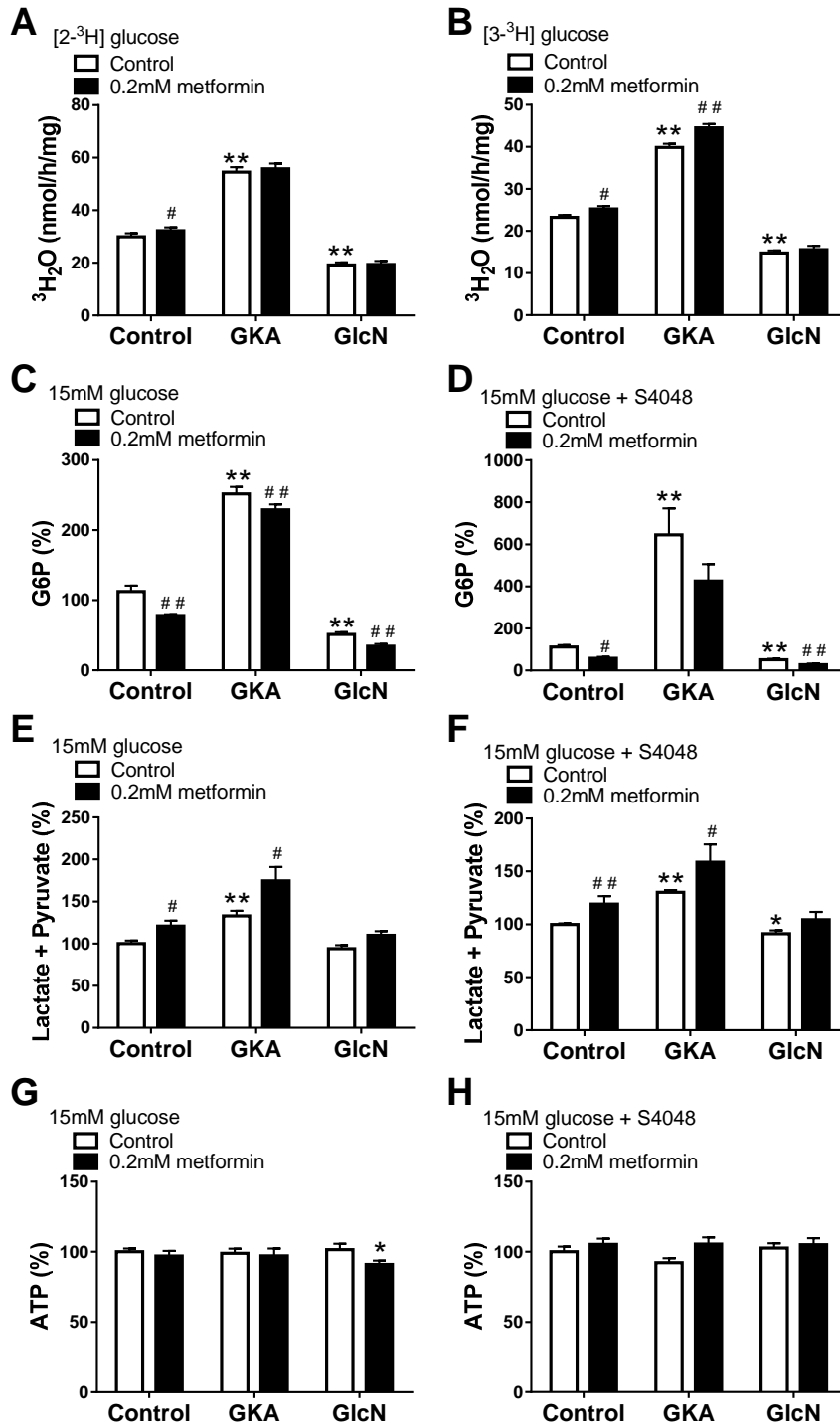


Figure 4.5 Inhibition of glucose phosphorylation by glucosamine (GlcN) but not by metformin

Mouse hepatocytes were pre-incubated with metformin for 2 hours, then [2-³H] glucose or [3-³H]-glucose, 15mM glucose and 10 μ M GKA or 5mM glucosamine (GlcN) in the absence (C, E, G) or presence (A, B, D, F, H) of 0.2 μ M S4048 for 1 hour. Mean \pm SEM, n=3-9. *p<0.05, **p<0.01 GKA or glucosamine effect. # P<0.05, ## P<0.01 metformin effect. Basal values were as in Table 3-1 and Table 3-2.

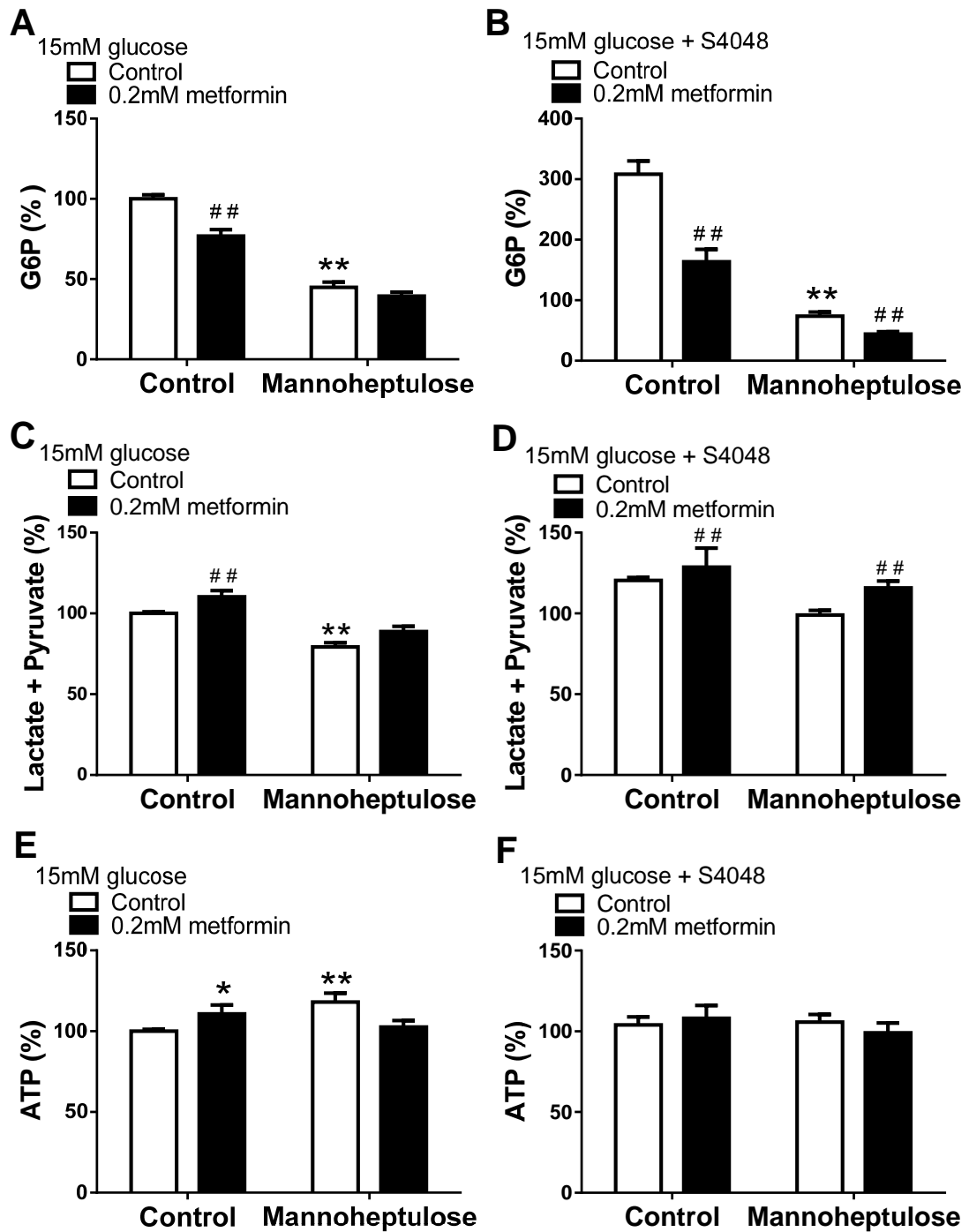


Figure 4.6 Metformin lowers G6P in the presence of the GK inhibitor mannoheptulose

Mouse hepatocytes were pre-incubated with metformin in the absence (A, C, E) or presence (B, D, F) of 0.2 μ M S4048 for 2 hours, then incubated with 10mM mannoheptulose for 1 hour. Mean \pm SEM, n=4-8. *p<0.05, **p<0.01. Basal values were as in Table 3-1 and Table 3-2.

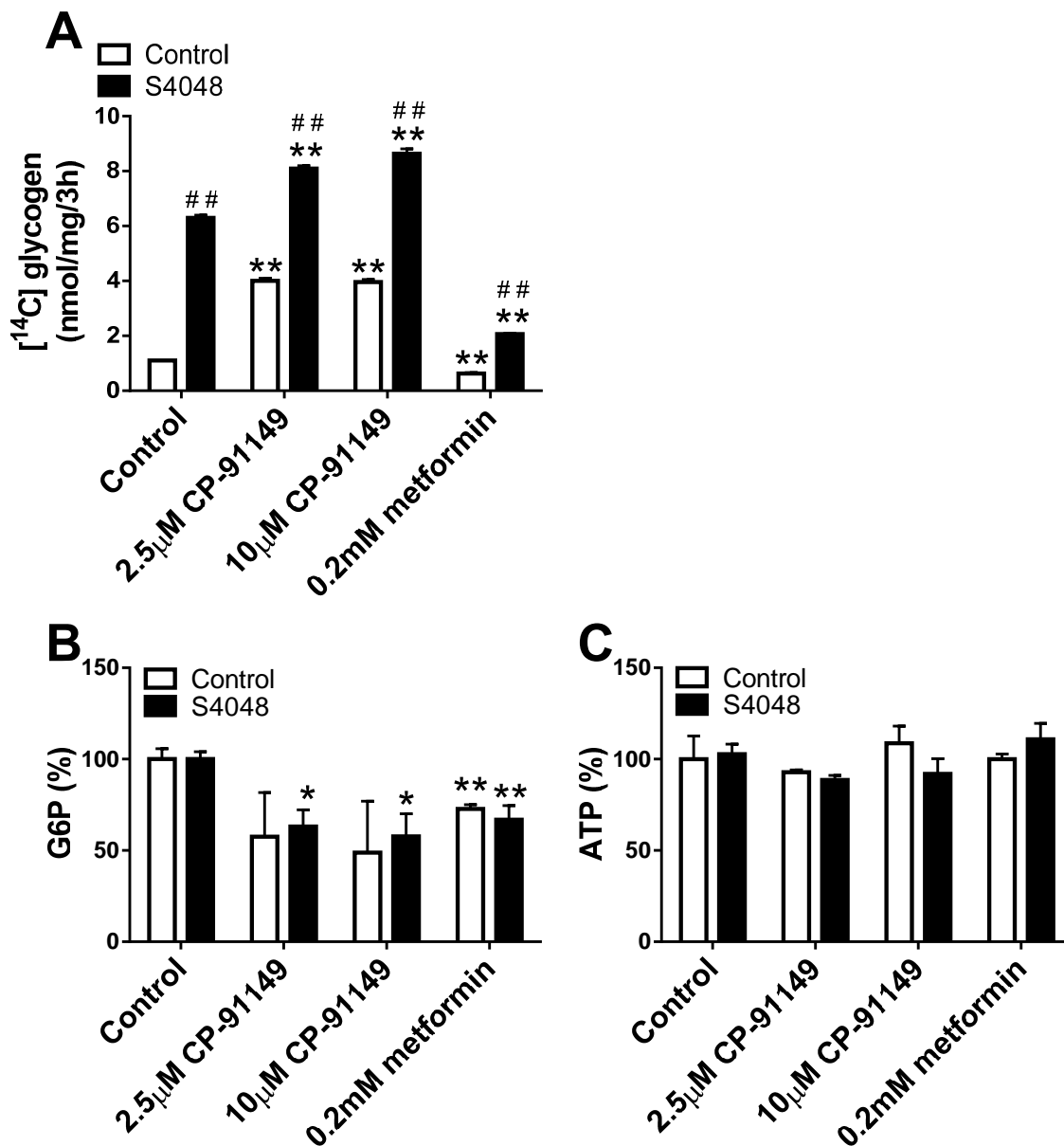


Figure 4.7 Metformin lowers G6P but inhibits glycogen synthesis

Mouse hepatocytes were pre-incubated with metformin for 2 hours, then incubated for a further 3 hours with CP-91149, 25mM glucose and D- [U-¹⁴C] glucose in the absence or presence of 0.2µM S4048. Mean ± SEM, n=1 (triplicate). *p<0.05, **p<0.01 CP-91149 or metformin effect. #P<0.05, ##P<0.01 S4048 effect.

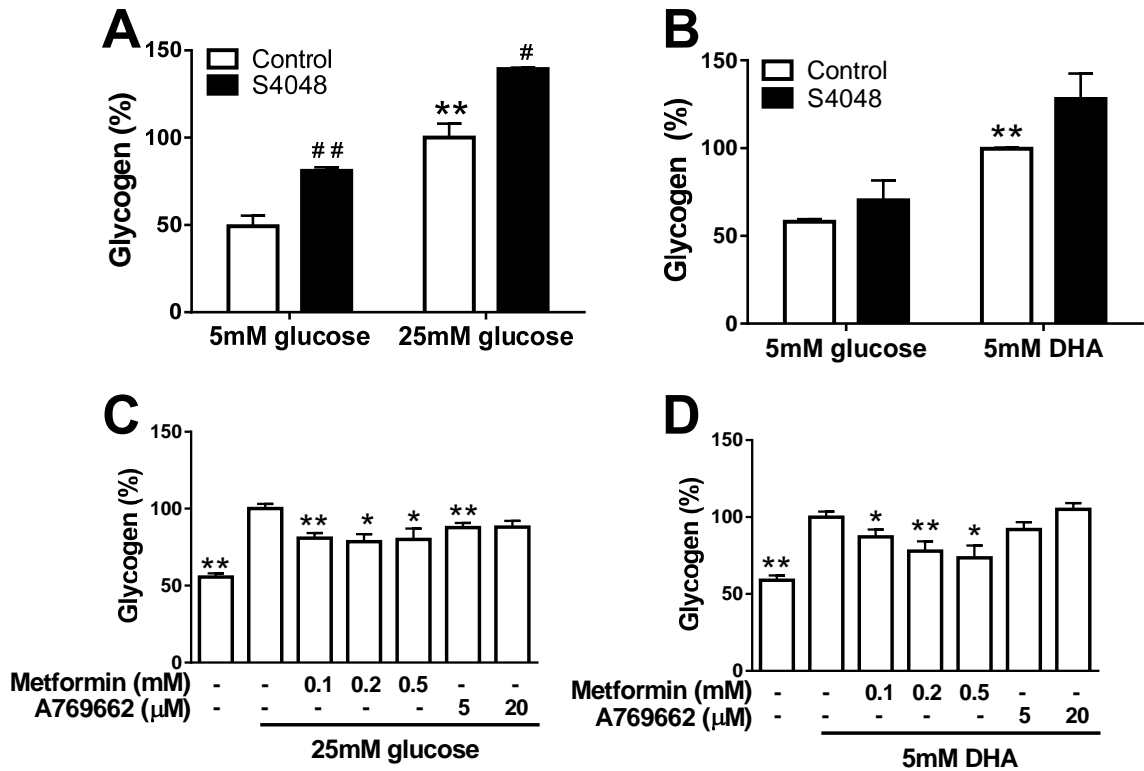


Figure 4.8 Metformin decreases glycogen accumulation with high glucose and DHA as substrates

Rat hepatocytes were pre-incubated with 5mM glucose and metformin or A769662 in the absence or presence of 2 μ M S4048 for 2 hours, then a further 2-3 hours with 25mM glucose (A, C) or 5mM DHA (B, D). Mean \pm S.E.M, n=1-3 (triplicate). *p<0.05, **p<0.01 glucose or metformin effect. # P<0.05, ## P<0.01 S4048 effect.

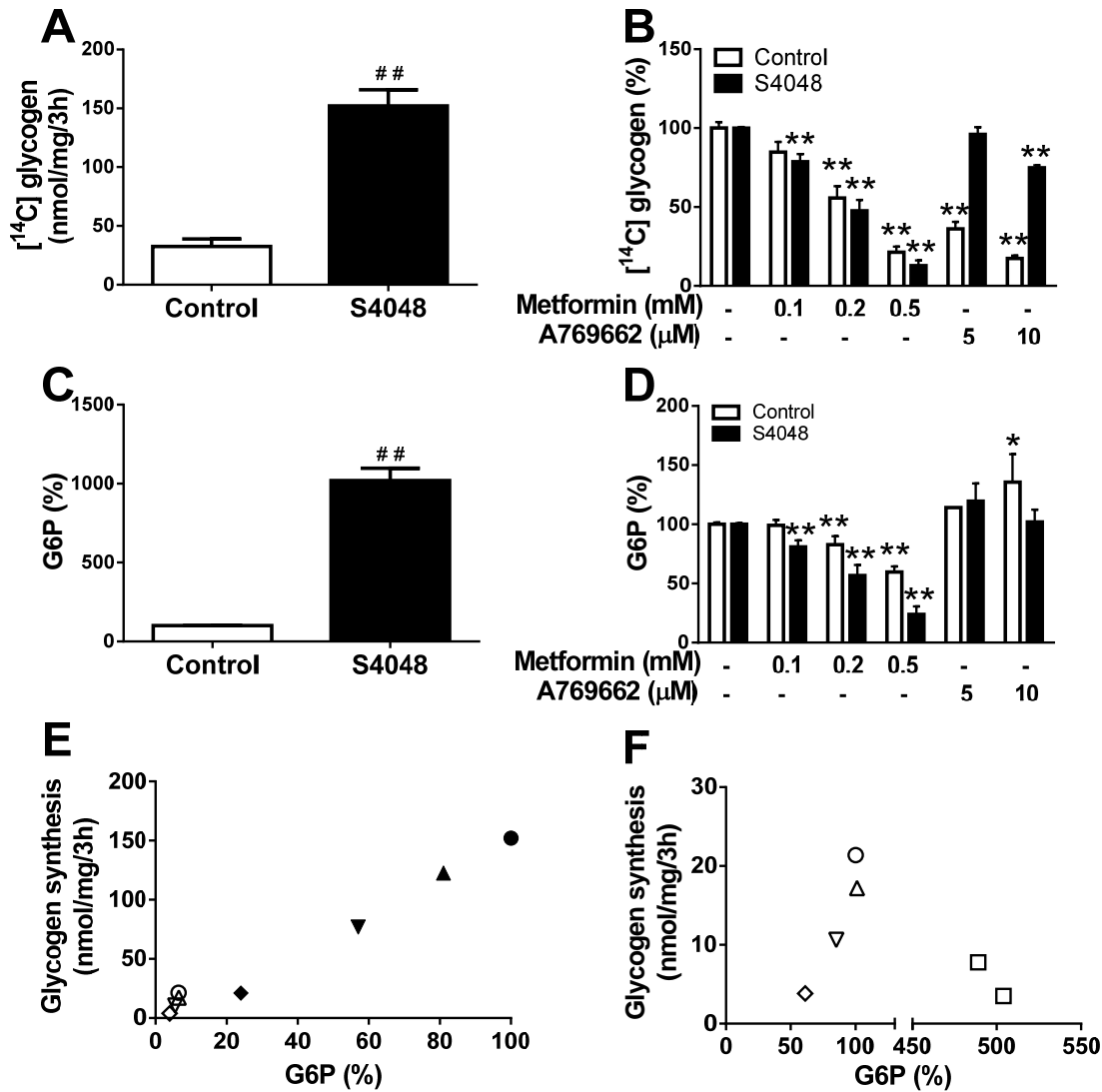
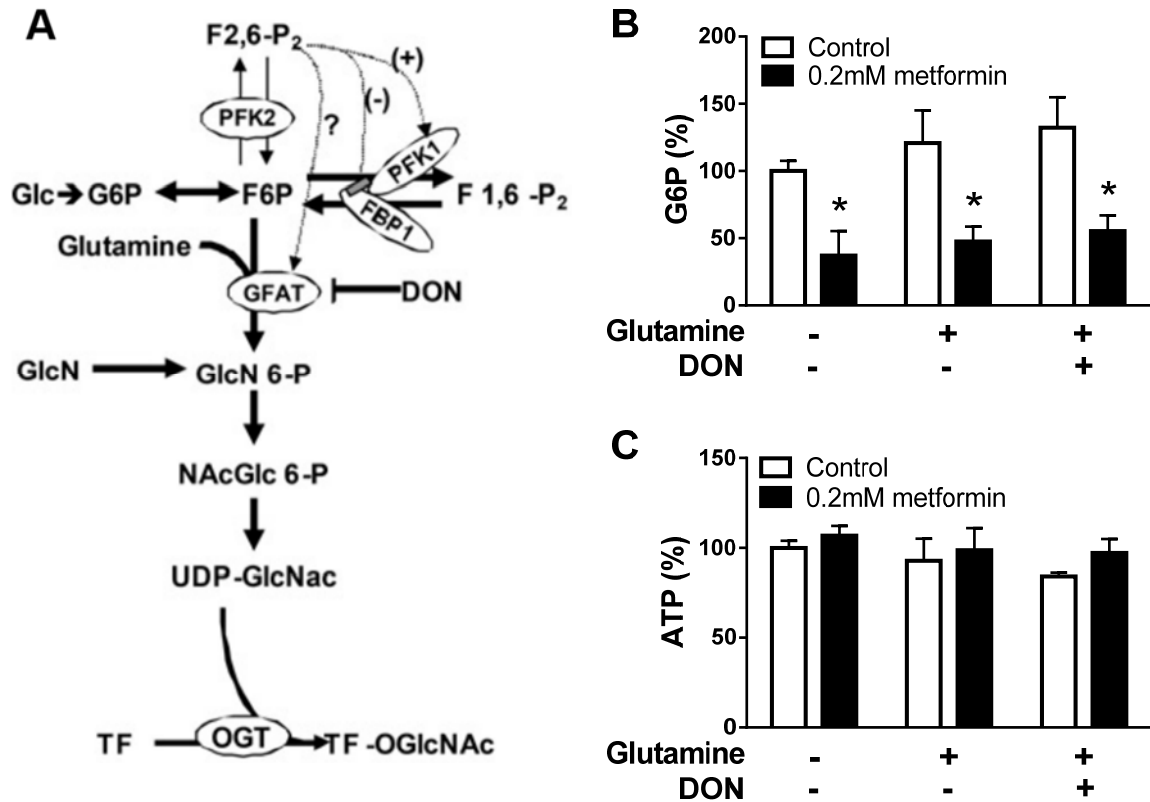


Figure 4.9 Inhibition of glycogen synthesis with metformin with not A769662 correlates with G6P

Rat hepatocytes were pre-incubated with metformin or A769662 for 2 hours, then incubated for a further 3 hours with 25mM glucose and D-[U-¹⁴C] glucose in the absence or presence of 0.2μM S4048. Mean ± SEM, n=3 (triplicate). *p<0.05, **p<0.01 glucose or metformin effect. #P<0.05, ##P<0.01 S4048 effect. Basal values were as in Table 3-1 and Table 3-2. (E, F) Correlation between cell G6P and glycogen synthesis with metformin in the presence of S4048 (filled)(r=0.96) and absence of S4048 (empty)(r=0.96), but no correlation with A769662.

- control, △ 0.1mM metformin, ▽ 0.2mM metformin, ◇ 0.5mM metformin,
- A769662, ● S4048, ▲ 0.1mM metformin + S4048, ▼ 0.2mM metformin + S4048,
- ◆ 0.5mM metformin + S4048.



(Arden et al., 2012)

Figure 4.10 Metformin lowers G6P independently of the hexosamine biosynthesis pathway

(A) Hexosamine biosynthesis pathway (Arden et al., 2012). F6P generated from G6P by PFK1 can enter HBP via GFAT which is inhibited by DON. Glucosamine (GlcN) enters the pathway after GFAT. (B, C) Mouse hepatocyte monolayers were cultured overnight with 10nM dexamethasone, 1nM insulin and 10 μ M DON. Cells were incubated with 0.2 μ M S4048 and metformin in the absence or presence of glutamine for 2 hours, then a further 1 hour with 25mM glucose. Mean \pm SEM, n=2. *P<0.05 metformin effect. Basal values were as in Table 3-1 and Table 3-2.

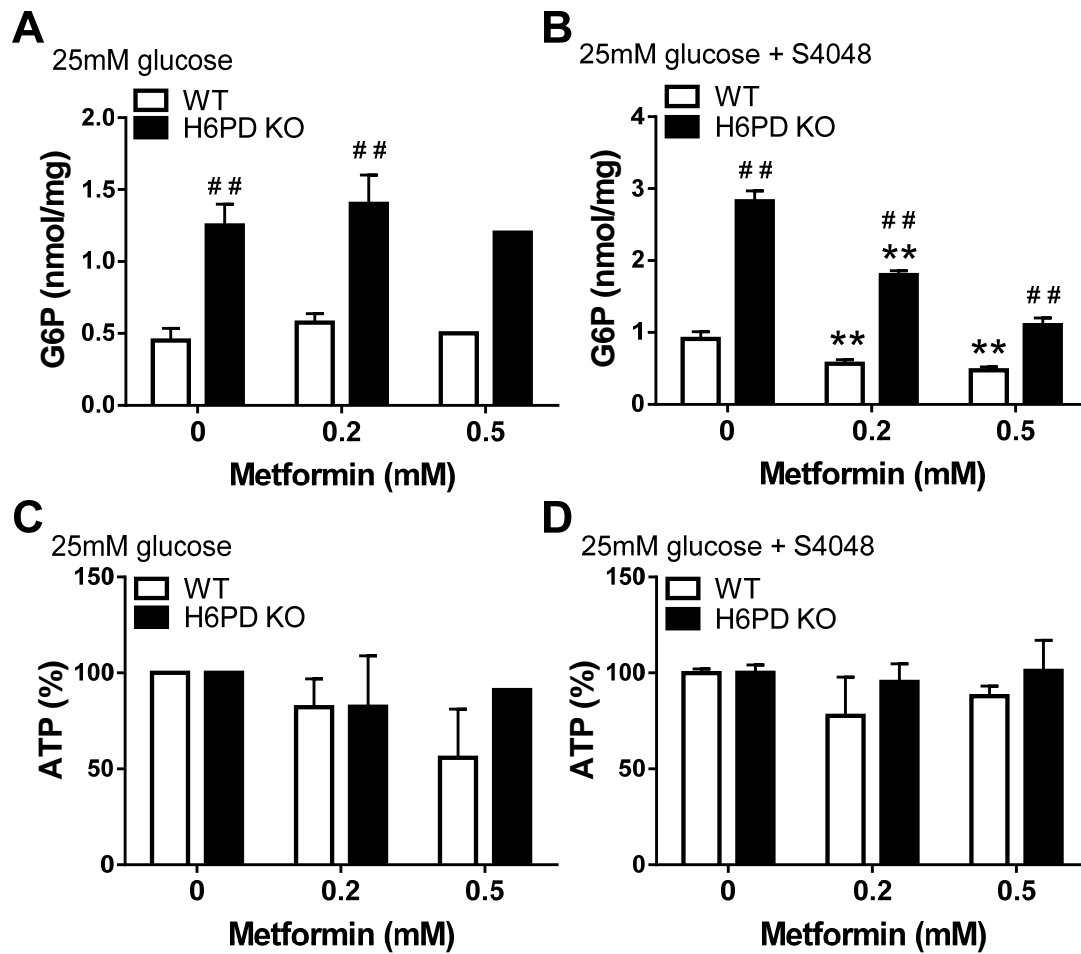


Figure 4.11 Metformin lowers G6P independently of hexose 6-phosphate dehydrogenase

Mouse hepatocytes were pre-incubated with metformin in the absence (A, C) or presence (B, D) of 0.2 μ M S4048 for 2 hours, then incubated for a further 1 hour with 25mM glucose. Mean \pm S.E.M. WT n=2, H6PD KO n=1. **p<0.01 metformin effect. ##p<0.01 KO effect.

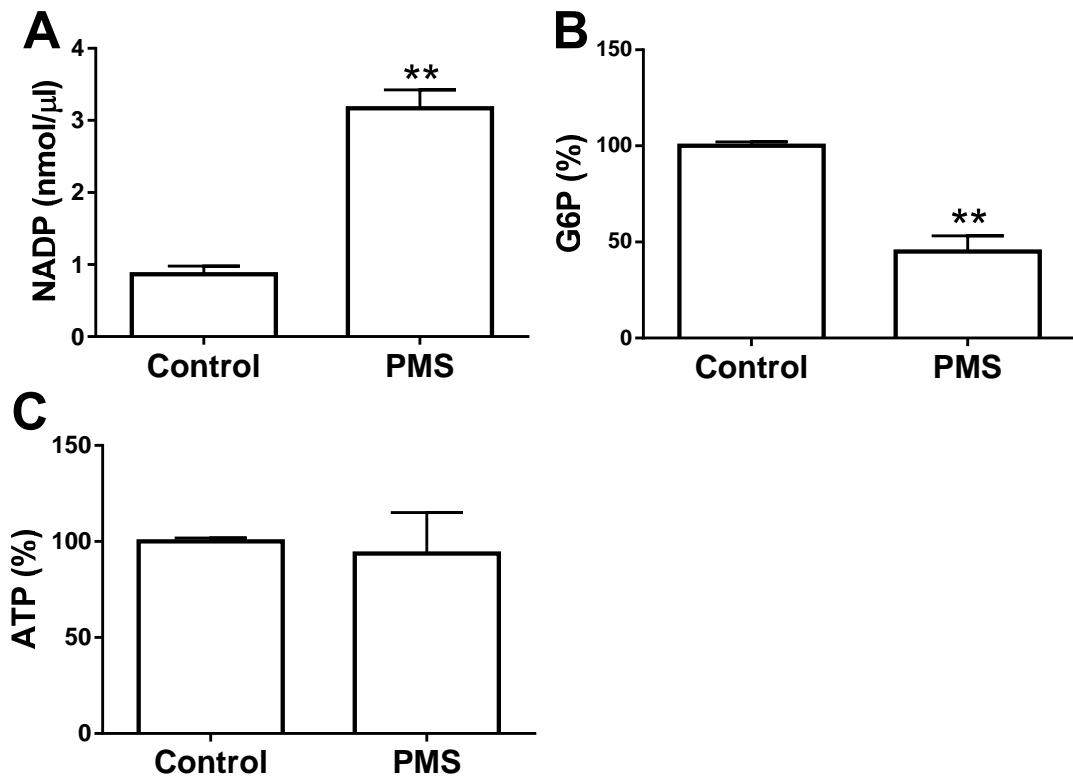


Figure 4.12 PMS increases NADP and decreases G6P

Rat hepatocytes were pre-incubated with 10 μ M PMS for 2 hours, then incubated for a further 15 minutes to 1 hour with 25mM glucose. Mean \pm S.E.M. **p<0.01. n=3-4.

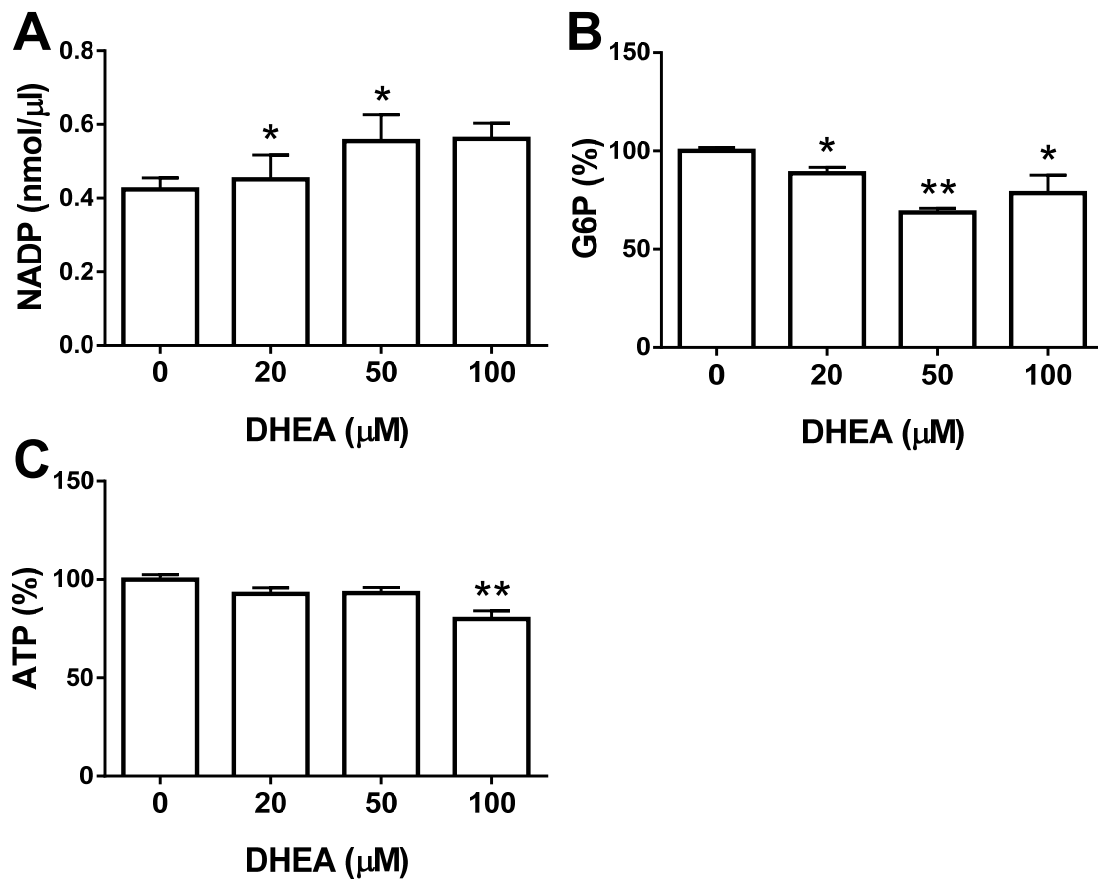


Figure 4.13 DHEA increases NADP and decreases G6P

Mouse hepatocyte were pre-incubated with 0.2-2 μM S4048 and DHEA for 30 minutes, then incubated with 25mM glucose for a further 1 hour. Mean \pm SEM, n=3-6. *p<0.05, **p<0.01.

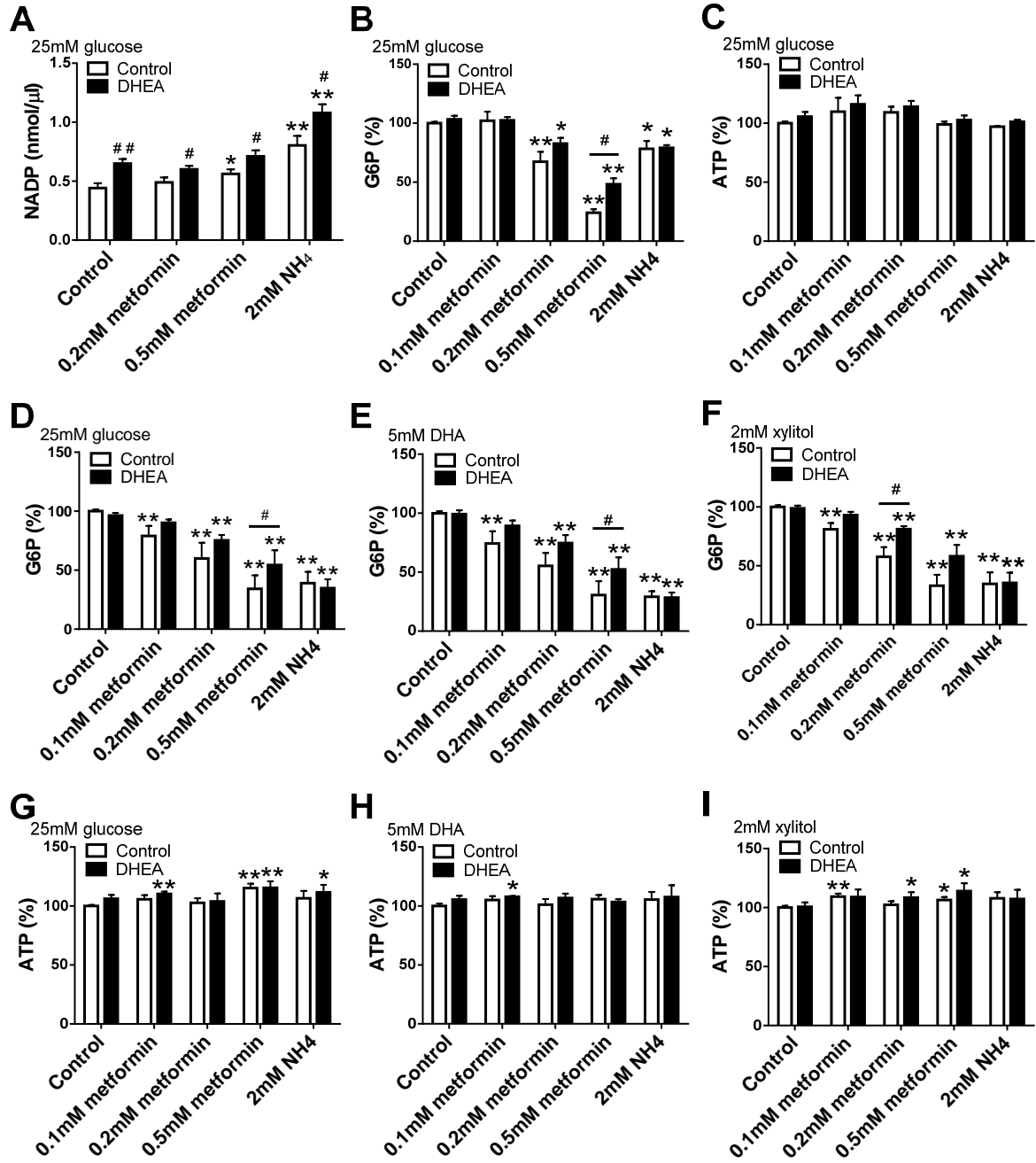


Figure 4.14 DHEA attenuates the decrease in G6P by metformin

Mouse hepatocytes (A-C) and rat hepatocytes (D-I) were pre-incubated with 0.2-2 μ M S4048, metformin and 10-20 μ M DHEA for 2 hours, then 1 hour with ammonium (NH₄⁺), 25mM glucose, 5mM DHA or 2mM xylitol. Mean \pm SEM n=4-8. Basal values were as in Table 3-1 and Table 3-2.

*p<0.05, **p<0.01 metformin or NH₄ effect. #P<0.05, ##P<0.01 DHEA effect.

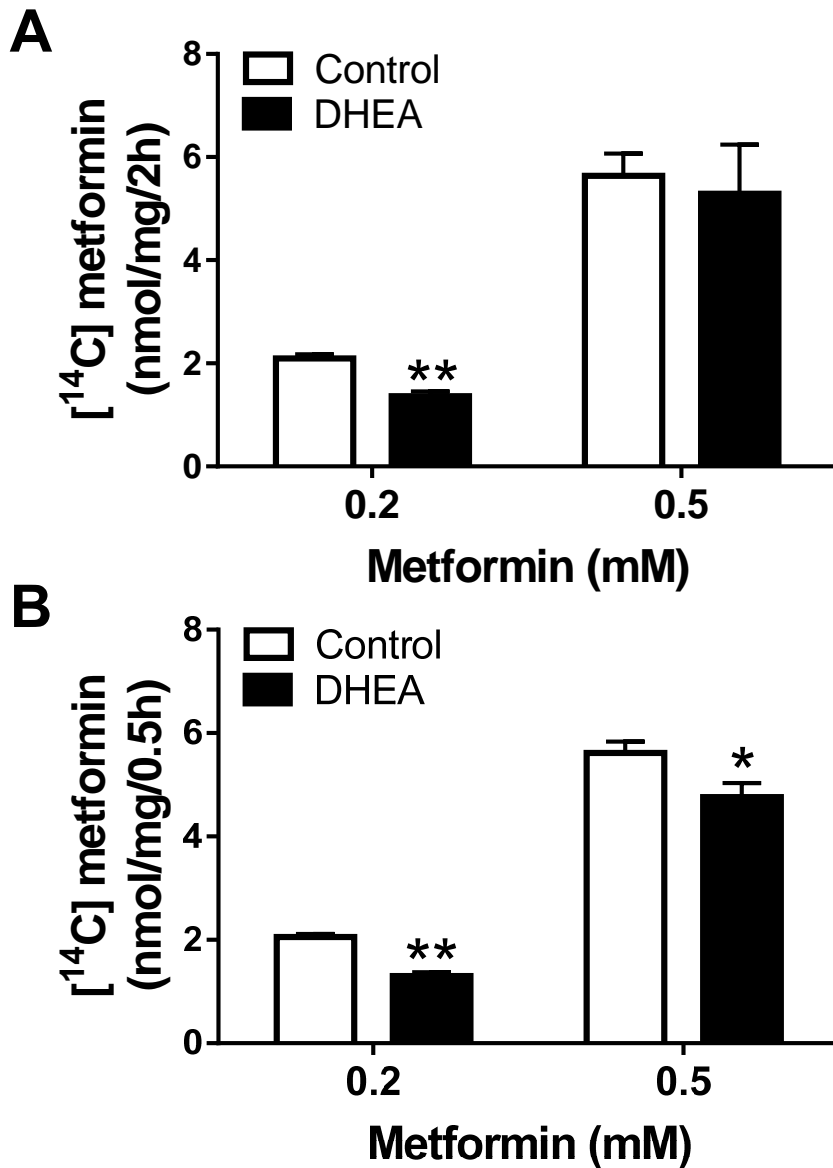


Figure 4.15 Effects of DHEA on [¹⁴C] metformin accumulation

Mouse hepatocytes were pre-incubated with [¹⁴C] metformin and metformin for 2 hours, and 20 μ M DHEA for either 2 hours (A) or 30 minutes (B), then a further 1 hour with 25mM glucose. Mean \pm SEM, n=3-4. *p<0.05, **p<0.01 DHEA effect.

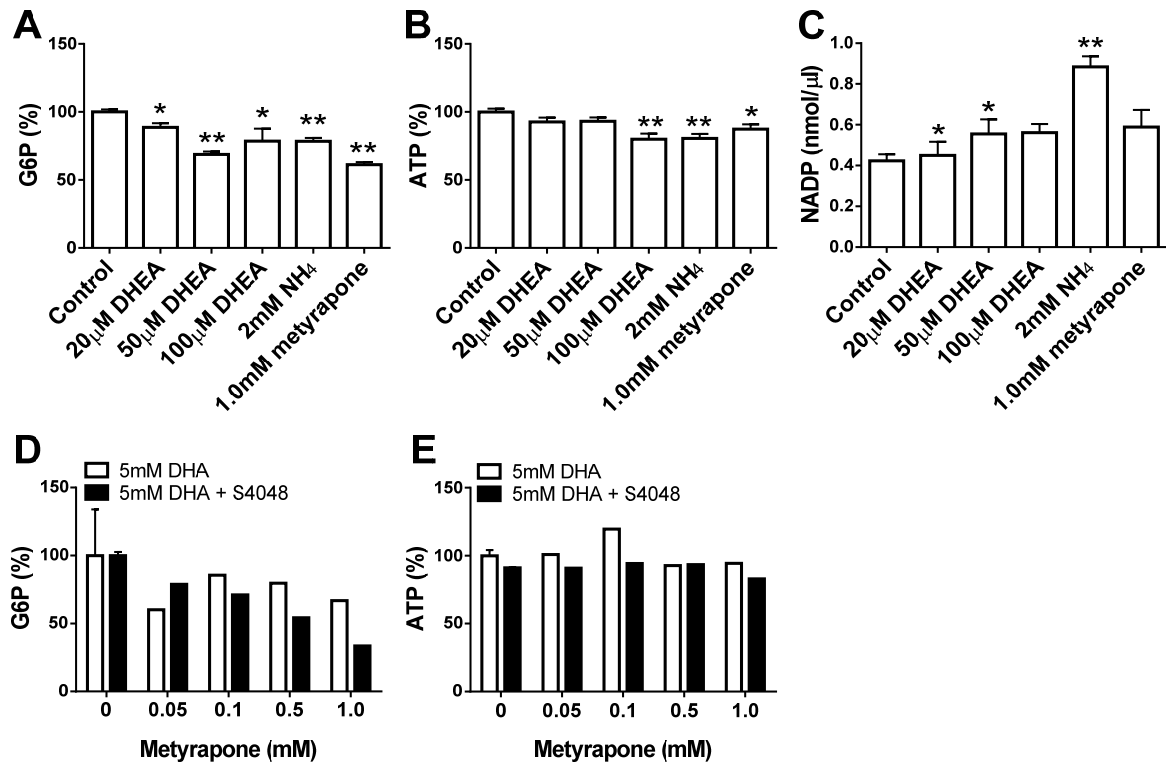


Figure 4.16 G6P is lowered by DHEA and metyrapone

Rat hepatocytes were pre-incubated with 0.2 μ M S4048 for 2 hours and DHEA for 30 minutes, then for a further 1 hour with ammonium (NH₄⁺), metyrapone and 25mM glucose (A-C). Rat hepatocytes were incubated for 1 hour with 2 μ M S4048, 0.05-1mM metyrapone and 5mM DHA (D, E). Mean \pm SEM, n=4-9 (A-C), n=1 (D-E) *p<0.05, **p<0.01. Basal values were as in Table 3-1 and Table 3-2.

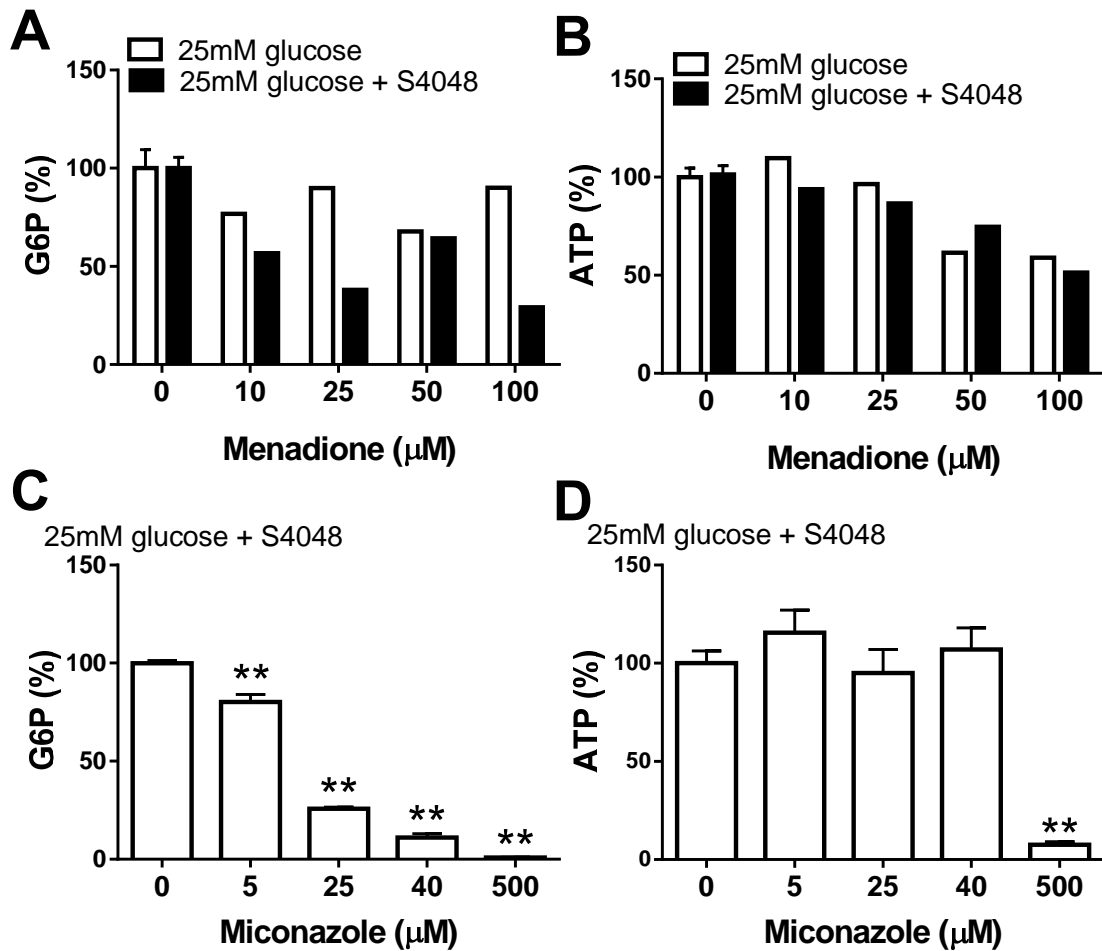


Figure 4.17 Menadione and miconazole lower G6P

Rat hepatocytes were incubated with 0.2-2 μM S4048, 0.05-1mM menadione, 0.05-1mM metyrapone, 5-500 μM miconazole and 25mM glucose for 1 hour. Mean \pm SEM, n=1-2. *p<0.05, **p<0.01. Basal values were as in Table 3-1 and Table 3-2.

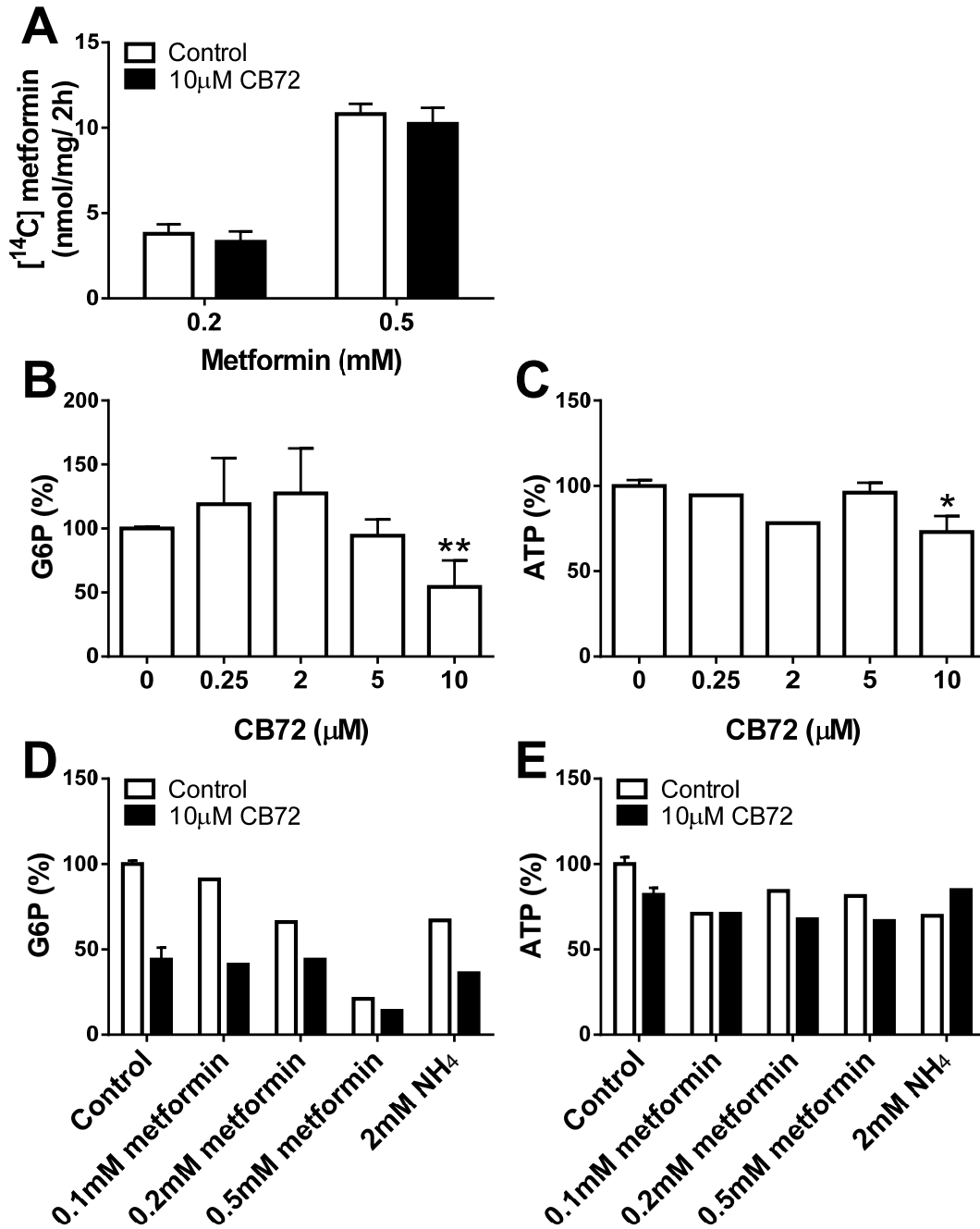


Figure 4.18 CB72 lowers G6P

Mouse hepatocytes were pre-incubated with $[^{14}\text{C}]$ metformin, metformin and CB72 for 2 hours, then a further 1 hour with 25mM glucose (A). Rat hepatocytes were preincubated with metformin and CB72 for 2 hours, then a further 1 hour with 2mM ammonium (NH_4) and 25mM glucose (B-E). Mean \pm SEM, n=3 (A), n=1-7 (B-E). *p<0.05, **p<0.01. Basal values were as in Table 3-1 and Table 3-2.

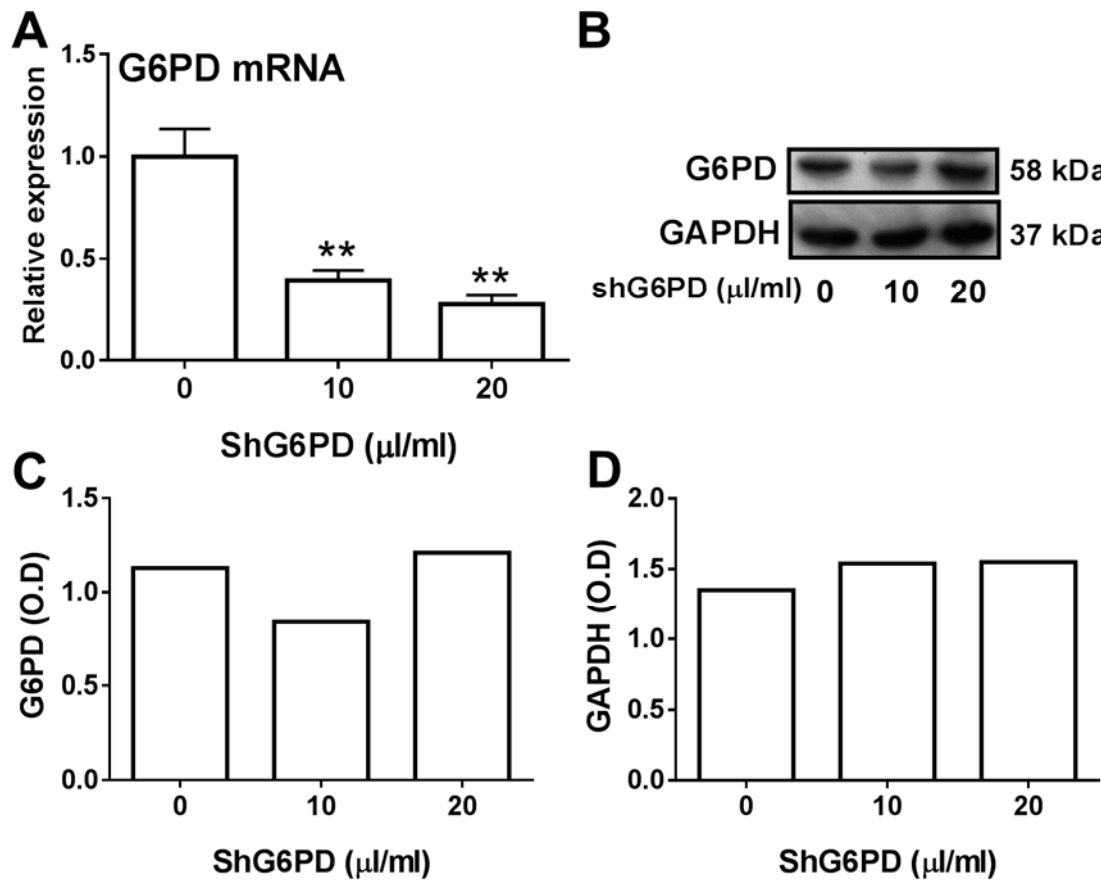


Figure 4.19 G6PD mRNA and protein in hepatocytes treated with short-hairpin RNA

Mouse hepatocyte monolayers were treated with 10-20 $\mu\text{l/ml}$ of an adenoviral vector for G6PD (shG6PD) and were cultured for 24 hours with 10nM dexamethasone and 1nM insulin. Mean \pm S.E.M. n=4 (A) * p <0.05, ** p <0.01.

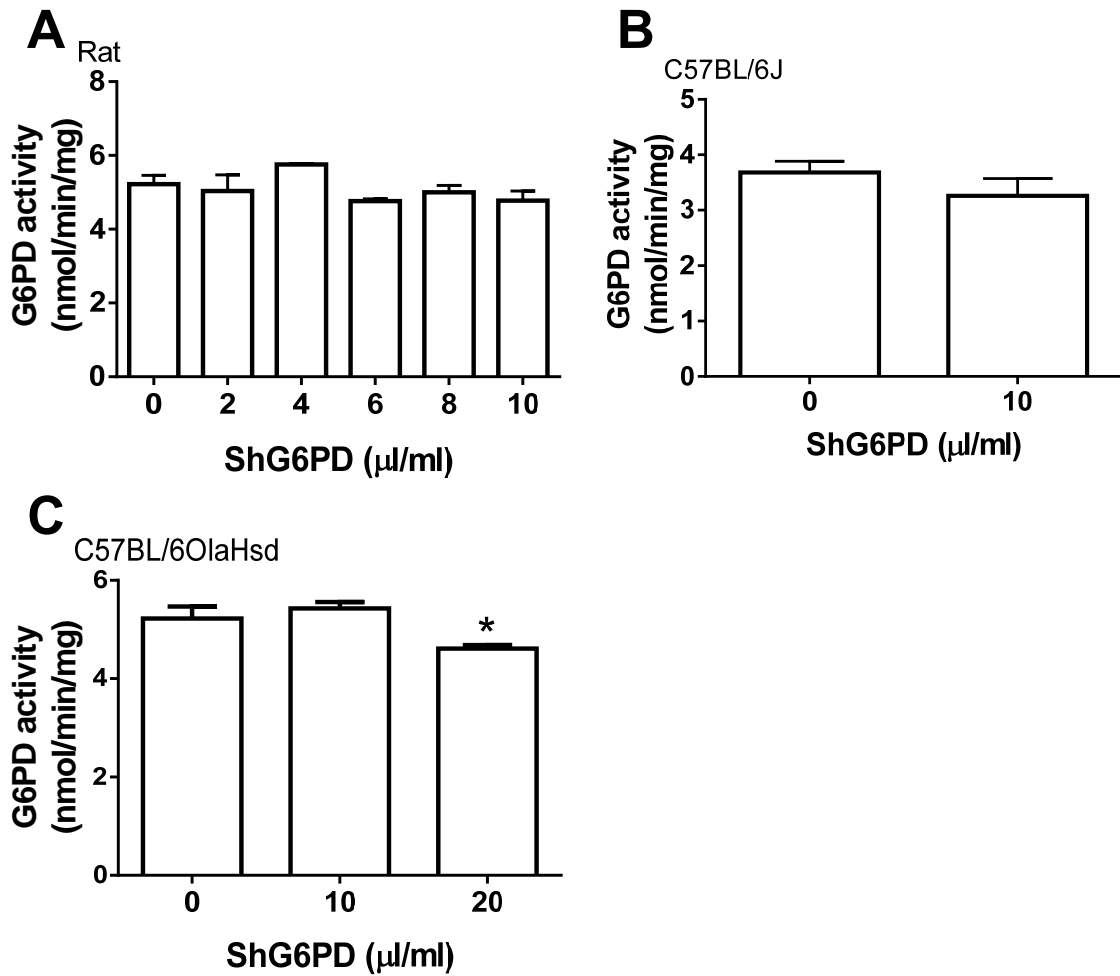


Figure 4.20 shG6PD decreases G6PD enzyme activity at high concentrations only

Rat (A) or mouse (B, C) hepatocyte monolayers were treated with 2-20 $\mu\text{l/ml}$ of an adenoviral vector for G6PD (shG6PD) and were cultured for 24 hours with 10nM dexamethasone and 1nM insulin. Mean \pm SEM, n=1-4. *p<0.05, **p<0.01.

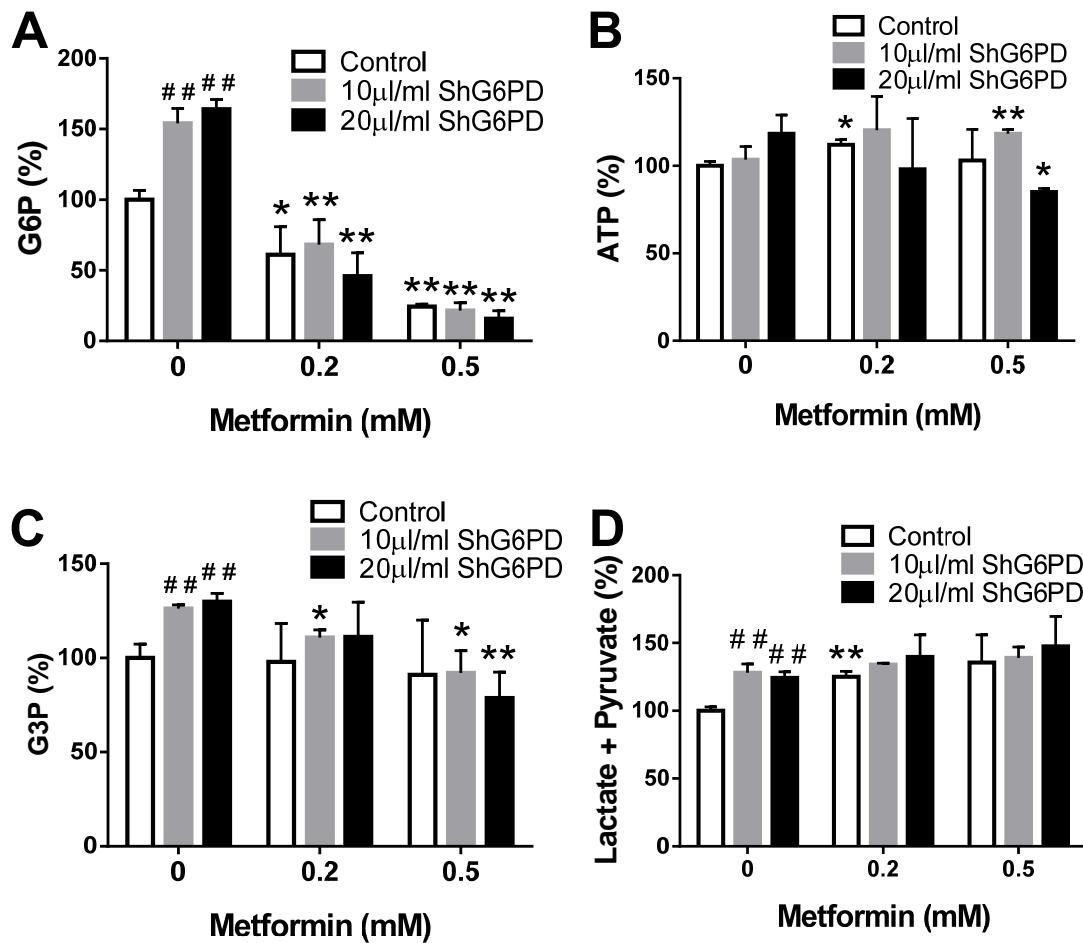


Figure 4.21 Metformin lowers G6P in the presence of ShG6PD

Mouse hepatocyte monolayers were treated with 2-20 μl/ml of an adenoviral vector for G6PD (shG6PD) and were cultured for 24 hours with 10 nM dexamethasone and 1 nM insulin. Cells were incubated with metformin and 0.2 μM S4048 for 2 hours and a further 1 hour with 25 mM glucose. Mean ± SEM, n=3. *p<0.05, **p<0.01 metformin effect. # p<0.05, ### p<0.01 shG6PD effect. Basal values were as in Table 3-1 and Table 3-2.

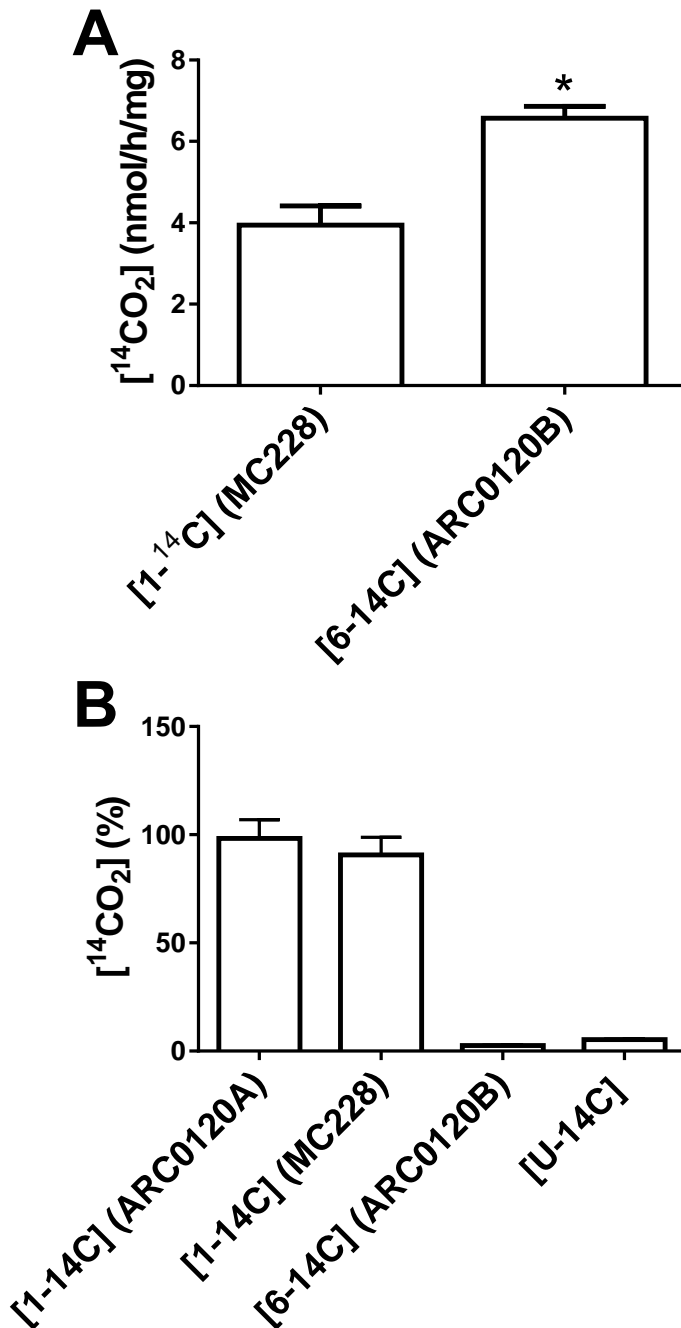


Figure 4.22 Higher rate of ¹⁴CO₂ formation from [6-¹⁴C] glucose than from [1-¹⁴C] glucose in mouse hepatocytes

(A) Mouse hepatocytes were incubated with MEM, 0.2 μ M S4048, 15mM glucose and [1-¹⁴C] glucose or [6-¹⁴C] glucose for 1 hour and ¹⁴CO₂ release was measured. Mean \pm SEM, n=4. *p<0.05. (B) The distribution of [¹⁴C] label on carbon-1 was determined by incubation of 0.1mM glucose with hexokinase (0.002 mg), G6PD (0.003 mg) and 6PGD (0.06 mg). Samples were removed at various time intervals for acidification and collection of ¹⁴CO₂, which was expressed as a percentage of total activity. This confirmed the purity (> 90%) of 2 different preparations of [1-¹⁴C] glucose (ARC120 and MC228). Mean \pm SEM, n=4.

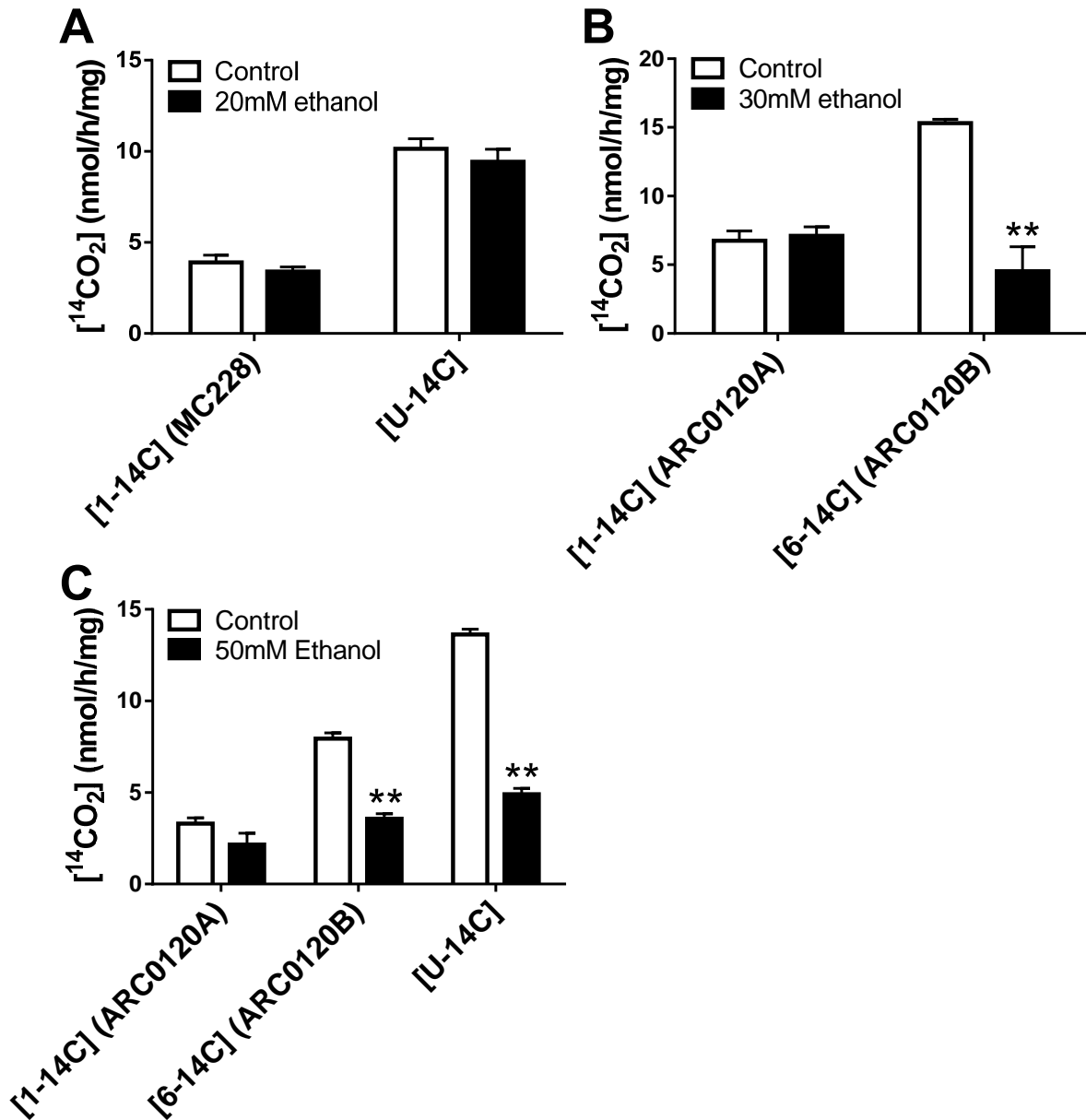


Figure 4.23 Inhibition of [6-¹⁴C] and [U-¹⁴C] glucose oxidation by high ethanol

Mouse hepatocytes were incubated with MEM, 0.2 μ M S4048, 15mM glucose, 20-50mM ethanol and [U-¹⁴C] glucose, [1-¹⁴C] glucose or [6-¹⁴C] glucose for 1 hour and ¹⁴CO₂ was collected. Mean \pm SEM, n=1. *p<0.05, **p<0.01.

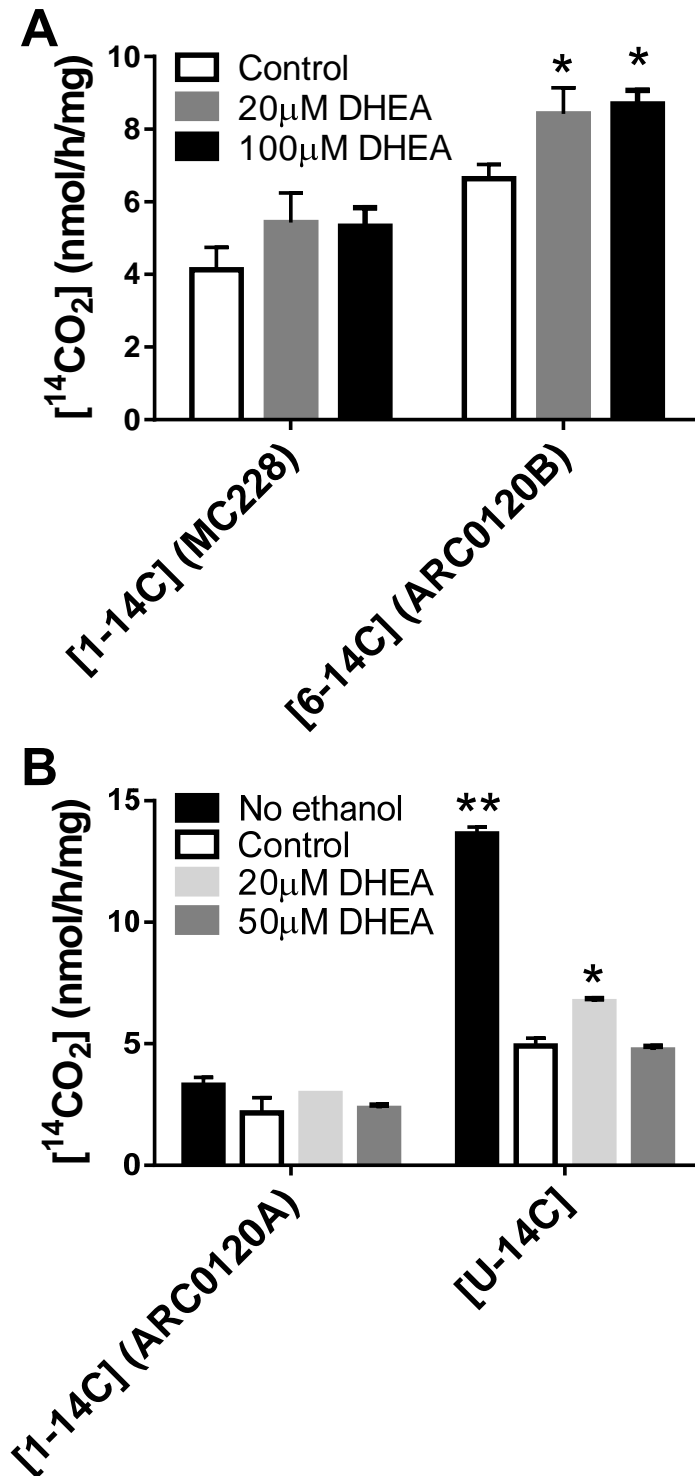


Figure 4.24 DHEA increases oxidation of [6- ^{14}C] glucose and [U- ^{14}C] glucose

Mouse hepatocytes were incubated with MEM, 0.2 μM S4048, 15mM glucose 20-100 μM DHEA and [U- ^{14}C] glucose, [1- ^{14}C] glucose or [6- ^{14}C] for 1 hour. Hepatocytes were incubated in the absence (A) or presence (B) of 50mM ethanol, and $^{14}\text{CO}_2$ was collected. Results = mean \pm SEM, n=1-3 (duplicate/ triplicate). *p<0.05, **p<0.01, #p<0.05, ##p<0.01.

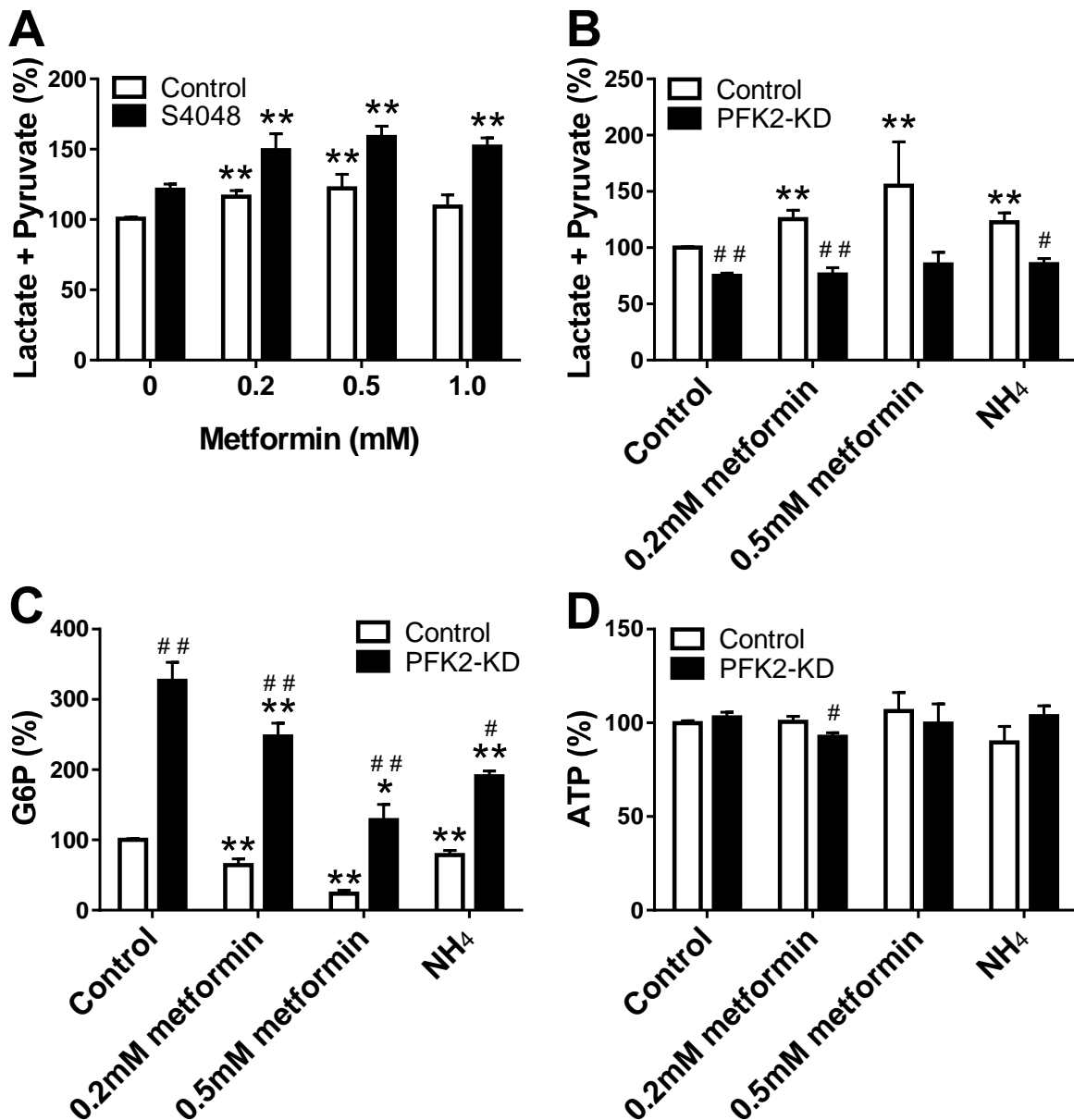


Figure 4.25 Inhibition of glycolysis and raised G6P by expression of a kinase deficient variant of PFK2/ FBP2

Mouse hepatocyte monolayers treated with an adenoviral vector for PFK-KD were cultured for 18 hours with 10nM dexamethasone and 1nM insulin. Cells were incubated with 0.2-2 μ M S4048 and metformin for 2 hours, then a further 1 hour with 25mM glucose and 2mM ammonium (NH₄). Mean \pm SEM, n=2-7. *p<0.05, **p<0.01 metformin or ammonium effect. #p<0.05, ##p<0.01 PFK2-KD effect. Basal values were as in Table 3-1 and Table 3-2.

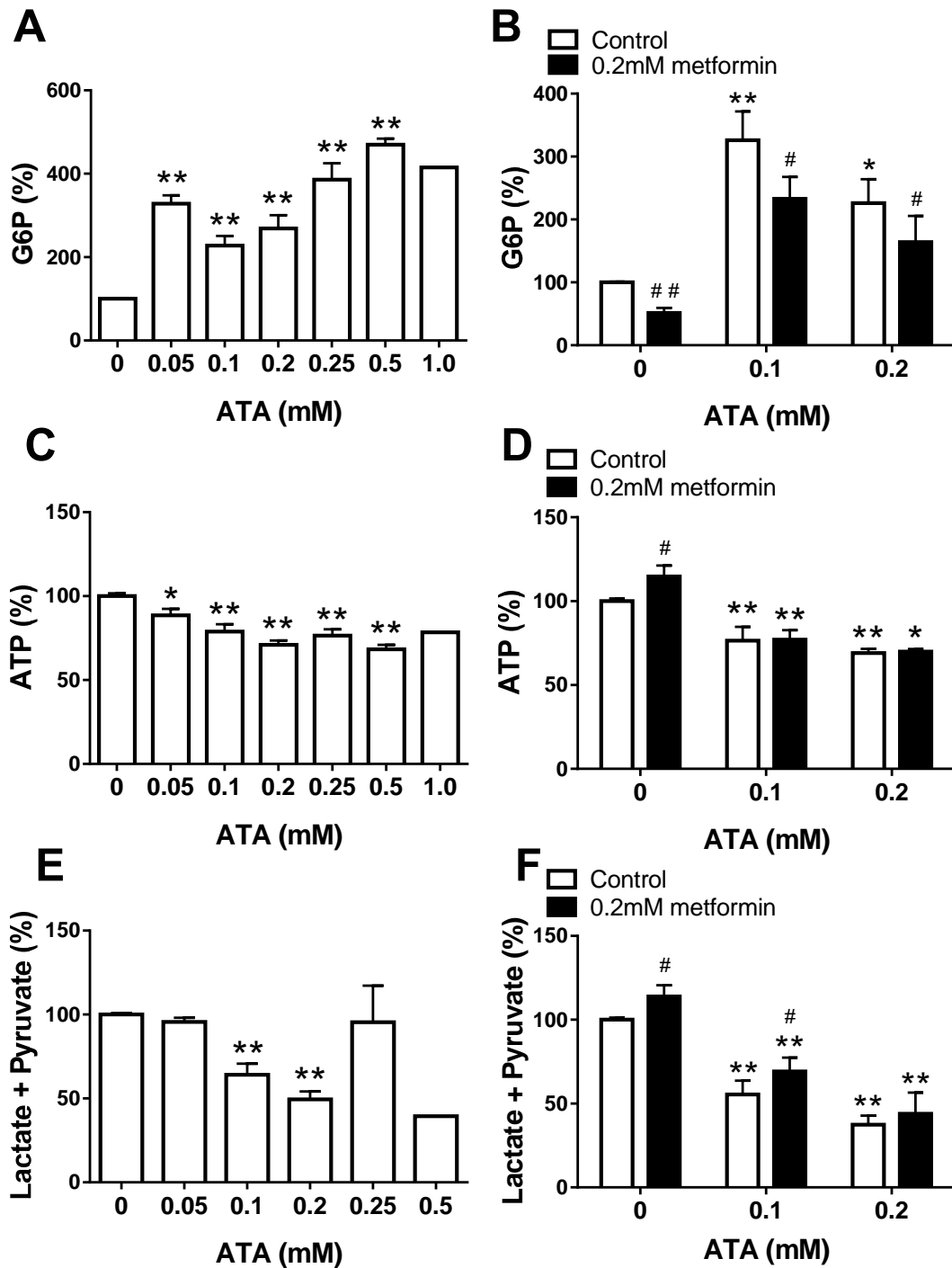


Figure 4.26 Inhibition of glycolysis and raised G6P with an inhibitor of PFK1

Mouse hepatocytes were incubated with 0.2-2 μ M S4048 and ATA or 0.2mM metformin for 2 hours, then a further 1 hour with 25mM glucose. Mean \pm SEM, n=1-18. *p<0.05, **p<0.01 ATA effect. #p<0.05, ##p<0.01 metformin effect. Basal values were as in Table 3-1 and Table 3-2.

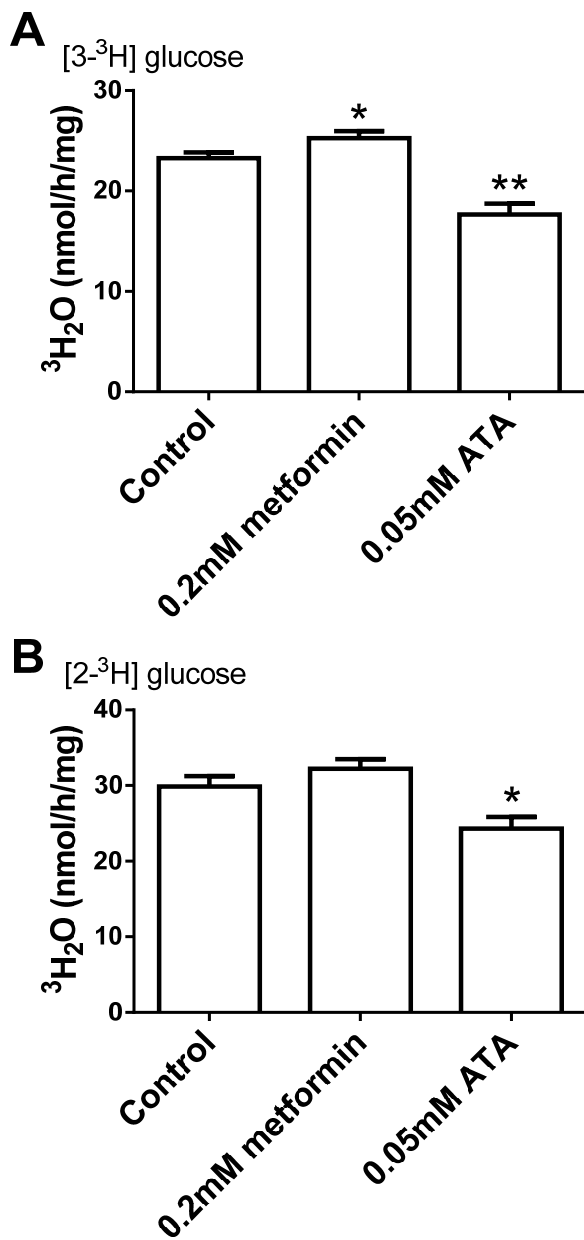


Figure 4.27 ATA inhibits the metabolism of [3-³H] and [2-³H] glucose

Mouse hepatocytes were pre-incubated with metformin or ATA for 2 hours and then incubated with MEM, 15mM glucose, 0.2 μ M S4048 and [3-³H]-glucose or [2-³H]-glucose for 1 hour. Mean \pm SEM, n=3. *p<0.05, **p<0.01.

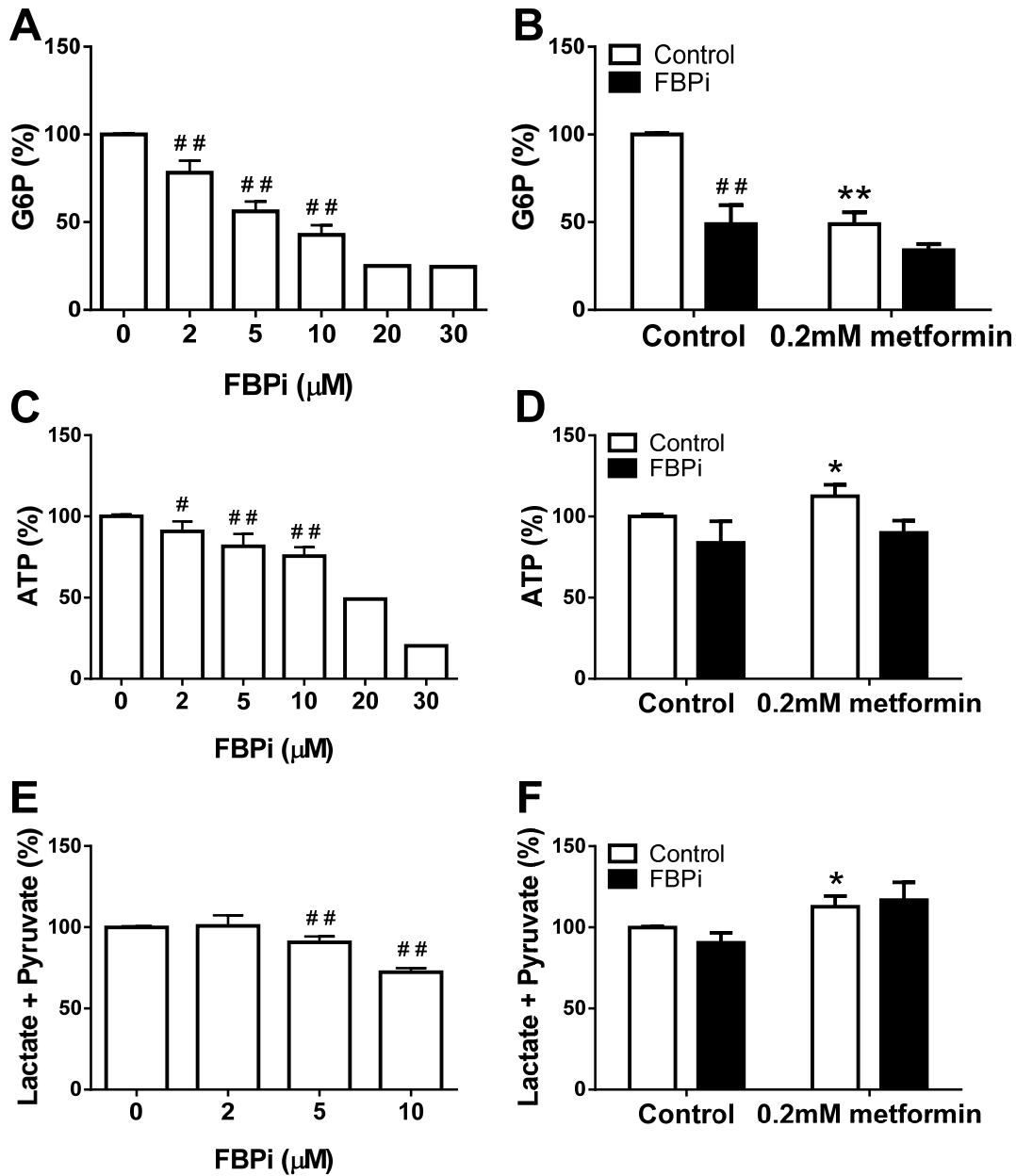


Figure 4.28 Lowering of G6P with an inhibitor of FBP1

Mice were pre-incubated with 0.2-2 μM S4048 and 2-30 μM FBPi (A, C, E) or 5 μM FBPi and metformin (B, D, F) for 2 hours, then a further 1 hour with 25mM glucose. Mean \pm SEM, n=1-17. *p<0.05, **p<0.01 metformin effect. #p<0.05, ##p<0.01 FBPi effect. Basal values were as in Table 3-1 and Table 3-2.

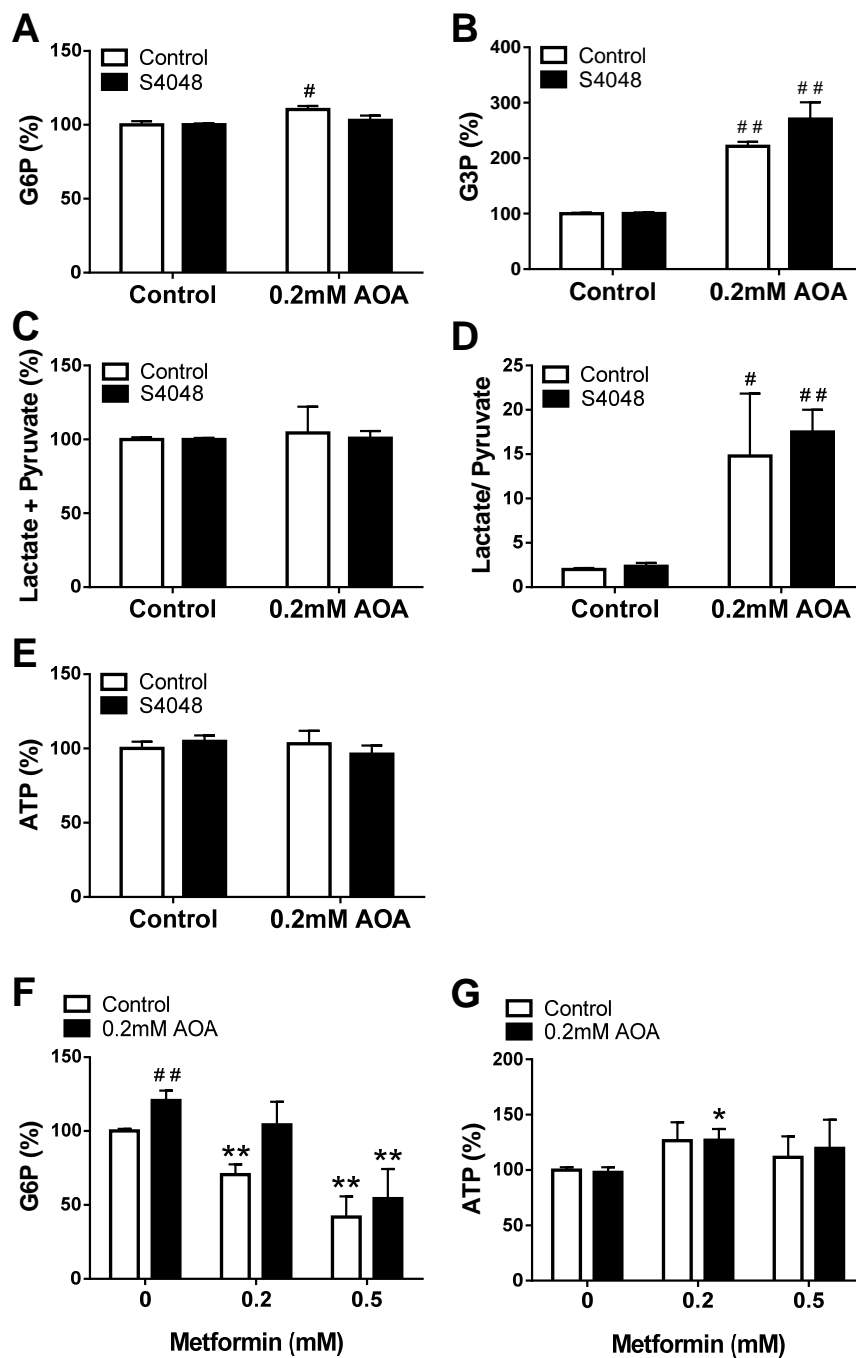


Figure 4.29 Inhibition of the malate-aspartate shuttle increases the lactate/ pyruvate ratio and causes a small increase in G6P

(A-E) Effects of AOA on cell metabolites, (F, G) effect of metformin with AOA on cell metabolites. Mouse hepatocytes were incubated with 25mM glucose and 0.2mM AOA in the absence or presence of 0.2-2 μ M S4048 for 1 hour. Mean \pm SEM, n=2-5. *p<0.05, **p<0.01 metformin effect. # p<0.05, ## p<0.01 AOA effect. Basal values were as in Table 3-1 and Table 3-2.

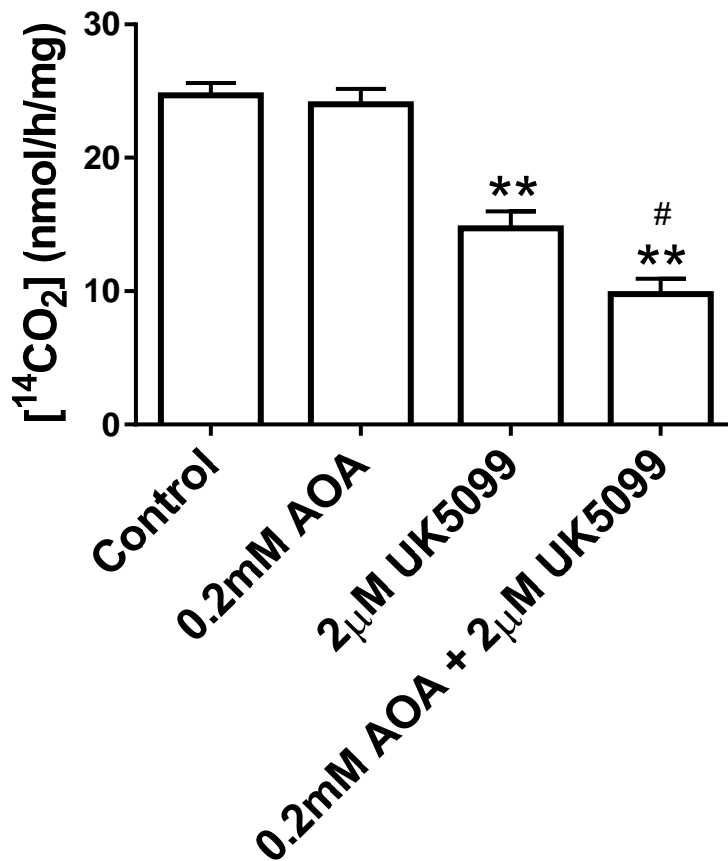


Figure 4.30 AOA inhibits glucose oxidation when combined with a pyruvate transport inhibitor

Mouse hepatocytes were incubated with MEM, 0.2µM S4048, 15mM glucose, [U- ^{14}C] glucose and 0.2mM AOA or 2µM UK099 for 1 hour, and $^{14}\text{CO}_2$ was collected. Mean \pm SEM, n=3. *p<0.05, **p<0.01, #p<0.05, ##p<0.01.

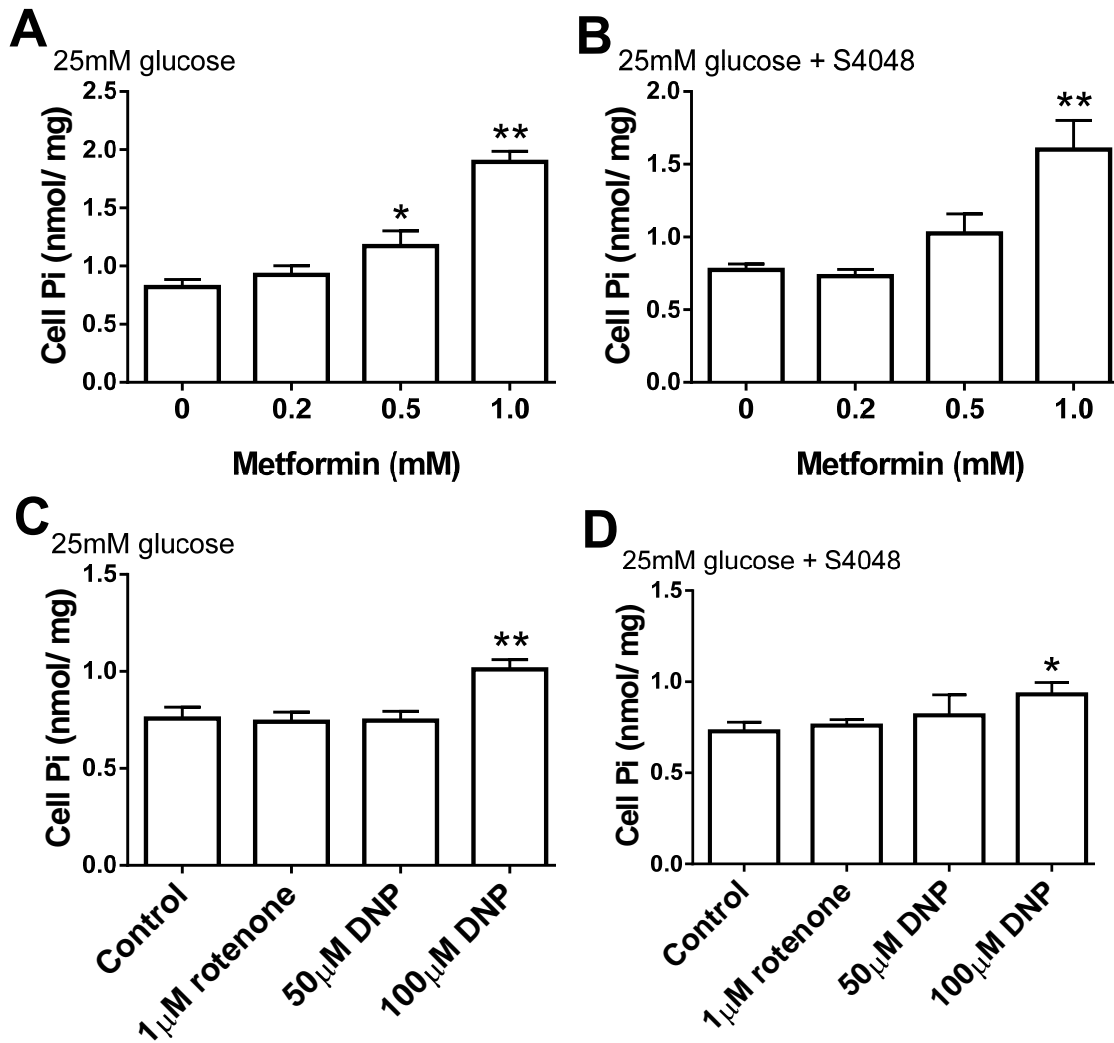


Figure 4.31 Metformin and DNP raise inorganic phosphate (Pi)

Mouse hepatocytes were pre-incubated in the absence of S4048 (A, C) or presence of 0.2 μM S4048 (B, D) and with metformin for 2 hours, then a further 1 hour with 25mM glucose and 1 μM rotenone or 50-100 μM DNP. Mean ± SEM, n=2-3. *p<0.05, **p<0.01.

Chapter 5: Discussion

5.1 Current status of hypotheses on the metformin mechanism

The evidence for inhibition of hepatic glucose production by metformin in man is derived primarily from chronic studies (2 to 26 weeks) (Natali & Ferrannini., 2006). Few studies have demonstrated lowering of blood glucose in T2D during an acute intravenous infusion of metformin (Sum et al., 1992). The chronic studies showed that metformin efficacy in lowering blood glucose correlates negatively with fasting glucose production and thereby with the severity of the diabetic state (Natali & Ferrannini., 2006) and that in non-diabetic subjects, stimulation of endogenous glucose production was found after 1-week exposure to metformin (Christensen et al., 2015). Whether metformin efficacy in man is due to chronic changes in gene expression rather than acute effects on metabolic flux is not known.

Studies in animal and cellular models have demonstrated acute inhibition of gluconeogenic flux and also gene repression of enzymes of gluconeogenesis by metformin which have been widely replicated (Stumvol et al., 1995; Hundal et al., 2000; Kim et al., 2008; He et al., 2009; Lee et al., 2010; Kim et al., 2012 a; Sajan et al., 2013; Cao et al., 2014; Petersen et al., 2017). It remains unsettled which of the effects of metformin that are observed in cellular model occur at therapeutic doses of the drug. Proposed mechanisms for the inhibition of gluconeogenic flux include: (i) lowering of cell ATP or the ATP/ADP ratio; (ii) activation of AMPK; (iii) raised AMP which counteracts glucagon signalling and inhibits FBP1; (iv) inhibition of mGpd and consequently a more reduced cytoplasmic redox state. Proposed mechanisms for the inhibition of gene expression of enzymes of gluconeogenesis include activation of AMPK. However, metformin also inhibits G6pc expression in AMPK-KO models in conjunction with depletion of cell ATP (Foretz et al., 2010). One current view on the metformin mechanism is that the therapeutic effects are most likely due to very modest effects at multiple sites and are not mediated by either inhibition of Complex 1 or by lowering of cell ATP (Bailey., 2017). An alternative possibility that would concur with the greater efficacy of metformin at higher fasting blood glucose levels (Natali & Ferrannini., 2006) is that metformin may counteract the effect of high glucose on hepatic gene regulation.

Work leading up to this project showed that metformin inhibits the effects of high glucose on induction of ChREBP target genes including Pklr and G6pc but has negligible effects on expression of these genes at basal glucose concentration. Because ChREBP is activated by cellular accumulation of intermediates of glucose metabolism such as G6P and F-2,6-P-2, it was hypothesized that metformin may exert its effect on G6pc and other ChREBP target genes by lowering the cellular concentration of metabolites of glucose such as G6P. The aims of this study were first to determine whether metformin lowers cellular G6P at cellular concentrations of metformin that are within the therapeutic range and if so in what substrate conditions. Secondly, to identify the mechanism by which metformin lowers G6P. Thirdly to determine whether the lowering of G6P can explain the counter-regulatory effects of metformin on gene regulation by high glucose.

Lowering of G6P by metformin in liver in vivo or in isolated hepatocytes was reported previously by 3 other laboratories (Owen et al., 2000; Fulgencio et al., 2001; Guigas et al., 2006). However, an increase in vivo has also been reported (Mithieux et al., 2002). The hepatocyte studies showed lowering of G6P by metformin concentrations of 2-10mM with either gluconeogenic precursors as substrate (Owen et al., 2000; Fulgencio et al., 2001) or with high glucose (Guigas et al., 2006). The lowering of G6P was explained by either inhibition of gluconeogenesis (Owen et al., 2000; Fulgencio et al., 2001) or by inhibition of glucose phosphorylation as a result of inhibition of glucokinase translocation (Guigas et al., 2006). In all three cases a role for ATP depletion was implicated. Owen et al. (2000) reported ~50% decrease in total G6P and F6P with 2mM metformin in hepatocytes, and a 60-61% decrease in G6P with 150-600mg/kg metformin in freeze-clamped livers which was accompanied by a 70% drop in the ATP/ADP ratio. Additionally, Fulgencio et al. (2001) reported a 50% decrease in G6P with 5mM metformin and a 70% decrease in ATP. Guigas et al (2006) observed a 20% decrease in G6P with 5mM metformin and ATP depletion by 40%. They demonstrated a correlation between inhibition of glucose production and ATP depletion. In the present study cell ATP was determined in all experiments in parallel with the measurement of G6P. This was particularly important first for establishing the range of concentrations of metformin that are effective in lowering cell G6P in conditions of preserved cell ATP.

Secondly, for studies on the metformin mechanism where inhibitors of mitochondrial function or G6P metabolising enzymes were used it was also important to establish whether these inhibitors mimicked metformin in conditions of maintained ATP.

The maximum concentration of metformin in the peripheral circulation in man is around 6 – 25 μ M (Kajbaf et al., 2016). However, higher concentrations are expected in the portal vein (Gormsen et al., 2016). Metformin accumulates slowly in liver (Owen et al., 2000) and reaches a tissue content that is 3-5 fold higher than the extracellular content (Wilcock & Bailey., 1994). A previous study on mice given an oral load of metformin (50 mg/kg) corresponding to the equivalent of the therapeutic dose in man showed a maximum liver content of 180 – 280 nmol/g or 1-1.5 nmol/mg protein if one assumes 200 mg protein per gram wet weight (Wilcock & Bailey., 1994). In order to study metformin concentrations over a range that include the “therapeutic equivalent” we determined the metformin content of cells after a 2-hour pre-incubation with a range of metformin concentrations (0.1 – 1mM). Using [¹⁴C] metformin we established that the cell content of metformin with this protocol is approximately 5 times the extracellular concentration which has been observed in vivo (Wilcock & Bailey., 1994), and also that at concentrations of 0.1-0.2mM it approximates the levels found in vivo (180-280 nmol/g) after a therapeutic load (50mg/kg) of metformin.

The concentration of G6P in the liver is dependent on the extracellular glucose concentration and on the activities of the enzymes involved in production of G6P from glucose, glycogen and gluconeogenesis, and in the clearance of G6P by glycolysis, the pentose phosphate pathway and conversion to UDP-glucose and G6pc in the lumen of the endoplasmic reticulum. In type 2 diabetes therapy, metformin is normally recommended to be taken with meals. In the absorptive state after a meal, liver G6P increases from 0.2mM to 0.4mM (Fernández-Novell et al., 1996) because of the increase in glucose concentration in the portal vein in conjunction with translocation of glucokinase from the nucleus to the cytoplasm (Aiston et al., 2004). In isolated hepatocytes the cell G6P concentration is a sigmoidal function of extracellular glucose concentration, and the magnitude of response to glucose is a function of glucokinase activity (Aiston et al., 2004). The initial hypothesis of this study was that if metformin inhibits glucokinase translocation as was reported in previous work (Guigas et al., 2006;

Mukhtar et al., 2008) with higher metformin concentrations then it would also attenuate the increase in G6P that occurs in response to high glucose. The results showed lowering of G6P by metformin in conditions of high glucose in the absence of inhibition of glucokinase translocation. The G6pc/G6PT is a strong candidate for regulating G6P levels because the K_m of G6Pase (2-3 mM) (van Schaftingen et al., 2002) is higher than the intracellular concentration of G6P which is in the range of 0.2-0.4mM after a meal (Fernández-Novell et al., 1996). However, we excluded a role for this system because the lowering of G6P by metformin was observed in the presence of S4048. The affinity of G6PD for G6P is high (0.052mM) (Wang & Engel., 2009) and below the physiological concentration of G6P in the absorptive state (0.2-0.4mM). However, flux through G6PD is regulated by changes in free NADP. The cell content of total NADP and NADPH is about 0.07 and 0.35 $\mu\text{mol/g}$ liver respectively (Bergmeyer., 1974). This represents both free and bound nucleotides, although the free concentrations of NADP and NADPH are assumed to be lower (Veech et al., 1969). The K_m of G6PD for NADP is 7 μM (Wang & Engel., 2009) meaning that an increase in NADP would be predicted to stimulate flux through G6PD. G6P is in equilibrium with F6P through PGI and the concentration of F6P in liver is around 0.05mM (Bergmeyer., 1974). The K_m of PFK1 for F6P is 50 -140 μM (Hue & Rider., 1987) and therefore within the physiological range of substrate concentration. However, PFK1 is a highly regulated enzyme (Hers & Hue., 1983). It is activated by F-2,6-P₂, AMP, NH₄⁺, Pi, OH⁻ and 6-PG, and inhibited by citrate, G3P and H⁺. Changes in these allosteric effectors can therefore alter the flux through PFK1 and thereby alter the concentration of hexose 6-phosphate. We therefore identified PFK1 as a candidate target for a metformin that is likely to alter cell G6P.

5.2 Metformin lowers G6P in hepatocytes

The present study supports the following conclusions on the G6P lowering effect. First, that metformin has a concentration dependent effect in lowering G6P which is observed at cellular loads of 1-2 nmol/ mg which correspond to the peak accumulation in the liver after an oral therapeutic load (Wilcock & Bailey., 1994) and the metformin effect increases progressively at concentrations up to 10-fold higher. At the highest concentrations of metformin (0.5-1.0mM) tested in this study we observed a small lowering of ATP in some experiments up to 16%, but ATP was not lowered with 0.1-

0.2mM metformin which corresponds to a comparable cell load as occurs in vivo after an oral therapeutic load of metformin (Wilcock & Bailey., 1994). Second, the effect of metformin on G6P is observed with both high glucose and with a variety of gluconeogenic precursors but not at basal glucose. Third, the fractional lowering of G6P by metformin was always greater in the presence of S4048 which raises G6P by inhibiting its metabolism by G6pc. Cumulatively, this indicates that metformin is most effective in conditions of high cellular metabolites, as would be expected to occur in metabolic disease. It is noteworthy that metformin efficacy in man correlates with the severity of the diabetes (Natali & Ferrannini., 2006) and furthermore metformin is ineffective in MODY-GK who are predicted to have low liver G6P levels because of the glucokinase mutation (Chakera et al., 2015).

5.3 Lowering of G6P by metformin is mimicked by inhibition of mitochondrial complex

1

One of the established effects of high metformin concentrations is the inhibition of Complex 1 (Owen et al., 2000; El-Mir et al., 2000; Bridges et al., 2014). This mechanism was shown in isolated mitochondria incubated with substrates of complex 1 and 2. In isolated hepatocytes and also in vivo, the inhibition of Complex 1 is supported by an increase in the mitochondrial redox state as determined from the ratio of 3-Hydroxybutyrate to acetoacetate (Owen et al., 2000). However, recent studies have also reported a more oxidised mitochondrial redox state (decreased NADH/NAD⁺ ratio) in vivo with lower doses of metformin in man and animal models (Madiraju et al., 2014; Qi et al., 2018; von Morze et al., 2018).

The present study supports the conclusion that the G6P lowering effect of metformin is mimicked by inhibition of Complex 1; depolarisation of mitochondria with an uncoupler and inhibition of NNT which is dependent on the mitochondrial proton motive force and results in elevated NADP, but not by inhibition of NADH transfer from the cytoplasm to the mitochondria with an inhibitor of the malate aspartate shuttle. Because metformin raised NADP, we considered the inhibition of NNT as a possible candidate for the G6P lowering. However, based on the lowering of G6P by metformin in hepatocytes from a mouse with a deletion in the NNT gene, we conclude that mechanisms other than inhibition of NNT must have a major role.

5.4 Metformin action involves mechanisms other than AMPK

Inhibition of complex 1 by metformin raises the AMP/ATP ratio which activates AMPK, the function of which is to maintain intracellular energy homeostasis (Owen et al., 2000; Foretz et al., 2010; Rena et al., 2017). One proposed mechanism by which metformin could restore the energy balance is by inhibiting gluconeogenesis (Zhou et al., 2001, Cao et al., 2014). However, metformin also inhibits hepatic glucose production in AMPK- KO mice in conditions of significant ATP depletion (Foretz et al., 2010). Therefore, the mechanism remains contentious, and does not rule out the involvement of both AMPK dependent and AMPK independent effects of metformin.

The following conclusions can be drawn from this study: first, metformin is able to lower G6P at concentrations that do not stimulate AMPK/ ACC phosphorylation (<0.5mM). Second, with a gluconeogenic substrate, pharmacological AMPK activators (A769662, C13 and 991) do not mimic the lowering of G6P by metformin. Third, Inhibition of glucose production by metformin (0.1-1.0mM) is not mimicked by AMPK activators consistent with the findings by Foretz et al. (2010) that metformin is able to inhibit gluconeogenesis in the absence of AMPK activation. Fourth, in contrast to metformin ($\geq 0.2\text{mM}$) which stimulated lactate and pyruvate production, AMPK activators inhibited lactate and pyruvate production. The AMPK activators also inhibited [$5\text{-}^3\text{H}$] glucose metabolism (indicating inhibition of flux through glycolysis/ pentose phosphate pathway) which was not mimicked by metformin. Together, this suggests metformin has an over-riding effect from its AMPK activating properties that accounts for the decrease in G6P and inhibition of glucose production as well as stimulation of glycolytic/ pentose phosphate pathway flux.

5.5 Metformin does not inhibit glucose phosphorylation

Previous studies showed inhibition of glucose phosphorylation by high metformin concentrations ($\geq 0.5\text{mM}$) (Guigas et al., 2006; Mukhtar et al., 2008). In these studies, we conclude that the lowering of G6P by metformin in conditions of high glucose cannot be explained by inhibition of glucose phosphorylation. This is supported by data showing that metformin (0.2-1.0mM) lowered G6P without inhibiting [$2\text{-}^3\text{H}$] glucose metabolism, which was observed in the presence of GK inhibitors. Additionally, we conclude that activation of AMPK causes a small inhibition of glucose phosphorylation. This is

supported by different classes of AMPK activators; A769662 which binds to an allosteric site and C13 which is an AMP mimetic. These findings are of interest because a previous study by Guigas et al., (2006) concluded that both metformin and AICAR inhibit glucose phosphorylation by a mechanism independent of AMPK that correlates with ATP depletion. However, their data shows stronger inhibition of glucose phosphorylation by AICAR than can be explained by ATP depletion alone. The present study provides an explanation for their observation.

5.6 Metformin inhibits glycogen synthesis: Possible roles of G6P depletion and Pi elevation

The present study supports the conclusion that the mechanism by which metformin lowers G6P is not by increased diversion of G6P to glycogen. In support of this, an inhibitor of glycogen phosphorylase (CP-91149) lowered G6P but stimulated glycogen synthesis. Metformin (0.1-0.5mM) also lowered G6P but this strongly correlated with inhibition of glycogen synthesis rather than stimulation. Two possible explanations can be offered for this correlation. First, that the lowering of G6P by metformin is due to activation of glycolysis and the lower cell G6P in turn causes activation of phosphorylase and inactivation of glycogen synthase, with consequent inhibition of glycogen synthesis. Accordingly, the lowering of G6P is the cause of the inhibition of glycogen synthesis. Second, if mitochondrial depolarisation causes an increase in cytoplasmic Pi through attenuation of the ATP-synthase and/ or through decreased uptake of Pi into mitochondria on the pH sensitive Pi-OH⁻ transporter, then the increase in cytoplasmic Pi concentrations would stimulate glycogenolysis by acting as a substrate for the enzyme and as an allosteric effector that stabilises the R-state thereby promoting phosphorylation of phosphorylase and inactivation of glycogen synthase.

Activation of glycogenolysis by the uncoupler DNP (100 μ M) through an increase in cytoplasmic Pi has been shown previously (Vanstapel et al. 1990). The present finding that metformin concentrations ranging from 0.1 to 0.5mM cause progressive inhibition of glycogen synthesis (in parallel with the G6P lowering) could be explained by both the decline in G6P and the rise in Pi. Because G6P and Pi have converse effects on phosphorylase (inactivation and activation respectively) through distinct binding sites (allosteric and active sites respectively), it can be hypothesized that the decline in G6P

and the increase in Pi caused by metformin would be expected to have synergistic effects on phosphorylase activation (and synthase inactivation). The present findings concur with 2 recent studies reporting stimulation of glycogenolysis or inhibition of glycogen synthesis by metformin. Hansen & McCormack., (2002) showed that 2mM metformin stimulated lactate production from glycogenolysis in rat hepatocytes and Otto et al., (2003) showed that lower concentrations of metformin (200 μ M) inhibited glycogen synthesis.

Previous work also showed that A769662 inactivated glycogen synthase (Bultot et al, 2012). We found that A769662 inhibited glycogen synthesis in the absence of S4048 and that this did not correlate with G6P. A769662 inhibited glycogen synthesis to a lesser extent in the presence of S4048 (which strongly activates glycogen synthesis by increasing G6P substantially). This could be due to an over-riding effect of elevated G6P or because A769662 does not cause AMPK phosphorylation in conditions of raised G6P.

5.7 Low metformin stimulates lactate and pyruvate formation but high metformin inhibits substrate oxidation

In this study we found that metformin (≥ 0.2 mM) stimulates lactate and pyruvate production in hepatocytes. The accumulation of lactate and pyruvate in the medium is an approximate measure of flux through glycolysis and the pentose phosphate pathway because part of the pyruvate formed is further metabolised in mitochondria. We found that metformin (0.5mM) inhibited substrate oxidation consistent with respiratory chain inhibition. Therefore, at metformin concentrations that inhibit Complex 1, the increase in lactate and pyruvate formation by metformin represents in part the inhibition of mitochondrial metabolism of pyruvate.

We found that at lower concentrations of metformin that correspond to the levels that accumulate in liver after a therapeutic dose (0.2mM), glycolysis was stimulated (indicated by stimulation of [3-³H] glucose metabolism and lactate and pyruvate production) in the absence of inhibition of mitochondrial oxidation. In principle the increase in lactate and pyruvate formation could arise by both glycolysis and the pentose phosphate pathway. However, several lines of evidence argue against stimulation of the pentose phosphate pathway as important in the metformin

mechanism. First, although the G6PD inhibitor DHEA partially counteracted the lowering of G6P by metformin, it did not inhibit pentose phosphate pathway flux as measured from [1-¹⁴C] glucose decarboxylation. Additionally, in the present study flux through the pentose phosphate pathway (from [1-¹⁴C] glucose decarboxylation) represented <1% of total lactate and pyruvate production.

Previous studies report that biguanides altered flux at the level of GAPDH/ phosphoglycerate kinase by the decrease in free ATP/ADP (Owen & Halestrap., 1993; Owen et al., 2000) which could explain the stimulation of lactate and pyruvate production, and a recent study suggested that metformin inhibits the glycerophosphate shuttle in the liver based on the increase in lactate/pyruvate ratio as a measure of the cytoplasmic NADH/NAD redox state (Madiraju et al., 2014) but whether the importance of this in man and rodent is contentious (Baur & Birnbaum., 2014). We found that metformin lowered G6P in conditions of a more reduced redox state and restricted flux through GAPDH with AOA, suggesting another target site is involved.

We concluded that PFK1/ FBP1 is the most likely site of control of G6P depletion by metformin. There are a number of candidate allosteric effectors of PFK1/ FBP1 (F-2,6-P₂, AMP and Pi) that could be involved in the G6P lowering effect of metformin. Several lines of evidence support this: first, stimulation of PFK1 with ammonium and ATA mimicked the lowering of G6P with metformin. Second, depleting F-2,6-P₂ with PFK2-KD increased G6P by 2-3 fold, consistent with the role of PFK1/FBP1 as a major determinant of cell G6P content. This was associated with inhibition of lactate and pyruvate production which was relatively small compared to the large increase in G6P. This supports the conclusion that a small fractional inhibition in flux through glycolysis results in a large increase in G6P. Al-Oanzi et al., (2017) reported lowering of F-2,6-P₂ by metformin (1-5mM) which would seem inconsistent with stimulation of glycolysis by metformin because F-2,6-P₂ is a very powerful activator of PFK1. However, the present findings of this study are consistent with a mechanism that is similar to what occurs during anoxia in liver. Anoxia results in inhibition of electron transport and thereby oxidative phosphorylation with a consequent increase in cell Pi but simultaneously with lowering of F-2,6-P₂ (Hue., 1982). In agreement with this, the present study shows that metformin (≥0.5mM) raised cell Pi which caused inhibition of glucose oxidation

indicating complex 1 inhibition. Although no inhibition of glucose oxidation was observed with 0.2mM metformin we observed an increase in Pi with the uncoupler, as expected from previous studies (Vanstapel et al., 1990). We cannot exclude the possibility that at 0.1-0.2mM metformin there is mild uncoupling and inhibition of Complex 1. The net effect of this would be lack of change in substrate oxidation but a decrease in proton motive force which would explain the inhibition of oxidative phosphorylation and therefore accumulation of Pi. Although a significant increase in cell Pi was only detected in this study with 0.5mM metformin we cannot exclude local changes in cytoplasmic Pi at low concentrations that are below the limit of detection. Because mitochondrial Pi is approximately 4-times greater than the cytoplasmic concentration (Akerboom et al., 1978), inhibition of oxidative phosphorylation by a decrease in proton gradient caused either by inhibition of Complex 1 or by uncoupling predicts decreased Pi entry into mitochondria and decreased consumption by oxidative phosphorylation, stimulating glycolysis at the level of PFK1.

5.8 Metformin counteracts the effects of high glucose on glucose regulated gene expression

In man, the evidence for inhibition of hepatic gluconeogenesis by metformin is derived mainly from chronic studies. Studies testing the acute effects of metformin on glucose production did not show significant effects (Sum et al., 1992). It remains uncertain whether the chronic effects of metformin are due to indirect mechanisms for example changes in hormones or blood fatty acids and triglycerides, or to changes in hepatic gene expression. The liver in T2D is characterised by increased rates of gluconeogenesis and lipogenesis. This could be in part due to activation of the transcription factor ChREBP or other transcription factors by the hyperglycaemia, and or raised levels of intracellular G6P as occurs in conditions of hyperglycaemia. ChREBP promotes induction of Pck1 and enzymes of de novo lipogenesis and as well as G6pc (Towle et al., 1997; Argaud et al., 1997; Arden et al., 2012; Dentin et al., 2012). Induction of G6pc by ChREBP in conditions of raised cell metabolites serves to restore intracellular metabolite homeostasis at the expense of worsening hyperglycaemia (Agius., 2016). Work leading up to this project showed that metformin at concentrations $\geq 0.5\text{mM}$ counteracts the effects of high glucose on the regulation of these ChREBP target genes and that the expression of G6pc

and Pklr correlate positively with intracellular G6P, whereas GK expression correlates negatively with cell G6P (Al-Oanzi et al., 2017). We therefore tested whether this could be observed at therapeutically relevant concentrations of metformin.

We concluded that metformin at physiological concentrations ($\geq 0.2\text{mM}$) counteracted the effect of high glucose on GK and G6pc gene expression in hepatocytes. The lowering of G6P by metformin correlated positively and negatively with G6pc and GK expression respectively and ATP was not depleted in these conditions. The effects of metformin on gene expression were not mimicked by AMPK activation and occurred at metformin concentrations that both did not stimulate (0.2mM) and stimulated ($\geq 0.5\text{mM}$) AMPK and ACC phosphorylation. Additionally, the AMPK activator A769662 had negligible effects on GK expression and counteracted the increase in G6pc expression with high glucose although to a lesser extent than metformin, and this was associated with raised G6P. A recent study implicated AMP as an allosteric inhibitor of ChREBP (Sato et al., 2016) which can explain this observation.

Therefore, therapeutic concentrations of metformin cause inhibition of hepatic glucose production as well as inhibition of gluconeogenic (G6pc) gene expression and stimulation of GK expression with high glucose. This correlated with a decrease in cell G6P, suggesting the changes in G6P by metformin may be involved in the regulation of these genes.

5.9 Summary

In this study we determined that metformin lowers cell G6P in hepatocytes incubated with high glucose and gluconeogenic precursors (DHA and xylitol) as substrates, but not at basal 5mM glucose. The lowest concentrations of metformin that were effective at lowering G6P ($0.1\text{-}0.2\text{mM}$) correspond to cellular drug loads of metformin ($1\text{-}2\text{ nmol/ mg}$ cell protein) that are within the levels reached in mouse models treated with a therapeutic dose (50 mg/ kg corresponding to 3g for a 60kg person) (Wilcock and Bailey., 1994). We found that the G6P lowering effect of metformin was mimicked by compounds that lower the proton gradient by either inhibition of Complex 1 or by uncoupling but not by pharmacological AMPK activators, suggesting this effect of metformin is independent of AMPK and is likely linked to depolarisation of the

mitochondria. We propose that mitochondrial depolarisation raises cell Pi in the cytosol as occurs also with an uncoupler. Pi is a strong allosteric activator of PFK1. Consequently, this stimulates glycolysis, lowering cell G6P. In our study, metformin lowered G6P in conditions where ATP was unaffected, or lowered marginally in comparison with previous studies. This can be explained by stimulation of flux through glycolysis by metformin which restores ATP, so the drop in ATP is not observed at the end of a fixed time point. We also propose that metformin counteracts the effects of high glucose on glucose regulated gene expression, and that repression of G6pc by metformin concurs with the lowering of G6P.

References

- 'Effect of intensive blood-glucose control with metformin on complications in overweight patients with type 2 diabetes (UKPDS 34). UK Prospective Diabetes Study (UKPDS) Group', (1998) *Lancet*, 352(9131), pp. 854-65.
- Agius, L. (2014) 'Lessons from glucokinase activators: the problem of declining efficacy', *Expert Opin Ther Pat*, 24(11), pp. 1155-9.
- Agius, L. (2015) 'Role of glycogen phosphorylase in liver glycogen metabolism', *Mol Aspects Med*, 46, pp. 34-45.
- Agius, L. (2016) 'Hormonal and Metabolite Regulation of Hepatic Glucokinase', *Annu Rev Nutr*, 36, pp. 389-415.
- Agius, L., Centelles, J. and Cascante, M. (2002) 'Multiple glucose 6-phosphate pools or channelling of flux in diverse pathways?', *Biochem Soc Trans*, 30(2), pp. 38-43.
- Agius, L. and Stubbs, M. (2000) 'Investigation of the mechanism by which glucose analogues cause translocation of glucokinase in hepatocytes: evidence for two glucose binding sites', *Biochem J*, 346 Pt 2, pp. 413-21.
- Aiston, S., Andersen, B. and Agius, L. (2003) 'Glucose 6-phosphate regulates hepatic glycogenolysis through inactivation of phosphorylase', *Diabetes*, 52(6), pp. 1333-9.
- Aiston, S., Green, A., Mukhtar, M. and Agius, L. (2004) 'Glucose 6-phosphate causes translocation of phosphorylase in hepatocytes and inactivates the enzyme synergistically with glucose', *Biochem J*, 377(Pt 1), pp. 195-204.
- Aiston, S., Hampson, L., Gomez-Foix, A.M., Guinovart, J.J. and Agius, L. (2001) 'Hepatic glycogen synthesis is highly sensitive to phosphorylase activity: evidence from metabolic control analysis', *J Biol Chem*, 276(26), pp. 23858-66.
- Aiston, S., Trinh, K.Y., Lange, A.J., Newgard, C.B. and Agius, L. (1999) 'Glucose-6-phosphatase overexpression lowers glucose 6-phosphate and inhibits glycogen synthesis and glycolysis in hepatocytes without affecting glucokinase translocation. Evidence against feedback inhibition of glucokinase', *J Biol Chem*, 274(35), pp. 24559-66.
- Akerboom, T.P., Bookelman, H., Zuurendonk, P.F., van der Meer, R. and Tager, J.M. (1978) 'Intramitochondrial and extramitochondrial concentrations of adenine nucleotides and inorganic phosphate in isolated hepatocytes from fasted rats', *Eur J Biochem*, 84(2), pp. 413-20.
- al-Habori, M., Peak, M., Thomas, T.H. and Agius, L. (1992) 'The role of cell swelling in the stimulation of glycogen synthesis by insulin', *Biochem J*, 282 (Pt 3), pp. 789-96.
- Al-Oanzi, Z.H., Fountana, S., Moonira, T., Tudhope, S.J., Petrie, J.L., Alshawi, A., Patman, G., Arden, C., Reeves, H.L. and
- Agius, L. (2017) 'Opposite effects of a glucokinase activator and metformin on glucose-regulated gene expression in hepatocytes', *Diabetes Obes Metab*, 19(8), pp. 1078-1087.
- An, H. and He, L. (2016) 'Current understanding of metformin effect on the control of hyperglycemia in diabetes', *J Endocrinol*, 228(3), pp. R97-106.
- Arden, C., Petrie, J.L., Tudhope, S.J., Al-Oanzi, Z., Claydon, A.J., Beynon, R.J., Towle, H.C. and Agius, L. (2011) 'Elevated glucose represses liver glucokinase and induces its regulatory protein to safeguard hepatic phosphate homeostasis', *Diabetes*, 60(12), pp. 3110-20.

- Arden, C., Tudhope, S.J., Petrie, J.L., Al-Oanzi, Z.H., Cullen, K.S., Lange, A.J., Towle, H.C. and Agius, L. (2012) 'Fructose 2,6-bisphosphate is essential for glucose-regulated gene transcription of glucose-6-phosphatase and other ChREBP target genes in hepatocytes', *Biochem J*, 443(1), pp. 111-23.
- Argaud, D., Kirby, T.L., Newgard, C.B. and Lange, A.J. (1997) 'Stimulation of glucose-6-phosphatase gene expression by glucose and fructose-2,6-bisphosphate', *J Biol Chem*, 272(19), pp. 12854-61.
- Argaud, D., Roth, H., Wiernsperger, N. and Leverve, X.M. (1993) 'Metformin decreases gluconeogenesis by enhancing the pyruvate kinase flux in isolated rat hepatocytes', *Eur J Biochem*, 213(3), pp. 1341-8.
- Arion, W.J., Canfield, W.K., Ramos, F.C., Schindler, P.W., Burger, H.J., Hemmerle, H., Schubert, G., Below, P. and Herling, A.W. (1997) 'Chlorogenic acid and hydroxynitrobenzaldehyde: new inhibitors of hepatic glucose 6-phosphatase', *Arch Biochem Biophys*, 339(2), pp. 315-22.
- Azzout, B. and Peret, J. (1984) 'Development of gluconeogenesis from dihydroxyacetone in rat hepatocytes during a feeding cycle and starvation', *Biochem J*, 218(3), pp. 975-81.
- Bailey, C.J. (2017) 'Metformin: historical overview', *Diabetologia*, 60(9), pp. 1566-1576.
- Bailey, C.J., Mynett, K.J. and Page, T. (1994) 'Importance of the intestine as a site of metformin-stimulated glucose utilization', *Br J Pharmacol*, 112(2), pp. 671-5.
- Bailey, C.J., Wilcock, C. and Scarpello, J.H. (2008) 'Metformin and the intestine', *Diabetologia*, 51(8), pp. 1552-3.
- Bannister, C.A., Holden, S.E., Jenkins-Jones, S., Morgan, C.L., Halcox, J.P., Scherthaner, G., Mukherjee, J. and Currie, C.J. (2014) 'Can people with type 2 diabetes live longer than those without? A comparison of mortality in people initiated with metformin or sulphonylurea monotherapy and matched, non-diabetic controls', *Diabetes Obes Metab*, 16(11), pp. 1165-73.
- Baranyai, J.M. and Blum, J.J. (1989) 'Quantitative analysis of intermediary metabolism in rat hepatocytes incubated in the presence and absence of ethanol with a substrate mixture including ketoleucine', *Biochem J*, 258(1), pp. 121-40.
- Baur, J.A. and Birnbaum, M.J. (2014) 'Control of gluconeogenesis by metformin: does redox trump energy charge?', *Cell Metab*, 20(2), pp. 197-9.
- Becker, T.C., Noel, R.J., Johnson, J.H., Lynch, R.M., Hirose, H., Tokuyama, Y., Bell, G.I. and Newgard, C.B. (1996) 'Differential effects of overexpressed glucokinase and hexokinase I in isolated islets. Evidence for functional segregation of the high and low Km enzymes', *J Biol Chem*, 271(1), pp. 390-4.
- Benziane, B., Bjornholm, M., Lantier, L., Viollet, B., Zierath, J.R. and Chibalin, A.V. (2009) 'AMP-activated protein kinase activator A-769662 is an inhibitor of the Na(+)-K(+)-ATPase', *Am J Physiol Cell Physiol*, 297(6), pp. C1554-66.
- Bergmeyer, H.U. and Gawehn, K. (1974) *Methods of enzymatic analysis*. Verlag Chemie.
- Berry, M.N., Gregory, R.B., Grivell, A.R., Phillips, J.W. and Schon, A. (1994) 'The capacity of reducing-equivalent shuttles limits glycolysis during ethanol oxidation', *Eur J Biochem*, 225(2), pp. 557-64.
- Berry, M.N., Phillips, J.W., Gregory, R.B., Grivell, A.R. and Wallace, P.G. (1992) 'Operation and energy dependence of the reducing-equivalent shuttles during lactate metabolism by isolated hepatocytes', *Biochim Biophys Acta*, 1136(3), pp. 223-30.
- Billin, A.N., Eilers, A.L., Queva, C. and Ayer, D.E. (1999) 'Mlx, a novel Max-like BHLHZip protein that interacts with the Max network of transcription factors', *J Biol Chem*, 274(51), pp. 36344-50.

- Bironaite, D. and Ollinger, K. (1997) 'The hepatotoxicity of rhein involves impairment of mitochondrial functions', *Chem Biol Interact*, 103(1), pp. 35-50.
- Bosca, L., Aragon, J.J. and Sols, A. (1985) 'Modulation of muscle phosphofructokinase at physiological concentration of enzyme', *J Biol Chem*, 260(4), pp. 2100-7.
- Bouche, C., Serdy, S., Kahn, C.R. and Goldfine, A.B. (2004) 'The cellular fate of glucose and its relevance in type 2 diabetes', *Endocr Rev*, 25(5), pp. 807-30.
- Boudaba, N., Marion, A., Huet, C., Pierre, R., Viollet, B. and Foretz, M. (2018) 'AMPK Re-Activation Suppresses Hepatic Steatosis but its Downregulation Does Not Promote Fatty Liver Development', *EBioMedicine*, 28, pp. 194-209.
- Bridges, H.R., Jones, A.J., Pollak, M.N. and Hirst, J. (2014) 'Effects of metformin and other biguanides on oxidative phosphorylation in mitochondria', *Biochem J*, 462(3), pp. 475-87.
- Brocklehurst, K.J., Payne, V.A., Davies, R.A., Carroll, D., Vertigan, H.L., Wightman, H.J., Aiston, S., Waddell, I.D., Leighton, B., Coghlan, M.P. and Agius, L. (2004) 'Stimulation of hepatocyte glucose metabolism by novel small molecule glucokinase activators', *Diabetes*, 53(3), pp. 535-41.
- Brown, M.S. and Goldstein, J.L. (2008) 'Selective versus total insulin resistance: a pathogenic paradox', *Cell Metab*, 7(2), pp. 95-6.
- Bultot, L., Guigas, B., Von Wilamowitz-Moellendorff, A., Maisin, L., Vertommen, D., Hussain, N., Beullens, M., Guinovart, J.J., Foretz, M., Viollet, B., Sakamoto, K., Hue, L. and Rider, M.H. (2012) 'AMP-activated protein kinase phosphorylates and inactivates liver glycogen synthase', *Biochem J*, 443(1), pp. 193-203.
- Bultot, L., Jensen, T.E., Lai, Y.C., Madsen, A.L., Collodet, C., Kviklyte, S., Deak, M., Yavari, A., Foretz, M., Ghaffari, S., Bellahcene, M., Ashrafian, H., Rider, M.H., Richter, E.A. and Sakamoto, K. (2016) 'Benzimidazole derivative small-molecule 991 enhances AMPK activity and glucose uptake induced by AICAR or contraction in skeletal muscle', *Am J Physiol Endocrinol Metab*, 311(4), pp. E706-e719.
- Buse, J.B., DeFronzo, R.A., Rosenstock, J., Kim, T., Burns, C., Skare, S., Baron, A. and Fineman, M. (2016) 'The Primary Glucose-Lowering Effect of Metformin Resides in the Gut, Not the Circulation: Results From Short-term Pharmacokinetic and 12-Week Dose-Ranging Studies', *Diabetes Care*, 39(2), pp. 198-205.
- Cabreiro, F., Au, C., Leung, K.Y., Vergara-Irigaray, N., Cocheme, H.M., Noori, T., Weinkove, D., Schuster, E., Greene, N.D. and Gems, D. (2013) 'Metformin retards aging in *C. elegans* by altering microbial folate and methionine metabolism', *Cell*, 153(1), pp. 228-39.
- Calabrese, M.F., Rajamohan, F., Harris, M.S., Caspers, N.L., Magyar, R., Withka, J.M., Wang, H., Borzilleri, K.A., Sahasrabudhe, P.V., Hoth, L.R., Geoghegan, K.F., Han, S., Brown, J., Subashi, T.A., Reyes, A.R., Frisbie, R.K., Ward, J., Miller, R.A., Landro, J.A., Londregan, A.T., Carpino, P.A., Cabral, S., Smith, A.C., Conn, E.L., Cameron, K.O., Qiu, X. and Kurumbail, R.G. (2014) 'Structural basis for AMPK activation: natural and synthetic ligands regulate kinase activity from opposite poles by different molecular mechanisms', *Structure*, 22(8), pp. 1161-1172.
- Cameron, A.R., Morrison, V.L., Levin, D., Mohan, M., Forteath, C., Beall, C., McNeilly, A.D., Balfour, D.J., Savinko, T., Wong, A.K., Viollet, B., Sakamoto, K., Fagerholm, S.C., Foretz, M., Lang, C.C. and Rena, G. (2016) 'Anti-Inflammatory Effects of Metformin Irrespective of Diabetes Status', *Circ Res*, 119(5), pp. 652-65.
- Cao, J., Meng, S., Chang, E., Beckwith-Fickas, K., Xiong, L., Cole, R.N., Radovick, S., Wondisford, F.E. and He, L. (2014) 'Low concentrations of metformin suppress glucose production in hepatocytes through AMP-activated protein kinase (AMPK)', *J Biol Chem*, 289(30), pp. 20435-46.

- Castillo-Quan, J.I. and Blackwell, T.K. (2016) 'Metformin: Restraining Nucleocytoplasmic Shuttling to Fight Cancer and Aging', *Cell*, 167(7), pp. 1670-1671.
- Chakera, A.J., Steele, A.M., Gloyn, A.L., Shepherd, M.H., Shields, B., Ellard, S. and Hattersley, A.T. (2015) 'Recognition and Management of Individuals With Hyperglycemia Because of a Heterozygous Glucokinase Mutation', *Diabetes Care*, 38(7), pp. 1383-92.
- Chen, E.C., Liang, X., Yee, S.W., Geier, E.G., Stocker, S.L., Chen, L. and Giacomini, K.M. (2015) 'Targeted disruption of organic cation transporter 3 attenuates the pharmacologic response to metformin', *Mol Pharmacol*, 88(1), pp. 75-83.
- Chen, S.Y., Pan, C.J., Nandigama, K., Mansfield, B.C., Ambudkar, S.V. and Chou, J.Y. (2008) 'The glucose-6-phosphate transporter is a phosphate-linked antiporter deficient in glycogen storage disease type Ib and Ic', *Faseb j*, 22(7), pp. 2206-13.
- Choi, J.M., Seo, M.H., Kyeong, H.H., Kim, E. and Kim, H.S. (2013) 'Molecular basis for the role of glucokinase regulatory protein as the allosteric switch for glucokinase', *Proc Natl Acad Sci U S A*, 110(25), pp. 10171-6.
- Chou, J.Y. and Mansfield, B.C. (2014) 'The SLC37 family of sugar-phosphate/phosphate exchangers', *Curr Top Membr*, 73, pp. 357-82.
- Christensen, M.M., Hojlund, K., Hother-Nielsen, O., Stage, T.B., Damkier, P., Beck-Nielsen, H. and Broesen, K. (2015) 'Endogenous glucose production increases in response to metformin treatment in the glycogen-depleted state in humans: a randomised trial', *Diabetologia*, 58(11), pp. 2494-502.
- Ciudad, C.J., Carabaza, A. and Guinovart, J.J. (1986) 'Glucose 6-phosphate plays a central role in the activation of glycogen synthase by glucose in hepatocytes', *Biochem Biophys Res Commun*, 141(3), pp. 1195-200.
- Cool, B., Zinker, B., Chiou, W., Kifle, L., Cao, N., Perham, M., Dickinson, R., Adler, A., Gagne, G., Iyengar, R., Zhao, G., Marsh, K., Kym, P., Jung, P., Camp, H.S. and Frevert, E. (2006) 'Identification and characterization of a small molecule AMPK activator that treats key components of type 2 diabetes and the metabolic syndrome', *Cell Metab*, 3(6), pp. 403-16.
- Cordero, M.D. and Violette, B. (2016) 'Editorial: AMPK: New Frontiers in Human Diseases', *Curr Drug Targets*, 17(8), p. 852.
- Corton, J.M., Gillespie, J.G., Hawley, S.A. and Hardie, D.G. (1995) '5-aminoimidazole-4-carboxamide ribonucleoside. A specific method for activating AMP-activated protein kinase in intact cells?', *Eur J Biochem*, 229(2), pp. 558-65.
- Cubeddu, L.X., Bonisch, H., Gothert, M., Molderings, G., Racke, K., Ramadori, G., Miller, K.J. and Schworer, H. (2000) 'Effects of metformin on intestinal 5-hydroxytryptamine (5-HT) release and on 5-HT₃ receptors', *Naunyn Schmiedebergs Arch Pharmacol*, 361(1), pp. 85-91.
- Cusi, K., Consoli, A. and DeFronzo, R.A. (1996) 'Metabolic effects of metformin on glucose and lactate metabolism in noninsulin-dependent diabetes mellitus', *J Clin Endocrinol Metab*, 81(11), pp. 4059-67.
- Davies, M.N., O'Callaghan, B.L. and Towle, H.C. (2008) 'Glucose activates ChREBP by increasing its rate of nuclear entry and relieving repression of its transcriptional activity', *J Biol Chem*, 283(35), pp. 24029-38.
- de la Iglesia, N., Mukhtar, M., Seoane, J., Guinovart, J.J. and Agius, L. (2000) 'The role of the regulatory protein of glucokinase in the glucose sensory mechanism of the hepatocyte', *J Biol Chem*, 275(14), pp. 10597-603.
- DeFronzo, R.A., Buse, J.B., Kim, T., Burns, C., Skare, S., Baron, A. and Fineman, M. (2016) 'Once-daily delayed-release metformin lowers plasma glucose and enhances fasting and postprandial GLP-1 and PYY: results from two randomised trials', *Diabetologia*, 59(8), pp. 1645-54.

- Dentin, R., Hedrick, S., Xie, J., Yates, J., 3rd and Montminy, M. (2008) 'Hepatic glucose sensing via the CREB coactivator CRTC2', *Science*, 319(5868), pp. 1402-5.
- Dentin, R., Tomas-Cobos, L., Foufelle, F., Leopold, J., Girard, J., Postic, C. and Ferre, P. (2012) 'Glucose 6-phosphate, rather than xylulose 5-phosphate, is required for the activation of ChREBP in response to glucose in the liver', *J Hepatol*, 56(1), pp. 199-209.
- Drahota, Z., Palenickova, E., Endlicher, R., Milerova, M., Brejchova, J., Vosahlikova, M., Svoboda, P., Kazdova, L., Kalous, M., Cervinkova, Z. and Cahova, M. (2014) 'Biguanides inhibit complex I, II and IV of rat liver mitochondria and modify their functional properties', *Physiol Res*, 63(1), pp. 1-11.
- Duca, F.A., Cote, C.D., Rasmussen, B.A., Zadeh-Tahmasebi, M., Rutter, G.A., Filippi, B.M. and Lam, T.K. (2015) 'Metformin activates a duodenal Ampk-dependent pathway to lower hepatic glucose production in rats', *Nat Med*, 21(5), pp. 506-11.
- Ducommun, S., Ford, R.J., Bultot, L., Deak, M., Bertrand, L., Kemp, B.E., Steinberg, G.R. and Sakamoto, K. (2014) 'Enhanced activation of cellular AMPK by dual-small molecule treatment: AICAR and A769662', *Am J Physiol Endocrinol Metab*, 306(6), pp. E688-96.
- Dujic, T., Causevic, A., Begovic, T., Malenica, M., Velija-Asimi, Z., Pearson, E.R. and Semiz, S. (2016) 'Organic cation transporter 1 variants and gastrointestinal side effects of metformin in patients with Type 2 diabetes', *Diabet Med*, 33(4), pp. 511-4.
- Dujic, T., Zhou, K., Tavendale, R., Palmer, C.N. and Pearson, E.R. (2016) 'Effect of Serotonin Transporter 5-HTTLPR Polymorphism on Gastrointestinal Intolerance to Metformin: A GoDARTS Study', *Diabetes Care*, 39(11), pp. 1896-1901.
- El-Mir, M.Y., Nogueira, V., Fontaine, E., Averet, N., Rigoulet, M. and Leverve, X. (2000) 'Dimethylbiguanide inhibits cell respiration via an indirect effect targeted on the respiratory chain complex I', *J Biol Chem*, 275(1), pp. 223-8.
- Fernandez-Novell, J.M., Arino, J. and Guinovart, J.J. (1994) 'Effects of glucose on the activation and translocation of glycogen synthase in diabetic rat hepatocytes', *Eur J Biochem*, 226(2), pp. 665-71.
- Fernandez-Novell, J.M., Roca, A., Bellido, D., Vilaro, S. and Guinovart, J.J. (1996) 'Translocation and aggregation of hepatic glycogen synthase during the fasted-to-refed transition in rats', *Eur J Biochem*, 238(2), pp. 570-5.
- Filhoulaud, G., Guillemain, G. and Scharfmann, R. (2009) 'The hexosamine biosynthesis pathway is essential for pancreatic beta cell development', *J Biol Chem*, 284(36), pp. 24583-94.
- Filhoulaud, G., Guilmeau, S., Dentin, R., Girard, J. and Postic, C. (2013) 'Novel insights into ChREBP regulation and function', *Trends Endocrinol Metab*, 24(5), pp. 257-68.
- Fitzpatrick, J.L., Ripp, S.L., Smith, N.B., Pierce, W.M., Jr. and Prough, R.A. (2001) 'Metabolism of DHEA by cytochromes P450 in rat and human liver microsomal fractions', *Arch Biochem Biophys*, 389(2), pp. 278-87.
- Fletterick, R.J. and Madsen, N.B. (1980) 'The structures and related functions of phosphorylase a', *Annu Rev Biochem*, 49, pp. 31-61.
- Florez, J.C. (2017) 'The pharmacogenetics of metformin', *Diabetologia*, 60(9), pp. 1648-1655.
- Fontaine, D.A. and Davis, D.B. (2016) 'Attention to Background Strain Is Essential for Metabolic Research: C57BL/6 and the International Knockout Mouse Consortium', *Diabetes*, 65(1), pp. 25-33.
- Fontaine, E. (2014) 'Metformin and respiratory chain complex I: the last piece of the puzzle?', *Biochem J*, 463(3), pp. e3-5.

- Foretz, M., Hebrard, S., Leclerc, J., Zarrinpashneh, E., Soty, M., Mithieux, G., Sakamoto, K., Andreelli, F. and Viollet, B. (2010) 'Metformin inhibits hepatic gluconeogenesis in mice independently of the LKB1/AMPK pathway via a decrease in hepatic energy state', *J Clin Invest*, 120(7), pp. 2355-69.
- Forslund, K., Hildebrand, F., Nielsen, T., Falony, G., Le Chatelier, E., Sunagawa, S., Prifti, E., Vieira-Silva, S., Gudmundsdottir, V., Pedersen, H.K., Arumugam, M., Kristiansen, K., Voigt, A.Y., Vestergaard, H., Hercog, R., Costea, P.I., Kultima, J.R., Li, J., Jorgensen, T., Levenez, F., Dore, J., Nielsen, H.B., Brunak, S., Raes, J., Hansen, T., Wang, J., Ehrlich, S.D., Bork, P. and Pedersen, O. (2015) 'Disentangling type 2 diabetes and metformin treatment signatures in the human gut microbiota', *Nature*, 528(7581), pp. 262-266.
- Fujimoto, Y., Torres, T.P., Donahue, E.P. and Shiota, M. (2006) 'Glucose toxicity is responsible for the development of impaired regulation of endogenous glucose production and hepatic glucokinase in Zucker diabetic fatty rats', *Diabetes*, 55(9), pp. 2479-90.
- Fulgencio, J.P., Kohl, C., Girard, J. and Pegorier, J.P. (2001) 'Effect of metformin on fatty acid and glucose metabolism in freshly isolated hepatocytes and on specific gene expression in cultured hepatocytes', *Biochem Pharmacol*, 62(4), pp. 439-46.
- Fullerton, M.D., Galic, S., Marcinko, K., Sikkema, S., Pulinilkunnil, T., Chen, Z.P., O'Neill, H.M., Ford, R.J., Palanivel, R., O'Brien, M., Hardie, D.G., Macaulay, S.L., Schertzer, J.D., Dyck, J.R., van Denderen, B.J., Kemp, B.E. and Steinberg, G.R. (2013) 'Single phosphorylation sites in Acc1 and Acc2 regulate lipid homeostasis and the insulin-sensitizing effects of metformin', *Nat Med*, 19(12), pp. 1649-54.
- Gabr, R.Q., El-Sherbeni, A.A., Ben-Eltriki, M., El-Kadi, A.O. and Brocks, D.R. (2017) 'Pharmacokinetics of metformin in the rat: assessment of the effect of hyperlipidemia and evidence for its metabolism to guanylurea', *Can J Physiol Pharmacol*, 95(5), pp. 530-538.
- Gautier-Stein, A., Soty, M., Chilloux, J., Zitoun, C., Rajas, F. and Mithieux, G. (2012) 'Glucotoxicity induces glucose-6-phosphatase catalytic unit expression by acting on the interaction of HIF-1alpha with CREB-binding protein', *Diabetes*, 61(10), pp. 2451-60.
- Gomez-Galeno, J.E., Dang, Q., Nguyen, T.H., Boyer, S.H., Grote, M.P., Sun, Z., Chen, M., Craigo, W.A., van Poelje, P.D., MacKenna, D.A., Cable, E.E., Rolzin, P.A., Finn, P.D., Chi, B., Linemeyer, D.L., Hecker, S.J. and Erion, M.D. (2010) 'A Potent and Selective AMPK Activator That Inhibits de Novo Lipogenesis', *ACS Med Chem Lett*, 1(9), pp. 478-82.
- Goransson, O., McBride, A., Hawley, S.A., Ross, F.A., Shpiro, N., Foretz, M., Viollet, B., Hardie, D.G. and Sakamoto, K. (2007) 'Mechanism of action of A-769662, a valuable tool for activation of AMP-activated protein kinase', *J Biol Chem*, 282(45), pp. 32549-60.
- Gormsen, L.C., Sundelin, E.I., Jensen, J.B., Vendelbo, M.H., Jakobsen, S., Munk, O.L., Hougaard Christensen, M.M., Brosen, K., Frokiaer, J. and Jessen, N. (2016) 'In Vivo Imaging of Human ¹¹C-Metformin in Peripheral Organs: Dosimetry, Biodistribution, and Kinetic Analyses', *J Nucl Med*, 57(12), pp. 1920-1926.
- Graham, G.G., Punt, J., Arora, M., Day, R.O., Doogue, M.P., Duong, J.K., Furlong, T.J., Greenfield, J.R., Greenup, L.C., Kirkpatrick, C.M., Ray, J.E., Timmins, P. and Williams, K.M. (2011) 'Clinical pharmacokinetics of metformin', *Clin Pharmacokinet*, 50(2), pp. 81-98.
- Gray, J.P., Karandrea, S., Burgos, D.Z., Jaiswal, A.A. and Heart, E.A. (2016) 'NAD(P)H-dependent quinone oxidoreductase 1 (NQO1) and cytochrome P450 oxidoreductase (CYP450OR) differentially regulate menadione-mediated alterations in redox status, survival and metabolism in pancreatic beta-cells', *Toxicol Lett*, 262, pp. 1-11.
- Griffin, S.J., Leaver, J.K. and Irving, G.J. (2017) 'Impact of metformin on cardiovascular disease: a meta-analysis of randomised trials among people with type 2 diabetes', *Diabetologia*, 60(9), pp. 1620-1629.
- Guigas, B., Bertrand, L., Taleux, N., Foretz, M., Wiernsperger, N., Vertommen, D., Andreelli, F., Viollet, B. and Hue, L. (2006) '5-Aminoimidazole-4-carboxamide-1-beta-D-ribofuranoside and metformin inhibit hepatic

- glucose phosphorylation by an AMP-activated protein kinase-independent effect on glucokinase translocation', *Diabetes*, 55(4), pp. 865-74.
- Guinez, C., Filhoulaud, G., Rayah-Benhamed, F., Marmier, S., Dubuquoy, C., Dentin, R., Moldes, M., Burnol, A.F., Yang, X., Lefebvre, T., Girard, J. and Postic, C. (2011) 'O-GlcNAcylation increases ChREBP protein content and transcriptional activity in the liver', *Diabetes*, 60(5), pp. 1399-413.
- Hampson, L.J. and Agius, L. (2005) 'Increased potency and efficacy of combined phosphorylase inactivation and glucokinase activation in control of hepatocyte glycogen metabolism', *Diabetes*, 54(3), pp. 617-23.
- Hansen, S.H. and McCormack, J.G. (2002) 'Application of (13)C-filtered (1)H NMR to evaluate drug action on gluconeogenesis and glycogenolysis simultaneously in isolated rat hepatocytes', *NMR Biomed*, 15(5), pp. 313-9.
- Hardie, D.G. (2018) 'Keeping the home fires burning: AMP-activated protein kinase', *J R Soc Interface*, 15(138).
- Hardie, D.G., Ross, F.A. and Hawley, S.A. (2012) 'AMPK: a nutrient and energy sensor that maintains energy homeostasis', *Nat Rev Mol Cell Biol*, 13(4), pp. 251-62.
- Harndahl, L., Schmoll, D., Herling, A.W. and Agius, L. (2006) 'The role of glucose 6-phosphate in mediating the effects of glucokinase overexpression on hepatic glucose metabolism', *Febs j*, 273(2), pp. 336-46.
- Havula, E. and Hietakangas, V. (2012) 'Glucose sensing by ChREBP/MondoA-Mlx transcription factors', *Semin Cell Dev Biol*, 23(6), pp. 640-7.
- Havula, E. and Hietakangas, V. (2012) 'Glucose sensing by ChREBP/MondoA-Mlx transcription factors', *Semin Cell Dev Biol*, 23(6), pp. 640-7.
- Hawley, S.A., Fullerton, M.D., Ross, F.A., Schertzer, J.D., Chevtzoff, C., Walker, K.J., Peggie, M.W., Zibrova, D., Green, K.A., Mustard, K.J., Kemp, B.E., Sakamoto, K., Steinberg, G.R. and Hardie, D.G. (2012) 'The ancient drug salicylate directly activates AMP-activated protein kinase', *Science*, 336(6083), pp. 918-22.
- Hawley, S.A., Ross, F.A., Chevtzoff, C., Green, K.A., Evans, A., Fogarty, S., Towler, M.C., Brown, L.J., Ogunbayo, O.A., Evans, A.M. and Hardie, D.G. (2010) 'Use of cells expressing gamma subunit variants to identify diverse mechanisms of AMPK activation', *Cell Metab*, 11(6), pp. 554-65.
- He, L., Chang, E., Peng, J., An, H., McMillin, S.M., Radovick, S., Stratakis, C.A. and Wondisford, F.E. (2016) 'Activation of the cAMP-PKA pathway Antagonizes Metformin Suppression of Hepatic Glucose Production', *J Biol Chem*, 291(20), pp. 10562-70.
- He, L., Sabet, A., Djedjos, S., Miller, R., Sun, X., Hussain, M.A., Radovick, S. and Wondisford, F.E. (2009) 'Metformin and insulin suppress hepatic gluconeogenesis through phosphorylation of CREB binding protein', *Cell*, 137(4), pp. 635-46.
- He, L. and Wondisford, F.E. (2015) 'Metformin action: concentrations matter', *Cell Metab*, 21(2), pp. 159-162.
- Heckman-Stoddard, B.M., DeCensi, A., Sahasrabudhe, V.V. and Ford, L.G. (2017) 'Repurposing metformin for the prevention of cancer and cancer recurrence', *Diabetologia*, 60(9), pp. 1639-1647.
- Heinz, S., Freyberger, A., Lawrenz, B., Schladt, L., Schmuck, G. and Ellinger-Ziegelbauer, H. (2017) 'Mechanistic Investigations of the Mitochondrial Complex I Inhibitor Rotenone in the Context of Pharmacological and Safety Evaluation', *Sci Rep*, 7, p. 45465.
- Heishi, M., Ichihara, J., Teramoto, R., Itakura, Y., Hayashi, K., Ishikawa, H., Gomi, H., Sakai, J., Kanaoka, M., Taiji, M. and Kimura, T. (2006) 'Global gene expression analysis in liver of obese diabetic db/db mice treated with metformin', *Diabetologia*, 49(7), pp. 1647-55.
- Herling, A.W., Burger, H., Schubert, G., Hemmerle, H., Schaefer, H. and Kramer, W. (1999) 'Alterations of

- carbohydrate and lipid intermediary metabolism during inhibition of glucose-6-phosphatase in rats', *Eur J Pharmacol*, 386(1), pp. 75-82.
- Herling, A.W., Burger, H.J., Schwab, D., Hemmerle, H., Below, P. and Schubert, G. (1998) 'Pharmacodynamic profile of a novel inhibitor of the hepatic glucose-6-phosphatase system', *Am J Physiol*, 274(6 Pt 1), pp. G1087-93.
- Hers, H.G. and Hue, L. (1983) 'Gluconeogenesis and related aspects of glycolysis', *Annu Rev Biochem*, 52, pp. 617-53.
- Hoek, J.B. and Rydstrom, J. (1988) 'Physiological roles of nicotinamide nucleotide transhydrogenase', *Biochem J*, 254(1), pp. 1-10.
- Howell, J.J., Hellberg, K., Turner, M., Talbott, G., Kolar, M.J., Ross, D.S., Hoxhaj, G., Saghatelian, A., Shaw, R.J. and Manning, B.D. (2017) 'Metformin Inhibits Hepatic mTORC1 Signaling via Dose-Dependent Mechanisms Involving AMPK and the TSC Complex', *Cell Metab*, 25(2), pp. 463-471.
- Hue, L. (1982) 'Role of fructose 2,6-bisphosphate in the stimulation of glycolysis by anoxia in isolated hepatocytes', *Biochem J*, 206(2), pp. 359-65.
- Hue, L. and Rider, M.H. (1987) 'Role of fructose 2,6-bisphosphate in the control of glycolysis in mammalian tissues', *Biochem J*, 245(2), pp. 313-24.
- Hult, M., Elleby, B., Shafqat, N., Svensson, S., Rane, A., Jornvall, H., Abrahmsen, L. and Oppermann, U. (2004) 'Human and rodent type 1 11beta-hydroxysteroid dehydrogenases are 7beta-hydroxycholesterol dehydrogenases involved in oxysterol metabolism', *Cell Mol Life Sci*, 61(7-8), pp. 992-9.
- Hundal, R.S., Krssak, M., Dufour, S., Laurent, D., Lebon, V., Chandramouli, V., Inzucchi, S.E., Schumann, W.C., Petersen, K.F., Landau, B.R. and Shulman, G.I. (2000) 'Mechanism by which metformin reduces glucose production in type 2 diabetes', *Diabetes*, 49(12), pp. 2063-9.
- Hunter, R.W., Foretz, M., Bultot, L., Fullerton, M.D., Deak, M., Ross, F.A., Hawley, S.A., Shpiro, N., Viollet, B., Barron, D., Kemp, B.E., Steinberg, G.R., Hardie, D.G. and Sakamoto, K. (2014) 'Mechanism of action of compound-13: an alpha1-selective small molecule activator of AMPK', *Chem Biol*, 21(7), pp. 866-79.
- Hunter, R.W., Foretz, M., Bultot, L., Fullerton, M.D., Deak, M., Ross, F.A., Hawley, S.A., Shpiro, N., Viollet, B., Barron, D., Kemp, B.E., Steinberg, G.R., Hardie, D.G. and Sakamoto, K. (2014) 'Mechanism of action of compound-13: an alpha1-selective small molecule activator of AMPK', *Chem Biol*, 21(7), pp. 866-79.
- Iizuka, K., Takeda, J. and Horikawa, Y. (2009) 'Glucose induces FGF21 mRNA expression through ChREBP activation in rat hepatocytes', *FEBS Lett*, 583(17), pp. 2882-6.
- International Diabetes Federation. *IDF Diabetes Atlas, 8th edn*. Brussels, Belgium: International Diabetes Federation. 2017. <http://www.diabetesatlas.org>
- Ishii, S., Iizuka, K., Miller, B.C. and Uyeda, K. (2004) 'Carbohydrate response element binding protein directly promotes lipogenic enzyme gene transcription', *Proc Natl Acad Sci U S A*, 101(44), pp. 15597-602.
- Johanns, M., Lai, Y.C., Hsu, M.F., Jacobs, R., Vertommen, D., Van Sande, J., Dumont, J.E., Woods, A., Carling, D., Hue, L., Viollet, B., Foretz, M. and Rider, M.H. (2016) 'AMPK antagonizes hepatic glucagon-stimulated cyclic AMP signalling via phosphorylation-induced activation of cyclic nucleotide phosphodiesterase 4B', *Nat Commun*, 7, p. 10856.
- Johnson, L.N. and Barford, D. (1993) 'The effects of phosphorylation on the structure and function of proteins', *Annu Rev Biophys Biomol Struct*, 22, pp. 199-232.
- Johnson, L.N., Snape, P., Martin, J.L., Acharya, K.R., Barford, D. and Oikonomakos, N.G. (1993) 'Crystallographic binding studies on the allosteric inhibitor glucose-6-phosphate to T state glycogen phosphorylase b', *J Mol*

Biol, 232(1), pp. 253-67.

Kabashima, T., Kawaguchi, T., Wadzinski, B.E. and Uyeda, K. (2003) 'Xylulose 5-phosphate mediates glucose-induced lipogenesis by xylulose 5-phosphate-activated protein phosphatase in rat liver', *Proc Natl Acad Sci U S A*, 100(9), pp. 5107-12.

Kabashima, T., Kawaguchi, T., Wadzinski, B.E. and Uyeda, K. (2003) 'Xylulose 5-phosphate mediates glucose-induced lipogenesis by xylulose 5-phosphate-activated protein phosphatase in rat liver', *Proc Natl Acad Sci U S A*, 100(9), pp. 5107-12.

Kahn, S.E., Cooper, M.E. and Del Prato, S. (2014) 'Pathophysiology and treatment of type 2 diabetes: perspectives on the past, present, and future', *Lancet*, 383(9922), pp. 1068-83.

Kajbaf, F., De Broe, M.E. and Lalau, J.D. (2016) 'Therapeutic Concentrations of Metformin: A Systematic Review', *Clin Pharmacokinet*, 55(4), pp. 439-59.

Katz, J. and Rognstad, R. (1966) 'The metabolism of tritiated glucose by rat adipose tissue', *J Biol Chem*, 241(15), pp. 3600-10.

Katz, J., Wals, P.A., Golden, S. and Rognstad, R. (1975) 'Recycling of glucose by rat hepatocytes', *Eur J Biochem*, 60(1), pp. 91-101.

Kauppinen, R.A., Sihra, T.S. and Nicholls, D.G. (1987) 'Aminooxyacetic acid inhibits the malate-aspartate shuttle in isolated nerve terminals and prevents the mitochondria from utilizing glycolytic substrates', *Biochim Biophys Acta*, 930(2), pp. 173-8.

Kean, E.A., Gutman, M. and Singer, T.P. (1971) 'Studies on the respiratory chain-linked nicotinamide adenine dinucleotide dehydrogenase. XXII. Rhein, a competitive inhibitor of the dehydrogenase', *J Biol Chem*, 246(8), pp. 2346-53.

Kim, Y.D., Kim, Y.H., Tadi, S., Yu, J.H., Yim, Y.H., Jeoung, N.H., Shong, M., Hennighausen, L., Harris, R.A., Lee, I.K., Lee, C.H. and Choi, H.S. (2012) 'Metformin inhibits growth hormone-mediated hepatic PDK4 gene expression through induction of orphan nuclear receptor small heterodimer partner', *Diabetes*, 61(10), pp. 2484-94.

Kim, Y.D., Li, T., Ahn, S.W., Kim, D.K., Lee, J.M., Hwang, S.L., Kim, Y.H., Lee, C.H., Lee, I.K., Chiang, J.Y. and Choi, H.S. (2012) 'Orphan nuclear receptor small heterodimer partner negatively regulates growth hormone-mediated induction of hepatic gluconeogenesis through inhibition of signal transducer and activator of transcription 5 (STAT5) transactivation', *J Biol Chem*, 287(44), pp. 37098-108.

Kim, Y.D., Park, K.G., Lee, Y.S., Park, Y.Y., Kim, D.K., Nedumaran, B., Jang, W.G., Cho, W.J., Ha, J., Lee, I.K., Lee, C.H. and Choi, H.S. (2008) 'Metformin inhibits hepatic gluconeogenesis through AMP-activated protein kinase-dependent regulation of the orphan nuclear receptor SHP', *Diabetes*, 57(2), pp. 306-14.

Koo, S.H., Flechner, L., Qi, L., Zhang, X., Sreaton, R.A., Jeffries, S., Hedrick, S., Xu, W., Boussouar, F., Brindle, P., Takemori, H. and Montminy, M. (2005) 'The CREB coactivator TORC2 is a key regulator of fasting glucose metabolism', *Nature*, 437(7062), pp. 1109-11.

Koo, S.H. and Towle, H.C. (2000) 'Glucose regulation of mouse S(14) gene expression in hepatocytes. Involvement of a novel transcription factor complex', *J Biol Chem*, 275(7), pp. 5200-7.

Kraev, A. (2014) 'Parallel universes of Black Six biology', *Biol Direct*, 9, p. 18.

Lai, Y.C., Kviklyte, S., Vertommen, D., Lantier, L., Foretz, M., Viollet, B., Hallen, S. and Rider, M.H. (2014) 'A small-molecule benzimidazole derivative that potently activates AMPK to increase glucose transport in skeletal muscle: comparison with effects of contraction and other AMPK activators', *Biochem J*, 460(3), pp. 363-75.

Landgraf, R.R., Goswami, D., Rajamohan, F., Harris, M.S., Calabrese, M.F., Hoth, L.R., Magyar, R., Pascal, B.D.,

- Chalmers, M.J., Busby, S.A., Kurumbail, R.G. and Griffin, P.R. (2013) 'Activation of AMP-activated protein kinase revealed by hydrogen/deuterium exchange mass spectrometry', *Structure*, 21(11), pp. 1942-53.
- Lavery, G.G., Walker, E.A., Draper, N., Jeyasuria, P., Marcos, J., Shackleton, C.H., Parker, K.L., White, P.C. and Stewart, P.M. (2006) 'Hexose-6-phosphate dehydrogenase knock-out mice lack 11 beta-hydroxysteroid dehydrogenase type 1-mediated glucocorticoid generation', *J Biol Chem*, 281(10), pp. 6546-51.
- Lee, J.M., Seo, W.Y., Song, K.H., Chanda, D., Kim, Y.D., Kim, D.K., Lee, M.W., Ryu, D., Kim, Y.H., Noh, J.R., Lee, C.H., Chiang, J.Y., Koo, S.H. and Choi, H.S. (2010) 'AMPK-dependent repression of hepatic gluconeogenesis via disruption of CREB.CRTC2 complex by orphan nuclear receptor small heterodimer partner', *J Biol Chem*, 285(42), pp. 32182-91.
- Li, M.V., Chen, W., Harmancey, R.N., Nuotio-Antar, A.M., Imamura, M., Saha, P., Taegtmeier, H. and Chan, L. (2010) 'Glucose-6-phosphate mediates activation of the carbohydrate responsive binding protein (ChREBP)', *Biochem Biophys Res Commun*, 395(3), pp. 395-400.
- Li, X., Kover, K.L., Heruth, D.P., Watkins, D.J., Moore, W.V., Jackson, K., Zang, M., Clements, M.A. and Yan, Y. (2015) 'New Insight Into Metformin Action: Regulation of ChREBP and FOXO1 Activities in Endothelial Cells', *Mol Endocrinol*, 29(8), pp. 1184-94.
- Lloyd, D.J., St Jean, D.J., Jr., Kurzeja, R.J., Wahl, R.C., Michelsen, K., Cupples, R., Chen, M., Wu, J., Sivits, G., Helmering, J., Komorowski, R., Ashton, K.S., Pennington, L.D., Fotsch, C., Vazir, M., Chen, K., Chmait, S., Zhang, J., Liu, L., Norman, M.H., Andrews, K.L., Bartberger, M.D., Van, G., Galbreath, E.J., Vonderfecht, S.L., Wang, M., Jordan, S.R., Veniant, M.M. and Hale, C. (2013) 'Antidiabetic effects of glucokinase regulatory protein small-molecule disruptors', *Nature*, 504(7480), pp. 437-40.
- Logie, L., Harthill, J., Patel, K., Bacon, S., Hamilton, D.L., Macrae, K., McDougall, G., Wang, H.H., Xue, L., Jiang, H., Sakamoto, K., Prescott, A.R. and Rena, G. (2012) 'Cellular responses to the metal-binding properties of metformin', *Diabetes*, 61(6), pp. 1423-33.
- M.N. Berry, A.M.E., G.J. Barritt (1991) *Laboratory Techniques in Biochemistry and Molecular Biology*. Amsterdam: Elsevier.
- Ma, L., Robinson, L.N. and Towle, H.C. (2006) 'ChREBP*MLx is the principal mediator of glucose-induced gene expression in the liver', *J Biol Chem*, 281(39), pp. 28721-30.
- Ma, L., Tsatsos, N.G. and Towle, H.C. (2005) 'Direct role of ChREBP.Mlx in regulating hepatic glucose-responsive genes', *J Biol Chem*, 280(12), pp. 12019-27.
- Madiraju, A.K., Erion, D.M., Rahimi, Y., Zhang, X.M., Braddock, D.T., Albright, R.A., Prigaro, B.J., Wood, J.L., Bhanot, S., MacDonald, M.J., Jurczak, M.J., Camporez, J.P., Lee, H.Y., Cline, G.W., Samuel, V.T., Kibbey, R.G. and Shulman, G.I. (2014) 'Metformin suppresses gluconeogenesis by inhibiting mitochondrial glycerophosphate dehydrogenase', *Nature*, 510(7506), pp. 542-6.
- Marks, P.A. and Banks, J. (1960) 'INHIBITION OF MAMMALIAN GLUCOSE-6-PHOSPHATE DEHYDROGENASE BY STEROIDS', *Proc Natl Acad Sci U S A*, 46(4), pp. 447-52.
- Martin-Montalvo, A., Mercken, E.M., Mitchell, S.J., Palacios, H.H., Mote, P.L., Scheibye-Knudsen, M., Gomes, A.P., Ward, T.M., Minor, R.K., Blouin, M.J., Schwab, M., Pollak, M., Zhang, Y., Yu, Y., Becker, K.G., Bohr, V.A., Ingram, D.K., Sinclair, D.A., Wolf, N.S., Spindler, S.R., Bernier, M. and de Cabo, R. (2013) 'Metformin improves healthspan and lifespan in mice', *Nat Commun*, 4, p. 2192.
- Massollo, M., Marini, C., Brignone, M., Emionite, L., Salani, B., Riondato, M., Capitanio, S., Fiz, F., Democrito, A., Amaro, A., Morbelli, S., Piana, M., Maggi, D., Cilli, M., Pfeffer, U. and Sambucetti, G. (2013) 'Metformin temporal and localized effects on gut glucose metabolism assessed using 18F-FDG PET in mice', *J Nucl Med*, 54(2), pp. 259-66.

- Mc, C.D. and Touster, O. (1957) 'The conversion in vivo of xylitol to glycogen via the pentose phosphate pathway', *J Biol Chem*, 229(1), pp. 451-61.
- McCreight, L.J., Bailey, C.J. and Pearson, E.R. (2016) 'Metformin and the gastrointestinal tract', *Diabetologia*, 59(3), pp. 426-35.
- McCune, S.A., Foe, L.G., Kemp, R.G. and Jurin, R.R. (1989) 'Aurintricarboxylic acid is a potent inhibitor of phosphofructokinase', *Biochem J*, 259(3), pp. 925-7.
- McGrane, M.M., El-Maghrabi, M.R. and Pilkis, S.J. (1983) 'The interaction of fructose 2,6-bisphosphate and AMP with rat hepatic fructose 1,6-bisphosphatase', *J Biol Chem*, 258(17), pp. 10445-54.
- Meadows, N.A., Saxty, B., Albury, M.S., Kettleborough, C.A., Ashcroft, F.M., Moore, A.L. and Cox, R.D. (2011) 'A high-throughput assay for modulators of NNT activity in permeabilized yeast cells', *J Biomol Screen*, 16(7), pp. 734-43.
- Meng, S., Cao, J., He, Q., Xiong, L., Chang, E., Radovick, S., Wondisford, F.E. and He, L. (2015) 'Metformin activates AMP-activated protein kinase by promoting formation of the alphabeta-gamma heterotrimeric complex', *J Biol Chem*, 290(6), pp. 3793-802.
- Meroni, G., Cairo, S., Merla, G., Messali, S., Brent, R., Ballabio, A. and Reymond, A. (2000) 'Mlx, a new Max-like bHLHZip family member: the center stage of a novel transcription factors regulatory pathway?', *Oncogene*, 19(29), pp. 3266-77.
- Miller, K.K., Al-Rayyan, N., Ivanova, M.M., Mattingly, K.A., Ripp, S.L., Klinge, C.M. and Prough, R.A. (2013) 'DHEA metabolites activate estrogen receptors alpha and beta', *Steroids*, 78(1), pp. 15-25.
- Miller, R.A., Chu, Q., Xie, J., Foretz, M., Viollet, B. and Birnbaum, M.J. (2013) 'Biguanides suppress hepatic glucagon signalling by decreasing production of cyclic AMP', *Nature*, 494(7436), pp. 256-60.
- Mithieux, G., Guignot, L., Bordet, J.C. and Wiernsperger, N. (2002) 'Intrahepatic mechanisms underlying the effect of metformin in decreasing basal glucose production in rats fed a high-fat diet', *Diabetes*, 51(1), pp. 139-43.
- Morris, R.C., Jr., Nigon, K. and Reed, E.B. (1978) 'Evidence that the severity of depletion of inorganic phosphate determines the severity of the disturbance of adenine nucleotide metabolism in the liver and renal cortex of the fructose-loaded rat', *J Clin Invest*, 61(1), pp. 209-20.
- Moyle, J. and Mitchell, P. (1973) 'The proton-translocating nicotinamide-adenine dinucleotide (phosphate) transhydrogenase of rat liver mitochondria', *Biochem J*, 132(3), pp. 571-85.
- Muirhead, R.P. and Hothersall, J.S. (1995) 'The effect of phenazine methosulphate on intermediary pathways of glucose metabolism in the lens at different glycaemic levels', *Exp Eye Res*, 61(5), pp. 619-27.
- Mukhtar, M.H., Payne, V.A., Arden, C., Harbottle, A., Khan, S., Lange, A.J. and Agius, L. (2008) 'Inhibition of glucokinase translocation by AMP-activated protein kinase is associated with phosphorylation of both GKRP and 6-phosphofructo-2-kinase/fructose-2,6-bisphosphatase', *Am J Physiol Regul Integr Comp Physiol*, 294(3), pp. R766-74.
- Nagamine, S., Horisaka, E., Fukuyama, Y., Maetani, K., Matsuzawa, R., Iwakawa, S. and Asada, S. (1997) 'Stereoselective reductive metabolism of metyrapone and inhibitory activity of metyrapone metabolites, metyrapol enantiomers, on steroid 11 beta-hydroxylase in the rat', *Biol Pharm Bull*, 20(2), pp. 188-92.
- Natali, A. and Ferrannini, E. (2006) 'Effects of metformin and thiazolidinediones on suppression of hepatic glucose production and stimulation of glucose uptake in type 2 diabetes: a systematic review', *Diabetologia*, 49(3), pp. 434-41.
- Niculescu, L., Veiga-da-Cunha, M. and Van Schaftingen, E. (1997) 'Investigation on the mechanism by which

- fructose, hexitols and other compounds regulate the translocation of glucokinase in rat hepatocytes', *Biochem J*, 321 (Pt 1), pp. 239-46.
- Nies, A.T., Koepsell, H., Winter, S., Burk, O., Klein, K., Kerb, R., Zanger, U.M., Keppler, D., Schwab, M. and Schaeffeler, E. (2009) 'Expression of organic cation transporters OCT1 (SLC22A1) and OCT3 (SLC22A3) is affected by genetic factors and cholestasis in human liver', *Hepatology*, 50(4), pp. 1227-40.
- Niewoehner, C.B., Gilboe, D.P. and Nuttall, F.Q. (1984) 'Metabolic effects of oral glucose in the liver of fasted rats', *Am J Physiol*, 246(1 Pt 1), pp. E89-94.
- Niewoehner, C.B., Gilboe, D.P., Nuttall, G.A. and Nuttall, F.Q. (1984) 'Metabolic effects of oral fructose in the liver of fasted rats', *Am J Physiol*, 247(4 Pt 1), pp. E505-12.
- Novelle, M.G., Ali, A., Dieguez, C., Bernier, M. and de Cabo, R. (2016) 'Metformin: A Hopeful Promise in Aging Research', *Cold Spring Harb Perspect Med*, 6(3), p. a025932.
- Olivier, S., Foretz, M. and Viollet, B. (2018) 'Promise and challenges for direct small molecule AMPK activators', *Biochem Pharmacol*, 153, pp. 147-158.
- Ota, S., Horigome, K., Ishii, T., Nakai, M., Hayashi, K., Kawamura, T., Kishino, A., Taiji, M. and Kimura, T. (2009) 'Metformin suppresses glucose-6-phosphatase expression by a complex I inhibition and AMPK activation-independent mechanism', *Biochem Biophys Res Commun*, 388(2), pp. 311-6.
- Otto, M., Breinholt, J. and Westergaard, N. (2003) 'Metformin inhibits glycogen synthesis and gluconeogenesis in cultured rat hepatocytes', *Diabetes Obes Metab*, 5(3), pp. 189-94.
- Ouyang, J., Parakhia, R.A. and Ochs, R.S. (2011) 'Metformin activates AMP kinase through inhibition of AMP deaminase', *J Biol Chem*, 286(1), pp. 1-11.
- Owen, M.R., Doran, E. and Halestrap, A.P. (2000) 'Evidence that metformin exerts its anti-diabetic effects through inhibition of complex 1 of the mitochondrial respiratory chain', *Biochem J*, 348 Pt 3, pp. 607-14.
- Owen, M.R. and Halestrap, A.P. (1993) 'The mechanisms by which mild respiratory chain inhibitors inhibit hepatic gluconeogenesis', *Biochim Biophys Acta*, 1142(1-2), pp. 11-22.
- Palmer, G., Horgan, D.J., Tisdale, H., Singer, T.P. and Beinert, H. (1968) 'Studies on the respiratory chain-linked reduced nicotinamide adenine dinucleotide dehydrogenase. XIV. Location of the sites of inhibition of rotenone, barbiturates, and piericidin by means of electron paramagnetic resonance spectroscopy', *J Biol Chem*, 243(4), pp. 844-7.
- Pan, C.J., Chen, S.Y., Jun, H.S., Lin, S.R., Mansfield, B.C. and Chou, J.Y. (2011) 'SLC37A1 and SLC37A2 are phosphate-linked, glucose-6-phosphate antiporters', *PLoS One*, 6(9), p. e23157.
- Patel, S. (2018) 'Polycystic ovary syndrome (PCOS), an inflammatory, systemic, lifestyle endocrinopathy', *J Steroid Biochem Mol Biol*.
- Pederson, B.A., Cheng, C., Wilson, W.A. and Roach, P.J. (2000) 'Regulation of glycogen synthase. Identification of residues involved in regulation by the allosteric ligand glucose-6-P and by phosphorylation', *J Biol Chem*, 275(36), pp. 27753-61.
- Petersen, M.C., Vatner, D.F. and Shulman, G.I. (2017) 'Regulation of hepatic glucose metabolism in health and disease', *Nat Rev Endocrinol*, 13(10), pp. 572-587.
- Preiss, D., Dawed, A., Welsh, P., Heggie, A., Jones, A.G., Dekker, J., Koivula, R., Hansen, T.H., Stewart, C., Holman, R.R., Franks, P.W., Walker, M., Pearson, E.R. and Sattar, N. (2017) 'Sustained influence of metformin therapy on circulating glucagon-like peptide-1 levels in individuals with and without type 2 diabetes', *Diabetes Obes Metab*, 19(3), pp. 356-363.

- Preuss, J., Richardson, A.D., Pinkerton, A., Hedrick, M., Sergienko, E., Rahlfs, S., Becker, K. and Bode, L. (2013) 'Identification and characterization of novel human glucose-6-phosphate dehydrogenase inhibitors', *J Biomol Screen*, 18(3), pp. 286-97.
- Proctor, W.R., Bourdet, D.L. and Thakker, D.R. (2008) 'Mechanisms underlying saturable intestinal absorption of metformin', *Drug Metab Dispos*, 36(8), pp. 1650-8.
- Pryor, H.J., Smyth, J.E., Quinlan, P.T. and Halestrap, A.P. (1987) 'Evidence that the flux control coefficient of the respiratory chain is high during gluconeogenesis from lactate in hepatocytes from starved rats. Implications for the hormonal control of gluconeogenesis and action of hypoglycaemic agents', *Biochem J*, 247(2), pp. 449-57.
- Quan, X., Uddin, R., Heiskanen, A., Parmvi, M., Nilson, K., Donolato, M., Hansen, M.F., Rena, G. and Boisen, A. (2015) 'The copper binding properties of metformin--QCM-D, XPS and nanobead agglomeration', *Chem Commun (Camb)*, 51(97), pp. 17313-6.
- Radziuk, J., Zhang, Z., Wiernsperger, N. and Pye, S. (1997) 'Effects of metformin on lactate uptake and gluconeogenesis in the perfused rat liver', *Diabetes*, 46(9), pp. 1406-13.
- Rena, G., Hardie, D.G. and Pearson, E.R. (2017) 'The mechanisms of action of metformin', *Diabetologia*, 60(9), pp. 1577-1585.
- Rena, G., Pearson, E.R. and Sakamoto, K. (2013) 'Molecular mechanism of action of metformin: old or new insights?', *Diabetologia*, 56(9), pp. 1898-906.
- Repiscak, P., Erhardt, S., Rena, G. and Paterson, M.J. (2014) 'Biomolecular mode of action of metformin in relation to its copper binding properties', *Biochemistry*, 53(4), pp. 787-95.
- Robinson, K.A., Weinstein, M.L., Lindenmayer, G.E. and Buse, M.G. (1995) 'Effects of diabetes and hyperglycemia on the hexosamine synthesis pathway in rat muscle and liver', *Diabetes*, 44(12), pp. 1438-46.
- Rognstad, R. and Katz, J. (1970) 'Gluconeogenesis in the kidney cortex. Effects of D-malate and amino-oxyacetate', *Biochem J*, 116(3), pp. 483-91.
- Rognstad, R., Wals, P. and Katz, J. (1975) 'Metabolism of [5-T]fructose by isolated liver cells', *J Biol Chem*, 250(22), pp. 8642-6.
- Rose, I.A. and O'Connell, E.L. (1961) 'Intramolecular hydrogen transfer in the phosphoglucose isomerase reaction', *J Biol Chem*, 236, pp. 3086-92.
- Ross, F.A., Jensen, T.E. and Hardie, D.G. (2016) 'Differential regulation by AMP and ADP of AMPK complexes containing different gamma subunit isoforms', *Biochem J*, 473(2), pp. 189-99.
- Ross, F.A., MacKintosh, C. and Hardie, D.G. (2016) 'AMP-activated protein kinase: a cellular energy sensor that comes in 12 flavours', *Febs j*, 283(16), pp. 2987-3001.
- Rudack, D., Chisholm, E.M. and Holten, D. (1971) 'Rat liver glucose 6-phosphate dehydrogenase. Regulation by carbohydrate diet and insulin', *J Biol Chem*, 246(5), pp. 1249-54.
- Rui, L. (2014) 'Energy metabolism in the liver', *Compr Physiol*, 4(1), pp. 177-97.
- Saheki, T., Iijima, M., Li, M.X., Kobayashi, K., Horiuchi, M., Ushikai, M., Okumura, F., Meng, X.J., Inoue, I., Tajima, A., Moriyama, M., Eto, K., Kadowaki, T., Sinasac, D.S., Tsui, L.C., Tsuji, M., Okano, A. and Kobayashi, T. (2007) 'Citrin/mitochondrial glycerol-3-phosphate dehydrogenase double knock-out mice recapitulate features of human citrin deficiency', *J Biol Chem*, 282(34), pp. 25041-52.

- Sajan, M.P., Ivey, R.A., 3rd and Farese, R.V. (2013) 'Metformin action in human hepatocytes: coactivation of atypical protein kinase C alters 5'-AMP-activated protein kinase effects on lipogenic and gluconeogenic enzyme expression', *Diabetologia*, 56(11), pp. 2507-16.
- Sampath-Kumar, R., Yu, M., Khalil, M.W. and Yang, K. (1997) 'Metyrapone is a competitive inhibitor of 11beta-hydroxysteroid dehydrogenase type 1 reductase', *J Steroid Biochem Mol Biol*, 62(2-3), pp. 195-9.
- Sanchez-Rangel, E. and Inzucchi, S.E. (2017) 'Metformin: clinical use in type 2 diabetes', *Diabetologia*, 60(9), pp. 1586-1593.
- Sanders, M.J., Ali, Z.S., Hegarty, B.D., Heath, R., Snowden, M.A. and Carling, D. (2007) 'Defining the mechanism of activation of AMP-activated protein kinase by the small molecule A-769662, a member of the thienopyridone family', *J Biol Chem*, 282(45), pp. 32539-48.
- Sato, S., Jung, H., Nakagawa, T., Pawlosky, R., Takeshima, T., Lee, W.R., Sakiyama, H., Laxman, S., Wynn, R.M., Tu, B.P., MacMillan, J.B., De Brabander, J.K., Veech, R.L. and Uyeda, K. (2016) 'Metabolite Regulation of Nuclear Localization of Carbohydrate-response Element-binding Protein (ChREBP): ROLE OF AMP AS AN ALLOSTERIC INHIBITOR', *J Biol Chem*, 291(20), pp. 10515-27.
- Schwartz, A.G. and Pashko, L.L. (2004) 'Dehydroepiandrosterone, glucose-6-phosphate dehydrogenase, and longevity', *Ageing Res Rev*, 3(2), pp. 171-87.
- Scott, J.W., Ling, N., Issa, S.M., Dite, T.A., O'Brien, M.T., Chen, Z.P., Galic, S., Langendorf, C.G., Steinberg, G.R., Kemp, B.E. and Oakhill, J.S. (2014) 'Small molecule drug A-769662 and AMP synergistically activate naive AMPK independent of upstream kinase signaling', *Chem Biol*, 21(5), pp. 619-27.
- Scott, J.W., van Denderen, B.J., Jorgensen, S.B., Honeyman, J.E., Steinberg, G.R., Oakhill, J.S., Iseli, T.J., Koay, A., Gooley, P.R., Stapleton, D. and Kemp, B.E. (2008) 'Thienopyridone drugs are selective activators of AMP-activated protein kinase beta1-containing complexes', *Chem Biol*, 15(11), pp. 1220-30.
- Senesi, S., Csala, M., Marcolongo, P., Fulceri, R., Mandl, J., Banhegyi, G. and Benedetti, A. (2010) 'Hexose-6-phosphate dehydrogenase in the endoplasmic reticulum', *Biol Chem*, 391(1), pp. 1-8.
- Seoane, J., Gomez-Foix, A.M., O'Doherty, R.M., Gomez-Ara, C., Newgard, C.B. and Guinovart, J.J. (1996) 'Glucose 6-phosphate produced by glucokinase, but not hexokinase I, promotes the activation of hepatic glycogen synthase', *J Biol Chem*, 271(39), pp. 23756-60.
- Seoane, J., Trinh, K., O'Doherty, R.M., Gomez-Foix, A.M., Lange, A.J., Newgard, C.B. and Guinovart, J.J. (1997) 'Metabolic impact of adenovirus-mediated overexpression of the glucose-6-phosphatase catalytic subunit in hepatocytes', *J Biol Chem*, 272(43), pp. 26972-7.
- Shaked, M., Ketzinel-Gilad, M., Cerasi, E., Kaiser, N. and Leibowitz, G. (2011) 'AMP-activated protein kinase (AMPK) mediates nutrient regulation of thioredoxin-interacting protein (TXNIP) in pancreatic beta-cells', *PLoS One*, 6(12), p. e28804.
- Shantz, L.M., Talalay, P. and Gordon, G.B. (1989) 'Mechanism of inhibition of growth of 3T3-L1 fibroblasts and their differentiation to adipocytes by dehydroepiandrosterone and related steroids: role of glucose-6-phosphate dehydrogenase', *Proc Natl Acad Sci U S A*, 86(10), pp. 3852-6.
- Shaw, R.J., Lamia, K.A., Vasquez, D., Koo, S.H., Bardeesy, N., Depinho, R.A., Montminy, M. and Cantley, L.C. (2005) 'The kinase LKB1 mediates glucose homeostasis in liver and therapeutic effects of metformin', *Science*, 310(5754), pp. 1642-6.
- Shih, H. and Towle, H.C. (1994) 'Definition of the carbohydrate response element of the rat S14 gene. Context of the CACGTG motif determines the specificity of carbohydrate regulation', *J Biol Chem*, 269(12), pp. 9380-7.
- Shin, N.R., Lee, J.C., Lee, H.Y., Kim, M.S., Whon, T.W., Lee, M.S. and Bae, J.W. (2014) 'An increase in the Akkermansia spp. population induced by metformin treatment improves glucose homeostasis in diet-

induced obese mice', *Gut*, 63(5), pp. 727-35.

Shu, Y., Sheardown, S.A., Brown, C., Owen, R.P., Zhang, S., Castro, R.A., Ianculescu, A.G., Yue, L., Lo, J.C., Burchard, E.G., Brett, C.M. and Giacomini, K.M. (2007) 'Effect of genetic variation in the organic cation transporter 1 (OCT1) on metformin action', *J Clin Invest*, 117(5), pp. 1422-31.

Sies, H., Akerboom, T.P. and Tager, J.M. (1977) 'Mitochondrial and cytosolic NADPH systems and isocitrate dehydrogenase indicator metabolites during ureogenesis from ammonia in isolated rat hepatocytes', *Eur J Biochem*, 72(2), pp. 301-7.

Sies, H., Summer, K.H. and Bucher, T. (1975) 'A process requiring mitochondrial NADPH: urea formation from ammonia', *FEBS Lett*, 54(2), pp. 274-8.

Slater, T.F. (1967) 'Oxidized and reduced nicotinamide-adenine dinucleotide phosphate in tissue suspensions of rat liver', *Biochem J*, 104(3), pp. 833-42.

Song, P., Kim, J.H., Ghim, J., Yoon, J.H., Lee, A., Kwon, Y., Hyun, H., Moon, H.Y., Choi, H.S., Berggren, P.O., Suh, P.G. and Ryu, S.H. (2013) 'Emodin regulates glucose utilization by activating AMP-activated protein kinase', *J Biol Chem*, 288(8), pp. 5732-42.

Sosnicki, S., Kapral, M. and Weglarz, L. (2016) 'Molecular targets of metformin antitumor action', *Pharmacol Rep*, 68(5), pp. 918-25.

Starkov, A.A. (2006) 'Protein-mediated energy-dissipating pathways in mitochondria', *Chem Biol Interact*, 163(1-2), pp. 133-44.

Stincone, A., Prigione, A., Cramer, T., Wamelink, M.M., Campbell, K., Cheung, E., Olin-Sandoval, V., Gruning, N.M., Kruger, A., Tauqeer Alam, M., Keller, M.A., Breitenbach, M., Brindle, K.M., Rabinowitz, J.D. and Ralser, M. (2015) 'The return of metabolism: biochemistry and physiology of the pentose phosphate pathway', *Biol Rev Camb Philos Soc*, 90(3), pp. 927-63.

Stoekman, A.K., Ma, L. and Towle, H.C. (2004) 'Mlx is the functional heteromeric partner of the carbohydrate response element-binding protein in glucose regulation of lipogenic enzyme genes', *J Biol Chem*, 279(15), pp. 15662-9.

Stumvoll, M., Nurjhan, N., Perriello, G., Dailey, G. and Gerich, J.E. (1995) 'Metabolic effects of metformin in non-insulin-dependent diabetes mellitus', *N Engl J Med*, 333(9), pp. 550-4.

Sugden, P.H. and Newsholme, E.A. (1975) 'The effects of ammonium, inorganic phosphate and potassium ions on the activity of phosphofructokinases from muscle and nervous tissues of vertebrates and invertebrates', *Biochem J*, 150(1), pp. 113-22.

Sullivan, J.E., Brocklehurst, K.J., Marley, A.E., Carey, F., Carling, D. and Beri, R.K. (1994) 'Inhibition of lipolysis and lipogenesis in isolated rat adipocytes with AICAR, a cell-permeable activator of AMP-activated protein kinase', *FEBS Lett*, 353(1), pp. 33-6.

Sum, C.F., Webster, J.M., Johnson, A.B., Catalano, C., Cooper, B.G. and Taylor, R. (1992) 'The effect of intravenous metformin on glucose metabolism during hyperglycaemia in type 2 diabetes', *Diabet Med*, 9(1), pp. 61-5.

Sundelin, E., Gormsen, L.C., Jensen, J.B., Vendelbo, M.H., Jakobsen, S., Munk, O.L., Christensen, M., Brosen, K., Frokiaer, J. and Jessen, N. (2017) 'Genetic Polymorphisms in Organic Cation Transporter 1 Attenuates Hepatic Metformin Exposure in Humans', *Clin Pharmacol Ther*, 102(5), pp. 841-848.

Tabidi, I. and Saggerson, D. (2012) 'Inactivation of the AMP-activated protein kinase by glucose in cardiac myocytes: a role for the pentose phosphate pathway', *Biosci Rep*, 32(3), pp. 229-39.

- Timmermans, A.D., Balteau, M., Gelinat, R., Renguet, E., Ginion, A., de Meester, C., Sakamoto, K., Balligand, J.L., Bontemps, F., Vanoverschelde, J.L., Horman, S., Beauloye, C. and Bertrand, L. (2014) 'A-769662 potentiates the effect of other AMP-activated protein kinase activators on cardiac glucose uptake', *Am J Physiol Heart Circ Physiol*, 306(12), pp. H1619-30.
- Towle, H.C., Kaytor, E.N. and Shih, H.M. (1997) 'Regulation of the expression of lipogenic enzyme genes by carbohydrate', *Annu Rev Nutr*, 17, pp. 405-33.
- Trautwein, C., Berset, J.D., Wolschke, H. and Kummerer, K. (2014) 'Occurrence of the antidiabetic drug Metformin and its ultimate transformation product Guanylurea in several compartments of the aquatic cycle', *Environ Int*, 70, pp. 203-12.
- Tsatsos, N.G. and Towle, H.C. (2006) 'Glucose activation of ChREBP in hepatocytes occurs via a two-step mechanism', *Biochem Biophys Res Commun*, 340(2), pp. 449-56.
- Turner, N., Li, J.Y., Gosby, A., To, S.W., Cheng, Z., Miyoshi, H., Taketo, M.M., Cooney, G.J., Kraegen, E.W., James, D.E., Hu, L.H., Li, J. and Ye, J.M. (2008) 'Berberine and its more biologically available derivative, dihydroberberine, inhibit mitochondrial respiratory complex I: a mechanism for the action of berberine to activate AMP-activated protein kinase and improve insulin action', *Diabetes*, 57(5), pp. 1414-8.
- Valencia, W.M., Palacio, A., Tamariz, L. and Florez, H. (2017) 'Metformin and ageing: improving ageing outcomes beyond glycaemic control', *Diabetologia*, 60(9), pp. 1630-1638.
- van de Werve, G., Lange, A., Newgard, C., Mechin, M.C., Li, Y. and Berteloot, A. (2000) 'New lessons in the regulation of glucose metabolism taught by the glucose 6-phosphatase system', *Eur J Biochem*, 267(6), pp. 1533-49.
- van Dijk, T.H., van der Sluijs, F.H., Wiegman, C.H., Baller, J.F., Gustafson, L.A., Burger, H.J., Herling, A.W., Kuipers, F., Meijer, A.J. and Reijngoud, D.J. (2001) 'Acute inhibition of hepatic glucose-6-phosphatase does not affect gluconeogenesis but directs gluconeogenic flux toward glycogen in fasted rats. A pharmacological study with the chlorogenic acid derivative S4048', *J Biol Chem*, 276(28), pp. 25727-35.
- Van Schaftingen, E. (1993) 'Glycolysis revisited', *Diabetologia*, 36(7), pp. 581-8.
- van Schaftingen, E. and Gerin, I. (2002) 'The glucose-6-phosphatase system', *Biochem J*, 362(Pt 3), pp. 513-32.
- Vanstapel, F., Waebens, M., Van Hecke, P., Decanniere, C. and Stalmans, W. (1990) 'The cytosolic concentration of phosphate determines the maximal rate of glycogenolysis in perfused rat liver', *Biochem J*, 266(1), pp. 207-12.
- Varjabedian, L., Bourji, M., Pourafkari, L. and Nader, N.D. (2018) 'Cardioprotection by Metformin: Beneficial Effects Beyond Glucose Reduction', *Am J Cardiovasc Drugs*, 18(3), pp. 181-193.
- Vasamsetti, S.B., Karnewar, S., Kanugula, A.K., Thatipalli, A.R., Kumar, J.M. and Kotamraju, S. (2015) 'Metformin inhibits monocyte-to-macrophage differentiation via AMPK-mediated inhibition of STAT3 activation: potential role in atherosclerosis', *Diabetes*, 64(6), pp. 2028-41.
- Veech, R.L., Eggleston, L.V. and Krebs, H.A. (1969) 'The redox state of free nicotinamide-adenine dinucleotide phosphate in the cytoplasm of rat liver', *Biochem J*, 115(4), pp. 609-19.
- Velasco, G., Geelen, M.J. and Guzman, M. (1997) 'Control of hepatic fatty acid oxidation by 5'-AMP-activated protein kinase involves a malonyl-CoA-dependent and a malonyl-CoA-independent mechanism', *Arch Biochem Biophys*, 337(2), pp. 169-75.
- Villar-Palasi, C. and Guinovart, J.J. (1997) 'The role of glucose 6-phosphate in the control of glycogen synthase', *Faseb j*, 11(7), pp. 544-58.
- Vincent, M.F., Bontemps, F. and Van den Berghe, G. (1992) 'Inhibition of glycolysis by 5-amino-4-

- imidazolecarboxamide riboside in isolated rat hepatocytes', *Biochem J*, 281 (Pt 1), pp. 267-72.
- Vincent, M.F., Marangos, P.J., Gruber, H.E. and Van den Berghe, G. (1991) 'Inhibition by AICA riboside of gluconeogenesis in isolated rat hepatocytes', *Diabetes*, 40(10), pp. 1259-66.
- von Morze, C., Ohliger, M.A., Marco-Rius, I., Wilson, D.M., Flavell, R.R., Pearce, D., Vigneron, D.B., Kurhanewicz, J. and Wang, Z.J. (2018) 'Direct assessment of renal mitochondrial redox state using hyperpolarized (13) C-acetoacetate', *Magn Reson Med*, 79(4), pp. 1862-1869.
- von Wilamowitz-Moellendorff, A., Hunter, R.W., Garcia-Rocha, M., Kang, L., Lopez-Soldado, I., Lantier, L., Patel, K., Pegg, M.W., Martinez-Pons, C., Voss, M., Calbo, J., Cohen, P.T., Wasserman, D.H., Guinovart, J.J. and Sakamoto, K. (2013) 'Glucose-6-phosphate-mediated activation of liver glycogen synthase plays a key role in hepatic glycogen synthesis', *Diabetes*, 62(12), pp. 4070-82.
- Vytla, V.S. and Ochs, R.S. (2013) 'Metformin increases mitochondrial energy formation in L6 muscle cell cultures', *J Biol Chem*, 288(28), pp. 20369-77.
- Wang, X.T. and Engel, P.C. (2009) 'An optimised system for refolding of human glucose 6-phosphate dehydrogenase', *BMC Biotechnol*, 9, p. 19.
- Wang, D.S., Jonker, J.W., Kato, Y., Kusuhara, H., Schinkel, A.H. and Sugiyama, Y. (2002) 'Involvement of organic cation transporter 1 in hepatic and intestinal distribution of metformin', *J Pharmacol Exp Ther*, 302(2), pp. 510-5.
- Wang, H. and Wollheim, C.B. (2002) 'ChREBP rather than USF2 regulates glucose stimulation of endogenous L-pyruvate kinase expression in insulin-secreting cells', *J Biol Chem*, 277(36), pp. 32746-52.
- Wang, Y., Botolin, D., Xu, J., Christian, B., Mitchell, E., Jayaprakasam, B., Nair, M.G., Peters, J.M., Busik, J.V., Olson, L.K. and Jump, D.B. (2006) 'Regulation of hepatic fatty acid elongase and desaturase expression in diabetes and obesity', *J Lipid Res*, 47(9), pp. 2028-41.
- Wang, Y.W., He, S.J., Feng, X., Cheng, J., Luo, Y.T., Tian, L. and Huang, Q. (2017) 'Metformin: a review of its potential indications', *Drug Des Devel Ther*, 11, pp. 2421-2429.
- Wilcock, C. and Bailey, C.J. (1991) 'Reconsideration of inhibitory effect of metformin on intestinal glucose absorption', *J Pharm Pharmacol*, 43(2), pp. 120-1.
- Wilcock, C. and Bailey, C.J. (1994) 'Accumulation of metformin by tissues of the normal and diabetic mouse', *Xenobiotica*, 24(1), pp. 49-57.
- Wilcock, C. and Bailey, C.J. (1994) 'Accumulation of metformin by tissues of the normal and diabetic mouse', *Xenobiotica*, 24(1), pp. 49-57.
- Witters, L.A. (2001) 'The blooming of the French lilac', *J Clin Invest*, 108(8), pp. 1105-7.
- Wollen, N. and Bailey, C.J. (1988) 'Inhibition of hepatic gluconeogenesis by metformin. Synergism with insulin', *Biochem Pharmacol*, 37(22), pp. 4353-8.
- Xiao, B., Sanders, M.J., Carmena, D., Bright, N.J., Haire, L.F., Underwood, E., Patel, B.R., Heath, R.B., Walker, P.A., Hallen, S., Giordanetto, F., Martin, S.R., Carling, D. and Gamblin, S.J. (2013) 'Structural basis of AMPK regulation by small molecule activators', *Nat Commun*, 4, p. 3017.
- Xu, M., Xiao, Y., Yin, J., Hou, W., Yu, X., Shen, L., Liu, F., Wei, L. and Jia, W. (2014) 'Berberine promotes glucose consumption independently of AMP-activated protein kinase activation', *PLoS One*, 9(7), p. e103702.
- Yamashita, H., Takenoshita, M., Sakurai, M., Bruick, R.K., Henzel, W.J., Shillinglaw, W., Arnot, D. and Uyeda, K. (2001) 'A glucose-responsive transcription factor that regulates carbohydrate metabolism in the liver', *Proc*

Natl Acad Sci U S A, 98(16), pp. 9116-21.

Yee, S.W., Chen, L. and Giacomini, K.M. (2012) 'The role of ATM in response to metformin treatment and activation of AMPK', *Nat Genet*, 44(4), pp. 359-60.

Zalitis, J. and Oliver, I.T. (1967) 'Inhibition of glucose phosphate isomerase by metabolic intermediates of fructose', *Biochem J*, 102(3), pp. 753-9.

Zhang, C.S., Jiang, B., Li, M., Zhu, M., Peng, Y., Zhang, Y.L., Wu, Y.Q., Li, T.Y., Liang, Y., Lu, Z., Lian, G., Liu, Q., Guo, H., Yin, Z., Ye, Z., Han, J., Wu, J.W., Yin, H., Lin, S.Y. and Lin, S.C. (2014) 'The lysosomal v-ATPase-Regulator complex is a common activator for AMPK and mTORC1, acting as a switch between catabolism and anabolism', *Cell Metab*, 20(3), pp. 526-40.

Zhang, C.S., Li, M., Ma, T., Zong, Y., Cui, J., Feng, J.W., Wu, Y.Q., Lin, S.Y. and Lin, S.C. (2016) 'Metformin Activates AMPK through the Lysosomal Pathway', *Cell Metab*, 24(4), pp. 521-522.

Zhang, Y. and Ye, J. (2012) 'Mitochondrial inhibitor as a new class of insulin sensitizer', *Acta Pharm Sin B*, 2(4), pp. 341-349.

Zhang, Y.L., Guo, H., Zhang, C.S., Lin, S.Y., Yin, Z., Peng, Y., Luo, H., Shi, Y., Lian, G., Zhang, C., Li, M., Ye, Z., Ye, J., Han, J., Li, P., Wu, J.W. and Lin, S.C. (2013) 'AMP as a low-energy charge signal autonomously initiates assembly of AXIN-AMPK-LKB1 complex for AMPK activation', *Cell Metab*, 18(4), pp. 546-55.

Zhou, G., Myers, R., Li, Y., Chen, Y., Shen, X., Fenyk-Melody, J., Wu, M., Ventre, J., Doebber, T., Fujii, N., Musi, N., Hirshman, M.F., Goodyear, L.J. and Moller, D.E. (2001) 'Role of AMP-activated protein kinase in mechanism of metformin action', *J Clin Invest*, 108(8), pp. 1167-74.

Zhou, H.Y., Hu, G.X., Lian, Q.Q., Morris, D. and Ge, R.S. (2012) 'The metabolism of steroids, toxins and drugs by 11beta-hydroxysteroid dehydrogenase 1', *Toxicology*, 292(1), pp. 1-12.

Zhou, K., Donnelly, L.A., Kimber, C.H., Donnan, P.T., Doney, A.S., Leese, G., Hattersley, A.T., McCarthy, M.I., Morris, A.D., Palmer, C.N. and Pearson, E.R. (2009) 'Reduced-function SLC22A1 polymorphisms encoding organic cation transporter 1 and glycemic response to metformin: a GoDARTS study', *Diabetes*, 58(6), pp. 1434-9.

Zhou, K., Yee, S.W., Seiser, E.L., van Leeuwen, N., Tavendale, R., Bennett, A.J., Groves, C.J., Coleman, R.L., van der Heijden, A.A., Beulens, J.W., de Keyser, C.E., Zaharenko, L., Rotroff, D.M., Out, M., Jablonski, K.A., Chen, L., Javorsky, M., Zidzik, J., Levin, A.M., Williams, L.K., Dujic, T., Semiz, S., Kubo, M., Chien, H.C., Maeda, S., Witte, J.S., Wu, L., Tkac, I., Kooy, A., van Schaik, R.H.N., Stehouwer, C.D.A., Logie, L., Sutherland, C., Klovins, J., Pirags, V., Hofman, A., Stricker, B.H., Motsinger-Reif, A.A., Wagner, M.J., Innocenti, F., t Hart, L.M., Holman, R.R., McCarthy, M.I., Hedderon, M.M., Palmer, C.N.A., Florez, J.C., Giacomini, K.M. and Pearson, E.R. (2016) 'Variation in the glucose transporter gene SLC2A2 is associated with glycemic response to metformin', *Nat Genet*, 48(9), pp. 1055-1059.